

## **INFORMATION TO USERS**

**This manuscript has been reproduced from the microfilm master. UMI films the text directly from the original or copy submitted. Thus, some thesis and dissertation copies are in typewriter face, while others may be from any type of computer printer.**

**The quality of this reproduction is dependent upon the quality of the copy submitted. Broken or indistinct print, colored or poor quality illustrations and photographs, print bleedthrough, substandard margins, and improper alignment can adversely affect reproduction.**

**In the unlikely event that the author did not send UMI a complete manuscript and there are missing pages, these will be noted. Also, if unauthorized copyright material had to be removed, a note will indicate the deletion.**

**Oversize materials (e.g., maps, drawings, charts) are reproduced by sectioning the original, beginning at the upper left-hand corner and continuing from left to right in equal sections with small overlaps.**

**Photographs included in the original manuscript have been reproduced xerographically in this copy. Higher quality 6" x 9" black and white photographic prints are available for any photographs or illustrations appearing in this copy for an additional charge. Contact UMI directly to order.**

**ProQuest Information and Learning  
300 North Zeeb Road, Ann Arbor, MI 48106-1346 USA  
800-521-0600**

**UMI<sup>®</sup>**



**UNIVERSITY OF ALBERTA**

**IMPROVING THE DESIGN OF OZONE CONTACTORS FOR MICROORGANISM  
REDUCTION WITH A STATIC MIXER**

**By**



**Stephen A. Craik**

**A THESIS SUBMITTED TO THE FACULTY OF GRADUATE STUDIES AND  
RESEARCH IN PARTIAL FULFILLMENT OF THE REQUIREMENTS FOR THE  
DEGREE OF DOCTOR OF PHILOSOPHY  
IN  
ENVIRONMENTAL ENGINEERING**

**DEPARTMENT OF CIVIL AND ENVIRONMENTAL ENGINEERING**

**EDMONTON, ALBERTA**

**FALL 2001**



**National Library  
of Canada**

**Acquisitions and  
Bibliographic Services**

**395 Wellington Street  
Ottawa ON K1A 0N4  
Canada**

**Bibliothèque nationale  
du Canada**

**Acquisitions et  
services bibliographiques**

**395, rue Wellington  
Ottawa ON K1A 0N4  
Canada**

*Your file Votre référence*

*Our file Notre référence*

**The author has granted a non-exclusive licence allowing the National Library of Canada to reproduce, loan, distribute or sell copies of this thesis in microform, paper or electronic formats.**

**The author retains ownership of the copyright in this thesis. Neither the thesis nor substantial extracts from it may be printed or otherwise reproduced without the author's permission.**

**L'auteur a accordé une licence non exclusive permettant à la Bibliothèque nationale du Canada de reproduire, prêter, distribuer ou vendre des copies de cette thèse sous la forme de microfiche/film, de reproduction sur papier ou sur format électronique.**

**L'auteur conserve la propriété du droit d'auteur qui protège cette thèse. Ni la thèse ni des extraits substantiels de celle-ci ne doivent être imprimés ou autrement reproduits sans son autorisation.**

**0-612-68923-9**

**Canada**

UNIVERSITY OF ALBERTA

LIBRARY RELEASE FORM

NAME OF AUTHOR: Stephen A. Craik

TITLE OF THESIS: IMPROVING THE DESIGN OF OZONE CONTACTORS FOR  
MICROORGANISM REDUCTION WITH A STATIC MIXER

DEGREE: DOCTOR OF PHILOSOPHY

YEAR THIS DEGREE GRANTED: 2001

Permission is hereby granted to the University of Alberta Library to reproduce single copies of this thesis and to lend or sell such copies for private, scholarly or scientific research purposes only.

The author reserves all other publication and other rights in association with the copyright in the thesis, and except for herein provided, neither the thesis nor any substantial portion thereof may be printed or otherwise reproduced in any material form whatever without the author's prior written permission.



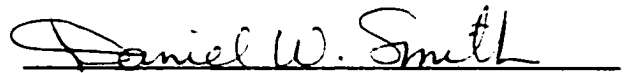
Stephen A. Craik

Dated: SEPT 4, 2001

UNIVERSITY OF ALBERTA

FACULTY OF GRADUATE STUDIES AND RESEARCH

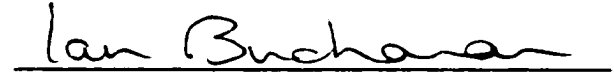
The undersigned certify that they have read, and recommend to the Faculty of Graduate Studies and Research for acceptance, a thesis entitled **IMPROVING THE DESIGN OF OZONE CONTACTORS FOR MICROORGANISM REDUCTION WITH A STATIC MIXER** submitted by **STEPHEN A. CRAIK** in partial fulfillment of the requirements for the degree of **DEGREE OF DOCTOR OF PHILOSOPHY IN ENVIRONMENTAL ENGINEERING**



Dr. D. W. Smith (Supervisor)



Dr. M. Belosevic (Co-supervisor)



Dr. I. D. Buchanan (Chair)



Dr. K. Nandakumar



Dr. F. E. Hicks



Dr. S. Duff (External Examiner)

Date Approved: **SEPT 4, 2001**

## **DEDICATION**

I dedicate the this thesis, and all the effort that went into it, to my wife, Shelley, for her love, support and inspiration from the start, through to the finish of this work and beyond, and to my baby daughter, Eva-Marie, who showed up somewhere in the middle, and, in ways she doesn't yet understand, provided me with some of the very same.

## ABSTRACT

*Cryptosporidium parvum* is an encysted parasite that has been linked to waterborne disease. In water treatment, the oocysts are resistant to chlorine but may be reduced or inactivated by aqueous ozone. A theoretical analysis based on established inactivation kinetics and chemical engineering principals showed that *C. parvum* inactivation by ozone will be limited by the mixing patterns that exist in many conventional ozone contactors. An alternative two-stage ozone contactor design concept, in which a static mixer is used to rapidly dissolve ozone, was proposed to improve the efficiency of microorganism inactivation. To test the fundamental assumptions of this concept, seeding experiments with *Bacillus subtilis* spores, *C. parvum* oocysts and *Giardia muris* cysts were carried out in a prototype contactor under rigorously controlled conditions. For *C. parvum* and *G. muris*, contactor efficiency was assessed by comparing measured inactivation to that predicted using kinetic models previously developed in batch reactor studies and available in the literature. For *B. subtilis* a batch reactor study was completed, and a new kinetic model, describing spore inactivation at temperatures ranging from 3 to 22°C and for pH 6 to 8, was developed.

In the prototype static mixer contactor, ozone gas-liquid mass transfer was determined mainly by the hydrodynamic conditions within the static mixer, which were given by the liquid superficial velocity (0.7 to 1.4 m/s) and the gas-liquid flowrate ratio (1.2 and 2.6%). For the dissolved ozone concentrations investigated, between 0.6 and 1.6 mg/L for *B. subtilis* spores and between 0.5 and 0.8 mg/L for *C. parvum* oocysts, inactivation was unaffected by static mixer hydrodynamic conditions and was determined mainly by contact with dissolved ozone in the reactive flow segment. Most importantly,

spore and oocyst inactivation approached that predicted based on the batch kinetic models and the assumption of plug flow behaviour in the contactor. Results with *Giardia muris* cysts were similar, but less definitive. It was concluded that the primary role of the static mixer in the two-stage contactor was to dissolve gaseous ozone rapidly and efficiently, and to thereby facilitate efficient microorganism reduction by contact with the dissolved ozone in the reactive flow segment.

## **ACKNOWLEDGEMENT**

I would like to gratefully acknowledge the support and guidance provided by both my graduate supervisor, Dr. Daniel W. Smith of the Environmental Engineering Program, and co-supervisor, Dr. Miodrag Belosevic of the Biological Sciences Department. I would also like to make a special acknowledgment to Dr. Gordon Russell Finch. Dr. Finch served as my original graduate supervisor until his untimely death in January of 2000. Dr. Finch supplied many of the initial ideas and the inspiration for the work described in this thesis, some of which did not become evident to me until several months after his untimely departure.

Many other individuals contributed to a greater or lesser extent during the project, in both concrete and abstract ways. These included fellow graduate students, post-doctoral fellows and technologists. I would like to particularly acknowledge the individuals in Dr. Belosevic's laboratory, without whom the parastilology work would not have been possible, or at least would have been orders of magnitude more difficult. These individuals included Cezary Kucharski, Shannon Lefevbre, Sarah Delorenzo, Dr. Norman Neumann and James Stafford. A special thanks goes to Mr. Emmanuel Guigard who assisted with most, if not all, of the experiments with the static mixer contactor.

I would also like to gratefully acknowledge the agencies that funded the work of this project. Funding was provided by the American Water Works Association Research Foundation and Vivendi/US Filter under the auspices of the AWWARF Tailored Collaboration Project Funding program. Finally, the Natural Sciences and Engineering Research Council of Canada (NSERC) provided me with personal financial support in the form of a post-graduate scholarship.

## TABLE OF CONTENTS

<b>1</b>	<b>INTRODUCTION .....</b>	<b>1</b>
1.1	EMERGING CHALLENGES IN DRINKING WATER TREATMENT .....	1
1.2	OZONE AS AN ALTERNATIVE FOR MICROORGANISM REDUCTION .....	2
1.3	THE ENGINEERING CHALLENGE .....	2
1.4	THESIS OBJECTIVE AND OVERVIEW .....	4
<b>2</b>	<b>BACKGROUND AND LITERATURE REVIEW .....</b>	<b>5</b>
2.1	TERMINOLOGY .....	5
2.2	ENCYSTED PROTOZOA IN DRINKING WATER.....	6
2.2.1	<i>Cryptosporidium parvum</i> and <i>Giardia lamblia</i> .....	6
2.2.2	Basic Biology .....	6
2.2.3	Species Identification .....	8
2.2.4	Human Health Effects .....	9
2.2.5	Oocysts and Cysts .....	11
2.2.6	Waterborne Disease.....	12
2.2.7	Reduction of Oocysts and Cysts by Conventional Water Treatment Processes .....	13
2.2.8	Regulatory Requirements.....	14
2.3	OZONE FOR REDUCTION OF ENCYSTED PROTOZOA .....	17
2.3.1	The Use of Ozone in Water Treatment .....	17
2.3.2	Ozone Solubility and Mass Transfer.....	17
2.3.3	Reaction and Decomposition of Aqueous Ozone .....	19
2.3.4	Health-Related By-Products.....	23
2.3.5	Effect of Ozone on Microorganisms .....	24
2.3.6	Kinetic Modeling of Microorganism Reduction by Ozone.....	27
2.3.7	Effect of Ozone on <i>Giardia</i> spp. ....	33
2.3.8	Effect of Ozone on <i>Cryptosporidium parvum</i> .....	37
2.3.9	Importance of the Method of Viability Determination .....	42
2.3.10	Scale-Up of Encysted Protozoa Inactivation by Ozone .....	44

2.3.11	Use of Bacterial Spores as Models for Ozone Inactivation of Encysted Protozoa .....	47
2.4	ROLE OF THE OZONE CONTACTOR IN MICROORGANISM REDUCTION .....	48
2.4.1	General Design Considerations for Ozone Contactors .....	48
2.4.2	Chemical Engineering Concepts .....	48
2.4.3	Impact of Mixing on Microorganism Reduction .....	52
2.4.4	Types of Ozone Contactors .....	53
2.4.5	Criteria for Ozone Contactor Design .....	54
2.4.6	Studies of Ozone Contactor Hydrodynamics .....	56
2.4.7	Influence of Gas-Liquid Contact .....	59
2.4.8	Use of Static Mixers for Ozone Contact .....	60
2.5	SUMMARY .....	63
3	EFFECT OF MIXING ON <i>CRYPTOSPORIDIUM PARVUM</i> INACTIVATION IN AN OZONE CONTACTOR - A THEORETICAL ANALYSIS .....	64
3.1	INTRODUCTION .....	64
3.2	CONTACTOR MODEL DEVELOPMENT .....	65
3.2.1	Scenario .....	65
3.2.2	Kinetic Models .....	65
3.2.3	Partially Segregated Flow Analysis .....	67
3.2.4	Segregated Flow Analysis .....	69
3.2.5	Numerical Calculations .....	70
3.3	SIMULATION RESULTS AND DISCUSSION .....	70
3.3.1	Simulation Plots .....	70
3.3.2	Effect of Residence Time Distribution .....	72
3.3.3	Effect of Micro-Mixing and Fluid Segregation .....	76
3.4	CONCLUSIONS .....	79
4	PROBLEM STATEMENT AND RESEARCH OBJECTIVES .....	81
4.1	PROBLEM STATEMENT .....	81
4.2	TWO-STAGE CONTACTOR DESIGN HYPOTHESIS .....	82
4.3	RESEARCH OBJECTIVES .....	83

<b>5</b>	<b>EXPERIMENTAL APPROACH</b> .....	<b>85</b>
5.1	CONCEPTUAL DESIGN OF AN EXPERIMENTAL OZONE STATIC MIXER CONTACTOR.....	85
5.2	MANIPULATED EXPERIMENTAL VARIABLES .....	87
5.3	INDEPENDENT CONTROL AND OZONE DISSOLUTION HYDRODYNAMICS AND DISSOLVED OZONE CONTACT .....	89
5.4	RESPONSE VARIABLES .....	89
5.5	VARIABLE CONTROL .....	91
5.6	SELECTION OF THE EXPERIMENTAL WATER SOURCE .....	91
<b>6</b>	<b>EXPERIMENTAL MATERIALS AND METHODS</b> .....	<b>93</b>
6.1	STATIC MIXER OZONE CONTACTOR MATERIALS AND METHODS.....	93
6.1.1	Details of the Experimental Static Mixer Ozone Contactor.....	93
6.1.2	Ozone Transfer Efficiency Measurements.....	96
6.1.3	Residence Time Distribution.....	98
6.1.4	Microorganism Inactivation Experiments With <i>B. subtilis</i> .....	100
6.1.5	Experiments With <i>C. parvum</i> .....	101
6.1.6	Experiments With <i>G. muris</i> .....	102
6.1.7	Dissolved Ozone Measurement.....	102
6.2	BATCH REACTOR EXPERIMENTS .....	105
6.3	<i>BACILLUS SUBTILIS</i> METHODS .....	107
6.3.1	Spore Production .....	107
6.3.2	Enumeration .....	108
6.4	<i>CRYPTOSPORIDIUM PARVUM</i> METHODS .....	108
6.4.1	Oocyst Production .....	108
6.4.2	Determination of Oocyst Infectivity in CD-1 Neonatal Mice.....	109
6.4.3	Interpretation of <i>C. parvum</i> Infectivity Data with the Logistic Dose Response Model .....	111
6.4.4	Characterization of Oocysts Used In Experiments .....	112
6.5	<i>GIARDIA MURIS</i> METHODS.....	114
6.5.1	Cyst Production .....	114

6.5.2	Development of a Quantitive Infectivity Model in C3H/HeN Mice.....	114
6.5.3	Infectivity Analysis In Experimental Samples.....	117
6.6	MISCELLANEOUS PROCEDURES .....	118
6.6.1	Ozone Demand-Free Materials .....	118
6.6.2	Ozone Demand-Free Phosphate Buffer.....	118
6.6.3	Measurement of Dissolved Combined Chlorine .....	118
6.6.4	Measurement of pH and Temperature.....	118
6.7	CALCULATIONS .....	119
6.7.1	Mean Residence Time.....	119
6.7.2	Average Concentration-Time Product .....	119
6.7.3	Microorganism Reduction.....	122
7	KINETICS OF OZONE INACTIVATION OF <i>BACILLUS SUBTILIS</i> SPORES ..	124
7.1	INTRODUCTION.....	124
7.2	BATCH REACTOR OZONATION TRIALS .....	125
7.2.1	Experimental Trials.....	125
7.2.2	Determination of Dissolved Ozone Concentration .....	126
7.2.3	Measured Spore Inactivation Curves .....	126
7.3	KINETIC MODELING .....	129
7.3.1	Development of a Two-Part Kinetic Model .....	129
7.3.2	Modeling Temperature Dependence .....	131
7.3.3	Model Regression to Experimental Data .....	132
7.4	EFFECT OF pH ON SPORE INACTIVATION .....	137
7.5	COMPARISON TO OTHER STUDIES .....	139
7.6	COMPARISON TO <i>CRYPTOSPORIDIUM PARVUM</i> .....	140
7.7	COMPARISON OF OZONE MEASUREMENT METHODS .....	143
7.8	SUMMARY OF BATCH REACTOR EXPERIMENTS WITH <i>BACILLUS SUBTILIS</i> SPORES .....	146
8	OZONE TRANSFER EFFICIENCY .....	147
8.1	INTRODUCTION.....	147
8.2	EXPERIMENTAL SYSTEM AND VARIABLES .....	147

8.3	PRELIMINARY EXPERIMENTS.....	148
8.4	TRANSFER EFFICIENCY DESIGNED EXPERIMENT.....	149
8.5	TRANSFER EFFICIENCY MODELING.....	153
8.6	MODEL PREDICTIONS.....	155
8.7	EFFECT OF WATER TEMPERATURE.....	157
8.8	DISCUSSION.....	158
9	INACTIVATION OF <i>BACILLUS SUBTILIS</i> SPORES IN THE STATIC MIXER CONTACTOR.....	162
9.1	INTRODUCTION.....	162
9.2	EXPERIMENTAL DESIGN.....	162
9.3	RESIDENCE TIME DISTRIBUTION.....	163
9.3.1	Determination of the Mean Residence Times.....	163
9.3.2	Effect of the Residence Time Distribution on Ozone Decomposition.....	166
9.4	FACTORIAL EXPERIMENT RESULTS.....	167
9.4.1	Selection of Dissolved Ozone Measurement Method.....	169
9.5	EFFECT OF STATIC MIXER HYDRODYNAMICS.....	171
9.5.1	Proposed Mechanisms for Enhanced Inactivation.....	171
9.5.2	Evidence for a Direct Effect: Spore Inactivation in the Static Mixer.....	172
9.5.3	Evidence for an Indirect Effect: Spore Inactivation in the Reactive Flow Segment.....	173
9.6	COMPARISON TO BATCH REACTORS.....	177
9.6.1	Experimental Conditions for Generation of the Batch Reactor Inactivation Curves.....	177
9.6.2	Modeling of the Batch Reactor Inactivation Curve.....	178
9.6.3	Interpretation of the Tailing Region as Spore Agglomeration.....	178
9.6.4	Interpretation by Segregated Flow Analysis.....	181
9.7	SUMMARY OF <i>B. SUBTILIS</i> SPORE EXPERIMENTS.....	184

<b>10</b>	<b>INACTIVATION OF <i>CRYPTOSPORIDIUM PARVUM</i> IN THE STATIC MIXER CONTACTOR</b> .....	<b>185</b>
10.1	INTRODUCTION.....	185
10.2	EXPERIMENTAL DESIGN .....	186
10.2.1	Static Mixer Contactor Challenge Experiments.....	186
10.2.2	Batch Reactor Experiments.....	187
10.3	CONTACTOR MODELING.....	187
10.3.1	Basis Approach .....	187
10.3.2	Kinetic Model of <i>C. parvum</i> Oocyst Inactivation.....	188
10.3.3	Predicted Inactivation in the Reactive Flow Segment .....	190
10.3.4	Predicted Inactivation in the Bubble Column .....	191
10.4	RESULTS OF CHALLENGE EXPERIMENTS .....	192
10.4.1	Ozonation Conditions.....	192
10.4.2	<i>C. parvum</i> Inactivation Measured by the CD-1 Neonatal Mouse Model .....	194
10.4.3	Measured <i>C. parvum</i> Oocyst Inactivation Curve .....	195
10.5	EFFECT OF STATIC MIXER HYDRODYNAMIC CONDITIONS ON <i>C. PARVUM</i> INACTIVATION .....	197
10.5.1	Direct Effect on <i>C. parvum</i> Inactivation .....	197
10.5.2	Indirect Effect on <i>C. parvum</i> Inactivation.....	197
10.6	VALIDATION OF THE BATCH KINETIC MODEL.....	199
10.6.1	Importance of Validation .....	199
10.6.2	<i>C. parvum</i> Inactivation in Batch Reactors Versus Kinetic Model-Prediction .....	199
10.6.3	Error Analysis .....	200
10.7	RESULTS OF MODELING ANALYSIS .....	201
10.7.1	Model Predictions .....	201
10.7.2	Comparison between Plug Flow and Segregated Flow Analysis.....	202
10.7.3	Comparison to Measured Inactivation .....	203
10.7.4	Comparison to <i>B. subtilis</i> Inactivation .....	205
10.8	SUMMARY OF <i>CRYPTOSPORIDIUM PARVUM</i> EXPERIMENTS .....	206

<b>11</b>	<b>INACTIVATION OF <i>GIARDIA MURIS</i> IN THE STATIC MIXER CONTACTOR</b> .....	<b>207</b>
11.1	INTRODUCTION.....	207
11.2	EXPERIMENTAL DESIGN.....	207
11.3	CONTACTOR MODELING.....	208
11.3.1	<i>G. muris</i> Kinetic Model.....	208
11.3.2	A Simplified Contactor Modeling Approach.....	210
11.4	CHALLENGE EXPERIMENT RESULTS.....	210
11.5	CYST INACTIVATION WITHIN THE STATIC MIXER.....	212
11.6	COMPARISON TO MODEL PREDICTIONS.....	213
11.7	SUMMARY OF <i>GIARDIA MURIS</i> EXPERIMENTS.....	215
<b>12</b>	<b>DISCUSSION AND SUMMARY</b> .....	<b>217</b>
12.1	THE PROBLEM STATEMENT REVISITED .....	217
12.2	FACTORS THAT DETERMINED MICROORGANISM INACTIVATION IN THE STATIC MIXER CONTACTOR .....	220
12.2.1	Effect of Turbulent Mixing on Mass Transfer and Microorganisms .....	220
12.2.2	Relationship Between Mass Transfer and Microorganism Reduction .....	222
12.2.3	Effect of Dissolved Ozone and Mixing.....	225
12.3	ENGINEERING SIGNIFICANCE.....	226
12.4	APPLICATION AT LARGER SCALES .....	228
<b>13</b>	<b>CONCLUSIONS</b> .....	<b>230</b>
<b>14</b>	<b>RECOMMENDATIONS</b> .....	<b>232</b>
<b>15</b>	<b>REFERENCES</b> .....	<b>234</b>
<b>APPENDIX A</b>	<b>INFORMATION FROM DOSE-RESPONSE EXPERIMENTS WITH <i>CRYPTOSPORIDIUM PARVUM</i> OOCYSTS AND <i>GIARDIA MURIS</i> CYSTS (CHAPTER 6)</b> .....	<b>271</b>

<b>APPENDIX B</b>	<b>INFORMATION FROM BATCH REACTOR OZONATION TRIALS WITH <i>BACILLUS SUBTILIS</i> (ATCC 6633) SPORES SUSPENDED IN PHOSPHATE BUFFERED WATER (CHAPTER 7).....</b>	<b>274</b>
<b>APPENDIX C</b>	<b>EXPERIMENTAL DATA AND INFORMATION FROM TRANSFER EFFICIENCY MEASUREMENT EXPERIMENTS WITH THE STATIC MIXER OZONE CONTACTOR (CHAPTER 8).....</b>	<b>278</b>
<b>APPENDIX D</b>	<b>EXPERIMENTAL DATA AND INFORMATION FROM CHALLENGE EXPERIMENTS WITH <i>BACILLUS SUBTILIS</i> SPORES IN THE EXPERIMENTAL STATIC MIXER CONTACTOR AND IN BATCH REACTORS (CHAPTER 9).....</b>	<b>282</b>
<b>APPENDIX E</b>	<b>INFORMATION FROM CHALLENGE EXPERIMENTS IN THE EXPERIMENTAL STATIC MIXER OZONE CONTACTOR AND BATCH OZONE REACTORS WITH <i>CRYPTOSPORIDIUM PARVUM</i> OOCYSTS (CHAPTER 10).....</b>	<b>287</b>
<b>APPENDIX F</b>	<b>INFORMATION FROM CHALLENGE EXPERIMENTS IN THE STATIC MIXER OZONE CONTACTOR AND BATCH OZONE REACTORS WITH <i>GIARDIA MURIS</i> CYSTS (CHAPTER 11).....</b>	<b>294</b>
<b>APPENDIX G</b>	<b>CALCULATION OF THE NUMBER OF OZONE MOLECULES TO OOCYSTS IN A DISSOLVED OZONE SOLUTION.....</b>	<b>300</b>
<b>APPENDIX H</b>	<b>CALCULATIONS OF HYDRODYNAMIC CONDITIONS WITHIN THE STATIC MIXER.....</b>	<b>302</b>
<b>APPENDIX I</b>	<b>CALCULATIONS OF THE HYDRODYNAMIC REGIME IN THE GREATER VANCOUVER DISTRICT GVRD COAQUITLAM FACILITY OZONE CONTACTOR.....</b>	<b>307</b>
<b>APPENDIX J</b>	<b>CURRICULUM VITAE.....</b>	<b>310</b>

## LIST OF TABLES

TABLE 2-1	COMPARISON OF INACTIVATION OF VARIOUS MICROORGANISMS BY CHLORINE COMPOUNDS .....	15
TABLE 2-2	SUMMARY OF REPORTED EXPERIMENTAL STUDIES ON INACTIVATION OF VARIOUS TYPES OF MICROORGANISMS BY OZONE IN WATER AND WASTEWATER.....	25
TABLE 2-3	THE EFFECT OF OZONE ON VARIOUS MICROORGANISMS – A COMPARISON..	26
TABLE 2-4	ALTERNATIVE KINETIC MODELS TO DESCRIBE REDUCTION OF MICROORGANISMS BY CHEMICAL REAGENTS. ....	32
TABLE 2-5	SUMMARY OF LABORATORY EXPERIMENTAL STUDIES ON THE EFFECT OF OZONE ON <i>GIARDIA</i> SPP. CYSTS.....	34
TABLE 2-6	SUMMARY OF LABORATORY EXPERIMENTAL STUDIES ON THE EFFECT OF OZONE ON <i>CRYPTOSPORIDIUM PARVUM</i> OOCYSTS.....	38
TABLE 5-1	MANIPULATED VARIABLES IN THE EXPERIMENTAL STATIC MIXER OZONE CONTACTOR. ....	88
TABLE 7-1	BEST-FIT PARAMETERS OF THE <i>BACILLUS SUBTILIS</i> SPORE INACTIVATION KINETIC MODEL .....	134
TABLE 7-2	ANALYSIS OF THE <i>BACILLUS SUBTILIS</i> KINETIC MODEL PREDICTION ERRORS.....	138
TABLE 8-1	RESULTS OF PRELIMINARY OZONE TRANSFER EFFICIENCY TRIALS WITH THE EXPERIMENTAL STATIC MIXER CONTACTOR.....	149
TABLE 8-2	SETTINGS OF THE TRANSFER EFFICIENCY DESIGNED EXPERIMENT FACTORS IN REAL AND CODED UNITS. ....	151
TABLE 8-3	RESULTS OF OZONE TRANSFER EFFICIENCY FACTORIAL DESIGNED EXPERIMENT ON THE EXPERIMENTAL STATIC MIXER CONTACTOR. ....	152
TABLE 8-4	ANALYSIS OF VARIANCE (ANOVA) RESULTS FOR THE TRANSFER EFFICIENCY MODEL LEAST-SQUARES LINEAR REGRESSION. ....	154
TABLE 8-5	EFFECT OF WATER TEMPERATURE ON OZONE TRANSFER EFFICIENCY IN THE STATIC MIXER CONTACTOR.....	158

TABLE 9-1	TARGET EXPERIMENTAL CONDITIONS FOR THE FACTORIAL DESIGNED EXPERIMENT ON THE EFFECT OF STATIC MIXER HYDRODYNAMIC CONDITIONS ON <i>BACILLUS SUBTILIS</i> SPORE INACTIVATION. ....	163
TABLE 9-2	SUMMARIZED RESULTS OF REPLICATE RESIDENCE TIME DETERMINATIONS AT MICROORGANISM SAMPLING LOCATIONS IN THE EXPERIMENTAL STATIC MIXER OZONE CONTACTOR. ....	166
TABLE 9-3	EXPERIMENTAL CONDITIONS FOR <i>BACILLUS SUBTILIS</i> SPORE INACTIVATION EXPERIMENTS IN THE EXPERIMENTAL STATIC MIXER OZONE CONTACTOR. ....	168
TABLE 9-4	COMPARISON OF MODEL-PREDICTED <i>BACILLUS SUBTILIS</i> SPORE INACTIVATION IN BATCH REACTORS AND IN THE EXPERIMENTAL STATIC MIXER OZONE CONTACTOR. ....	183
TABLE 10-1	SUMMARY OF OZONATION CONDITIONS FOR THE <i>CRYPTOSPORIDIUM PARVUM</i> CHALLENGE EXPERIMENTS IN THE STATIC MIXER CONTACTOR....	193
TABLE 10-2	MEASURED AND MODEL-PREDICTED <i>CRYPTOSPORIDIUM PARVUM</i> OOCYST INACTIVATION IN THE EXPERIMENTAL STATIC MIXER OZONE CONTACTOR. ....	195
TABLE 11-1	SUMMARY OF OZONATION CONDITIONS FOR THE <i>GIARDIA MURIS</i> CHALLENGE EXPERIMENTS WITH THE EXPERIMENTAL STATIC MIXER CONTACTOR. . ....	211
TABLE 11-2	MEASURED AND MODEL-PREDICTED <i>GIARDIA MURIS</i> CYST INACTIVATION IN THE EXPERIMENTAL STATIC MIXER OZONE CONTACTOR.....	212
TABLE 12-1	ESTIMATED HYDRODYNAMIC CONDITIONS WITHIN THE STATIC MIXER. ....	220
TABLE A-1	RESULTS OF FIVE DOSE RESPONSE EXPERIMENTS WITH EXPERIMENTAL <i>C. PARVUM</i> OOCYSTS.....	272
TABLE A-2	INFORMATION FROM <i>G. MURIS</i> DOSE-RESPONSE EXPERIMENTS WITH ADULT-MALE C3H/HeN MICE USED TO DEVELOP THE LATENT PERIOD DOSE-RESPONSE MODEL.....	223
TABLE B-1	BATCH REACTOR OZONATION TRIALS WITH <i>BACILLUS SUBTILIS</i> SPORES AT 3°C.....	275

TABLE B-2	BATCH REACTOR OZONATION TRIALS WITH <i>BACILLUS SUBTILIS</i> SPORES AT 12°C.....	276
TABLE B-3	BATCH REACTOR OZONATION TRIALS WITH <i>BACILLUS SUBTILIS</i> SPORES AT 22°C.....	277
TABLE C-1	INFORMATION FROM OZONE TRANSFER EFFICIENCY EXPERIMENTS WITH THE STATIC MIXER OZONE CONTACTOR.....	279
TABLE D-1	STATIC MIXER CONTACTOR CHALLENGE EXPERIMENTS WITH <i>B. SUBTILIS</i> SPORES: OZONATION CONDITIONS BASED ON UV 260 ABSORBANCE METHOD .....	283
TABLE D-2	STATIC MIXER CONTACTOR CHALLENGE EXPERIMENTS WITH <i>B. SUBTILIS</i> SPORES: OZONATION CONDITIONS BASED ON THE INDIGO TRISULPHONATE METHOD.....	284
TABLE D-3	MICROORGANISM ENUMERATION INFORMATION FROM LABORATORY STUDY WITH STATIC MIXER OZONE CONTACTOR EXPERIMENTS WITH <i>B. SUBTILIS</i> SPORES.....	285
TABLE D-4	BATCH REACTOR OZONATION TRIALS WITH <i>B. SUBTILIS</i> SPORES AT 16°C.....	286
TABLE E-1	STATIC MIXER CONTACTOR EXPERIMENTS WITH <i>CRYPTOSPORIDIUM</i> <i>PARVUM</i> OOCYSTS: OZONATION CONDITIONS BASED ON UV 260 ABSORBANCE METHOD.....	288
TABLE E-2	STATIC MIXER CONTACTOR EXPERIMENTS WITH <i>CRYPTOSPORIDIUM</i> <i>PARVUM</i> OOCYSTS: OZONATION CONDITIONS BASED ON INDIGO TRISULPHONATE METHOD.....	289
TABLE E-3	INFECTIVITY ANALYSIS IN THE STATIC MIXER CONTACTOR EXPERIMENTS WITH <i>CRYPTOSPORIDIUM PARVUM</i> OOCYSTS.....	290
TABLE E-4	OZONATION CONDITIONS IN BATCH OZONE REACTOR EXPERIMENTS WITH <i>CRYPTOSPORIDIUM PARVUM</i> OOCYSTS.....	292
TABLE E-5	INFECTIVITY ANALYSIS WITH THE NEONATAL CD-1 MOUSE INFECTIVITY ASSAY IN THE BATCH OZONE REACTOR EXPERIMENTS WITH <i>CRYPTOSPORIDIUM PARVUM</i> OOCYSTS.....	293

<b>TABLE F-1</b>	<b>STATIC MIXER OZONE CONTACTOR EXPERIMENTS WITH <i>GIARDIA MURIS</i> CYSTS: OZONATION CONDITIONS BASED ON THE UV 260 ABSORBANCE METHOD.....</b>	<b>295</b>
<b>TABLE F-2</b>	<b>STATIC MIXER OZONE CONTACTOR EXPERIMENTS WITH <i>GIARDA MURIS</i> CYSTS: OZONATION CONDITIONS BASED ON THE INDIGO TRISULPHONATE METHOD.....</b>	<b>296</b>
<b>TABLE F-3</b>	<b>LATENT PERIOD INFECTIVITY ANALYSIS IN ADULT-MALE C3H HEN MICE FOR STATIC MIXER OZONE CONTACTOR EXPERIMENTS WITH <i>GIARDIA MURIS</i>.....</b>	<b>298</b>
<b>TABLE F-4</b>	<b>BATCH OZONATION TRIALS WITH <i>GIARDIA MURIS</i> CYSTS AND SIMPLIFIED HOM MODEL PREDICTIONS.....</b>	<b>299</b>

## LIST OF FIGURES

FIGURE 1-1	GROWTH IN OZONE APPLICATIONS IN WATER TREATMENT .....	3
FIGURE 2-1	POSSIBLE FORMS OF MICROORGANISM REDUCTION INACTIVATION CURVES .....	30
FIGURE 2-2	DEPICTION OF A TYPICAL CONVENTIONAL MULTI-CHAMBER FINE BUBBLE DIFFUSER (FBD) OZONE CONTACTOR .....	54
FIGURE 2-3	POTENTIAL HYDRODYNAMIC FLOW PATTERN IN A TYPICAL CONVENTIONAL MULTI-CHAMBER FINE BUBBLE DIFFUSER OZONE CONTACTOR. ....	58
FIGURE 3-1	THE EXIT AGE DISTRIBUTION IN A HYPOTHETICAL OZONE CONTACTOR AS A FUNCTION OF THE NUMBER OF CFSTRs IN SERIES.....	71
FIGURE 3-2	SIMULATION OF THE EFFECT OF CONTACTOR HYDRODYNAMICS ON <i>C.</i> <i>PARVUM</i> INACTIVATION FOR THE CASE OF NO OZONE DECOMPOSITION ( $k_d =$ $0 \text{ MIN}^{-1}$ ) .....	73
FIGURE 3-3	SIMULATION OF THE EFFECT OF CONTACTOR HYDRODYNAMICS ON <i>C.</i> <i>PARVUM</i> INACTIVATION FOR THE CASE OF OZONE DECOMPOSITION WITH $k_d = 0.1 \text{ MIN}^{-1}$ .....	74
FIGURE 3-4	SIMULATION OF THE EFFECT OF CONTACTOR HYDRODYNAMICS ON <i>C.</i> <i>PARVUM</i> INACTIVATION FOR THE CASE OF OZONE DECOMPOSITION WITH $k_d = 0.2 \text{ MIN}^{-1}$ .....	75
FIGURE 3-5	EFFECT OF FLUID SEGREGATION ON THE OZONATION REQUIREMENTS FOR 2 LOG-UNITS INACTIVATION OF <i>CRYPTOSPORIDIUM PARVUM</i> IN AN OZONE CONTACTOR. ....	77
FIGURE 4-1	DESCRIPTION OF THE TWO-STAGE OZONE CONTACTOR DESIGN HYPOTHESIS. ....	82
FIGURE 5-1	SIMPLIFIED SCHEMATIC OF THE EXPERIMENTAL OZONE STATIC MIXER CONTACTING SYSTEM. ....	85
FIGURE 5-2	PHOTOGRAPH OF THE DISASSEMBLED STATIC MIXER WITH INTERNAL MIXING ELEMENTS REMOVED. ....	86

FIGURE 6-1	DETAILED SCHEMATIC OF THE EXPERIMENTAL STATIC MIXER OZONE CONTACTOR. ....	93
FIGURE 6-2	DETAIL OF THE INTERNALS OF THE SULZER SMV STATIC MIXER .....	95
FIGURE 6-3	APPARATUS USED FOR SAMPLING AND DETERMINATION OF OZONE CONCENTRATION IN STATIC MIXER OZONE CONTACTOR FEED GAS AND OFF GAS. ....	98
FIGURE 6-4	APPARATUS USED FOR MICROORGANISM INACTIVATION EXPERIMENTS IN WELL-MIXED BATCH REACTORS WITH CONTINUOUS DISSOLVED OZONE MONITORING BY UV ABSORBANCE. ....	106
FIGURE 6-5	DOSE-RESPONSE OF <i>CRYPTOSPORIDIUM PARVUM</i> OOCYSTS USED IN EXPERIMENTAL TRIALS AND MAXIMUM LIKELIHOOD FIT OF LOGIT DOSE-RESPONSE MODEL. ....	113
FIGURE 6-6	PATTERN OF CYST SHEDDING IN THE FECES OF C3H/HeN MICE INFECTED WITH FRESH <i>GIARDIA MURIS</i> CYSTS IN A DOSE-RESPONSE EXPERIMENT. ....	116
FIGURE 6-7	LATENT PERIOD, <i>LP</i> , IN THE C3H/HeN MICE AS A FUNCTION OF THE NUMBER OF FRESH <i>GIARDIA MURIS</i> CYSTS IN THE ORAL INOCULUM, <i>D</i> . ....	117
FIGURE 6-8	TYPICAL OZONE CONCENTRATION PROFILE IN THE REACTIVE FLOW SEGMENT OF THE STATIC MIXER OZONE CONTACTOR.....	120
FIGURE 6-9	TYPICAL OZONE CONCENTRATION PROFILE IN A BATCH REACTOR EXPERIMENT .....	121
FIGURE 7-1	OZONE INACTIVATION OF <i>BACILLUS SUBTILIS</i> SPORES IN OZONE DEMAND-FREE BUFFERED LABORATORY WATER AT 3°C.....	127
FIGURE 7-2	OZONE INACTIVATION OF <i>BACILLUS SUBTILIS</i> SPORES IN OZONE DEMAND-FREE BUFFERED LABORATORY WATER AT 12°C.....	128
FIGURE 7-3	OZONE INACTIVATION OF <i>BACILLUS SUBTILIS</i> SPORES IN OZONE DEMAND-FREE BUFFERED LABORATORY WATER AT 22°C.....	128
FIGURE 7-4	COMPARISON OF MODEL-PREDICTED AND MEASURED INACTIVATION OF <i>BACILLUS SUBTILIS</i> SPORES AT 3°C. ....	135
FIGURE 7-5	COMPARISON OF MODEL-PREDICTED AND MEASURED INACTIVATION OF <i>BACILLUS SUBTILIS</i> SPORES AT 12°C. ....	135

FIGURE 7-6	COMPARISON OF MODEL-PREDICTED AND MEASURED INACTIVATION OF <i>BACILLUS SUBTILIS</i> SPORES AT 22°C.....	136
FIGURE 7-7	HISTOGRAM OF THE <i>BACILLUS SUBTILIS</i> OZONE INACTIVATION KINETIC MODEL PREDICTION ERRORS.....	136
FIGURE 7-8	COMPARISON OF MODEL-PREDICTED OZONE INACTIVATION CURVES OF <i>BACILLUS SUBTILIS</i> ATCC 6633 SPORES AND <i>CRYPTOSPORIDIUM PARVUM</i> OOCYSTS AT 22°C.....	141
FIGURE 7-9	COMPARISON OF MODEL-PREDICTED OZONE INACTIVATION CURVES OF <i>BACILLUS SUBTILIS</i> ATCC 6633 SPORES AND <i>CRYPTOSPORIDIUM PARVUM</i> OOCYSTS AT 12°C.....	142
FIGURE 7-10	COMPARISON OF MODEL-PREDICTED OZONE INACTIVATION CURVES OF <i>BACILLUS SUBTILIS</i> ATCC 6633 SPORES AND <i>CRYPTOSPORIDIUM PARVUM</i> OOCYSTS AT 3°C.....	143
FIGURE 7-11	RATIO OF THE AVERAGE DISSOLVED OZONE CONCENTRATION IN THE <i>BACILLUS SUBTILIS</i> SPORE BATCH REACTOR EXPERIMENTS AS DETERMINED BY THE INDIGO TRISULPHONATE METHOD AND THE DIRECT UV ABSORBANCE METHOD..	145
FIGURE 8-1	MANIPULATED AND RESPONSE VARIABLES IN THE OZONE TRANSFER EFFICIENCY EXPERIMENTS.....	148
FIGURE 8-2	TYPICAL DISSOLVED OZONE PROFILES IN THE STATIC MIXER OZONE CONTACTOR BUBBLE COLUMN AT HIGH AND LOW $G/Q_F$ SETTINGS.....	150
FIGURE 8-3	COMPARISON OF MODEL-PREDICTED AND MEASURED OZONE TRANSFER EFFICIENCY.....	155
FIGURE 8-4	EXAMPLES OF TRANSFER EFFICIENCY MODEL PREDICTIONS..	156
FIGURE 9-1	EXAMPLES OF THE EXIT AGE DISTRIBUTION, $E(t)$ , MEASURED AT THE OUTLET OF THE BUBBLE COLUMN.....	164
FIGURE 9-2	EXAMPLES OF THE EXIT AGE DISTRIBUTION, $E(t)$ , MEASURED AT FOUR DIFFERENT LOCATIONS IN THE REACTIVE FLOW SEGMENT (RFS).....	165
FIGURE 9-3	RESULTS OF DUPLICATE CHALLENGE TRIALS WITH <i>BACILLUS SUBTILIS</i> SPORES AT DIFFERENT STATIC MIXER HYDRODYNAMIC CONDITIONS	

	BASED ON OZONE CONCENTRATION DETERMINED USING THE INDIGO TRISULPHONATE MEASUREMENT METHOD.....	170
FIGURE 9-4	RESULTS OF DUPLICATE CHALLENGE TRIALS WITH <i>BACILLUS SUBTILIS</i> SPORES AT DIFFERENT STATIC MIXER HYDRODYNAMIC CONDITIONS BASED ON OZONE CONCENTRATION DETERMINED USING THE UV ABSORBANCE MEASUREMENT METHOD. ....	171
FIGURE 9-5	BOX AND WHISKER DIAGRAM OF MEASURED <i>BACILLUS SUBTILIS</i> SPORE INACTIVATION ACROSS THE STATIC MIXER ITSELF.....	173
FIGURE 9-6	EFFECT OF HYDRODYNAMIC CONDITIONS WITHIN THE STATIC MIXER ON THE <i>BACILLUS SUBTILIS</i> SPORE INACTIVATION CURVE IN THE STATIC MIXER OZONE CONTACTOR.....	174
FIGURE 9-7	BEST-FIT CURVE OF <i>BACILLUS SUBTILIS</i> SPORE INACTIVATION IN THE EXPERIMENTAL STATIC MIXER CONTACTOR.....	175
FIGURE 9-8	EFFECT OF STATIC MIXER HYDRODYNAMIC CONDITIONS ON PREDICTION ERRORS OF THE AVERAGE <i>BACILLUS SUBTILIS</i> SPORE INACTIVATION MODEL.....	176
FIGURE 9-9	COMPARISON BETWEEN <i>BACILLUS SUBTILIS</i> SPORE INACTIVATION MEASURED IN THE STATIC MIXER CONTACTOR AND <i>BACILLUS SUBTILIS</i> SPORE INACTIVATION MEASURED IN BATCH REACTORS .....	177
FIGURE 9-10	LINEAR REGRESSION FIT OF THE <i>BACILLUS SUBTILIS</i> SPORE INACTIVATION MODEL TO SPORE INACTIVATION MEASURED IN THE BATCH REACTOR OZONATION TRIALS.. .....	179
FIGURE 9-11	COMPARISON BETWEEN <i>BACILLUS SUBTILIS</i> SPORE INACTIVATION MEASURED IN THE STATIC MIXER CONTACTOR AND SPORE INACTIVATION MEASURED IN BATCH REACTORS .....	180
FIGURE 10-1	MEASURED INACTIVATION OF <i>CRYPTOSPORIDIUM PARVUM</i> OOCYSTS IN THE EXPERIMENTAL STATIC MIXER OZONE CONTACTOR .....	196
FIGURE 10-2	BOX AND WHISKER DIAGRAM OF MEASURED <i>CRYPTOSPORIDIUM PARVUM</i> INACTIVATION MEASURED DIRECTLY AT THE INLET AND OUTLET OF THE STATIC MIXER.....	198

<b>FIGURE 10-3</b>	<b>COMPARISON OF MODEL-PREDICTED AND MEASURED BATCH REACTOR INACTIVATION OF THE <i>CRYPTOSPORIDIUM PARVUM</i> OOCYSTS USED IN THE STATIC MIXER CONTACTOR EXPERIMENTS .....</b>	<b>201</b>
<b>FIGURE 10-4</b>	<b>COMPARISON OF MODEL-PREDICTED AND MEASURED <i>CRYPTOSPORIDIUM PARVUM</i> OOCYST INACTIVATION AT THE OUTLET OF THE REACTIVE FLOW SEGMENT IN THE EXPERIMENTAL STATIC MIXER CONTACTOR.....</b>	<b>204</b>
<b>FIGURE 11-1</b>	<b>INACTIVATION OF <i>GIARDIA MURIS</i> BY OZONE IN BATCH REACTORS AS DETERMINED BY LATENT PERIOD INFECTIVITY ANALYSIS IN C3H/HEN MICE .....</b>	<b>209</b>
<b>FIGURE 11-2</b>	<b>BOX AND WHISKER DIAGRAM OF MEASURED <i>GIARDIA MURIS</i> INACTIVATION AT THE INLET AT OUTLET OF THE STATIC MIXER. ....</b>	<b>213</b>
<b>FIGURE 11-3</b>	<b>INACTIVATION OF <i>GIARDIA MURIS</i> IN THE EXPERIMENTAL STATIC MIXER OZONE CONTACTOR AT DIFFERENT SUPERFICIAL VELOCITIES IN THE STATIC MIXER.....</b>	<b>215</b>
<b>FIGURE 12-1</b>	<b>DEPICTION OF OZONE CONCENTRATION PROFILES IN MICROORGANISM INACTIVATION PROCESSES FOR TWO PHYSICAL CASES .....</b>	<b>224</b>

## **LIST OF ABBREVIATIONS AND NOMENCLATURE**

### **ABBREVIATIONS**

<b>AOP</b>	<b>Advanced Oxidation Process</b>
<b>APHA</b>	<b>American Public Health Administration</b>
<b>ATCC</b>	<b>American Type Culture Collection</b>
<b>AWWA</b>	<b>American Water Works Association</b>
<b>AWWARF</b>	<b>American Water Works Association Research Foundation</b>
<b>CFSTR</b>	<b>Continuous-Flow Stirred Tank Reactor</b>
<b>CFU</b>	<b>Colony Forming Unit</b>
<b>CFD</b>	<b>Computational Fluid Dynamics</b>
<b>Cum.</b>	<b>Cumulative</b>
<b>D/DPB</b>	<b>Disinfection/Disinfectant By-Product</b>
<b>DPD</b>	<b><i>N,N</i>-Diethyl-<i>p</i>-PhenyleneDiamine colorimetric method for total chlorine</b>
<b>FBD</b>	<b>Fine Bubble Diffuser</b>
<b>FEA</b>	<b>Finite Element Analysis</b>
<b>GAC</b>	<b>Granular Activated Carbon</b>
<b>GVRD</b>	<b>Greater Vancouver Regional District</b>
<b>HAAs</b>	<b>HaloAcetic Acids (<math>\mu\text{g/L}</math>)</b>
<b>HPC</b>	<b>Heterotrophic Plate Count</b>
<b>HRT</b>	<b>Hydraulic Residence Time (min)</b>
<b>ID</b>	<b>Internal Diameter (mm)</b>
<b>ID<sub>50</sub></b>	<b>parasite dose required for a 50% rate of infection</b>
<b>IESWTR</b>	<b>Interim Enhanced Surface Water Treatment Rule</b>
<b>LT2ESWTR</b>	<b>Long Term 2 Enhanced Surface Water Treatment</b>
<b>MCL</b>	<b>Maximum Contaminant Level (<math>\mu\text{g/L}</math>)</b>

## **ABBREVIATIONS (CONTINUED)**

<b>na</b>	<b>not applicable</b>
<b>nd</b>	<b>not done</b>
<b>NTP</b>	<b>Normal Temperature and Pressure (0°C and 760 mmHg)</b>
<b>NTU</b>	<b>Nephelometric Turbidity Units</b>
<b>ODF</b>	<b>Ozone Demand-Free</b>
<b>PFA</b>	<b>Plug Flow Analysis</b>
<b>PFR</b>	<b>Plug Flow Reactor</b>
<b>PVC</b>	<b>Polyvinyl Chloride</b>
<b>RFS</b>	<b>Reactive Flow Segment</b>
<b>RTD</b>	<b>Residence Time Distribution</b>
<b>SE</b>	<b>Standard Error</b>
<b>SFA</b>	<b>Segregated Flow Analysis</b>
<b>SMX</b>	<b>Static MiXer</b>
<b>SWTR</b>	<b>Surface Water Treatment Rule</b>
<b>Temp.</b>	<b>Temperature (°C)</b>
<b>THMs</b>	<b>Trihalomethanes (µg/L)</b>
<b>TOC</b>	<b>Total Organic Carbon (mg C/L)</b>
<b>US</b>	<b>United States</b>
<b>UK</b>	<b>United Kingdom</b>
<b>US EPA</b>	<b>United States Environmental Protection Agency</b>
<b>UV</b>	<b>Ultraviolet</b>
<b>WEF</b>	<b>Water Environment Federation</b>

## **SYMBOLS USED**

$a$	specific gas-liquid interfacial surface area ( $\text{m}^2/\text{m}^3$ )
$A_{260}$	absorbance at 260 nm measured in a 10 mm cell
$A_{600}$	absorbance at 600 nm measured in a 10 mm cell
$C$	concentration of ozone in the aqueous phase (mg/L)
$C_a$	applied ozone represented as concentration (mg/L)
$C_{avg}$	average ozone concentration (mg/L)
$C^*$	concentration of ozone in the liquid phase in equilibrium with the gas phase (mg/L)
$Ct$	generic concentration $\times$ time product (mg $\times$ min/L)
$C_{avg}t_b$	average ozone concentration $\times$ time product in the batch reactor (mg $\times$ min/L)
$C_{avg}t_m$	average ozone concentration $\times$ time product in the static mixer contactor (mg $\times$ min/L)
$C_f$	final ozone concentration in the batch reactor or at outlet of the reactive flow segment in the static mixer contactor (mg/L)
$C_0$	initial ozone concentration in the batch reactor or at the inlet of reactive flow segment in the static mixer contactor (mg/L)
$C_t$	concentration of dissolved tracer at time $t$ (mg/L)
$C_{avg,t}$	Average concentration of dissolved tracer at times $t$ and $t-1$ (mg/L)
$d$	number of live (oo)cysts in inoculum to each mouse estimated from infectivity model
$d_0$	total number of (oo)cysts in inoculum to each mouse based on hemocytometer counts
$D/uL$	dispersion number
$\mathcal{D}$	molecular diffusivity ( $\text{m}^2/\text{s}$ )
$e$	energy dissipation rate (J/kg/s)

## **SYMBOLS USED (Continued)**

$E(t)$	exit age distribution function determined from tracer tests
$E_A$	activation energy (kJ/mol)
$F$	value of the Fisher $F$ -statistic in ANOVA
$f$	sensitivity coefficient for indigo trisulphonate procedure
$g$	gravitational acceleration (9.82 m/s <sup>2</sup> )
$G$	velocity gradient (s <sup>-1</sup> )
$G$	gas volumetric flow rate (L/min)
$G/Q_f$	gas to liquid flow rate ratio (%)
$h_L$	head loss (m)
$H$	height of the bubble column in the static mixer contactor (m)
$i$	index for summation operations
$I$	inactivation ratio in base 10 logarithm
$J$	number of CFSTRs in the CFSTR-in-series model
$k$	Chick-Watson kinetic model rate constant, natural logarithm (L/mg/min)
$k'$	Chick-Watson kinetic model rate constant, base 10 logarithm (L/mg/min)
$k_i$	rate constant for inactivation of individual spores (L/mg/min)
$k_a$	rate constant for inactivation of agglomerated spore units (L/mg/min)
$k_d$	first-order rate coefficient for ozone decomposition (min <sup>-1</sup> )
$k_H$	Hom kinetic model rate constant, natural logarithm (L/mg/min)
$k'_H$	Hom kinetic model rate constant, base 10 logarithm (L/mg/min)
$k_L$	local liquid film mass transfer coefficient (m <sup>-2</sup> min <sup>-1</sup> )
$k_L a$	bulk liquid film mass transfer parameter (min <sup>-1</sup> )
$L$	length (m)
$L_{sm}$	length of the static mixer (m)
$LP$	latent period of infection (d)
$L$	likelihood function

## **SYMBOLS USED (Continued)**

$m$	kinetic parameter of the Hom kinetic model of ozone inactivation
$M$	gas-liquid mass transfer rate in mass per unit time (mg/min)
$N$	concentration of live microorganisms after a specified ozone treatment (no. /mL)
$N_0$	concentration of live microorganisms before ozone treatment (no. /mL)
$N_i$	concentration of individual spores (no. /mL)
$N_a$	concentration of agglomerated spore units (no. /mL)
$n_c$	number of critical targets required for spore inactivation
$n$	kinetic parameter of the Hom kinetic model of ozone inactivation
$n$	number of measurements
$N_{Re}$	dimensionless Reynold's number
$P$	power input (kW)
$P$	proportion of neonatal CD-1 mice that are positive for infection
$p$ -value	probability of a type I error in a hypothesis test
$\Delta p$	pressure drop (kPa)
$Q_f$	static mixer feed water flow rate (L/min)
$Q_{RFS}$	reactive flow segment water flow rate, (L/min)
$R$	universal gas constant, 0.08205 (L·atm/mol/K)
$r$	fraction of the spore population with a higher resistance to ozone
$s$	standard deviation
$S$	microorganism survival ratio
$S_g$	segregation number
$t$	time (min or s)
$\bar{t}$	mixing time scale (min or s)
$t_{10}$	time required for 10% of the injected tracer to exit the system (min or s)
$t_{90}$	time required for 90% of the injected tracer to exit the system (min or s)
$t_{98}$	time required for 98% of the injected tracer to exit the system (min or s)

## **SYMBOLS USED (Continued)**

$t_b$	batch contact time (min or s)
$t_m$	mean residence time (min or s)
$t_{\alpha/2}$	value of the Student t-distribution
$\Delta t$	time step for numerical integration (s)
$T$	temperature (°C)
$TE$	ozone mass transfer efficiency (%)
$V$	volume (L)
$V_g$	gas volume (L) at 0°C and 760 mmHg
$Y$	concentration of ozone in the gas phase (mg/L or g/m <sup>3</sup> )
$Y_f$	concentration of ozone in contactor feed gas (mg/L or g/m <sup>3</sup> )
$Y_o$	concentration of ozone in contactor off-gas (mg/L or g/m <sup>3</sup> )

## **GREEK SYMBOLS**

$\alpha$	acceptable probability level for hypothesis testing
$\beta_0$	parameter of the <i>C. parvum</i> logit dose-response model
$\beta_1$	parameter of the <i>C. parvum</i> logit dose-response model
$\chi^2_{p,\alpha}$	The Chi-square distribution with $p$ degrees of freedom and $1 - \alpha$ level of confidence
$\varepsilon$	model prediction error
$\gamma$	the incomplete gamma function
$\eta$	The Kolmogoroff mixing scale (m)
$\mu$	viscosity (N·s/m)
$\pi$	the value 3.1416
$\theta$	The Arrhenius temperature dependence coefficient of inactivation rate constants
$\rho$	density (kg/m)
$\sigma_\theta^2$	variance of the normalized residence time distribution
$\tau$	total theoretical residence time or space time (min or s)
$\tau_i$	theoretical residence time or space time in individual reactors in the tanks-in-series model (min or s)

## **UNITS**

°C	degrees Celsius
g	grams
h	hours
J	Joules
kg	kilograms
kPa	kilopascals
L/min	liters per minute
m	metres
min	minutes
mg/L	milligrams per liter
mL	milliliters
mol	gram moles ( $6.02 \times 10^{23}$ molecules)
mm	millimetres
m/s	meters per second
M	molar
N	normal
µg/L	micrograms per liter
µL	microlitres
µm	micrometres
s	seconds

# 1 INTRODUCTION

## 1.1 EMERGING CHALLENGES IN DRINKING WATER TREATMENT

The reduction and control of pathogenic microorganisms in public drinking water supplies through application of treatment processes was one of the most significant public health achievements of the twentieth century. Introduction of filtration and chlorination in water treatment during the earlier part of that century almost eradicated waterborne outbreaks of cholera and typhoid in major North American cities (Okun 1996). Chlorination was very quickly proven to be a highly capable and inexpensive treatment technique for reduction of pathogenic bacteria. For many years, there was little incentive to improve upon the engineering science of microorganism reduction processes, nor to investigate alternatives to chlorine.

In the latter part of the century, new microbial threats emerged in the form of the parasites *Giardia lamblia* and *Cryptosporidium parvum*. In the environmentally robust encysted form, these protozoan parasites proved to be much more resistant to the effects of conventional chlorination than are bacteria and viruses. Moreover, they have been increasingly identified as causes of waterborne disease in humans. At the same time, the level of awareness and concern over the potential long-term human health effects of ingestion of the chemical by-products formed during chlorination and other chemical treatment processes has increased (Tate and Fox Arnold, 1990). Federal drinking water regulations in the United States have now set simultaneous requirements for reduction of encysted protozoa and maximum allowable limits on the concentration of these chemical by-products in drinking water (U. S. Environmental Protection Agency, 1998a, 1998b). These recent historical events in the water treatment industry have forced environmental engineers to look for more rational and precise methods of water treatment facility design. The challenge is to strike the correct balance between risk of microbial contamination and disease on the one hand, and the long-term health effects of low level chemical exposure on the other, and to do so within reasonable economic cost constraints. This challenge must be met through selection of appropriate treatment methods and through rational process design.

## **1.2 OZONE AS AN ALTERNATIVE FOR MICROORGANISM REDUCTION**

The limitations and health concerns associated with chlorination have prompted exploration of alternatives for control of microorganisms in drinking water, such as the oxidant chemical ozone. Several laboratory studies have now confirmed that ozone is an effective biocidal agent against encysted protozoa (Finch et al. 1993a; Gyürék et al. 1999; Hirata et al., 2000; Kanjo et al., 2000; Korich et al., 1990; Li et al. 2001; Oppenheimer et al. 2000; Perrine et al., 1990; Ransome et al. 1993, Rennecker et al. 1999; Somiya et al. 2000a, 2000b). In addition, ozone does not produce the same suite of chemical by-products as does chlorination (Singer, 1990). The rapid growth in the number of water treatment applications of ozone in North America (Figure 1-1) in the past decade and a half is not surprising. Ozone, however, is not without limitations. Ozonation systems are technically complex to design and to operate, are difficult to optimize, and are relatively capital and operating cost intensive (Glaze, 1990). It has also now been established that ozonation of some natural waters may also produce undesirable by-products that are of potential concern to human health (Singer, 1990). For example, ozonation of waters that contain low levels of the innocuous bromide ion results in the generation of bromate ion, a chemical believed to cause cancer in laboratory animals (Amy et al., 2000).

## **1.3 THE ENGINEERING CHALLENGE**

In the past, design of ozonation facilities in water treatment has been based more on experience and empirical sets of rules and less on complete understanding of the underlying processes involved. Ozone is an extremely reactive gas of limited solubility. In most water treatment applications, gaseous ozone produced on site is dissolved into the water and an aqueous ozone concentration is generated (Langlais et al. 1991). Once dissolved, ozone engages in complex chemistry that includes auto-decomposition and reaction with various constituents of the water, in addition to reaction with microorganisms (Hoigné, 1988). To date, most of the engineering effort has been directed at improving the efficiency of ozone dissolution, increasing system reliability and reducing costs. Less effort has been dedicated to understanding and optimizing the role of the ozone contactor as a reactor for microorganism reduction. And, for most applications, this approach has sufficed.

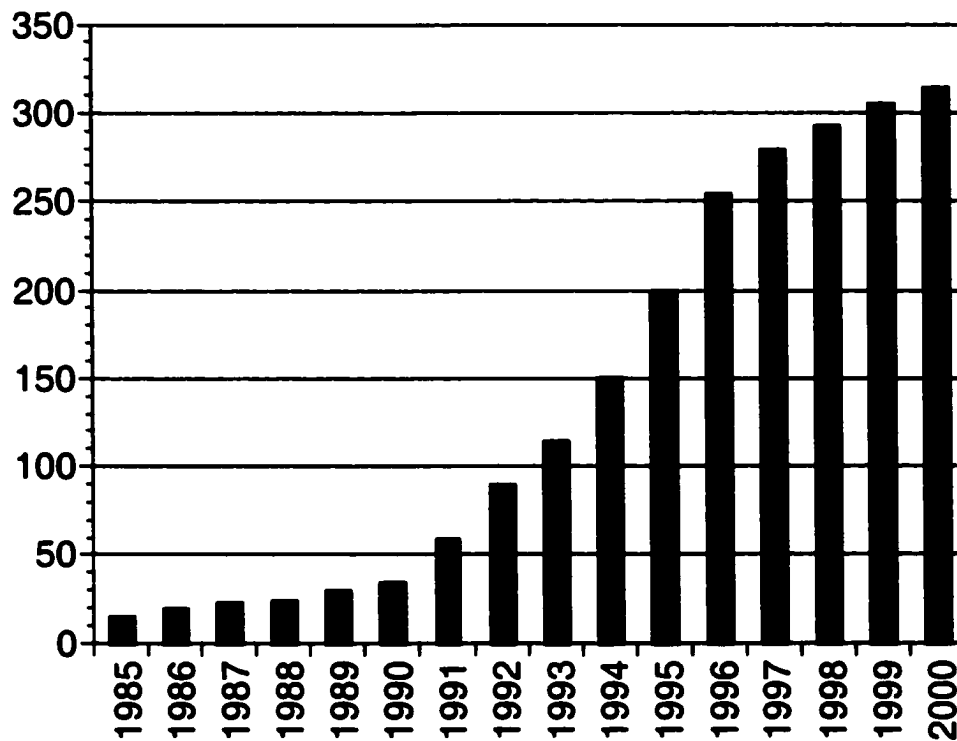


Figure 1-1 Growth in ozone applications in water treatment. The vertical axis shows the number of installed ozone facilities in drinking water treatment application in the United States from 1985 to 2000 (after Overbeck (2000)).

The new emphasis on ozone as the primary protection against resistant encysted protozoa has prompted a more detailed examination ozone contactor design. The fundamentals of the reaction between dissolved ozone and encysted protozoa has been intensively studied in laboratory reactors, and the understanding has improved considerably in the past several years. The designer of water treatment facilities must be able to extrapolate this fundamental knowledge to full-scale operation with some level of confidence and assurance of real world performance. In full-scale ozone contactors, however, additional factors come into play. Variables such as gas-liquid contacting and the complex hydrodynamic environment that exists in conventional ozone contactors may

impact the efficiency of protozoa reduction (Do-quang, 2000a, 2000b). The significance of these variables, however, is not fully understood.

#### **1.4 THESIS OBJECTIVE AND OVERVIEW**

The objective of this thesis was to explore the possibility of improving the hydrodynamic design of an ozone contactor and optimizing microorganism reduction through the use of an in-line static mixer for ozone dissolution. The potential impact of ozone contactor hydrodynamics on the efficiency of *C. parvum* reduction was examined using chemical reactor engineering principles. Based on this theoretical analysis and a review of the literature regarding the hydrodynamics of conventional ozone contactors, it was argued that a two-stage ozone contactor design may achieve more reliable microorganism reduction than conventional designs. The principal hypothesis was that, in such a design, the mass transfer process can be effectively separated from the microorganism reduction operation. This design approach will provide efficient and predictable reduction of microorganisms and will also simplify engineering analysis and process scale-up of the ozonation process.

The main body of the thesis describes an experimental program that was designed to rigorously test the two-stage contactor hypothesis. The core of the research involved measurement of microorganism reduction efficiency in an experimental static mixer ozone contactor under various operating conditions. In particular, the relationship between the hydrodynamic conditions of gas-liquid contact within the static mixer, ozone mass transfer efficiency and microorganism reduction was carefully examined. In order to determine to what extent the findings may be generalized, three microorganisms were studied. These were (1) spores of the aerobic bacteria *Bacillus subtilis* (2) encysted *C. parvum* oocysts and (3) encysted *G. lamblia*.

## 2 BACKGROUND AND LITERATURE REVIEW

### 2.1 TERMINOLOGY

The process of adding oxidant chemicals to control microorganisms in drinking water treatment has traditionally been referred to as “disinfection”. In water treatment, disinfection has been defined as “a process designed for the deliberate reduction of a number of pathogenic microorganisms” (Haas 1990). The term “disinfection”, however, means the complete elimination of human disease-causing microorganisms from the water. In this thesis the term “microorganism reduction” is used to refer to engineered processes in which the goal is to ensure the protection of public health by removal or destruction of all types of microorganisms, not only those that are known human pathogens. The latter term also recognizes explicitly that treatment processes will typically not render drinking water completely free of viable microorganisms but will reduce their number to acceptable levels.

Throughout this thesis, the term inactivation is used to characterize microorganism reduction by ozone. This term reflects that ozone, under most application conditions, does not physically remove or destroy microorganisms present in the water, but renders them non-infective. Used in this sense, inactivation is considered to represent just one of several microorganism reduction mechanisms. In water and wastewater treatment literature, the survival ratio is usually defined as  $N/N_0$  where  $N_0$  and  $N$  are the concentrations of infectious microorganisms in the water before and after a specific treatment. The inactivation ratio is defined as  $I = -\log_{10}(N/N_0)$  and is often represented in terms of base 10 log-units. For example, 99% inactivation was equivalent to 2 log-units and 99.9% inactivation was equivalent to 3 log-units. Unless otherwise noted, the term “log” referred to the base 10 logarithm.

## **2.2 ENCYSTED PROTOZOA IN DRINKING WATER**

### **2.2.1 *Cryptosporidium parvum* and *Giardia lamblia***

*Cryptosporidium* and *Giardia* are the genus names of two distinct groups of unicellular parasitic microorganisms, both members of the kingdom protozoa that are known to infect a variety of vertebrate animals. *C. parvum* and *G. lamblia* are the species that cause the gastrointestinal diseases in humans known as cryptosporidiosis and giardiasis, respectively. Discovery of organisms of the genus *Giardia* has been attributed to Antony van Leeuwenhoek (1632-1723), the inventor of the microscope, Clifford Dobell (1886-1949) and Vilem Lambl (1824-1895) (Meyer 1990a). It was not until 1954, when Rendtorff (1954) conducted experiments with human volunteers, that *Giardia spp.* organisms were discovered to cause illness in humans. *G. lamblia* is now recognized as a common intestinal parasite of humans with recognized pathological effects (Marshall et al. 1997; Meyer 1990a; Thompson and Reynoldson 1993). The first documented waterborne outbreak of giardiasis in North America occurred in 1965-66 and several other outbreaks of giardiasis have since been documented (Craun 1990).

E. E. Tyzzer first described the life cycle stages of *C. parvum* in the gut of laboratory mice in 1912 (Current and Garcia 1991). It was not until 1976, however, that the first cases of human cryptosporidiosis were reported (Nime et al. 1976) and not until 1985 that the first documented outbreak of human cryptosporidiosis traced to contamination of water supply was reported (D'Antonio et al. 1985). Since then, *C. parvum* has become one of the most important microbiological contaminants in drinking water treatment both in North America and other parts of the world in terms of its' prevalence in water sources and association with waterborne disease (Smith and Rose 1998).

### **2.2.2 Basic Biology**

Although both parasites are often discussed in the same breath in the water treatment industry, *Cryptosporidium* and *Giardia* species are biologically distinct and belong to different major groupings of protozoan parasites (Cox 1993). Species of the genus *Cryptosporidium* are members of the coccidian or sporozoan group, which are

characterized by a lack of means of locomotion within the host. The *C. parvum* life cycle is similar to that of other coccidian parasites and involves several development stages, including both asexual and sexual reproduction stages, that all occur within a single host. The infectious stage is the environmentally resistant sporulated oocyst that contains four motile sporozoites. Subsequent to oral ingestion of the oocyst by the host, the six major development life stages are (Current and Garcia 1991):

1. excystation, the release of infective sporozoites through a suture in the oocyst wall, invasion of the epithelial cells of the gastrointestinal tract and formation of trophozoites;
2. merogony, the asexual division within host epithelial cells;
3. gametogony, the formation of micro- and macro-gametes for sexual reproduction;
4. fertilization, the union of micro- and macro-gametes to form a zygote;
5. development of the zygote into an oocyst;
6. sporogony, formation of infective sporozoites within the oocyst wall.

From a public health perspective, two of the significant aspects of the lifecycle of *C. parvum* are (1) it is intracellular and (2) it involves autoinfective stages. Subsequent to invasion of host epithelial cells in step 1, developmental stages take place within a parasitophorous vacuole that forms within the host cells, but external to the cell cytoplasm. The parasitophorous vacuole protects the parasite from attack by the host immune system and may also provide some measure of protection from the effects of antimicrobial drugs. This helps to explain the difficulty in clearing the infection experienced by some individuals, and also why efforts to develop drug therapies to treat human cryptosporidiosis have been unsuccessful (Clark 1999). During merogony, (step 2) trophozoites form merozoites, which invade adjacent cells and produce more merozoites. In step 5, most of the zygotes form environmentally resistant oocysts, with a thick, two-layered wall that are passed into the environment with the feces. The infective cycle starts anew when oocysts are ingested by a new host. A smaller fraction of the zygotes are believed to form thin-walled oocysts, which later liberate their sporozoites within the gastrointestinal tract of the same host, re-invade the host cells and repeat the life cycle (Current and Garcia 1991). These two autoinfective stages contribute to the

severity of the illness and also result in excretion of large numbers of parasites by infected hosts.

Species of *Giardia* are members of the group of protozoan parasites known as the intestinal flagellates. Unlike *C. parvum*, the flagellates have relatively simple extracellular life cycles that consist of two stages with reproduction by asexual binary fission. The biology, life cycle and ultrastructure of *Giardia* spp. have been described in detailed reviews by Feely and co-workers (1990) and Thompson and Reynoldson (1993). In the infective stage, which takes place outside the host, the trophozoites are protected within an environmentally resistant cyst, typically with two trophozoites per cyst. The host stage commences when cysts enter the host by ingestion of fecally contaminated water or food. During excystation, the trophozoites emerge from the cysts in the host duodenum. The motile trophozoites then attach to the surface of the epithelial cell layer of the villi in the duodenum and jejunum, and undergo binary division in the intestine. As they pass through the colon, some of the trophozoites become encysted within a protective wall and are excreted in the feces as cysts to re-initiate the life cycle.

### **2.2.3 Species Identification**

The proper classification of the various species and strains of *Cryptosporidium* and *Giardia* that have been identified, and determination of host specificity, is a topic of ongoing research and controversy. Originally, over 40 species of *Giardia* were identified based on host occurrence (Thompson and Reynoldson 1993). Most authorities now prefer the species grouping proposed by Filice (1952), which describes three distinct morphologies of trophozoites. These are *G. muris*, which infects mice, *G. agilis*, which infects amphibians, and a human infective form that has been identified over the years as *Lambliia intestinalis*, *G. intestinalis*, *G. enterica*, *G. duodenalis* and *G. lamblia* (Meyer 1990b).

In addition to *C. parvum*, which is believed to infect both humans and other mammals, there are several other *Cryptosporidium* species that infect a diversity of both domestic and wild animals, including mammals, birds and fish. In his recent review, Fayer (1997) identified seven other species of *Cryptosporidium*, in addition to *C. parvum*, based on morphology and host specificity. These other species and the animals they are

associated with are *C. muris* (rodents and cattle), *C. meleagridis* (birds), *C. baileyi* (birds), *C. serpentis* (reptiles), *C. nasorum* (fish), *C. wrairi* (guinea pigs) and *C. felis* (cats). Some of these species have been known for sometime to causes health problems in farm animals that result in significant economic loss (de Graaf et al. 1999). Both *Cryptosporidium* and *Giardia* species are very common in dairy cows and especially calves (de Graaf et al. 1999; Garber et al. 1994; Xiao et al. 1993; Xiao and Herd 1994). For example the prevalance of *C. parvum* and *G. lamblia* in diary calves in British Columbia was found to be 59% and 73%, respectively, based on stool examination (Olson et al. 1997).

Although the details and epidemiological significance of zoonotic transmission are not completely understood, most authorities recognize that giardiasis and cryptosporidiosis may be transmitted to humans from various animals (Current and Garcia 1991; Thompson and Reynoldson 1993). The introduction of molecular biology techniques, such as DNA hybridization, has improved the ability of microbiologists to characterize the various parasite isolates on the basis of genetic composition. These techniques have exposed the existence of considerable genetic heterogeneity amongst *G. lamblia* and *C. parvum* isolates and indicate that a series of host-adapted genotypes, strains or species of the parasites may exist (Morgan et al. 1999; Thompson and Reynoldson 1993). A review of recent genetic studies supports the concept that there are at least two, and probably more, genetically distinct isolates of *C. parvum* species (Clark 1999). One genotype is host specific and infects humans exclusively. The other is a zoonotic that infects both animals and humans. At this point in time, it is not clear what the implications of this genetic diversity will be for the design of water treatment processes.

#### **2.2.4 Human Health Effects**

Both *C. parvum* and *G. lamblia* are transmitted to humans mainly by ingestion of food or water contaminated with infectious (oo)cysts. The potential for disease transmission is amplified by the relatively low oral doses that are required to cause infection in humans. In human volunteer experiments with *G. lamblia*, a dose of as low as 10 cysts per individual was sufficient to cause infection (Rendtorff 1954). A single

orally administered *G. muris* cyst was sufficient to cause infection in mice (Labatiuk et al. 1991). An oral dose of 30 *C. parvum* oocysts was found to be sufficient to cause infection in healthy adult humans (DuPont et al. 1995). In the same study, the median infective *C. parvum* dose (ID<sub>50</sub>) was determined to be 132 oocysts. Water treatment industry professionals must consider that parasite virulence may be much higher in immuno-compromised individuals or in children than is indicated by these experiments with healthy adult volunteers.

Cryptosporidiosis and giardiasis share clinical symptoms common to other other gastrointestinal illnesses. Giardiasis often manifests itself as acute diarrhea, with symptoms that might include nausea, anorexia, intestinal uneasiness, malaise and low-grade fever, or as a chronic illness. Symptoms appear after an incubation period of about 12 to 19 days and commonly resolve spontaneously. Compared to giardiasis, the gastrointestinal symptoms of cryptosporidiosis are more consistent and intense. The diarrhea is most often described as profuse, watery and “cholera-like” (Current and Garcia 1991). In healthy, immuno-competent individuals the disease is self-limiting and resolves in 3 to 12 days. However, in individuals with compromised immune systems, particularly those suffering from acquired immuno-deficiency syndrome (AIDS), the disease is chronic and may contribute to premature death (Current and Garcia 1991).

Cryptosporidiosis and giardiasis are widely distributed worldwide at an endemic level in both industrialized and developing countries. Prevalence of the diseases is most common in crowded urban areas of developing nations where sanitation is poorest. Based on inspections of stool, one study found that rate of infection of *C. parvum* in diarrhea cases was 2.2% in industrialized countries and 8.5% in developing countries (Crawford and Vermund 1988). According to another estimation, as many as 250 to 500 million infections may occur annually in Asia, Africa and Latin America (Current and Garcia 1991). *G. lamblia* remains the most frequently isolated intestinal parasite in the world and the most frequently identified etiologic agent in waterborne disease outbreaks (Marshall et al. 1997). The rates of giardiasis in clinical cases of acute diarrhea has been reported to range from 2 to 44% in developing countries, with a higher frequency among children (Islam 1990). Health consequences, such as retardation of growth and normal development retardation have been associated with high rates of giardiasis in children

(Thompson and Reynoldson 1993). Recent studies suggest that in developing countries cryptosporidiosis is common in children less than one year of age and contributes to malnutrition (Clark 1999). Health officials believe the incidence of infectious diseases, including cryptosporidiosis and giardiasis, is expanding both in North America and in the rest of the world (Marshall et al. 1997).

Several drug therapies have been used against giardiasis with varying degrees of clinical success, including quinacrine, metronidazole, furazolidone and paromomycin (Davidson 1990). Although the drug therapies are often effective against giardiasis, the drawbacks include adverse reactions and side effects, long dose regimes, poor palatability, cost and potential treatment failure (Thompson and Reynoldson 1993). There is still no effective cure for human cryptosporidiosis, although some progress has been made in the therapeutic treatment of immuno-compromised patients (Clark 1999). Provision of an uncontaminated drinking water supply, then, is still one of the best measures for control of cryptosporidiosis and giardiasis.

### **2.2.5 Oocysts and Cysts**

*C. parvum* oocysts and *G. lamblia* cysts are fully infectious when they are released with the feces of an infected animal or human. Only the environmentally resistant oocyst and cysts can survive outside the host, and therefore, it is these encysted forms that are of most interest and relevance to environmental engineers. In water, oocysts and cysts behave as microscopic particles. *C. parvum* oocysts are spherical and about 4 to 6  $\mu\text{m}$  in diameter. *G. lamblia* cysts are larger and more elliptical in shape, with dimensions of 8 to 12  $\mu\text{m}$  long by 7 to 10  $\mu\text{m}$  wide. Using column settling tests and a Monte Carlo analysis, oocysts and cysts freely suspended in clean water were found to settle according to Stoke's law with settling velocities of 0.35 and 1.4  $\mu\text{m/s}$ , respectively (Medema et al. 1998). Oocysts and cysts in natural aquatic habitats, therefore, will most likely remain suspended in the water column and be readily transported with the bulk water flow.

Electron microscopy has shown that the *C. parvum* oocyst wall is about 0.03 to 0.07  $\mu\text{m}$  thick and is composed of two distinct layers separated by a space (Reduker et al. 1985). The thin outer layer is decomposed by hypochlorite but the thicker inner layer is

resistant to the chemical. A suture in the oocyst wall dissolves during excystation and allows the motile sporozoites to emerge. A more recent electron microscopy study of the oocyst wall suggests a complex lattice structure of some unknown material that is reinforced by a layer of filamentous proteinaceous material on the inner surface (Harris and Petry 1999). The *Giardia* spp. cyst wall is about 0.3 to 0.5  $\mu\text{m}$  thick and is composed of a layer of proteinaceous fibers arranged in a felt-like web (Feely et al. 1990). Although the chemical composition and functioning of the cyst and oocyst walls are poorly understood, it is well established that both parasites, in their encysted forms, will retain their viability for extended periods (days to months) in a range of aquatic environments (Chauret et al. 1998; Fayer et al. 1998; Robertson et al. 1992; Wickramanayake et al. 1985).

### **2.2.6 Waterborne Disease**

The results of numerous surveys that have been carried out since the late 1980's show that both parasites are relatively widespread in surface waters (LeChevallier et al. 1991a; LeChevallier et al. 1991b; Ongerth 1989; Ongerth and Stibbs 1987; Roach et al. 1993; Rose et al. 1991a; Smith et al. 1993; Smith et al. 1995; Wallis et al. 1996). According to a recent review, *Cryptosporidium* spp. oocysts have been found in over 80% and 50% of untreated surface waters, and in 26% and 37% of treated drinking waters, in the United States (US) and the United Kingdom (UK), respectively (Smith and Rose 1998). It is not surprising that the Center for Disease Control in the United States reports that, of the 25 disease outbreaks associated with supplied drinking water that were reported 1993-94, and for which the etiologic agent was identified, 10 were caused by either *G. lamblia* or *C. parvum* (Kramer et al. 1996). A recent review lists 19 documented waterborne outbreaks of cryptosporidiosis that have occurred in the US, the UK and Japan (Smith and Rose 1998). The most notorious of these is the outbreak that occurred in 1993 in the City of Milwaukee, Wisconsin (US), and which may have affected as many as 403,000 persons (MacKenzie et al. 1994). An informal list of cryptosporidiosis outbreaks is maintained on the website of the Parasitology Laboratory at Kansas State University (<http://www.ksu.edu/parasitology/water>). Sixty-nine outbreaks are listed and the majority of these are associated with problems in the drinking

water supply. In the US, *G. lamblia* is still the most frequently identified etiologic agent in waterborne disease outbreaks (Marshall et al. 1997).

A review of 35 waterborne cryptosporidiosis outbreaks in the US and Canada revealed both filtered and unfiltered surface water supplies, and even groundwater systems, are vulnerable to this parasite (Craun et al. 1998). In most of these outbreaks, sources of contamination and treatment deficiencies were identified. However, cryptosporidiosis outbreaks have occurred in public water systems using conventional treatment processes that were in compliance with federal and local regulations at the time of the outbreak (Solo-Gabriele and Neumeister 1996). Craun noted that the available epidemiological information and the quality of monitoring information are insufficient to estimate the endemic risk of cryptosporidiosis from consumption of potable water (Craun et al. 1998). As an alternative, analytic risk assessment approaches that are based on information from human dose-response studies have been used to establish the acceptable levels of infectious *G. lamblia* cysts and *C. parvum* oocysts in drinking water and to determine water treatment requirements (Haas et al. 1996; Rose et al. 1991b). Based on an acceptable level of annual infection risk of 1 infection in 10,000 persons, the average reduction requirements for drinking water treatment plants in North America has been estimated to be 5.4 log-units for cysts and 4.5 log-units for oocysts (LeChevallier and Norton 1995).

### **2.2.7 Reduction of Oocysts and Cysts by Conventional Water Treatment Processes**

Laboratory-, pilot- and demonstration-scale studies have determined that well-designed and properly operated conventional water treatment processes will provide some measure of physical removal of *Giardia* spp. cysts and *Cryptosporidium* spp. oocysts. Both conventional and direct filtration processes, using anthracite coal and sand media, were demonstrated to be capable of greater than 2 log-units of cysts and oocysts reduction when coagulation was optimized (Nieminski et al. 1995; Ongerth and Pecoraro 1995; Patania et al. 1995). Non-conventional processes, such as slow sand filtration (Logsdon 1988), dissolved air flotation (Plummer et al. 1995) and diatomaceous earth filtration (Ongerth 1990; Schuler and Ghosh 1990; Schuler et al. 1991), have also been shown to be effective for reduction of cysts and oocysts. In small-scale testing,

ultrafiltration membrane filtration processes have demonstrated almost complete parasite removal (Jacangelo et al. 1995). Application of membrane processes, such as ultrafiltration, is currently limited to smaller communities with relatively clean water sources.

An additional barrier to physical treatment is required for protection of public health from the risk of encysted protozoa, especially when surface water is used as the source. The most common chemical agent used in North America for primary control of microorganisms in both filtered and unfiltered water supplies has been chlorine. The estimated treatment required, in terms of the concentration-time (*Ct*) product, for inactivation of various microorganisms by chlorine compounds is summarized in Table 2-1. The *Ct* products required for 2 log-unit inactivation *G. lamblia* cysts are much greater than those for vegetative bacteria or viruses, but are still within the realm of practical application in the water treatment. The same is not true for *C. parvum* oocysts. The *Ct* products for only 1 log-unit reduction of *C. parvum* oocysts by chlorine would require several hours of contact time even at relatively warm water temperatures. As indicated in Table 2-1 the *Ct* products required for *Giardia* spp. are much greater at lower temperature. Though the data are not yet available, the same trend can be expected for *C. parvum*. This has recently been confirmed experimentally (Li et al. 2001, Oppenheimer et al. 2000). The much greater resistance of the encysted protozoa to chlorination, together with the desire to reduce the formation of health-related chlorination by-products, has encouraged the consideration of alternative oxidant chemicals like chlorine dioxide and ozone.

### **2.2.8 Regulatory Requirements**

The emergence of encysted protozoa as a health problem in drinking water has greatly influenced the development of new drinking water regulations, particularly in the United States. In 1989, the United States Environmental Protection Agency (US EPA) introduced the Surface Water Treatment Rule (SWTR), the first regulation that dealt specifically with control of encysted protozoa (U.S. Environmental Protection Agency 1989). According to the SWTR, water treatment systems are required to provide treatment that is capable of ensuring 3 log-units reduction of *G. lamblia* cysts and 4 log-

Table 2-1 Comparison of inactivation of various microorganisms by chlorine compounds

Microorganism	Compound	Temp °C	pH	Ct for 2 log-units inactivation mg×min/L	Reference
<i>E. coli</i>	Free Cl <sub>2</sub>	23	7	0.014	Leahy et al. (1987)
		5	6.5	0.24	
Poliovirus (Mahoney)	Free Cl <sub>2</sub>	20	6	0.2	Leahy et al. (1987)
		5	6	1.01	
Coxsackievirus B5	Free Cl <sub>2</sub>	20	6	0.5 to 0.7	Leahy et al. (1987)
		5	6	1.25	
<i>Entamoeba histolytica</i> (cysts)	Free Cl <sub>2</sub>	27 - 30	7	20	Leahy et al. (1987)
<i>Naegleria</i> spp. (cysts)	Free Cl <sub>2</sub>	25	7.4	26 to 34	Langlais et al. (1990)
<i>Acanthamoeba</i> spp (cysts)	Free Cl <sub>2</sub>	25	7.4	> 81	Langlais et al. (1990)
<i>G. lamblia</i> (cysts)	Free Cl <sub>2</sub>	25	7	< 15	Leahy et al. (1987)
		5	7	90 to 170	
<i>G. muris</i> (cysts)	Free Cl <sub>2</sub>	25	7	45 to 26	Leahy et al. (1987)
		5	7	449 to 1010	
	NH <sub>2</sub> Cl	18	7	144 to 246	Hoff (1986)
		3	7	496	
<i>C. parvum</i> (oocysts)	Free Cl <sub>2</sub>	22	6	<sup>1</sup> 1700 to 4000	Gyürék et al. (1997) Korich et al. (1990)
		25	7	4800	
	NH <sub>2</sub> Cl	25	8	3300 to 7000	Gyürék et al. (1997) Korich et al. (1990)
		22	9 to 10	7200	

<sup>1</sup>Ct products for *C. parvum* are for 1 log-unit inactivation.

units reduction of viruses through a combination of physical and chemical treatment. New regulations are currently being developed by the US EPA specifically to address *C. parvum*. The Interim Enhanced Surface Water Treatment Rule (IESWTR), promulgated

in 1998, sets a maximum contaminant level goal of zero for *Cryptosporidium* species in drinking water and requires that a utility demonstrate 2 log-units removal of oocysts (U.S. Environmental Protection Agency 1998b).

Unlike the SWTR for *G. lamblia*, the IESWTR does not specify a set of chemical *Ct* requirements for *Cryptosporidium* spp. inactivation. Rather, the removal target is to be achieved through use of conventional or direct filtration operated under appropriate coagulant conditions and optimized to meet specific turbidity requirements. The US EPA has delayed setting *Ct* requirements for *Cryptosporidium* spp. for ozone due to the state of scientific uncertainty surrounding the various studies that have investigated the effects of ozone on the parasite (U.S. Environmental Protection Agency 1999). It is expected that this scientific uncertainty will be resolved in the near future and that *Ct* requirements for *C. parvum* will be established in the Long Term 2 Enhanced Surface Water Treatment (LT2ESWTR) Rule scheduled for promulgation in 2002.

At the same time that the above rules are setting requirements for removal or inactivation of encysted protozoa, a concurrent set of US EPA rules will address the potential human health concerns that are associated with the use of oxidant chemicals and their by-products. Chlorine reacts with organic compounds present in the source water to form trihalomethanes (THMs), haloacetic acids (HAAs) and other undesirable organic by-products (Tate and Fox Arnold 1990). While the specific human health effects of exposure to these individual compounds through drinking water remains uncertain, epidemiological studies and laboratory studies with mice have indicated an association between consumption of chlorinated water with increased incidences of various forms of cancer (Tate and Fox Arnold 1990). To address these potential human health concerns, the Stage 1 Disinfection/Disinfectant By-Product (D/DPB) Rule was promulgated by the US EPA in 1998. The rule sets maximum limits and goals for the concentrations of chlorine, chloramine, chlorine dioxide, THMs, HAAs, chlorite and bromate in drinking water (U.S. Environmental Protection Agency 1998a). In the future, water treatment processes will need to be more carefully selected, and more precisely designed and controlled in order to achieve the appropriate balance between protection from microbial contamination and the potential long-term chemical risks.

## **2.3 OZONE FOR REDUCTION OF ENCYSTED PROTOZOA**

### **2.3.1 The Use of Ozone in Water Treatment**

The development of ozone generator technology made possible the first large-scale installation of ozone for drinking water treatment in 1893 in the Netherlands. Installations in France, Germany and the United States soon followed with the primary intended purpose of bacterial reduction (Langlais et al. 1991). With the introduction of chlorination, a much less expensive alternative, interest in the use of ozone for bacterial reduction declined. Although France has continued to use ozone as the primary means of microorganism reduction until the present (Le Paulouë and Langlais 1999), application of ozone in water treatment in other parts of the world has been limited, until recently, to other recognized beneficial uses. These include reduction of taste and odour, oxidation and removal of iron and manganese, reduction of colour, control of algal growth and biofouling, enhancement of chemical coagulation, nitrification of ammonia, reduction of THM formation potential and oxidation of specific micropollutants (Glaze 1987; Singer 1990). Ozone can also be used to enhance biological removal of total organic carbon in combination with granular activated carbon beds, or can be coupled with ultraviolet light or hydrogen peroxide in advanced oxidation processes (AOPs) to destroy a range of organic micro-pollutants in water (Singer 1990).

In 1977, there were only five operating ozone installations in public drinking water systems in the United States, and most of these were originally designed for the purposes of taste and odour control or THM precursor removal (Glaze 1987). The new environmental regulations requiring protozoan removal and reduction of chlorination by-products have generated a marked increase in the use of ozone for water treatment in the United States. As of 1997, the number of ozone installations for water treatment in that country had grown to more than 200 (Rice 1999).

### **2.3.2 Ozone Solubility and Mass Transfer**

Ozone, molecular formula  $O_3$ , is an extremely reactive and unstable gas at ambient conditions. Consequently, the gas must be generated on site for immediate use. The conventional method for ozone generation for water and wastewater treatment is

from either dry air or oxygen in commercial corona discharge generators (Glaze 1987). The use of medium frequency corona discharge generators with oxygen as a feed gas is increasing due to better ozone yields and higher concentrations of ozone in the ozonized gas (Schulz and Prendeville 1993).

It is generally believed that to be effective against microorganisms, ozone gas must first be dissolved into the water to be treated (Langlais et al. 1991, Singer 1990). Electrical generation of ozone is expensive and the solubility of the gas in water is limited. Ozone dissolution efficiency is, therefore, one of the critical design aspects of any ozonation system. Consequently, both the equilibrium and kinetic aspects of ozone dissolution into water have been the subjects of considerable study and have been reviewed by several authors (Kuo and Yocum 1982; Langlais et al. 1991; Masschelein 1982a). The solubility of ozone in water is greater than that of oxygen and nitrogen, but less than that of carbon dioxide and chlorine (Masschelein 1982a). For the range of concentrations normally encountered in water treatment (less than 20 mg/L) ozone solubility obeys Henry's law, which states that the concentration of the dissolved gas is proportional to the partial pressure in the gas phase (Masschelein 1982a). The effect of water quality variables, such as temperature, pH, ionic strength and salt content, on the Henry's law constant for ozone is well documented (Langlais et al. 1991; Sotelo et al. 1989).

Lewis and Whitman two-film theory has frequently been used to describe and model the gas-liquid mass transfer of ozone in water and wastewater treatment (Kuo and Yocum 1982; Langlais et al. 1991; Masschelein 1982a). The molecular diffusivity of dissolved ozone in water is  $1.74 \times 10^{-9} \text{ m}^2/\text{s}$  at 20°C and, like diatomic oxygen, the overall rate of ozone transport is generally considered to be controlled by the rate of mass transfer within the liquid film (Langlais et al. 1991; Masschelein, 1982a). According to the two-film theory the local rate of ozone mass transfer into water,  $M$ , in mass per unit time can be described by:

$$M = k_L a (C^* - C) \quad \text{Equation 2-1}$$

where  $C$  and  $C^*$  are the concentrations of ozone in the bulk liquid and in equilibrium with the bulk gas, respectively,  $k_L$  is local liquid-film mass transfer coefficient, and  $a$  is the specific gas-liquid interfacial surface area.

Measurement of the specific interfacial surface areas,  $a$ , in many gas-liquid contacting systems is difficult. The bulked parameter  $k_L a$ , therefore, is usually used as the engineering design parameter to describe the mass transfer in a gas-liquid system. Langlais and co-workers (1991) have summarized  $k_L a$  correlations for various different types of ozone contacting systems including bubble-diffuser columns, mechanically stirred reactors and packed towers. Probably the best-studied type of ozone contacting system has been the vertical bubble-diffuser column. Several groups of researchers have applied two-film theory and estimates of  $k_L a$  to model pilot-scale ozone bubble-diffuser columns for various water and wastewater situations (Le Sauze et al. 1993; Mariñas et al. 1993; Roustan et al. 1987; Smith and Zhou 1994; Zhou et al. 1994). The understanding of the mass transfer in bubble-column systems has improved with direct measurement of bubble size and size distribution using sophisticated techniques, including a laser particle dynamics analyzer (Zhou and Smith 2000) and photographic techniques (Roustan et al. 1996). The presence of very fast reactions may also affect the rate of mass transfer and will tend to enhance the rate of mass transfer in ozone systems beyond that predicted by two-film theory (Mehta et al. 1989). For most water and wastewater situations, however, the disappearance of ozone is sufficiently slow that enhancement of the mass transfer process by chemical reaction will be insignificant and liquid side mass transfer resistance will dominate (Zhou et al. 1994).

### **2.3.3 Reaction and Decomposition of Aqueous Ozone**

Ozone has a standard electrode potential of 2.07 V and is one of strongest chemical oxidants known (Glaze 1990). The chemistry of ozone in aqueous solution is complex and the precise nature of the various reactions that ozone may participate in depends on the properties of and the compounds present in the specific water. The categories of ozonation reactions in water have been described as (Hoigné 1988):

1. direct reaction of molecular ozone with organic or inorganic substrates;
2. decomposition of ozone into a series of highly reactive secondary oxidants;
3. formation of additional secondary oxidants from ozone reacting with other solutes; and
4. subsequent reactions of these secondary oxidants with inorganic or organic substrate.

Although molecular ozone is a strong oxidant and is thermodynamically favoured to react with numerous substances, many of these reactions are extremely slow and are controlled by kinetics. Hoigné and associates (1983a; 1983b; 1985) studied the direct reaction of molecular ozone with a variety of organic and inorganic compounds and measured second-order rate constants that varied over several orders of magnitude. They determined that the reaction of molecular ozone with organic substrates is highly selective and that molecular ozone reacts mainly by electrophilic attack on electron dense sites of specific functional groups. The range of compounds with which molecular ozone reacts rapidly in water treatment situations is, therefore, limited and includes unsaturated aromatic and olefin compounds and simple amines. Compounds such as benzene react only very slowly, while saturated alkyl compounds do not react at all. Less is known about the end-products of the reaction between ozone and organic compounds, but lower molecular weight organic compounds such as aldehydes, ketones, acids and even polymers are formed (Hoigné 1988).

The rate and mechanism of ozone decomposition in water have been matters of considerable scientific inquiry and controversy. Grasso and Weber (1989) list 25 studies that have been published on the topic between 1913 and 1988. Two models for the auto-decomposition of ozone in pure water have been favoured in the literature; those postulated by Staehelin and Bader (1982) and by Tomiyasu and co-workers (1985). Both models propose a free-radical chain reaction process in which the chain is initiated by reaction of molecular ozone with hydroxyl ion,  $\text{OH}^-$ . Propagation proceeds through a series of reactions that generate several free-radical intermediate species, including  $\text{HO}_2$ ,  $\text{HO}_2^-$ ,  $\text{O}_3^-$ ,  $\text{O}_2^-$  and  $\text{OH}^\bullet$ . These free-radical intermediates react with molecular ozone to propagate the chain. The two reaction pathways differ in the mechanisms of hydroxide

initiation, and the presence and role of the various postulated intermediate species (Chelkowska et al. 1992).

Various kinetic models for the aqueous decomposition of ozone have been presented in the literature. Reported values for the apparent order of the decomposition reaction with respect to ozone concentration vary from 0 to 2 (Grasso and Weber 1989). Staehelin and Hoigné (1982) concluded that the rate of ozone decomposition in pure water is limited by reaction with hydroxide ion in the initiation step, and therefore, for a given pH, the decomposition of ozone in pure water should be first-order with respect to ozone. Tomiyasu and co-workers (1985) proposed the following expression that included both first- and second-order terms to describe the rate of disappearance of ozone in pure waters:

$$\frac{d[O_3]}{dt} = k_1[O_3][OH^-] + k_2[O_3]^2[OH^-] \quad \text{Equation 2-2}$$

In Equation 2-2,  $k_1$  and  $k_2$  are rate constants.

The presence of organic and inorganic impurities in natural waters, which may act as either promoters or inhibitors of ozone decomposition, complicates the deterministic investigations of ozone decomposition rates. It is fairly well established, however, that the rate of decomposition of molecular ozone in natural waters increases with pH and in the presence of hydrogen peroxide, and decreases in the presence scavenging agents such as carbonate or bicarbonate ions, alkyl groups and tertiary alcohols (Staehelin and Hoigné 1985). Humic compounds present in natural waters may act as either promoters or inhibitors of ozone decomposition, depending on the composition of other impurities in the water (Staehelin and Hoigné 1985). Yurteri and Gurol (1988) proposed a first-order rate expression to describe the disappearance of ozone in natural waters of the following form:

$$-\frac{d[O_3]}{dt} = w[O_3] \quad \text{Equation 2-3}$$

The reaction rate constant,  $w$ , is a function of the pH, the total organic carbon (TOC) and alkalinity of the water and given by:

$$\log w = B_0 + a \cdot pH + b \cdot \log(\text{TOC}) - c \cdot \log(\text{alkalinity}/10) \quad \text{Equation 2-4}$$

The parameters of this model were determined by fitting Equation 2-4 to the value of  $w$  measured in 96 synthetically prepared waters with different combinations of TOC, pH and alkalinity. When they tested it with various natural waters, Yurteri and Gurol found that the model they developed could predict  $w$  to within  $\pm 25\%$  of the measured value. The measured first-order rate constants in the 11 waters tests ranged from  $0.4 \text{ hr}^{-1}$  to  $20 \text{ hr}^{-1}$  at  $20^\circ\text{C}$ .

Hoigné and Bader (1994) proposed that, in most cases, ozone decomposition in natural waters is adequately approximated as a two-step process. Part of the ozone is consumed by instantaneous or very rapid reactions that occur within seconds of addition of the ozone to the water. Instantaneous ozone demand is followed by a much more gradual decomposition of ozone that can be approximated as a first-order process. The two parameters that characterize ozone decomposition, the instantaneous demand and slow decomposition half-life, are considered to be distinct and measurable characteristics of the water (Richard 1994; Roustan et al. 1998). Oke and Smith (1998), however, observed that a first-order decomposition assumption, while valid for clean water, provided a poor fit to the ozone decomposition profile measured in natural surface waters. They proposed a decomposition model in which the first-order rate constant,  $k_w$ , changes continuously as a function of the amount of ozone consumed by the reaction,  $\Delta[\text{O}_3]$ , as follows:

$$-\frac{d[\text{O}_3]}{dt} = k_w [\text{O}_3] \quad \text{Equation 2-5}$$

$$k_w = a + be^{-c[O_3]}$$

Equation 2-6

Although the model fit the observed ozone decomposition well, Oke and Smith were unable to correlate the ozone decomposition model parameters ( $a$ ,  $b$  and  $c$ ) to the measured water quality parameters.

Hoigné and Bader (1994) commented that because of the potential for synergistic effects, it is generally difficult to predict the rate of ozone decomposition based solely on analytical characterization of the water. Ozone reaction in water is also influenced by temperature (Morooka et al. 1979; Roth and Sullivan 1983). The Arrhenius activation energies for reaction between ozone and specific reactants are typically between of 35 to 50 kJ/mol. Nevertheless, it is difficult to predict the effect of temperature on the overall ozone decomposition rate in natural waters (Hoigné and Bader 1994). Clearly, then, direct measurement of ozone decomposition in natural water is preferred for the purposes of ozone facility design.

### **2.3.4 Health-Related By-Products**

One of the advantages of ozone over conventional chlorination is that it does not produce the same range of halogenated by-products. Reaction between ozone and organic contaminants present in the water, however, produces a unique set of by-products with uncertain health effects. These include, but are probably not limited to, aldehydes, organic peroxides, epoxides, ketones, carboxylic acids and other aliphatic and hydroxylated aromatic forms (Singer 1990). Ozonation of water containing bromide ion,  $Br^-$ , leads to the formation of the inorganic by-product bromate,  $BrO_3^-$  (Amy et al. 2000). Health concerns linked to consumption of bromate ion have led to the establishment of maximum allowable level of 10  $\mu\text{g/L}$  in potable water in the US (U.S. Environmental Protection Agency 1998a). In addition to economic considerations, by-product considerations provide an additional motive for rational and efficient design of ozone facilities.

### **2.3.5 Effect of Ozone on Microorganisms**

The efficacy of ozone against various types of microorganisms in water or wastewater has been demonstrated in numerous studies. For a summary see Table 2-2. Examples of the dissolved ozone *Ct* requirements for inactivation of various microorganisms are provided in Table 2-3. The biocidal effectiveness of ozone varies considerably with both type and species of microorganism. Viruses tend to be somewhat more resistant than vegetative bacteria, while encysted amoebas are considerably more resistant. Sensitivity to ozone of different species of human enteroviruses has been observed to vary by as much as a factor of forty (Roy et al. 1982b). In one comparative study, the relative resistance to ozone was determined for several species of microorganisms using identical ozone exposure protocols, and was determined to be (increasing order of resistance): poliovirus 1, *E. coli*, hepatitis A virus, *Legionella pneumophila* serogroup 6 and *Bacillus subtilis* spores (Herbold et al. 1989). When comparing the *Ct* products required for 2 log-unit inactivation by ozone (Table 2-3) with those for chlorine (Table 2-1) the much greater effectiveness of ozone for all types of microorganisms is evident.

Interpretation of the results of individual experimental studies of the effect of aqueous ozone on microorganisms is complicated by the instability and reactivity of ozone in aqueous solutions. For example, aqueous ozone is less stable at higher temperature. A given initial concentration of aqueous ozone will, therefore, tend to be less effective against microorganisms as the temperature is increased, all other things being equal. However, using appropriate experimental designs and data analysis methods, several researchers have demonstrated that the intrinsic rate of inactivation of viruses and bacteria by aqueous ozone increases with temperature according to an Arrhenius type dependence (Farooq et al. 1977b; Roy et al. 1981a). This increased biocidal effectiveness at higher temperatures tends to counterbalance the effect of decreased ozone stability. Similarly, the effect of pH on inactivation of bacteria by ozone has been shown to be minimal in the range of pH 5.7 to 10 in experiments where the ozone concentration was maintained constant (Farooq et al. 1977a). On the other hand, viruses were found to be more resistant to ozone at acidic pH than at neutral pH (Roy et al. 1981a).

**Table 2-2 Summary of reported experimental studies on inactivation of various types of microorganisms by ozone in water and wastewater.**

<b>Type of Microorganism</b>	<b>Study Citation</b>
<b>Viruses</b>	Botzenhart et al. (1993); Coin et al. (1967); Coin et al. (1964); Finch and Fairbairn (1991); Hall and Sobsey (1993); Herbold et al. (1989); Katzenelson et al. (1974); Katzenelson et al. (1979); Kim et al. (1980); Roy et al. (1981a); Roy et al. (1982a); Roy et al. (1982b); Sproul et al. (1982)
<b>Vegetative Bacteria</b>	Botzenhart et al. (1993); Broadwater et al. (1973); Burleson et al. (1975); Farooq et al. (1977a); Fetner and Ingols (1956); Finch et al. (1988); Gyürék and Finch (1998); Hamelin and Chung (1974); Harakeh and Butler (1984); Harakeh and Butler (1985); Herbold et al. (1989); Hunt and Mariñas (1999); Majumdar et al. (1973); Scott and Lesher (1963); Zhou and Smith (1994)
<b>Sporulated Bacteria</b>	Botzenhart et al. (1993); Broadwater et al. (1973); Choe (1998); Facile et al. (2000); Herbold et al. (1989)
<b>Yeast</b>	Farooq et al. (1977a)
<b>Amoeba</b>	Langlais et al. (1990)

In a conventional ozonation process (as opposed to a process in which ozone decomposition and formation of radical intermediates is intentionally promoted), molecular ozone, not the radical products of ozone reactions, is believed to be the chemical species primarily responsible for microorganism inactivation. From a

theoretical viewpoint, hydroxyl radicals are not expected to play a significant role as biocidal agents because they will likely be consumed by reaction with dissolved substrates before they have an opportunity to react with dispersed particles (Hoigné and Bader 1975). Within the microbial cell, hydroxyl radical activity is likely to be inhibited by the near-neutral pH and high bicarbonate concentration (Langlais et al. 1991). Experimental evidence tends to support the molecular ozone hypothesis. Conditions that favour increased hydroxyl radical formation, such as basic pH, UV light and addition of hydrogen peroxide did not enhance inactivation of bacteria or viruses beyond the effect of molecular ozone alone (Farooq et al. 1977b; Harakeh and Butler 1985; Wolfe et al. 1989a). Further, the presence of a bicarbonate radical scavenging agent appeared to improve rather than hinder inactivation of enteroviruses (Harakeh and Butler 1985). In another study, humic acid had a significant effect on the rate of ozone disappearance but had little effect on the reaction rate constant between ozone and *E. coli* cells (Hunt and Mariñas 1999). The authors concluded that this was evidence that molecular ozone, rather than radicals, was responsible for bacterial inactivation.

Table 2-3 The effect of ozone on various microorganisms – a comparison.

Microorganism	Temp. °C	pH	Ct for 2 log-unit inactivation mg×min /L	Reference
<i>E. coli</i>	5	6 to 7	0.02	Langlais et al. (1991)
<i>Poliovirus 1</i>	5	6 to 7	0.1 to 0.2	Langlais et al. (1991)
<i>Rotavirus</i>	5	6 to 7	0.006 to 0.06	Langlais et al. (1991)
<i>Naegleria gruberi</i> (cysts)	5		4.23	Langlais et al. (1991)
<i>Acanthamoeba</i> spp. (cysts)	25	7.4	1.0 to 1.12	Langlais et al. (1990)
<i>Naegleria</i> spp. (cysts)	25	7.4	0.3 to 0.70	Langlais et al. (1991)

Despite the many experimental studies that have been done with ozone (Table 2-2) there is little consensus on the mode of action of ozone on microorganisms. The chemical selectivity of molecular ozone results in very different rates of reaction with different cellular biomolecules. Polysaccharides, phospholipids and amine sugars react slowly, therefore, the chemical action of ozone on the cell surface and wall is expected to be weak (Langlais et al. 1991). Amino acids and nucleic acids react fairly rapidly, therefore, proteins in the cell membrane and nucleic acids within the cell are potential sites of ozone attack (Langlais et al. 1991). Conclusions from various experimental studies differ. The primary mode of action of ozone against viruses has been proposed to be damage to the capsid protein (Kim et al. 1980; Riesser et al. 1977; Sproul et al. 1982), direct damage to the nucleic acid within the capsid (Roy et al. 1981b), or a combination of both (Shinriki et al. 1988). Working with bacterial cells, one group of workers postulated that ozone does not permeate the cells, but rather attacks the bacterial cell surface, alters the cell membrane permeability and ultimately causes either lysis, or leakage of cell components (Scott and Lesher 1963). Others, in contrast, proposed that ozone permeates bacterial cell membranes and degrades the DNA, causing loss of viability (Hamelin and Chung 1974; Ishizaki et al. 1987). Most of the *E. coli* cells exposed to ozone were rendered non-viable before any noticeable structural changes were observed in the cells (Hunt and Mariñas 1999). This observation tends to support a hypothesis wherein ozone permeates the cell and the lethal effect is by damage to biochemical molecules or processes within the cell.

### **2.3.6 Kinetic Modeling of Microorganism Reduction by Ozone**

The rational design of ozone contactors for microorganism reduction requires an understanding of the inactivation kinetics of the microorganisms of interest. Harriet Chick (1908) proposed the notion that inactivation of microorganisms by chemical agents is a rate-governed process that is analogous to a bi-molecular chemical reaction where one reactant is some vital component bacterial protoplasm and the other is the chemical agent. In experiments with anthrax spores exposed to dissolved phenol, she found that the rate of spore disappearance could be described consistently by a first-order relationship of the following form:

$$-\frac{dN}{dt} = kN \quad \text{Equation 2-7}$$

where  $N$  is the number of surviving bacteria at a given time and  $k$  is a rate constant.

Chick noted that the rate was also function of the chemical concentration and, to account for this, Watson (1908) proposed the modified rate equation:

$$-\frac{dN}{dt} = kC^n N \quad \text{Equation 2-8}$$

In Equation 2-8,  $C$  is concentration of the chemical agent and the  $n$  is known as the coefficient of dilution. The value of  $n$  can also be thought of as the number of molecules required to react with one molecule of a vital component, such as a particular protein, of a single microorganism to cause a lethal effect. Integration of Equation 2-8 yields the generalized form of the pseudo first-order Chick-Watson rate law:

$$-\ln \frac{N}{N_0} = kC^n t \quad \text{Equation 2-9}$$

The more common base 10 logarithm form of the Chick-Watson rate law is:

$$-\log \frac{N}{N_0} = k' C^n t \quad \text{Equation 2-10}$$

In Equations 2-9 and 2-10,  $N_0$  is the initial number of live microorganisms and  $N$  the number of surviving microorganisms after at time,  $t$ . If  $n$  is set equal to unity, the level of

inactivation is proportional to the simple product of the oxidant concentration,  $C$ , and the contact time,  $t$ . Equation 2-10 is the basis for the use by the US EPA of the  $Ct$  product as the main criteria for design and performance analysis of microorganism reduction processes (Malcolm Pirnie Inc. and HDR Engineering Inc. 1991). The popularity of the  $Ct$  product approach is that it is relatively simple to understand and to use for design and regulatory purposes.

Microorganism inactivation has been described as a multi-step physical-chemical process that includes mixing of the chemical in the bulk fluid, transport from the bulk fluid to the surface of the microorganism, diffusion through the microorganism cell wall, migration within the microorganism, and reaction at the site of lethal effect (Haas 1981). The treatment of microorganism inactivation by a chemical agent as a simple bi-molecular reaction is, therefore, a simplification of a much more complex process. It is not surprising, then, that observed microorganism inactivation rate curves tend to deviate from the Chick-Watson rate law and often exhibit the non-linear behaviour illustrated in Figure 2-1. *Shoulder* behaviour occurs when the initial rate of inactivation is very low and results in an apparent lag between the addition of the chemical and the onset of measurable inactivation. Explanations for a *shoulder* include poor mixing or the requirement of diffusion of the chemical to the site of action. More mechanistic explanations are based on target theory and include the requirement for damage to a minimum number of vulnerable target sites (multi-target) or completion of a series of distinct damaging reactions (series-event) in order to cause death of a microorganism (Hiatt 1964; Wei and Chang 1975). *Tailing* behaviour is often observed in the survival curves of bacterial spores and viruses when the rate of inactivation decreases with extent of exposure and (Cerf 1977; Clark et al. 1994; Hiatt 1964). Explanations of *tailing* fall into two categories, the vitalistic and the mechanistic. In the vitalistic theory, resistance to the lethal agent differs between individuals in a heterogeneous population. Mechanistic explanations include a complex inactivation mechanism, adaptation of the individuals during the treatment, clumping of microorganisms, heterogeneity of treatment and error in enumeration of survivors (Cerf 1977).

Different types of kinetic behavior have been reported for reduction of bacteria and viruses by ozone. The existence of an apparent critical threshold ozone concentration

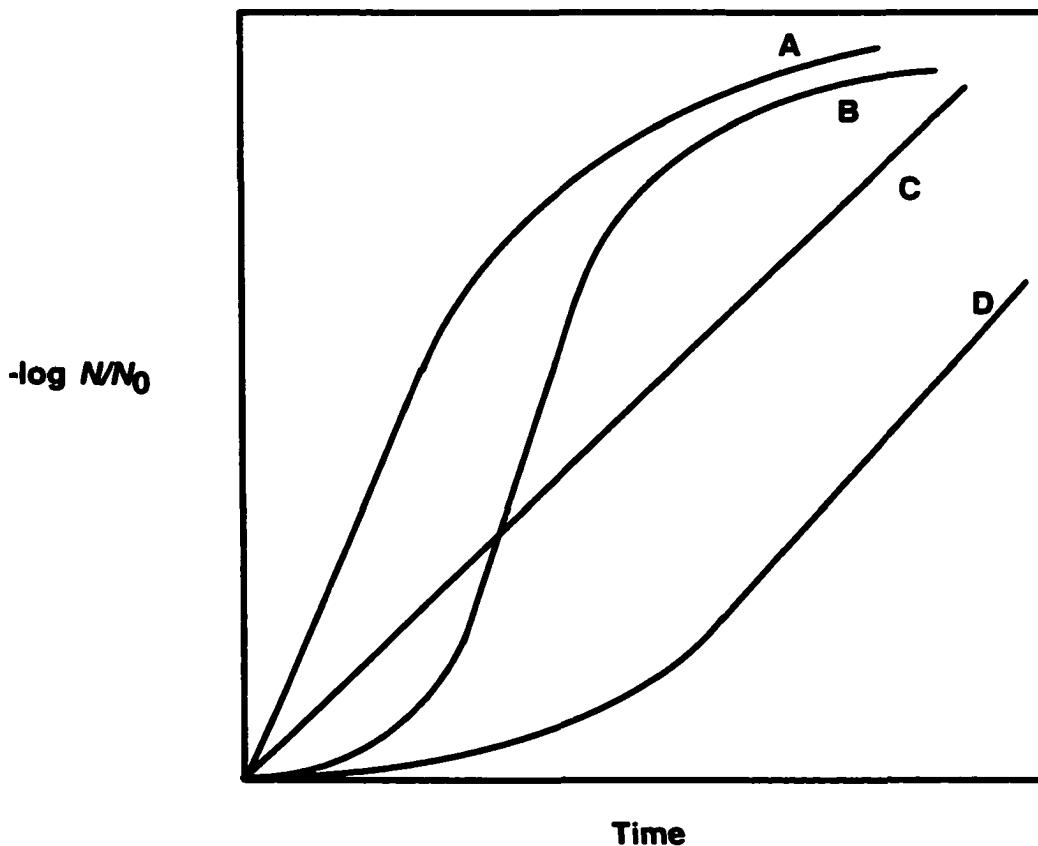


Figure 2-1 Possible forms of microorganism reduction inactivation curves

- A = presence of *tailing*
- B = presence of a *shoulder* and *tailing*
- C = adherence to Chick-Watson rate law
- D = presence of a *shoulder*

required for lethal effect is often observed. Some researchers have reported an “all or nothing” effect with both vegetative and sporulated bacteria, wherein inactivation was essentially complete above the threshold concentration (Broadwater et al. 1973). Others have reported Chick-Watson type inactivation kinetics above the threshold (Fetner and Ingols 1956; Hamelin and Chung 1974). The existence of two distinct Chick-Watson type kinetic regions, a region of low inactivation rate below the threshold and one with

higher inactivation above the threshold, has also been reported (Majumdar et al. 1973). In contrast, many other researchers did not observe a significant threshold but reported non-linear inactivation kinetic behaviour with a reduced inactivation rate at higher ozone exposures (Choe 1998; Farooq et al. 1977a; Finch et al. 1988; Gyürék and Finch 1998; Katzenelson et al. 1974; Katzenelson et al. 1979; Roy et al. 1982b; Zhou and Smith 1994). The use of ultrasound both before ozone exposure and during ozone exposure has been found to increase the rate of microorganism inactivation of both virus and vegetative bacteria (Burleson et al. 1975; Dahi 1976; Harakeh and Butler 1985; Katzenelson et al. 1974). Ultrasound may loosen or promote the break-up of aggregated microorganisms, thereby making the individual microorganisms in the aggregates more vulnerable to ozone. It is often not clear if the differences in reported kinetic behaviour represent the true differences in the response to ozone of the various microorganisms studied, or if they arise from differences in the experimental protocols used between the various studies.

Several alternative kinetic formulations have been proposed to describe non-linearities observed in experimental inactivation curves. Some of these are summarized in Table 2-4. Many of these, such as the multi-target, series-event and the Monod model, are based on a proposed reaction mechanism. Others, like the Hom and the rational model, are based solely on empirical observation. A few studies have rigorously compared different models using statistical techniques, but no one model has emerged as a universal solution for all situations. Based on computed regression correlation coefficients and standard errors, the Chick-Watson model was found to fit as well as the Hom and the Monod models for inactivation of coliform bacteria by chlorine in the case where the concentration of chlorine was constant (Haas and Karra 1984a). However, the Selleck model was preferred for the case in which chlorine demand and decomposition was significant (Haas and Karra 1984b). The Hom model was found to better represent inactivation of *G. lamblia* cysts by free chlorine than the Chick-Watson model when the two models were compared using the method of maximum likelihood (Haas and Heller 1990). Using non-linear regression and error-in-variables techniques, five models representing three basic phenomena were compared for the case of *E. coli* inactivation by ozone in a completely-mixed reactor (Zhou and Smith 1994). The more complex models

Table 2-4 Alternative kinetic models to describe reduction of microorganisms by chemical reagents.

Model	Formulation	System(s) Studied	Mechanistic Basis	Reference(s)
Chick-Watson	$-\frac{dN}{dt} = -k'NC^n$	anthrax spores and phenol	bimolecular reaction	Chick (1908; Watson (1908)
Hom	$-\frac{dN}{dt} = -k'NC^n t^{m-1}$	chlorination of coliform bacteria in wastewater	empirical modification of Chick-Watson	Hom (1972)
Rational	$-\frac{dN}{dt} = -k'N^x C^n$	ozonation of poliovirus in wastewater	empirical modification of Chick-Watson	Majumdar et al. (1973)
Gard	$-\frac{dS}{dt} = \frac{kS}{1+k'Cl}$	poliovirus and formaldehyde	decrease in permeability of spore viral coat	Gard (1957); Hiatt (1964)
Selleck	$-\frac{dS}{dt} = \frac{nC}{b} S^{\frac{n+1}{n}}$	chlorination of coliform in wastewater	none	Selleck et al. (1978)
Modified Gard	$-\frac{dS}{dt} = k_1 C^n S^{(1+k_1/k)}$	ozonation of <i>E. coli</i> in wastewater	empirical modification of Selleck model	Zhou and Smith (1994)
Monod	$\ln S = \frac{-k_2 C \beta}{C + K_D} \left[ t + \frac{e^{-k_1 t (C + K_D)} - 1}{k_1 (C + K_D)} \right]$	chlorination of poliovirus	2-step process with intermediate state of receptor sites bound with oxidant	(Haas 1980)
Multi-Target	$S = 1 - \left( 1 - e^{-kCl} \right)^{n_c}$	ultraviolet exposure of various microorganisms	finite number, $n_c$ , of discrete critical targets per organism	Kimball (1953); Severin et al. (1983)
Series-Event (Poisson)	$N = N_0 e^{-kCl} \sum_{i=1}^{l-1} \frac{(kCl)^i}{i!}$	ultraviolet exposure bacteria and virus, and chlorine inactivation of amoebic cysts	inactivation of microorganism requires series of $l$ first-order steps	Severin et al. (1983); Wei and Chang (1975)
Multi-Poisson	$N = \sum_{j=1}^n \left[ N_j^0 e^{-k_j t} \sum_{i=1}^{l-1} \frac{(k_j t)^i}{i!} \right]$	chlorine inactivation of amoebic cysts	$n$ types of microorganisms with different number of required steps	Wei and Chang (1975)

Notes:  $k, k', k_1, k_2, K_D, b, \beta, n, n_c, l, i, x,$  = parameters of the various models

provided only a marginally better fit to observations than the Chick-Watson model with a dilution coefficient of  $n = 3.3$ . Others found that, of several models tested, a Hom model modified to incorporate a first-order ozone disappearance term provided the best fit to heterotrophic plate count bacteria inactivation data (Gyürék and Finch 1998).

### **2.3.7 Effect of Ozone on *Giardia* spp.**

Laboratory studies that have been conducted to determine the effect of ozone on cysts of *Giardia* spp. are summarized in (Table 2-5). Wherever possible, an estimate of the ozone *Ct* product required for 2 log-units of cyst inactivation determined from the experimental results is included for each study. These *Ct* values provide an approximate basis for comparison of cyst sensitivity to ozone determined in the various studies. Wickramanayake and co-workers carried out the first set of studies using human source *G. lamblia* cysts and mouse source *G. muris* cysts suspended in phosphate buffered de-ionized water (Wickramanayake et al. 1984a; Wickramanayake et al. 1984b). The cysts were exposed to a constant ozone concentration by continuously dispersing ozonized gas through the suspension in a well-mixed semi-batch reactor. Using *in vitro* excystation as a measure of cyst viability, they found that the *Ct* products required for 2 log-units inactivation with ozone (Table 2-5) were approximately two orders of magnitude less than those reported previously for free chlorine (Table 2-1). The efficacy of ozone against the cysts was also found to be a function of both pH and temperature. At 7°C, significantly greater *Ct* products were required for equivalent cyst inactivation than at 25°C. The *Ct* products required for cyst inactivation at pH 5 and 7 were approximately double those required at pH 9. The authors also reported similar enhancement of inactivation at alkaline pH with *Naegleria gruberi* cysts. This pH sensitivity of protozoan cysts contrasts with what has been observed with bacteria (Farooq et al. 1977a) and leads to speculation that the pH may play a role in the permeability of the protozoan cyst wall.

Table 2-5 Summary of laboratory experimental studies on the effect of ozone on *Giardia* spp. cysts.

Study	Species	Viability Method	Water Matrix	Type of Reactor	Temp. °C	pH	Ct for 2 log-units inactivation mg×min/L	Reference
1	<i>G. lamblia</i>	<i>in vitro</i> excystation	buffered pure water	semi-batch	5	7	0.53	Wickramanayake et al. (1984a)
					25	7	0.17	
2	<i>G. muris</i>	<i>in vitro</i> excystation	buffered pure water	semi-batch	5	7	1.94	Wickramanayake et al. (1984b)
					25	7	0.27	
3	<i>G. muris</i>	<i>in vitro</i> excystation, flourogenic dye exclusion, and infectivity in mice	buffered pure water	batch	22	6.7	na	Labatiuk et al. (1991)
4	<i>G. muris</i>	infectivity in mice	various natural waters	batch	5 to 22	5.7 to 7.6	na	Labatiuk et al. (1992b)
5	<i>G. lamblia</i>	Infectivity in gerbils	buffered pure water	batch	22	6.9	< 1.0	Finch et al. (1994); Finch et al. (1993b); Labatiuk et al. (1992a)
	<i>G. muris</i>	infectivity in mice			22	6.7 to 7.6	0.1	

Notes: na = value not available from information provided.

Finch, Labatiuk and co-workers at University of Alberta conducted a series of studies in which *G. muris* and *G. lamblia* cysts were exposed to dissolved ozone and hydrogen peroxide in well-stirred batch reactors (Finch et al. 1993a; Finch et al. 1994; Labatiuk 1992; Labatiuk et al. 1992a; Labatiuk et al. 1992b; Labatiuk et al. 1994; Labatiuk et al. 1991). These researchers used infectivity in mice and gerbils to assess cyst viability following exposure to ozone, rather than the *in vitro* excystation method used by previous researchers. *G. muris* cyst infectivity was determined using a model in which the size of the infective inoculum was a function of the latent period of cyst shedding in the feces of adult male C3H/HeN mice (Labatiuk et al. 1991). *G. lamblia* cyst infectivity was determined using a mongolian gerbil model in which the number of gerbils positive for infection was related to the size of infective inoculum through a logit dose response (Finch et al. 1993b). Inactivation of both species was found to be a linear function of dissolve ozone *Ct* product up to approximately 2 or 3 log-units, but was a non-linear function of *Ct* above 3 log-units (Finch et al. 1993b). Even at the highest ozone exposures (*Ct* greater than 2 mg×min/L at 22°C), a small fraction of the cysts remained infectious. The Hom kinetic model (Haas and Joffe 1994; Hom 1972) was use to model the non-linear inactivation curve. The form of the kinetic model, which incorporated a first-order description of the rate of ozone disappearance in the batch reactor, was:

$$-\log \frac{N}{N_0} = k'_H C_0^n \int_0^t (\exp - k_d t)^n t^m dt \quad \text{Equation 2-11}$$

where  $k_d$  is the first-order rate of ozone decomposition measured for each trial. The equation was solved numerically and the values of the best-fit kinetic parameters, computed using maximum likelihood criteria, were  $k'_H = 1.04$ ,  $m = 0.84$  and  $n = 0.12$  (Finch et al. 1993b).

Direct comparison of the results of these two experimental studies is difficult because the ozone exposure conditions and the resulting inactivation levels were

different. Wickramanyake and co-workers studied ozone *Ct* products of less than 0.3 mg×min/L at 25°C and observed inactivation levels of less than 2.3 log-units (Wickramanayake et al. 1984a; Wickramanayake et al. 1984b). The Finch/Labatiuk group, in comparison, concentrated their effort on *Ct* products that were greater than 0.6 mg×min/L with resulting inactivation that was greater than 3 log-units (Finch et al. 1993b). Nevertheless, the estimated ozone *Ct* product required for 2 log-units inactivation obtained by extrapolating the results of the Finch/Labatiuk group are in the same range as those determined by Wickramanyake and co-workers.

*G. muris* cysts have been proposed as a useful model for *G. lamblia* for use in microorganism reduction experiments with chlorine (Leahy et al. 1987). The advantages of the murine form for use in experiments are: (1) the cysts are relatively easy to produce, (2) they do not infect humans, (3) they consistently exhibit a high rate of excystation *in vitro*, and (4) they are somewhat more resistant to chlorine than are *G. lamblia* cysts. Using *in vitro* excystation, Wickramanayake and co-workers (1984a; 1984b) found *G. muris* cysts to be about 2 to 4 times more resistant to ozone than *G. lamblia* cysts when compared on the basis of *Ct* requirements. Finch and co-workers (1993b), on the other hand, reported that the resistance of *G. muris* and *G. lamblia* to ozone was not significantly different when determined using infectivity assays in mice and the mongolian gerbil, respectively. The disparity in the findings of these two studies may be linked to differences in the viability assays used. In any event, *G. muris* is a useful, and perhaps conservative, model for *G. lamblia* in experimental studies with ozone.

The experimental evidence supports the hypothesis that molecular ozone is responsible for inactivation of *Giardia* spp. cysts in ozonation systems and radical decomposition products exert little influence. When compared on the basis of molecular ozone *Ct* product, cyst inactivation in reactors in which hydroxyl radicals were promoted by addition of hydrogen peroxide was equivalent to cyst inactivation in reactors in which hydroxyl radicals were inhibited by addition of carbonate ion (Labatiuk et al. 1994). The performance of the carbonate-stabilized system was considered superior because the lifetime of the added ozone was longer. In a pilot-scale study with natural surface water, the ozone *Ct* required for inactivation of *G. muris* was the same with or without addition of hydrogen peroxide (Wolfe et al. 1989b).

### **2.3.8 Effect of Ozone on *Cryptosporidium parvum***

Since 1989, there has been significant interest in the effects of ozone on *C. parvum* oocysts. As a consequence, the number of reported laboratory studies with ozone and *C. parvum*, summarized in Table 2-6, exceeds the number of similar studies with the *Giardia* spp. (Table 2-5). This reflects the current high profile of *C. parvum* as a human health concern in water treatment and the promise of ozone as a method for controlling this parasite. Synthesis of the results of the various studies in Table 2-6 is complicated by the diversity in the experimental protocols used and the range of ozonation conditions investigated. Important differences in protocols include the oocyst source host, the method used to measure the loss of oocyst viability, the water matrix used in experiments, and the type of reactor used for the ozone exposure. Other potentially important differences between studies that are not captured in Table 2-6 include the specific strain of oocysts used, the oocyst purification and storage methods, and the age of the oocysts. In addition the analytical method used to measure dissolved ozone, and the way in which the dissolved ozone  $Ct$  was calculated may affect comparisons between studies.

As a result, there is considerable variability in the  $Ct$  products required for 2 log-units oocyst inactivation reported in these studies. This variability creates a dilemma for those responsible for developing engineering design or performance criteria for ozonation systems. Nevertheless, it is clear that *C. parvum* is considerably more resistant to ozone than are most other microorganisms (Tables 2-3 and 2-5). Estimated  $Ct$  products for 2 log-unit inactivation of *C. parvum* are on the order of 10 to 20 times greater than for *Giardia* spp. While the earliest reported studies (Korich et al. 1990; Peeters et al. 1989; Perrine et al. 1990) demonstrated the potential of ozone, the range of experimental conditions was limited, the datasets were small and the infectivity analysis methods were not quantitative. The information from these studies was not sufficient to develop rigorous engineering design criteria for ozonation systems. The value of subsequent studies was often limited by the use of *in vitro* assays for determination of oocyst viability (Campbell et al. 1997; Parker et al. 1993; Ransome et al. 1993). (See discussion of viability methods in Section 2.3.9).

Table 2-6 Summary of laboratory experimental studies on the effect of ozone on *Cryptosporidium parvum* oocysts.

Study	Oocyst Source	Viability Method	Water Matrix	Type of Reactor	Temp. °C	pH	Ct for 2 log-units inactivation mg×min/L	Reference
1	Bovine	infectivity in neonatal Swiss OF1 mice	buffered laboratory water	batch	na	na	na	Peeters et al. (1989)
2	Bovine	infectivity in BALB/c Mice in-vitro excystation	buffered laboratory water	semi-batch	25 25	7 7	5 to 10 3.8	Korich et al. (1990)
3	Horses	infectivity in rats	distilled water	batch	20	6.9 to 7.1	2.6	Perrine et al. (1990)
4	Animal	<i>in vitro</i> excystation	borehole water	batch	10	7	> 19	Ransome et al. (1993)
5	Bovine	fluorogenic dyes (DAPI/PI)	na	batch semi-batch	5 20 5	na na na	> 50 10 to 12 > 0	Parker et al. (1993)
6	Human	In vitro excystation and DAPI/PI	na	batch	20		6 <sup>1</sup>	Campbell et al. (1997)
7	Bovine	neonatal CD-1 mouse	buffered laboratory water	batch	7 22	6.9 6.9	5.1 to 10.4 1.7 to 8.1	Finch et al. (1993a); Finch et al. (1994)
8	Bovine	neonatal CD-1 mouse	buffered laboratory water	batch	22	6 to 8	4.4 to 4.9	(Gyürék et al. 1999)

<sup>1</sup>An approximate value of Ct product was estimated from the information presented in the study.

Table 2-6 (Continued)

Study	Oocyst Source	Viability Method	Water Matrix	Type of Reactor	Temp. °C	pH	Ct for 2 log-unit inactivation mg×min/L	Reference
9	Bovine	neonatal CD-1 mouse	buffered laboratory water	batch	1 5 13 22	6 to 8	42 to 43 28 to 29 11.8 to 12.4 4.6 to 4.7	Finch and Li (1999); Li et al. (2001)
10	Bovine	in vitro excystation	buffered laboratory water	semi-batch	5 15 25	7	32.5 9.6 3.8	Rennecker et al. (1999)
11	Bovine	neonatal NMRI mice	buffered laboratory water	batch	20	7	2.5 to 4 <sup>1</sup>	de Traversay et al. (1999)
12	Human	SCID mice	de-ionized water	semi-batch	5 23	na	10 3	Kanjo et al. (2000)
13	Human	SCID mice	buffered laboratory water	semi-batch	20	7	<sup>1</sup> 3 to 6	Hirata et al. (2000)
14	Human	ATP	de-ionized water	batch	20	na	<sup>1</sup> 9	Somiya et al. (2000a); Somiya et al. (2000b)
15	Bovine	neonatal CD-1 mice	various natural waters	continuous stirred tank(s)	3 10 22	6.2 to 8.2	22 to 52 7.6 to 18 1.2 to 2.9	Oppenheimer et al. (2000)

<sup>1</sup>An approximate value of the Ct product was estimated from information presented in the study.

Perhaps the most comprehensive quantitative study and rigorous modeling effort of the effect of ozone on *C. parvum* oocysts was undertaken by Finch and co-workers at the University of Alberta (Finch et al. 1993a; Finch et al. 1994; Finch and Li 1999; Gyürék et al. 1999; Li et al. 2001). These researchers set out to carefully determine the inactivation kinetics of the *C. parvum*-ozone system using well-defined protocols and a quantitative mouse infectivity assay, and to use this information to develop engineering design and performance criteria. Others have pursued a similar course using a modified *in vitro* exystation method to assess oocyst viability, rather than infectivity (Rennecker et al. 1999). Recent studies using oocysts derived from human hosts are indicating a level of resistance to ozone that is comparable to that reported in the earlier studies that used bovine-derived oocysts (Hirata et al. 2000; Kanjo et al. 2000). A recently completed comprehensive study of oocyst inactivation in several natural surface waters suggests that the water matrix has little effect on the oocyst inactivation kinetics except at extreme values of water quality parameters (Oppenheimer et al. 2000).

In the University of Alberta study, highly purified oocysts were suspended in a matrix of ozone demand-free phosphate buffered ultra-pure water in order to minimize extraneous ozone reactions. A unique batch reactor system that provided continuous monitoring of the dissolved ozone system ensured complete information regarding exposure to dissolved ozone. Infectivity reduction was measured using a neonatal CD-1 mouse model and was interpreted quantitatively using a logistic oocyst dose-response model (Ernest et al. 1986; Finch et al. 1993c). Quality control was ensured by determining the infective properties of each batch of oocysts used in experimental trials in dose-response experiments. Using these rigorous protocols, a comprehensive dataset was compiled over the course of the study period that comprised 62 independent ozonation experiments at temperatures ranging from 1°C to 37°C and pH ranging from 6 to 8 (Li et al. 2001). Both first-order ( $n = 1$ ) Chick-Watson and non-linear Hom kinetic models were developed to describe oocyst inactivation. For both models, the time-variable ozone concentration was accounted for by assuming first-order disappearance as per Equation 2-11. The incomplete gamma function was used to obtain an analytical solution to the modified Hom model of Equation 2-11, thereby, increasing the robustness

of the model fit. The incomplete gamma formulation of the Hom model, first proposed by Hass and Joffe (1994), is given by:

$$-\log \frac{N}{N_0} = \frac{mk'_H C_0^n}{(nk_d)^m} \gamma(m, nk_d t) \quad \text{Equation 2-12}$$

where  $\gamma(m, nk_d t)$  is the incomplete gamma function. The model is valid when  $m > 0$  and  $nk_d t \geq 0$ .

To account for the temperature variation of oocyst sensitivity to ozone, the inactivation rate constant  $k'_H$  was expanded to incorporate an Arrhenius-type temperature dependence according to:

$$\frac{k'_{H,T}}{k'_{H,22}} = \theta^{T-22} \quad \text{Equation 2-13}$$

In Equation 2-13,  $k'_{H,22}$  is the value of the rate constant at 22°C, and  $k'_{H,T}$  is the value of the rate constant at temperature,  $T$ . The adequacy of the model was tested using non-linear regression with maximum likelihood criteria. Based on an analysis of the residuals and the value of variance parameter in the maximum likelihood function, the Hom model was found to be superior to the Chick-Watson model (Gyürék et al. 1999; Li et al. 2001). Best-fit values of the kinetic parameters for the Hom model with temperature correction were  $\theta = 1.080$ ,  $k'_{H,22} = 0.68$ ,  $n = 0.71$  and  $m = 0.73$  (Li et al. 2001). The values of the  $n$  and  $m$  parameters are less than unity but are close in value. This indicates both contact time and ozone concentration are equally important for *C. parvum* inactivation, but that there is tailing in the inactivation curve. Water pH was found to have little effect on the intrinsic oocyst inactivation kinetics, although it did affect the rate of ozone disappearance. This observation is consistent with the hypothesis that molecular ozone is the principle agent responsible for microorganism inactivation. Other researchers arrived

at the same conclusion after observing that addition of hydrogen peroxide did not enhance oocyst inactivation by ozone (de Traversay et al. 1999).

In contrast to the conclusion of the University of Alberta kinetic study, other researchers have reported that a first-order Chick-Watson model adequately described *C. parvum* oocyst inactivation by ozone (Oppenheimer et al. 2000; Rennecker et al. 1999). The reason for the discrepancy is not clear, although differences in the experiment reactor configurations may have been contributing factors. One of these research groups reported a distinct shoulder effect that may have been related to the use of *in vitro* excystation to determine infectivity reduction (Rennecker et al. 1999). The other research teams used infectivity in mice and did not observe a shoulder. Other researchers have also observed the dependence of oocyst inactivation on water temperature although the magnitude of this dependence has differed from study to study (Finch and Black 1994; Finch et al. 1993a; Kanjo et al. 2000; Li et al. 2001; Oppenheimer et al. 2000; Parker et al. 1993; Rennecker et al. 1999). Reported activation energies range from 51.7 kJ/mol to 102 kJ/mol. In comparison, the activation energies computed for *G. lamblia* and *G. muris* were 40 kJ/mol and 70 kJ/mol, respectively (Li et al. 2001).

### **2.3.9 Importance of the Method of Viability Determination**

A crucial aspect in any experimental study on the effect of chemical agents on encysted protozoa is the choice of the assay used to determine the viability of the (oo)cysts following ozone exposure. The summaries in Tables 2-5 and 2-6 indicate that a variety of different assays have been used. However, these different assays can be categorized into two main types; infectivity assays and *in vitro* assays. The principal advantage of the *in vitro* assays, like *in vitro* excystation and fluorogenic or vital dyes techniques is that, compared with animal infectivity, they are much easier, more rapid, and much less expensive to carry out. The disadvantage is that these techniques do not directly measure the ability of the parasite to cause infection in a host and may not necessarily be good indicators of the infectious potential of parasites exposed to environmental stresses.

*In vitro* excystation measures the ability of the parasite to emerge from the cyst, or to excyst, when exposed to test-tube conditions that simulate the gastrointestinal tract

of a warm-blooded host (Korich et al. 1990; Schaefer 1990; Woodmansee 1987). Parasites that excyst are considered to be alive and infectious while those that do not are considered to be dead. *In vitro* excystation has been the preferred method for determination of the effect of chlorine compounds on *Giardia* spp. cysts (Haas et al. 1998; Jarroll et al. 1981; Jarroll et al. 1980; Leahy et al. 1987; Rubin et al. 1989) and has been shown to correlate with animal infectivity in at least one study (Hoff et al. 1985). Labatiuk and co-workers (1991) compared *in vitro* excystation and a fluorescein diacetate-ethidium bromide dye assay to infectivity in mice for *G. muris* cysts exposed to ozone. They found that, while the fluorogenic dye assay significantly overestimated cyst infectivity in mice, *in vitro* excystation results were not significantly different than those generated using animal infectivity. On the other hand, Taghi-Kilani and co-workers (1996) found that *in vitro* excystation significantly underestimated *G. muris* inactivation by ozone, while two commercial nucleic acid stains provided a better correlation to infectivity.

Korich and co-workers (1990) reported that both animal infectivity and *in vitro* excystation indicated loss of viability of ozone exposed *C. parvum* oocysts, while the vital dyes fluorescein diacetate and propidium iodide were found to be unreliable indicators of loss of viability. Others have reported inconsistencies between vital dye, *in vitro* excystation or infectivity assays for determination of the effect of ozone on *C. parvum* oocysts and have recommended animal infectivity as the most reliable method (Black et al. 1996; Bukhari et al. 2000; Campbell et al. 1997). Examination of Table 2-6 shows that, in general, studies using *in vitro* assays tend to overestimate ozonation requirements for a given inactivation level when compared to studies using infectivity assays. In direct comparisons, several research groups have found that *in vitro* excystation overestimates the viability of oocysts exposed to ozone compared to animal infectivity (Bukhari et al. 2000; Hirata et al. 2000; Kanjo et al. 2000). On the other hand, Rennecker and others found that a modified *in vitro* excystation protocol gave more consistent results and better agreement with infectivity assays for ozone exposed oocysts (Rennecker et al. 1999). Recently, it has been shown that *C. parvum* oocysts that did not excyst *in vitro* were still able to cause infection in mice (Neumann et al. 2000). Conversely, both *in vitro* excystation and a commercial nucleic acid dye stain kit grossly

overestimated the infectivity of *G. muris* cysts and *C. parvum* oocysts exposed to ultraviolet light (Bukhari et al. 1999; Craik et al. 2000).

Therefore, *in vitro* assays, including excystation and vital stains, should be used with caution. For rigorous research work, animal infectivity assays are preferred whenever possible because they provide the best available measure of the ability of the parasite to cause illness in humans (Black et al. 1996; Bukhari et al. 2000; Labatiuk et al. 1991). An added advantage of infectivity assays is that they can potentially be used to measure inactivation ratios of greater than 3 log-units, while the practical limit of *in vitro* techniques is approximately 2 log-units (Labatiuk et al. 1991). *In vitro* infectivity assays based on cell culture techniques have now been developed for *C. parvum* (Di Giovanni et al. 1999; Rochelle et al. 1997; Slifko et al. 1997; Slifko et al. 1999). Application of these techniques, however, has been limited mostly to the problem of detecting live parasites in environmental water samples. As of yet, there are no reported studies in which cell culture assays have been tested for determination of the viability of ozone-exposed oocysts.

### **2.3.10 Scale-Up of Encysted Protozoa Inactivation by Ozone**

Limited studies have been conducted in either pilot-scale or larger water treatment facilities to determine the reduction of encysted protozoa by ozone. This is in part due to the expense and logistical difficulties in carrying out this type of work, and in part due to technical challenges in recovery and enumeration of parasites. Reliance on direct measurement of reduction of encysted protozoa naturally present in the source water of an operating water treatment facility as an indicator of the efficacy of full-scale ozone processes is not practical. One difficulty is that cysts and oocysts are typically not present in sufficient numbers in the source water to enable determination of inactivation by ozone to any significant extent (LeChevallier and Norton 1995). In addition, the analytical methods that have been used to measure the numbers of cysts and oocyst in the inlet and outlet of water treatment facilities do not measure the viability of the parasites (LeChevallier and Norton 1995; LeChevallier et al. 1995). In a test on a large pilot facility that consisted of pre-ozonation, coagulation, flocculation and direct filtration steps, removal of heterotrophic plate count bacteria was determined to be 1 to 2 log-

units higher with ozonation. Assessment of cysts and oocyst inactivation was not successful because they were only present in sufficient numbers to be counted in the filter backwash water (Nieminski and Bradford 1991).

The most common approach to assessing scale-up of microorganism reduction processes is to conduct challenge experiments on pilot-scale facilities wherein the feed is seeded with a concentrate parasite preparation. Wallis and co-workers (1990) seeded the feed to a continuous-flow pilot-scale (0.15 m diameter × 2 m tall) ozone bubble column with both *G. duodenalis* and *G. muris* cysts. Using *in vitro* excystation and infectivity in mice, they found the level inactivation to be proportional to the dissolved ozone *Ct* product. Based on examination of exposed cysts by transmission electron microscopy, the authors concluded that ozone compromised the integrity of the cyst wall, and resulted in degradation of the cytoplasmic elements of the cysts even when the wall and membrane appeared intact. In a bubble column of similar size, Wolfe, Scott and co-workers (Scott et al. 1992; Wolfe et al. 1989b) observed that dissolved ozone concentration, and not applied dose, turbidity or hydrogen peroxide addition, was the main factor that determined inactivation of seeded *G. muris* cysts.

Labatiuk (1992) found that inactivation of *G. muris* added to a semi-batch ozone contactor equipped with a Rushton turbine for dispersal of gaseous ozone was similar to that observed in batch experiments with dissolved ozone. Because it was done in a semi-batch system, this study was not a complete test of the scale-ability of batch experimental results to the continuous-flow systems that are typical of water treatment facilities. In a well-designed study, reduction of *Giardia muris* cysts, MS2 bacteriophage and *E. coli* in a pilot-scale ozone bubble column contactor was compared to inactivation based on a non-linear batch kinetic model (Haas et al. 1995; Haas et al. 1998). The variability in the measured microorganism reduction was 2 log-units or greater in repeat trials, therefore, interpretation of the results was difficult.

In a series of studies conducted by the United States Environmental Protection Agency, *C. parvum*, *C. muris* and *G. muris* were seeded into the feed water of a 0.15 m diameter × 2.65 m tall pilot-scale countercurrent flow bubble diffuser column (Miltner et al. 1997; Owens et al. 1994; Owens et al. 1995). Based on a mouse infectivity assay, the

*Ct* required for 2 log-units of inactivation of *C. parvum* oocysts was somewhat higher than *Ct* requirements measured in previous laboratory studies where infectivity was used (Table 2-6). The difference may have been due back-mixing in the contactor. A mechanistic model pilot was later developed to predict the levels of *C. parvum* inactivation observed in the US EPA pilot study (Tomiak et al. 1998). Ozone mass transfer was modeled using two-film theory with axial dispersion in the liquid phase, and *C. parvum* reduction by ozone was modeled using the pseudo first-order model of Rennecker and co-workers (1999). Model predictions were within about 1 log-unit of measured inactivation and the mismatch was attributed to analytical variation and imperfections in the hydrodynamic model. One potential problem in this comparison is that the model predictions were based on a kinetic model that used *in vitro* excystation to determine inactivation. Inactivation in the pilot study experiments was determined using a mouse infectivity assay.

A pilot-scale ozone contacting system that consisted of two 0.10 m diameter × 3.2 m tall columns arranged in series was subject to challenge tests with *C. parvum* oocysts (States et al. 2000). At the measured dissolved ozone *Ct* values, the authors reported dramatically lower oocyst inactivation (less than 0.5 log-units) in the pilot system than would be expected by extrapolation of laboratory results. The authors concluded that bench-scale results could not be reliably extrapolated to a flow system and attributed the poor performance of the contactor “poorer ozone contact”, though they did not elaborate on the precise meaning of this phrase.

Judging from these pilot-scale studies, there are good indications that the same concepts determined in laboratory studies, such as the importance of dissolved ozone *Ct* in determining the extent of inactivation, seem to apply to these larger-scale systems. However, the data set is sparse, is limited to mostly bubble-column systems and the outcomes have been mixed. In addition, there is some question as to how well bubble-systems represent the performance of the large diffuser basins that are typical of full-scale ozone contactors. The ability of design engineers to transfer the results from laboratory studies to full-scale continuous-flow treatment situations remains uncertain.

### **2.3.11 Use of Bacterial Spores as Models for Ozone Inactivation of Encysted Protozoa**

Traditional indicators of microbial water quality, like the total and fecal coliform bacteria, are not appropriate for determining the effectiveness of protozoan parasites reduction by ozone. Proposed alternative surrogate microorganisms for assessment of treatment processes include sporulated aerobic bacteria (Nieminski and Bellamy 1998; Rice et al. 1996; Toenniessen and Johnson 1970), sporulated sulphite-reducing anaerobes (Hijnen et al. 1997) and heterotrophic plate count bacteria (Nieminski and Bellamy 1998). The properties of an ideal model organism that can be used to evaluate ozonation processes include:

1. comparable resistance to ozone as *C. parvum*, with the same sensitivity to water quality variables like temperature and pH;
2. predictable ozone inactivation kinetics;
3. easy and inexpensive to produce in substantial titres;
4. easy and inexpensive to enumerate; and
5. non-pathogenic to humans.

Aerobic bacterial spores of *Bacillus* species have been shown to demonstrate considerable resistance to inactivation by ozone (Botzenhart et al. 1993; Broadwater et al. 1973; Choe 1998; Facile et al. 2000; Herbold et al. 1989; Owens et al. 2000). In batch reactors, cultured spores of *B. cereus* were found to have similar resistance to ozone as *C. parvum* oocysts (Finch and Choe 1999). However, *B. cereus* is an agent of food poisoning in humans (Goepfert et al. 1972) and is, therefore, not an ideal model organism. In pilot-trials, both indigenous aerobic spores and a pure strain of *B. subtilis* spores were found to be more than twice as resistant to ozone as were *C. parvum* oocysts (Owens et al. 2000) suggesting that these non-human pathogenic species of *Bacillus* might serve as good model organisms for ozonation processes.

The kinetics of inactivation of natural aerobic spores and a pure strain of *B. subtilis* spores by ozone were measured at 22°C and were modeled using a modified Hom equation (Facile et al. 2000). At the 2 log-unit level, resistance of the spores to ozone was found to be comparable to that reported for *C. parvum* oocysts in other work.

However, unlike *C. parvum*, the rate of spore inactivation was found to be a significant function of pH. Further, indigenous spores were found to be less resistant to ozone than were the cultured spores. The authors cautioned that the resistance to ozone might depend on the source of the spores. Others have also reported that the resistance of various species of aerobic spores to chemical agents may differ (Barbeau et al. 1999; Broadwater et al. 1973).

## **2.4 THE ROLE OF THE OZONE CONTACTOR IN MICROORGANISM REDUCTION**

### **2.4.1 General Design Considerations for Ozone Contactors**

The two main design goals of an ozone contacting system intended primarily for microorganism reduction are to dissolve the gaseous ozone efficiently, and to provide the appropriate conditions of dissolved ozone contact that will achieve the required reduction of the target microorganisms. Ozone dissolution is a mass transfer problem, aspects of which were discussed in Section 2.3.2. In order to effectively optimize the microorganism reduction function, the designer of an ozone contacting system must simultaneously consider:

1. the fundamental kinetics of microorganism inactivation by dissolved ozone;
2. the ozone demand of the water and the rate of ozone reaction and decomposition; and
3. the effect of fluid mixing and hydrodynamics.

The first two factors have been considered in previous sections. The third will now be addressed. Other factors that must also be considered as part of the overall facility design include feed gas-preparation, choice of ozone generation technology, process off-gas treatment, and process monitoring and control (Masschelein 1982a).

### **2.4.2 Chemical Engineering Concepts**

The same theoretical principles that have been developed by chemical engineers to describe the effect of mixing on the extent of conversion in chemical reactors can, and have been to some extent, applied to evaluate the impact of contactor hydrodynamics on

microorganism reduction in water treatment. The theoretical basis for describing the effects of fluid mixing and non-ideal flow on the conversion in chemical reactors is well established in the chemical engineering literature and excellent reviews are found in texts by Levenspiel (1972) and Nauman and Buffham (1983). In general, the conversion of a reactant in a homogeneous continuous-flow chemical reaction system is determined by the intrinsic reaction kinetics, the residence time distribution (RTD), and the degree of fluid segregation (Levenspiel 1972).

The two idealized flow patterns that are most often used to approximate real systems are the continuous-flow stirred tank reactor (CFSTR) and the plug flow reactor (PFR). Feed material entering an ideal CFSTR immediately disperses and mixes completely with the reactor contents. In a PFR, on the other hand, there is no back-mixing or dispersion. Feed entering the reactor moves from the inlet to the outlet in an orderly fashion, like a plug. For reactions with positive order, as are most microorganism reduction processes, the ideal PFR flow condition provides the highest possible conversion for a given hydraulic detention time (Levenspiel 1972). The flow pattern and, therefore, the conversion in real reactors is generally considered to lie somewhere between the two idealized extremes of the CFSTR and PFR, although it is possible for poorly mixed real reactors to display performance that is inferior to that of a CFSTR (Nauman and Buffham 1983).

Flow patterns in real reactors typically deviate from these two idealized flow concepts and may be characterized by stagnant zones, regions of bypass flow or short-circuiting, back-mixing or dispersion. It is often convenient to use the RTD to characterize the non-ideal flow pattern of a real reactor. Using the nomenclature of Levenspiel (1972), the RTD can be described by the age distribution of fluid leaving a reaction vessel,  $E(t)$ . The advantage of the RTD concept in practice is that  $E(t)$  can be readily determined for real reactor vessels, or contacting basins in water treatment plants, through pulse- or step-input tracer tests. Alternatively, the flow pattern can be modeled using conceptual mixing models. The most popular model used to describe non-ideal mixing in both chlorine contacting basins and ozone contactors has been the CFSTR-in-series model (Bellamy 1995; Do-Quang et al. 2000b; Lawler and Singer 1993; Lev and Regli 1992b; Reddy et al. 1997; Roustan et al. 1993; Roustan et al. 1996). In this model,

the contactor is considered to behave as a series of  $J$  ideal CFSTRs. The single model parameter,  $J$ , describes the deviation from ideal mixing conditions. When  $J = 1$ , the reactor behaves as an ideal CFSTR. As  $J$  increases the residence time distribution and the conversion approaches that of an ideal PFR. Other models that have been used to model the hydrodynamics in ozone contactors include the axial dispersion model (Bellamy 1995; Le Sauze et al. 1993; Mariñas et al. 1993; Reddy et al. 1997; Zhou et al. 1994) and the back-flow mixed cell model (Smith and Zhou 1994; Zhou et al. 1994).

In addition to the residence time distribution, which describes the macro-mixing pattern in the reactor, conversion may also depend on the degree of segregation or micro-mixing of the fluid. At one extreme, the fluid is said to be perfectly micro-mixed. As the fluid flows through the reactor, there is complete exchange of material at the scale of the individual molecules or particles. This condition is generally associated with a high degree of turbulent mixing. At the other extreme, there is no mixing at the molecular scale. The fluid behaves as a series of discrete clumps, or agglomerates, as it flows through the reactor from inlet to outlet. In this case, the fluid is considered fully segregated. In real reactors, the fluid is likely to be in a partially segregated state, and is neither perfectly micro-mixed nor fully segregated. It should be noted here that the micro-mixing and segregation are distinct from the macro-mixing pattern described the residence time distribution. Reactors with identical residence time patterns may have very different levels of micro-mixing (Levenspiel 1972).

If the flow is completely segregated, overall conversion can be calculated by integrating the exit age distribution with the conversion expected in a batch reactor operating at the same feed conditions. Mathematically, this is given by (Levenspiel 1972):

$$\frac{C}{C_0} = \int_0^{\infty} \left( \frac{C}{C_0} \right)_{batch} E(t) dt \quad \text{Equation 2-14}$$

where  $C_0$  and  $C$  are, respectively, the concentrations of reactant at the inlet or outlet of the flow reactor or at the beginning and end of the batch reaction time. Equation 2-14, therefore, represents a very simple way of combining information from laboratory batch reactors with a directly measurable flow characteristic in order to predict conversion in a larger flow system. In water and wastewater treatment, the term “segregated flow analysis” has been used to describe the analysis of Equation 2-14 (Haas 1988; Haas et al. 1995; Haas et al. 1998; Lawler and Singer 1993; Lev and Regli 1992b; Trussell and Chao 1977).

Segregated flow analysis yields exact conversion when the reaction kinetics are uni-molecular first-order, or for any kinetics when the flow is indeed completely segregated. To investigate the effect of deviations from the segregated flow assumption on conversion, Zwietering (1959) introduced the concept of maximum mixedness. He presented a differential equation that describes conversion in a reactor in which the fluid was perfectly micro-mixed at all locations, and for any reaction kinetics and residence time distribution. The degree of fluid segregation becomes important for conditions of very high conversion, non-linear kinetics and deviations from plug flow. For positive-order reactions, conversion will be highest in the completely segregated flow reactor and lowest in the perfectly micro-mixed reactor, and will lie somewhere between the two fluid mixing extremes for intermediate levels of segregation. Unfortunately, Zwietering presented analytical solutions for only a few relatively simple cases, such as first-order uni-molecular reactions. Mechanistic models have been proposed to describe conversion for intermediate degrees of segregation, however, these are largely theoretical and of limited practical value (Nauman and Buffham 1983). Mixing models such as the CFSTR-in-series or the axial dispersion model incorporate an intrinsic level of segregation and, therefore, conversion based on these models will lie between the extremes of complete segregation and maximum mixedness (Nauman and Buffham 1983).

The segregation number has been proposed as a measure of the degree of fluid segregation in a reactor. The segregation number,  $S_g$ , is related to the molecular diffusivity of the reactants,  $\mathcal{D}$ , the mixing time-scale,  $\bar{t}$ , and minimum turbulent eddy size

determined from Kolmogoroff mixing theory.  $S_g$  can be estimated from the following equation:

$$S_g = \frac{\mu^{3/2}}{4\pi^2 \rho^{3/2} e^{1/2} D \bar{t}} \quad \text{Equation 2-15}$$

where  $\rho$  and  $\mu$  are the density and viscosity of the water, respectively, and  $e$  is the energy dissipation rate. For a second-order reaction, the fluid segregation was shown to have an observable effect on conversion for  $S_g > 0.1$  and to become important when  $S_g > 1$ .

### 2.4.3 Impact of Mixing on Microorganism Reduction

Microorganism reduction processes are vulnerable to the effects of both the residence time distribution and the degree of segregation because inactivation kinetics are generally not first-order, the hydrodynamics of contactors usually diverge from plug flow, and the target conversion efficiencies are often very high, typically exceeding 99%. A few theoretical studies have investigated the potential effect of contactor mixing on the efficiency of microorganism reduction in chlorine contactors by combining chemical reaction engineering principles with microbe inactivation kinetics. Trussell and Chao (1977) used fully segregated flow analysis to demonstrate the potential effects of dispersion and back-mixing in a chlorine contactor on coliform reduction. Haas (1988) compared reduction of *Escherichia coli* in a hypothetical chlorine contactor assuming complete segregation, partial segregation and perfect micro-mixing. He used the procedure of Zwietering (1959) to model the micro-mixed case and a CFSTR-in-series model to represent partial segregation. The effects of the residence time distribution and micro-mixing on *E. coli* reduction were most pronounced at the highest inactivation levels. Reduction in a perfectly micro-mixed contactor was up to 2 log-units less than in a segregated flow contactor when the inactivation level was 5 to 6 log-units. Using a CFSTR-in-series mixing model to represent partial segregation, Lawler and Singer (1993) calculated greater inactivation of *G. lamblia* in a completely segregated chlorine contactor compared to a partially segregated contactor. With a macro-mixing condition

equal to 10 CFSTRs in series, predicted microorganism reduction was 4.1 log-units with complete segregation versus 3.6 log-units with partial segregation. Both Lawler and Singer (1993) and Haas (1988) noted that the fluid in chlorine contactors in drinking water treatment is likely to be closer to a micro-mixed state than a completely segregated state.

#### **2.4.4 Types of Ozone Contactors**

In their review of ozone engineering applications, Langlais and co-authors (1991) list a number of different technologies that have been employed to dissolved ozone into water or a waster water treatment. These include:

1. conventional fine bubble diffusion;
2. turbine mixers;
3. injectors and static mixers;
4. packed columns;
5. spray chambers;
6. deep U-tube;
7. sweeping porous plate diffuser contactor; and
8. submerged static radial turbine contactor.

Of these, the conventional fine bubble diffuser (FBD) is the most commonly employed ozone dissolution technique both in Europe and the United States (Langlais et al. 1991). A typical FBD contactor is illustrated in Figure 2-2. The contactor consists of a rectangular basin that is sub-divided into a series of chambers by walls or baffles. The water flows through the contactor in an up-and-over pattern. In one or more of the chambers, ozonized gas is dispersed into the water at the bottom through an array of porous diffusers, and off-gas is collected above the water level. The total number of chambers, the number of chambers to which ozone is added, and the arrangement of baffles varies between installations. Advantages of the FBD, as noted by Langlais and co-authors (1991), are that it is established and familiar technology, the ozone transfer efficiency is usually greater than 90%, there are no moving parts and hydraulic head loss is low. Disadvantages include the requirement for deep contact basins in order to achieve

good ozone transfer, clogging of diffusers and the possibility of vertical channeling of the bubbles.

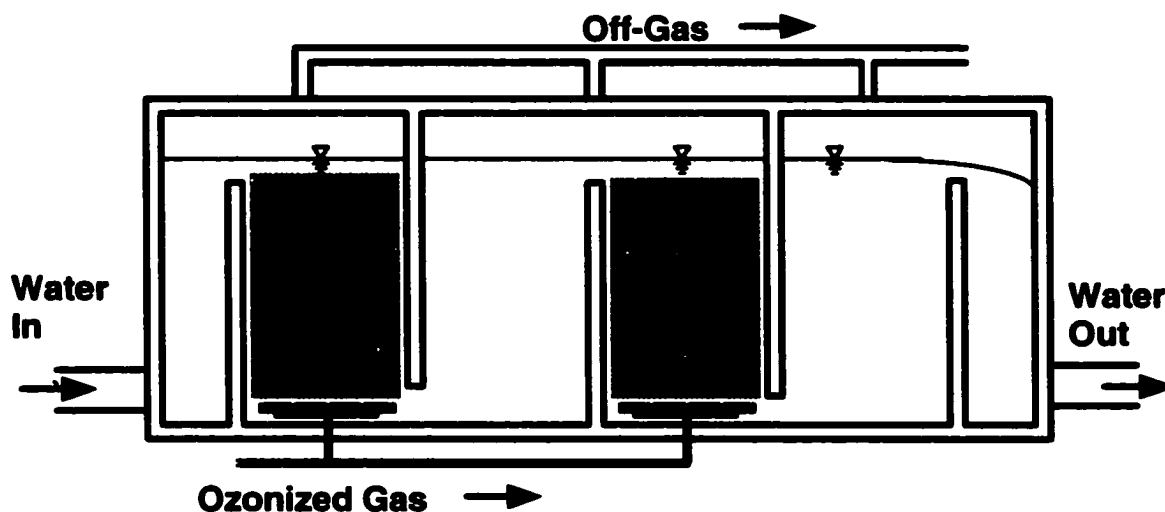


Figure 2-2 Depiction of a typical conventional multi-chamber fine bubble diffuser (FBD) ozone contactor consisting of four chambers with ozone addition to the first and third chamber.

#### 2.4.5 Criteria for Ozone Contactor Design

Design of ozone systems for water treatment has lacked a rigorous scientific and engineering basis and has been based largely on previous experience and empirical “rules-of-thumb”. In France the historical “rule-of-thumb” was to maintain a minimum ozone concentration of 0.4 mg/L for 4 min (Langlais et al. 1991) because this exposure was found to be sufficient to inactivate poliovirus under ideal laboratory conditions (Coin et al. 1964). To account for potential effects of hydraulic short-circuiting, the hydraulic detention time of full-scale contactors was typically increased to 10 to 12 minutes (Langlais et al. 1991). In the United States formal design criteria for ozonation systems in water treatment were introduced with the 1989 US EPA Surface Water Treatment Rule in the form of  $Ct$  requirements for inactivation of bacteria, viruses and *Giardia* spp. cysts

(U.S. Environmental Protection Agency 1989). The USEPA  $Ct$  requirements for reduction of cysts by ozone were based on the results of laboratory studies (Malcolm Pirnie Inc. and HDR Engineering Inc. 1991). Conventional FBD ozone contactors, however, are much more complicated physical systems than are laboratory reactors. Gas-liquid mass transfer, ozone demand and decomposition reactions, and microorganism reduction all take place in the same continuous-flow vessel. A complicated two-phase hydrodynamic flow pattern and a distribution of residence times add to the physical complexity.

Given these complexities, the following question is raised: What values of  $C$  and  $t$  should be used in the determination of  $Ct$  for full-scale ozone contactors in order to ensure target microorganism reduction? To account for non-ideal macro-mixing patterns in full-scale ozone contactors, the guidance manual to the SWTR recommends the use of the  $t_{10}$  as the time variable rather than either the theoretical residence time,  $\tau$ , or the measured mean residence time,  $t_m$  (Malcolm Pirnie Inc. and HDR Engineering Inc. 1991). The  $t_{10}$  is the time required for 10% of the total amount of tracer added to influent stream of a contactor in a pulse tracer experiment to exit the contactor in the effluent stream. For an ideal plug flow contactor, all of the tracer molecules exit the contactor at the exactly the same time, the theoretical residence time,  $\tau$ , and the value of the ratio of  $t_{10}/\tau$  is unity. The mixing patterns in real ozone contactors inevitably deviate from plug flow and the measured  $t_{10}$  values are often considerably less than  $\tau$ . The use of the  $t_{10}$  derived from tracer experiments is intended as a conservative safety measure, and one that is simple to understand and is easy to use by water utilities.

Although selection of  $t_{10}$  as the characteristic time appears somewhat arbitrary and empirical, it was based on a theoretical analysis conducted by Lev and Regli (1992b). In their analysis, Lev and Regli used a CFSTR-in-series mixing model with segregated flow analysis, and made the simplifying assumptions of constant ozone concentration and first-order microorganism inactivation kinetics. They concluded that the  $t_{10}$  will provide an adequate safety margin provided that the target inactivation levels are not too high or that the deviations from plug flow are not too large. A similar theoretical approach was used to generate guidelines for selecting the characteristic concentration,  $C$  (Lev and Regli 1992a). Requirement of the use of the  $t_{10}$  as the characteristic time has been

criticized as too conservative a measure for chlorine contacting facilities (Lawler and Singer 1993). Others have argued that the  $Ct$  design process of the US EPA does not capture the complex interrelationships between contactor hydrodynamics and the spatial and temporal distribution of ozone within full-scale ozone contactors (Bellamy 1995).

The American Water Works Association Research Foundation (AWWARF) sponsored a project to develop alternatives to the  $Ct$  method that would enable more accurate site-specific determination of microorganism reduction requirements. The integrated disinfection design framework, or IDDF emerged from that effort (Bellamy et al. 2000; Bellamy et al. 1997). The IDDF adopted reaction engineering methods that were used by others to analyze the effect of mixing on microorganism reduction, and formalized these into a calculation procedure that integrated oxidant demand and decomposition, microorganisms reduction kinetics and contactor hydrodynamics determined from tracer tests. The IDDF is directed toward analysis of existing facilities rather than design of new facilities.

#### **2.4.6 Studies of Ozone Contactor Hydrodynamics**

Since the introduction of the US EPA SWTR requirements, a number of engineering studies have appeared in the literature describing the hydrodynamics of ozone contactors in operation at water treatment facilities. The majority of the published studies have been with FBD contactors (Henry and Freeman 1995; Martin et al. 1992; Martin et al. 1995; Reddy et al. 1997; Roustan et al. 1993). Tracer tests on several full-scale FBD contactors have revealed that there is usually considerable divergence from perfect plug flow in these contactors. Reported values of the  $t_{10}/\tau$  ratio, an approximate measure of the approach to perfect plug flow and the hydrodynamic efficiency, have ranged from approximately 0.40 to 0.70 (Bellamy 1995; Do-Quang et al. 2000a; Martin et al. 1995). In one study that surveyed 12 full-scale FBD contactors in the United Kingdom and France, the  $t_{10}/\tau$  ranged from 0.41 to 0.67 and the number of CFSTRs that best described the measured residence time distribution was between 4 and 7 (Do-Quang et al. 2000a).

In response to the US EPA SWTR requirements for microorganism reduction, engineers have attempted to increase the  $t_{10}/\tau$  ratio of FBD contactors by installing more

baffles or by making other modifications. As the number of baffles and chambers are increased in an FBD contactor, the flow regime and residence time distribution will tend to better approach that of perfect plug flow. In a pilot-scale study, the  $t_{10}/\tau$  ratio was found to improve considerably when the number of baffles and chambers was increased (Do-Quang et al. 2000a). Newer contactors, designed primarily for microorganism reduction, have been built with as many as six chambers in order to improve the hydrodynamic efficiency (Coffey and Gramith 1994; Reddy et al. 1997). However, as noted by Langlais and co-authors (1991), there are practical limits to the number of chambers. Other modifications, other than baffle installation, may also yield improvements. By appropriate adjustments to the height and spacing of the baffles in a 1/5 size prototype of a 5-chamber design, the  $t_{10}/\tau$  ratio improved from 0.5 to 0.67 (Heathcote and Drage 1995).

Computational fluid dynamics (CFD) and finite element analysis (FEA) modeling techniques suggested the presence of large recirculation zones and areas of dead volume in three out of four full-scale FBD contactors that were studied (Henry and Freeman 1995). An example of the type of flow pattern predicted by the CFD study contactor is shown in Figure 2-3. The CFD analysis further predicted that the  $t_{10}/\tau$  ratio could be improved by increasing the depth to length ratio in each contactor cell or by adding vanes or wall foils at strategic locations (Henry and Freeman 1995). The hydrodynamic efficiency in FBD contactors is also sensitive to the conditions of gas dispersion. Gas addition has been observed to increase the degree of back-mixing and liquid dispersion in small-scale bubble columns (Mariñas et al. 1993; Nieminski 1990; Roustan et al. 1996). In a small-scale FBD contactor, the  $t_{10}/\tau$  ratio increased with higher gas-to-liquid flow rate ratio,  $G/Q_f$ , and when the gas was distributed to all chambers versus addition to only one chamber (Do-Quang et al. 2000a). The same effects were confirmed in full-scale contactors (Martin et al. 1992; Reddy et al. 1997).

The potential impact of contactor hydrodynamics on *G. lamblia* and *C. parvum* inactivation in full-scale ozone contactors has been studied by theoretical analysis with the CFSTR-in-series mixing model. Increasing the number of CSFTRs in series from 3 to 10 in a hypothetical contactor resulted in a predicted decrease in the residence time required for 2 log-units of *G. lamblia* inactivation by a factor of almost two (Roustan et

al. 1991). For *C. parvum* a similar increase in hydrodynamic efficiency resulted in a reduction in the required residence time by a factor of more than three (Do-Quang et al. 2000b). No studies have reported on the effect of contactor hydrodynamics on the efficiency of the reduction of either *Giardia* spp. cysts or *Cryptosporidium* oocysts based on direct measurement.

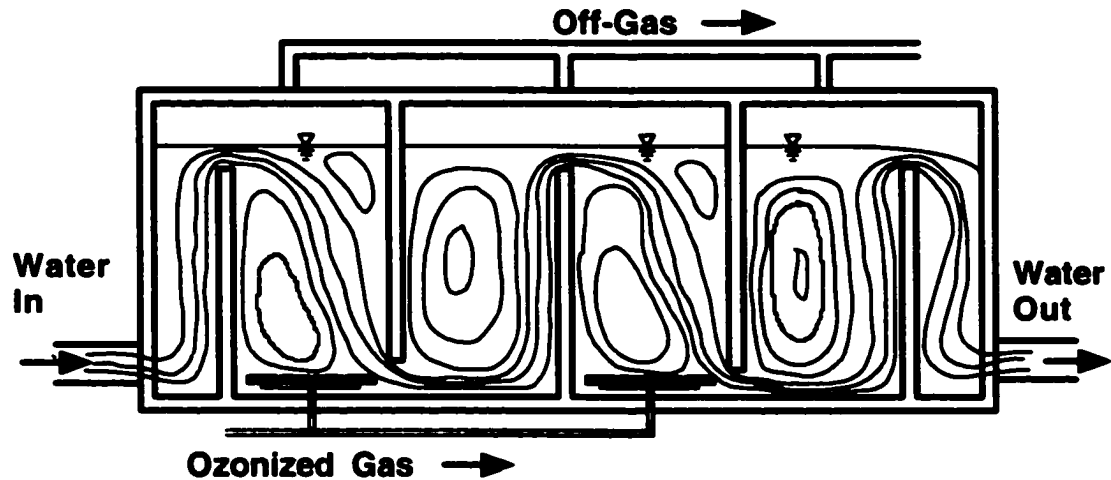


Figure 2-3 Potential hydrodynamic flow pattern in a typical conventional multi-chamber fine bubble diffuser ozone contactor. Flow streamlines are adapted from results of the computational fluid dynamics study of Henry and Freeman (1995).

These hydrodynamic studies expose the limitation inherent in the design of FBD contactors when considered for microorganism reduction. The gas-liquid contacting requirement in an FBD results in physical contactor designs and hydrodynamic conditions that are less than ideal for efficient microorganism reduction. This arises because contactor geometries are dictated primarily by mass transfer requirements, and not by hydrodynamic considerations. For example, the up-and-over configuration is dictated by the need to provide opportunity for contact between the ozone bubbles and the water. Further, FBD contactor height and width are determined by ozone transfer

efficiency requirements and the area required for diffusers (Joost et al. 1989; Rakness et al. 1988).

#### **2.4.7 Influence of Gas-Liquid Contact**

The implicit assumption underlying the discussion of contactor hydrodynamics thus far has been that the intrinsic microorganism inactivation rate at any point in the contactor depends on the local dissolved ozone concentration only. There are suggestions in the literature that other factors may influence the rate of microorganism inactivation by ozone, particularly in gas-liquid systems. Some authors have proposed that contact with bubbles of gaseous ozone may enhance microorganism inactivation in ozone contactors (Haas 1990; Masschelein et al. 1975; Masschelein et al. 1976; Masschelein 1982b). Gaseous ozone has been shown to be an effective bactericide as long as sufficient humidity is present (Dahi and Lund 1980; Ishizaki et al. 1986). The presence of ozone gas bubbles together with dissolved ozone was found to enhance the inactivation of the bacteria *Mycobacterium fortuitum* and the yeast *Candida parapsilosis* by about 1 log-unit as compared to exposure to dissolved ozone alone (Farooq et al. 1977a). The authors speculated that, because of their surface active properties, microorganisms would tend to concentrate in the liquid film at the gas-liquid interface, and would thus be exposed to both gaseous ozone and a higher concentration of ozone than in the bulk liquid (Farooq et al. 1978). In a continuous-flow laboratory-scale bubble column, standard plate count bacteria in secondary wastewater were more effectively inactivated when the ozone bubbles were smaller, given the same dissolved ozone concentration (Ahmad and Farooq 1984). It was postulated that this was due to the increased gas-liquid contact surface area associated with the finer gas bubbles. In a comparison of different contacting systems, including porous diffusers, ejectors and mixing turbines, the ozone concentration in the water necessary for a given level of *Actinomyces* reduction was found to be lower if the energy dissipated during gas-liquid mixing was higher (Masschelein 1982b). The authors attributed this effect to an increase in the rate of exposure of the microorganisms to the surface of gaseous ozone bubbles. In the same study, the same authors also reported that the rate of ozone reaction with picric acid, a slowly reacting phenolic compound, was proportional to the surface area of gas-

liquid contact in a dispersed bubble reactor. The reported information in these studies, however, was often not sufficient to distinguish whether the observed effects were due to an increased degree of direct contact between microorganisms and gaseous ozone, or to an increase in the ozone mass transfer rate that accompanied smaller bubble size.

The findings of other researchers, however, tend to contradict the gas-bubble hypothesis. Scaccia and Rosen (1978) argued and that inactivation of microorganisms would be equivalent in any type of contactor as long as the absorbed ozone dose was the same. They provided supporting evidence for their argument by comparing fecal coliform inactivation in three types of gas-liquid ozone contactors. Finch and Smith (1991) found that inactivation of *E. coli* in wastewater exposed to gaseous ozone in a semi-batch gas-liquid contact tank stirred with a Rushton turbine was less efficient at higher rates of energy input. They concluded that the design of ozone contactors for microorganism reduction should ideally consist of a gas-liquid contact stage for mass transfer, followed by a plug flow reactor for dissolved ozone contact and microorganism reduction.

The varied results of these experiments suggest that the role of ozone bubbles and gas-liquid contact may be system dependent. In addition, the studies were limited to microorganisms that are relatively rapidly inactivated by ozone, such as vegetative bacteria or yeast. No information is available on the effects of gas-liquid contact on microorganisms that are more resistant to ozone, such as sporulated bacteria or encysted protozoa like *Cryptosporidium parvum* or *Giardia lamblia*.

#### **2.4.8 Use of Static Mixers for Ozone Contact**

Several other methods for dissolving gaseous ozone in water have been experimented with in addition to the conventional FBD contactor, however, most of these have seen only limited application (Langlais et al. 1991; Masschelein 1982a). The deep U-tube contactor has been promoted in France as a means of improving hydrodynamic efficiency, although this was not proven in a test on a full-scale installation (Roustan et al. 1993). Another type of contactor that has been pilot-tested in the United States is the side-stream venturi injector with a downflow tube. The advantage of this contactor is that it can achieve both high dissolved ozone concentrations and mass transfer

efficiencies and is well-adapted to the use of modern high concentration ozone gas feeds (Schulz et al. 1995).

Static mixers, also called motion-less mixers, consist of a series of stationary mixing elements mounted inside a section of pipe or duct. They have been used in the chemical process and food industries for applications ranging from the mixing of highly viscous fluids, like polymers, to absorbance of gases into non-viscous liquids (Myers et al. 1997; Rader et al. 1989). As the fluid mixture flows through the elements of the static mixer, it is sheared, sub-divided into smaller elements, and recombined many times. Fluid kinetic energy is rapidly dissipated resulting in a highly micro-mixed, homogenous fluid with a radially uniform concentration. In gas-liquid contacting systems, high rates of mass transfer are promoted by formation of very fine bubbles, the surfaces of which are renewed constantly by coalescence and redistribution of the fluids, and by high turbulence (Grosz-Röll et al. 1982). The short residence times and rapid energy dissipation within static mixers make them particularly useful for enhancing the yield of very fast and competitive reactions where mass transfer and degree of micro-mixing are the rate controlling steps (Bourne et al. 1992). For this reason, static mixers are useful for the rapid mixing of coagulation chemicals in water treatment (Schulgen et al. 1996).

Static mixers have been available as an option for ozone dissolution for some time (Masschelein 1982a). Langlais and co-authors (1991) list the principle advantages of static mixers, and other in-line contactors, for ozone contacting as follows:

1. They are simple systems with no moving parts that require little maintenance.
2. They provide good mixing and mass transfer.
3. Much smaller contacting vessels are required compared to FBD contactors because of the very short residence times within the mixers.

The main disadvantage of static mixers in drinking water treatment facilities is that the pressured drop incurred may create the need for additional pumping and energy expenditure.

The benefits of using a static mixer, or any other in-line mixing devices, for improving the efficiency of microorganism reduction processes in water treatment have been explored only to a limited extent. Zhu and co-workers (1989a) found that, in an

experimental static mixer system, inactivation of *E. coli* in wastewater was controlled by the mass transfer rate within the static mixer and even proposed a mathematical relationship between inactivation and the mass transfer coefficient. However, it is not clear from the experimental design if these researchers were able to separate the effects on the microorganisms of mass transfer from those of contact with dissolved ozone. After studying the hydrodynamics of several conventional fine bubble diffuser contactors, Martin and co-workers (1992) recommended the use of static mixers as an alternative for ozone dissolution. They argued that a static mixer used in combination with a plug-flow contactor would provide the best microorganism reduction. The design concept of a rapid mass transfer stage followed by a microorganism reduction stage is similar to that suggested by Finch and Smith (1991). The concept was later tested to a very limited extent in a pilot study. The focus of the work was ozone transfer efficiency and oxidation of atrazine and limited information on the reduction of heterotrophic plate count (HPC) bacteria was provided (Martin and Galey 1994).

Others studied HPC and fecal coliform bacteria reduction in a static mixer ozone contactor (Bonnard et al. 1999). The experimental design, however, did not allow the effect of the static mixer on microorganism reduction to be determined separately from the effects of other system parameters, such as contact time. Recently, enhanced reduction of *C. parvum* oocysts was reported when the microorganisms were pre-contacted with dissolved chlorine in a static mixer relative to pre-contact in an empty pipe (Heindel et al. 1999). This finding suggests that vigorous mixing within the static mixer might increase the efficacy of the chlorine by loosening, or otherwise altering, the oocyst wall.

Few documented full-scale examples of static mixer ozonation systems are available. Zhu and co-workers (1990) described a small installation in which hospital wastewater was contacted with ozone in a static mixer for a 0.1 min contact time with applied ozone doses ranging from 20 to 45 mg/L. Reduction of *E. coli* in the wastewater was 3 to 5 log-units. Martin and co-workers (1995) described an  $84 \times 10^3 \text{ m}^3/\text{d}$  static mixer installation at the Melun-Arvigny water treatment plant in France. Ozone was contacted with a side-stream of plant water flow in one static mixer and was then further blended with the main flow in a second static mixer. Additional contact time of 6.2

minutes with dissolved ozone was provided in an “up and over” style, 4-chamber contactor. No microorganism reduction or hydrodynamic performance data was available.

## **2.5 SUMMARY**

New requirements to provide reduction of encysted protozoa, particularly *C. parvum*, have increased the need for a better understanding of ozone contactor design. Considerable information has been gained from batch and semi-batch reactor studies and the rate of reaction between *C. parvum* oocysts and dissolved ozone is now fairly well, but not completely, understood. For the purposes of water treatment process design and public health protection, animal infectivity remains the most reliable method of determining the effects of ozone on these parasites. The influence of ozone contactor hydrodynamics on microorganism reduction efficiency, however, is less well understood. Based on consideration of chemical reaction engineering principles and measurements of residence time distributions, conventional full-scale ozone contactor designs are not conducive to efficient microorganism reduction. It has been suggested that a better design would promote rapid ozone dissolution followed by contact with dissolved molecular ozone under plug flow conditions. Very little experimental work has been conducted to verify the effect of ozone contactor hydrodynamics on microorganism reduction or to demonstrate alternative contactor designs. No studies have been reported in which the effect of mixing in ozone contactors on *C. parvum* inactivation was experimentally investigated. The effect of gas-liquid contacting conditions on *C. parvum* oocysts remains largely unexplored. It is, therefore, uncertain how well the information generated in batch and semi-batch reactors can be extended to larger-scale continuous flow ozone contacting systems.

### **3 EFFECT OF MIXING ON *CRYPTOSPORIDIUM PARVUM* INACTIVATION IN AN OZONE CONTACTOR - A THEORETICAL ANALYSIS**

#### **3.1 INTRODUCTION**

Chemical reactor engineering theory predicts that both the macro-mixing characteristics and the degree of fluid segregation, or micro-mixing, may influence conversion in chemical reactors. The extent to which micro-mixing is important is dictated by the reaction kinetics of the particular system under consideration, the macro-mixing and the extent of conversion. The potential impact of these hydrodynamic factors on inactivation of *C. parvum* oocysts in ozone contactors has been investigated only to a limited extent. The theoretical reaction engineering analysis of Do-Quang and co-workers (2000b), using a CFSTR-in-series mixing model, considered only two macro-mixing conditions, equivalent to 3 and 10 CFSTRs in series, and a fixed rate of ozone decomposition. The analysis was also restricted to the assumption of first-order Chick-Watson inactivation kinetics. Others have found that *C. parvum* inactivation by ozone is better represented by a non-linear kinetic model (Gyürék et al. 1999; Li et al. 2001). Further, the fluid micro-mixing condition was limited to the case of partial segregation that is intrinsic to the CFSTR-in-series model.

The objective of the theoretical mathematical analysis presented in this chapter was to predict the effect of hydrodynamic conditions in a hypothetical single-phase ozone contactor on *C. parvum* inactivation over a wider range of macro-mixing states. Both first-order and non-linear kinetic models of *C. parvum* inactivation by dissolved ozone at 22°C (Gyürék et al. 1999) were used as the basis for a series of mathematical simulations. Partial and complete fluid segregation micro-mixing cases were considered using a modeling approach similar to that used by others for the case of fecal coliform and *G. lamblia* cyst inactivation by chlorine compounds (Haas 1988; Lawler and Singer 1993). The influence of ozone decomposition rate was also examined.

## 3.2 CONTACTOR MODEL DEVELOPMENT

### 3.2.1 Scenario

The case of a hypothetical dissolved ozone contactor was considered in which gaseous ozone was dissolved into the water in an upstream step. Both the feed and the outlet streams of the contactor were assumed to be perfectly micro-mixed with respect to both microorganisms and dissolved ozone. Between the inlet and the outlet the fluid was in either a partially segregated or a completely segregated mixing state. Segregated flow analysis, wherein the residence time distribution was integrated directly with kinetic models of *C. parvum* inactivation by dissolved ozone, was used to simulate complete fluid segregation. A CFSTR-in-series mixing model that incorporated the same kinetic models was used to simulate partial fluid segregation.

### 3.2.2 Kinetic Models

The fundamental kinetic assumption in the analysis was that the local rate of *C. parvum* inactivation at any point within the contactor was determined by the dissolved ozone concentration according to either a Chick-Watson or a Hom model. The Chick-Watson model was described in both differential and integrated form in Equations 2-8 and 2-10. The differential and the integrated forms of the Hom model were given by, respectively:

$$-\frac{dN}{dt} = k_H m N C^n t^{m-1} \quad \text{Equation 3-1}$$

$$-\log \frac{N}{N_0} = k'_H C^n t^m \quad \text{Equation 3-2}$$

where  $k'_H = k_H/\ln(10)$ . This parameter adjustment was required to convert from natural base  $e$  logarithm to the base 10 logarithm form more commonly used in the water treatment field. Model parameters were adopted from the work of Gyürék and co-

workers (1999) on inactivation of *C. parvum* oocysts in phosphate buffered ultrapure water at 22°C and pH 6 to 8, and were:

First-Order Chick-Watson Model:  $k' = 0.37 \text{ min}^{-1}, n = 1$

Hom model:  $k'_H = 0.68 \text{ min}^{-1}, n = 0.70, m = 0.73$

Although various orders for the rate of ozone decomposition in natural water have been reported (Grasso and Weber 1989), for simplicity, a simple first-order relationship was used in the simulations. The differential and integrated forms were, respectively:

$$-\frac{dC}{dt} = k_d C \quad \text{Equation 3-3}$$

$$C = C_0 \exp(-k_d t) \quad \text{Equation 3-4}$$

In these equations,  $C$  represented the local dissolved ozone concentration in the contactor,  $C_0$  was the dissolved ozone concentration at the inlet of the contactor, and  $k_d$  was the first-order ozone decomposition rate constant.

First-order ozone decomposition was incorporated mathematically into the differential form of the batch microorganism kinetic models by inserting Equation 3-4 into Equation 2-8, for Chick-Watson kinetics, or into Equation 3-1, for Hom kinetics. The resulting differential equations were then integrated from  $t = 0$  to  $t = t$  yielding the following expressions for inactivation ratio in a batch or perfect plug flow reactor:

Chick-Watson:  $-\log \frac{N}{N_0} = \frac{k' C_0^n}{k_d n} [1 - \exp(-k_d t)] \quad \text{Equation 3-5}$

$$\text{Hom:} \quad -\log \frac{N}{N_0} = \frac{mk'_H C_0^n}{(nk_d t)^m} \gamma(m, nk_d t) \quad \text{Equation 3-6}$$

The analytical solution to the Hom model case was derived using the incomplete Gamma function,  $\gamma$ , and is valid when  $m > 0$  and  $nk_d t > 0$  (Haas and Joffe 1994). The gamma function was solved in Microsoft Excel 2000 using `Gammadist(nk_d t, m, 1, true) * exp(-Gammaln(m))` (Gyürék et al. 1999).

### 3.2.3 Partially Segregated Flow Analysis

To simulate non-ideal macro-mixing, the contactor was considered to be equivalent to a series of identical continuous-flow, perfectly stirred tank reactors (CFSTRs) as follows:



The extent of back-mixing in the contactor was described by the single parameter  $J$ , the number of CFSTRs in the series. A single perfect CFSTR was represented by setting  $J$  equal to 1. As  $J$  was increased, the extent of back-mixing decreased and the macro-mixing and residence time distribution approached that of perfect plug flow. In each of the CFSTRs in the series, the fluid was considered to be perfectly micro-mixed, however, there was no mixing between the individual CFSTRs. Conceptually, therefore, this mixing model represented a condition of partial fluid segregation (Lawler and Singer 1993).

Solution of the overall reactor problem required a mass balance for both dissolved ozone and microorganisms for each of the  $J$  CFSTRs in the series. Given first-order ozone decomposition as described by Equation 3-3, a mass balance yielded the following expression for the ozone concentration,  $C_i$ , in the  $i$ th CFSTR:

$$\frac{C_i}{C_{i-1}} = \frac{1}{1 + \tau_i k_d} \quad \text{Equation 3-7}$$

In Equation 3-7,  $\tau_i$  was the space time in each CFSTR in the series and was equal to the contactor hydraulic residence time divided by the number of CFSTRs (i.e.  $\tau_i = \tau_T / J$ ). A similar expression was derived for the concentration of live *C. parvum* oocysts in the *i*th CFSTR,  $N_i$ , by incorporating the differential form of the inactivation kinetic models (Equations 2-8 and 3-1) into the mass balance. The solutions for each of the two kinetic formulations were:

$$\text{Chick-Watson:} \quad \frac{N_i}{N_{i-1}} = \frac{1}{1 + \tau_i k C} \quad \text{Equation 3-8}$$

$$\text{Hom:} \quad \frac{N_i}{N_{i-1}} = \frac{1}{1 + \tau_i k_H m C^n t^{m-1}} \quad \text{Equation 3-9}$$

In Equation 3-9, the  $t$  variable arising from the Hom kinetic formulation presented a unique problem. The Hom formulation was originally derived from kinetic studies in batch reactors where  $t$  represents the duration of the ozone exposure (Hom 1972). In the CFSTR-in-series model,  $t$  in *i*'th reactor was defined as follows:

$$t = i \frac{\tau_i}{J} \quad \text{Equation 3-10}$$

Substituting Equation 3-10 into Equation 3-9 yielded the following equation:

$$\frac{N_i}{N_{i-1}} = \frac{1}{1 + \frac{i^{m-1} \tau_i^m k_H m C^n}{J^{m-1}}} \quad \text{Equation 3-11}$$

*C. parvum* oocyst infectivity reduction in a hypothetical contactor with mixing equivalent to  $J$  CFSTRs was determined by solving simultaneously the algebraic set of equations that described  $i = 1$  to  $J$  reactors. For each reactor, these were Equation 3-7 and either Equation 3-9 (Chick-Watson kinetics) or Equation 3-11 (Hom kinetics).

### 3.2.4 Segregated Flow Analysis

The residence time distribution for the segregated flow analysis case was generated from the following equation that describes the exit age distribution function for a series of identical CFSTRs (Levenspiel 1972):

$$E(t) = \frac{t^{J-1}}{\tau_i^J (J-1)!} \exp\left(-\frac{t}{\tau_i}\right) \quad \text{Equation 3-12}$$

For segregated flow analysis, *C. parvum* inactivation was determined by replacing the chemical concentration in Equation 2-14 with the concentration of live microorganisms. The resulting expression was:

$$\frac{N}{N_0} = \int_{t=0}^{t=\infty} \left( \frac{N}{N_0} \right)_{\text{batch}} E(t) dt \quad \text{Equation 3-13}$$

where  $(N/N_0)_{\text{batch}}$  was the survival ratio determined from a batch reactor kinetic model of microorganism inactivation. Substituting Equations 3-5 and 3-6 into Equation 3-13 yielded the following integral expressions for *C. parvum* inactivation for the segregated flow case with either Chick-Watson or Hom kinetics:

**Chick-Watson:**

$$\frac{N}{N_0} = \int_{t=0}^{t=\infty} \text{antilog} \left\{ \frac{-k' C_0^n}{k_d n} [1 - \exp(-k_d t n)] \right\} E(t) dt \quad \text{Equation 3-14}$$

**Hom:**

$$\frac{N}{N_0} = \int_{t=0}^{t=\infty} \text{antilog} \left\{ \frac{-m k'_H C_0^n}{(n k_d)^m} \cdot \gamma(m, n k_d t) \right\} E(t) dt \quad \text{Equation 3-15}$$

**3.2.5 Numerical Calculations**

The algebraic set of equations that described the  $J$  CFSTRs of the partially segregated fluid contactor was solved using a spreadsheet program in Microsoft Excel 2000<sup>®</sup>. For segregated flow analysis, Equations 3-14 and 3-15 were integrated numerically using the trapezoid rule with a calculation interval of 1 s. Smaller calculation intervals were tested, but were found to provide the same solution to within 0.1% of the 1 s step size. Numerical calculations were done in Microsoft Excel 2000. Calculations were performed for a hypothetical ozone contactor with a total theoretical residence time,  $\tau$ , of 15 min. A residence time of approximately 15 min would be typical for an ozone contactor designed primarily for *C. parvum* reduction.

**3.3 SIMULATION RESULTS AND DISCUSSION****3.3.1 Simulation Plots**

A corollary of reaction engineering theory is that a certain hydrodynamic mixing condition gives rise to a unique residence time distribution. The converse, however, is not necessarily true (Levenspiel 1972). Different degrees of fluid micro-mixing or macro-mixing patterns within the reactor may give rise to identical residence time distributions. In the hypothetical ozone contactor simulations, the macro-mixing condition and the residence time distribution for both partial and complete fluid

segregation cases was defined by the value of the hydrodynamic parameter,  $J$ . Figure 3-1 shows the computed exit age distribution,  $E(t)$ , as a function of  $J$  for a total theoretical residence time,  $\tau$ , of 15 min. For  $J = 1$ , the  $E(t)$  curve was identical to that of a single ideal CFSTR. As  $J$  increased and the degree of back-mixing decreased the  $E(t)$  peak became progressively narrower, and approached that of a perfect plug flow reactor. For a given  $J$ , the exit age distribution,  $E(t)$ , and macro-mixing characteristics of the partially segregated and completely segregated fluid contactors were identical. However, the extent of micro-mixing was determined by the assumptions implicit in segregated flow analysis of Equation 3-13 and the micro-mixing characteristics intrinsic to the CFSTR-in-series model.

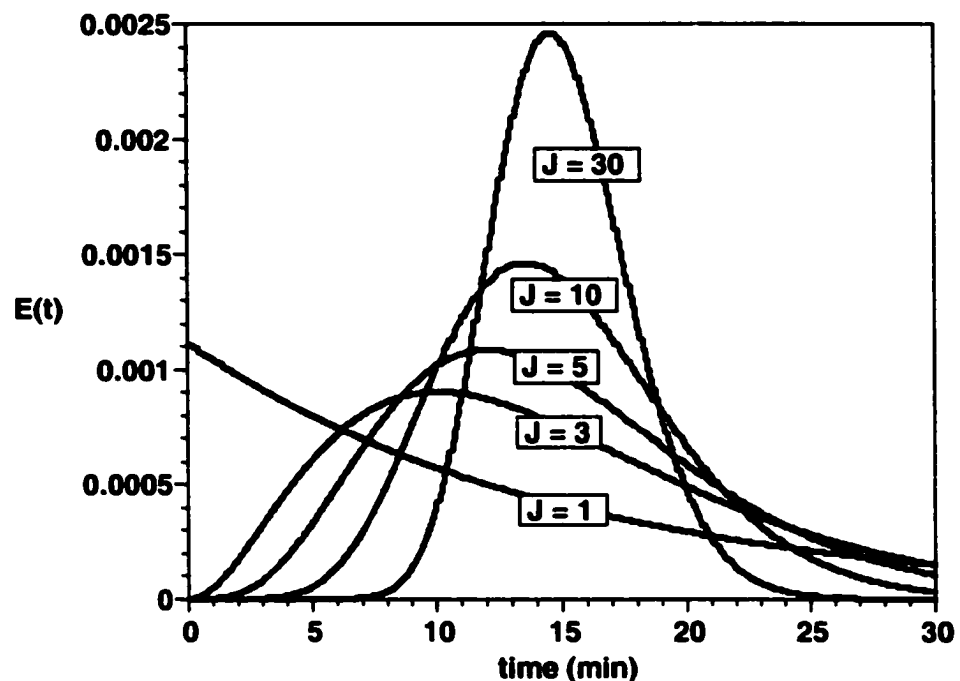


Figure 3-1 The exit age distribution in a hypothetical ozone contactor as a function of the number of CFSTRs in series,  $J$ , for a total theoretical residence time,  $\tau$ , of 15 min.

The results of a series of contactor simulations are presented in the plots of Figures 3-2, 3-3 and 3-4. For each simulation, the total theoretical residence time,  $\tau$ , in

the hypothetical zone contactor was 15 min. Each plot in these figures gives the predicted inactivation of *C. parvum* at 22°C on the vertical axis as a function of the macro-mixing parameter,  $J$ , on the horizontal axis. Simulation results for both complete and partial segregation are compared on the same set of plot axes. Two levels of ozone treatment and inactivation were examined by adjusting the value of the initial ozone concentration,  $C_0$ . The set of plotted curves at the top of each figure shows the simulation results based on the first-order Chick-Watson inactivation kinetic model. At the bottom, the simulation results at identical ozonation conditions but with the non-linear Hom kinetic model are provided.

### 3.3.2 Effect of Residence Time Distribution

The simulations of Figures 3-2, 3-3 and 3-4 have important implications for *C. parvum* inactivation in conventional multi-basin fine bubble diffuser ozone contactors. The predicted level of *C. parvum* inactivation increased as the value of  $J$  increased and the degree of back-mixing in the contactor decreased. This observation follows directly from chemical reaction engineering theory and was thus expected. What was more interesting, and significant, was that the predicted level of inactivation was most sensitive to the value of  $J$  for  $J$  between 1 and 10. The  $J$  values of operating conventional multi-basin fine bubble diffuser ozone contactors lie within this hydrodynamic range. One survey of ozone contactors operating in water treatment plants in the UK reported  $J$  values that ranged from 4 to 7 for conventional designs (Do-Quang et al. 2000a). Further, the effect  $J$  in this range on inactivation was greatest when the ozone treatment and the inactivation level were higher. In one simulation (top of Figure 3-2) for example, an increase in  $J$  from 4 to 7 resulted in a 0.7 log-unit increase in the inactivation level from 2.5 to 3.2 log-units. When the value of  $J$  was increased further to 30, predicted inactivation increased to 4.6 log-units. The macro-mixing hydrodynamics in conventional ozone contactors, therefore, are not likely to be conducive to efficient *C. parvum* inactivation, especially if the target inactivation level is greater than 2 log-units. Substantial improvements in inactivation could be achieved by modification of hydrodynamic design.

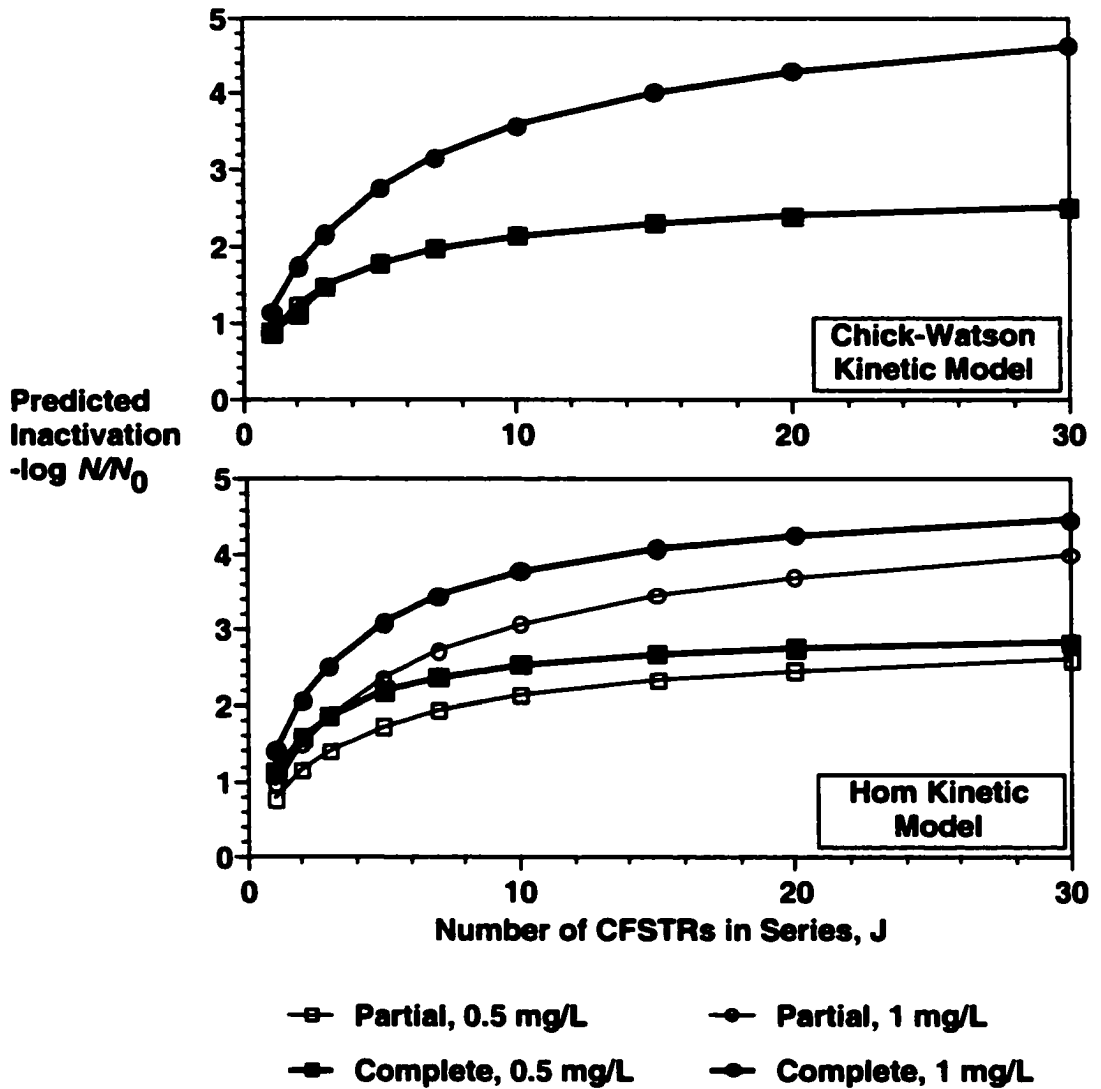


Figure 3-2 Simulation of the effect of contactor hydrodynamics on *C. parvum* inactivation at 22°C for the case of no ozone decomposition ( $k_d = 0 \text{ min}^{-1}$ ) and both complete and partial fluid segregation.

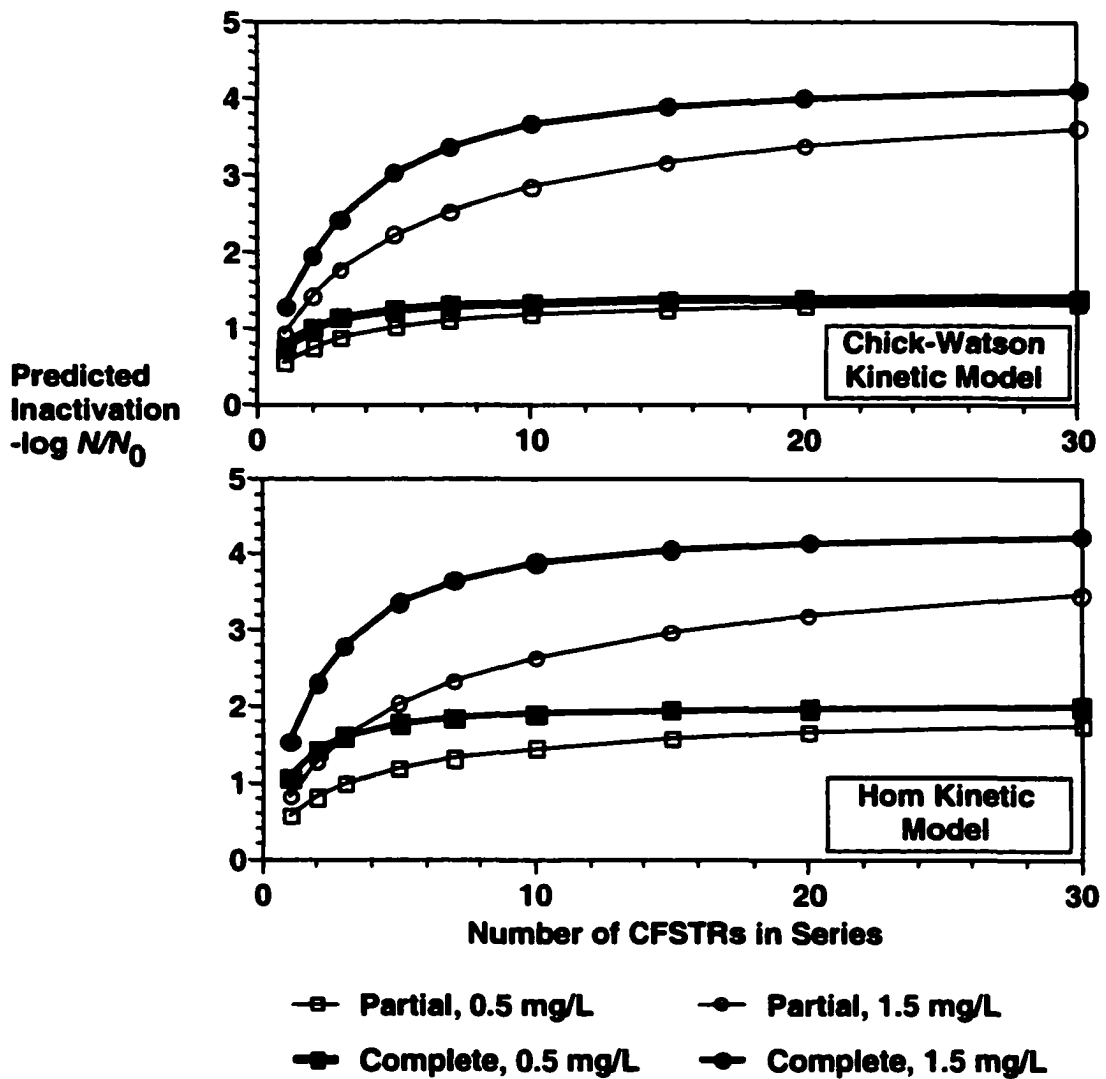


Figure 3-3 Simulation of the effect of contactor hydrodynamics on *C. parvum* inactivation at 22°C for the case of ozone decomposition with  $k_d = 0.1 \text{ min}^{-1}$ , and both complete and partial fluid segregation.

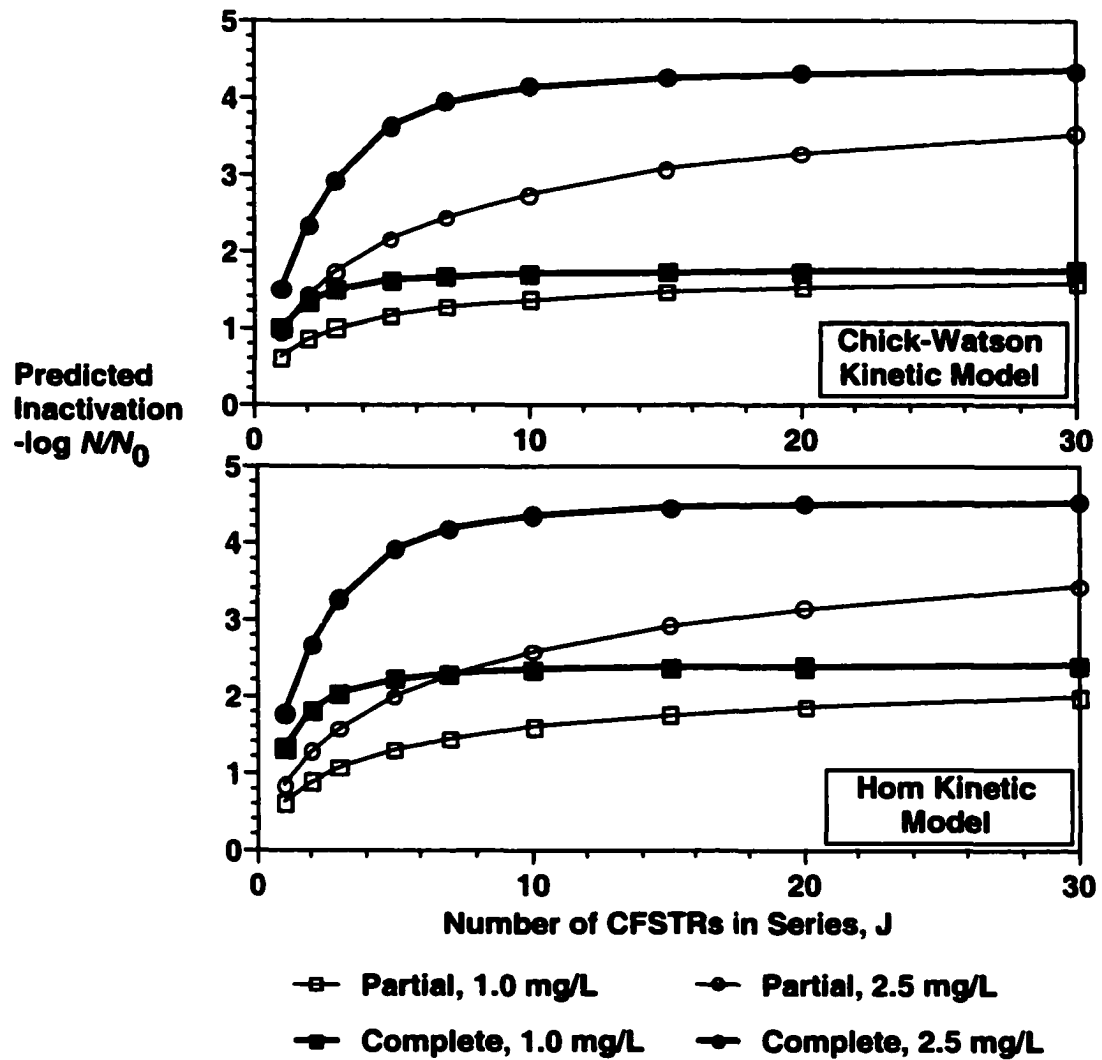


Figure 3-4 Simulation of the effect of contactor hydrodynamics on *C. parvum* inactivation at 22°C for the case of ozone decomposition with  $k_d = 0.2 \text{ min}^{-1}$ , and both complete and partial fluid segregation.

### 3.3.3 Effect of Micro-Mixing and Fluid Segregation

The effect of micro-mixing on inactivation was influenced by several factors including the microorganism kinetics, the ozone decomposition kinetics, the macro-mixing condition and the level of inactivation. In all simulation cases, except one, and at all macro-mixing conditions, inactivation in the partially segregated contactor was lower than in the completely segregated contactor. That is, greater micro-mixing resulted in less inactivation. The exception was the case of no ozone decomposition ( $k_d = 0$ ) and first-order Chick-Watson inactivation kinetics for which predicted inactivation for complete and partial segregation was equal (top of Figure 3-2). For this case, the kinetic system was reduced to a uni-molecular first-order process. According to chemical reaction engineering theory, conversion in this type of system is unaffected by micro-mixing (Levenspiel 1972). When either a non-linear inactivation kinetic model or a non-zero ozone decomposition rate was introduced into the simulations, deviations between predicted inactivation for complete and partial segregation were observed. Integration of first-order ozone decomposition with first-order Chick-Watson microorganism inactivation resulted in a kinetic system that was second-order overall and was thereby influenced by the degree of fluid segregation (top of Figure 3-3). The deviation between complete and partial segregation, and the importance of micro-mixing, increased as the value of the first-order decomposition rate constant,  $k_d$ , was increased from 0.1 to 0.2  $\text{min}^{-1}$  (Figure 3-3 and 3-4).

The effect of micro-mixing on inactivation was greatest at lower values of  $J$ , or greater back-mixing, but diminished gradually when the hydrodynamic condition approached that of perfect plug flow. The greatest deviation between the complete and partially segregated fluid cases was observed to occur at  $J$  of between approximately 4 and 7, which corresponds to the macro-mixing region of conventional ozone contactors. *C. parvum* inactivation in the conventional contactors, therefore, will not only be limited by macro-mixing, but might also be adversely impacted by micro-mixing. According to the simulations, the potential magnitude of the micro-mixing effect is considerable. For example, with an ozone decomposition rate of 0.2  $\text{min}^{-1}$ , an initial ozone concentration of 2.5 mg/L and macro-mixing equivalent to  $J = 5$  CFSTRs-in-series, the predicted inactivation for complete segregation was almost 2 log-units greater than for partial

segregation (3.9 versus 2.0 log-units, bottom of Figure 3-4. Even for the lower ozone treatment of 1.0 mg/L, the magnitude of the micro-mixing effect was almost 1 log-unit (2.2 versus 1.3 log-units).

The potential impact of this analysis in terms of achieving a target level of *C. parvum* inactivation was examined in Figure 3-5. This figure plots the initial ozone concentration required to achieve 2 log-unit inactivation as a function of macro-mixing for both complete and partially segregated fluids. Hom inactivation kinetics at 22°C and a first-order ozone decomposition constant,  $k_d$ , equal to  $0.1 \text{ min}^{-1}$  were assumed. The results indicated that the degree of micro-mixing will have a considerable effect on the ozonation requirements. At macro-mixing conditions that are typical of conventional fine bubble diffuser contactors ( $J = 4$  to  $7$ ), the partially segregated contactor required approximately twice the ozone for the same level of inactivation.

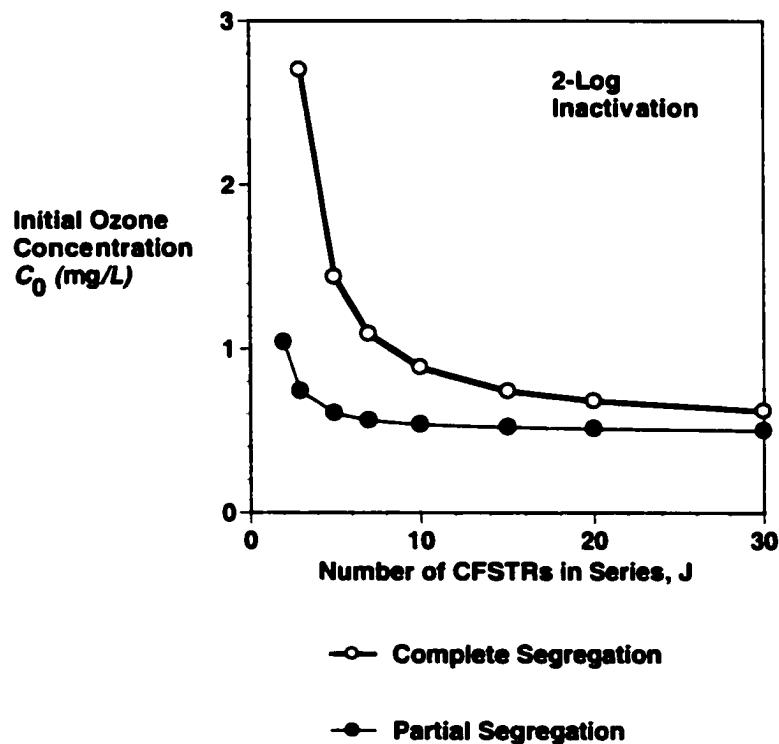


Figure 3-5 Effect of fluid segregation on the ozonation requirements for 2 log-units inactivation of *Cryptosporidium parvum* in an ozone contactor.

In theory, then, *C. parvum* inactivation will be influenced by the degree of micro-mixing that exists in conventional contactors. Lawler and Singer (1993) observed that the complete fluid segregation condition was unlikely in chlorine contactors because of the low viscosity of water. Haas (1988) arrived at a similar conclusion based on determination of the segregation number,  $S_g$ , for a typical chlorine contactor. In an ozone contactor, the segregation number for ozone can be estimated from Equation 2-15:

$$S_g = \frac{\mu^{3/2}}{4\pi^2 \rho^{3/2} e^{1/2} \mathcal{D} \bar{t}} \quad \text{Equation 2-15}$$

As indicated by Equation 2-15, the degree of segregation is inversely proportional to the rate of energy dissipation, and therefore, the degree of turbulent mixing. In the absence of mechanical mixing or mixing induced by gas addition, the rate of energy dissipation,  $e$ , is related to the loss of hydraulic head and can be estimated from:

$$e = \frac{\gamma h_L}{\rho \bar{t}} \quad \text{Equation 3-16}$$

An order of magnitude estimate of the segregation number was calculated by assuming that typical values of the mixing time and hydraulic head loss in an ozone contactor are on the order of  $\bar{t} = 15$  min (900 s) and  $h_L = 0.1$  m. Values for the properties of water and diffusivity of ozone used in the calculation were: viscosity,  $\mu = 0.957 \times 10^{-3}$  N·s·m<sup>-2</sup>; specific weight,  $\gamma = 9.78 \times 10^3$  N·m<sup>-3</sup>; density,  $\rho = 998$  kg·m<sup>-3</sup>; and diffusivity  $\mathcal{D} = 1.74 \times 10^{-9}$  m<sup>2</sup>·s<sup>-1</sup>. Substituting these values into Equations 3-16 and 2-15 yielded the following estimates for energy dissipation and segregation number, respectively:

$$e = \frac{(9.78 \times 10^3 \text{ N} \cdot \text{m}^{-3}) (0.1 \text{ m})}{(998 \text{ kg} \cdot \text{m}^{-3}) (900 \text{ s})} = 1.1 \times 10^{-3} \frac{\text{m}^2}{\text{s}^3}$$

and

$$S_r = \frac{(0.957 \times 10^{-3} \text{ N} \cdot \text{s} \cdot \text{m}^{-2})^{3/2}}{4(3.14)^2 (998 \text{ kg} \cdot \text{m}^{-3})^{3/2} (1.1 \times 10^{-3} \text{ m}^2 \text{s}^{-3})^{1/2} (1.74 \times 10^{-9} \text{ m}^2 \text{s}^{-1})(900 \text{ s})} = 0.0005$$

At segregation numbers of less than 0.1, segregation was shown to have little effect on the conversion of second-order reactions, and conversion was equal to the micro-mixed condition (Nauman and Buffham 1983). The estimated segregation number of 0.0005 for this hypothetical ozone contactor without gas addition is, therefore, more than two orders magnitude less than the threshold value at which segregation may be expected to play a role in determining conversion. In ozone bubble diffusion chambers, addition of gas will tend to decrease the segregation number even further. It, therefore, seems unlikely that segregation will have a significant effect on inactivation of *C. parvum* inactivation in a conventional ozone contactor. It further follows that the assumption of partial segregation would be more accurate and appropriate for predicting *C. parvum* inactivation for ozone contactors. Haas (1988) found that, for the case of fecal coliform reduction by chlorine, the CFSTR-in-series model yielded predictions that were approximately midway between those of a perfectly micro-mixed contactor and a completely segregated contactor. Assumption of partial segregation may lead to overestimates of *C. parvum* inactivation in fine bubble diffuser contactors that are both back-mixed and micro-mixed. The magnitude of the error introduced by the assumption of partial segregation, however, will tend to decrease as the level of back-mixing decreases and the residence time distribution approaches that of perfect plug flow.

### 3.4 CONCLUSIONS

The theoretical analysis presented in this chapter indicated that the hydrodynamics of ozone contactors have an important impact on the efficiency of *C. parvum* inactivation. In conventional multi-chamber fine bubble diffuser ozone contactors, inactivation will be limited by both the macro-mixing and micro-mixing regimes. The fluid in a typical ozone contactor is likely to be closer to a micro-mixed than a segregated condition, and, therefore, the assumptions of segregation will likely

lead to overestimation of inactivation. The micro-mixing effect becomes more significant the greater the extent of back-mixing, the greater the ozone decomposition rate and the greater the desired level of inactivation. Micro-mixing is associated with turbulence, therefore, the optimum hydrodynamic design of an ozone contactor would be one in which turbulence is minimized. To achieve this, energy input by mechanical mixing and energy dissipation by head loss should be minimized during dissolved ozone contact. Given the low viscosity of water, however, some degree of micro-mixing is probably inevitable in ozone contactors. To minimize the effect of micro-mixing and to maximize inactivation, contactors should, therefore, be designed primarily to reduce back-mixing. The objective should be to provide a residence time distribution with behaviour that approaches that of perfect plug flow as much as possible.

## **4 PROBLEM STATEMENT AND RESEARCH OBJECTIVES**

### **4.1 PROBLEM STATEMENT**

The current challenges of microorganism control in drinking water supply described in Chapter 2 have generated a need for more precise design and engineering analysis of microorganism reduction processes. Traditional ozone contactor design, represented by the conventional fine bubble diffuser contactor, falls short of fulfilling this need. The review in Chapter 2 discussed how the dual role of the conventional fine bubble diffuser contactors as gas-liquid mass transfer and contacting chambers makes them less than ideal as reactors for optimum microorganism inactivation. The theoretical analysis presented in Chapter 3 demonstrated that hydrodynamic conditions in ozone contactors will have a considerable influence on the efficiency of *C. parvum* inactivation. The design limitation of conventional FBD ozone contactors was captured by Haas (1990):

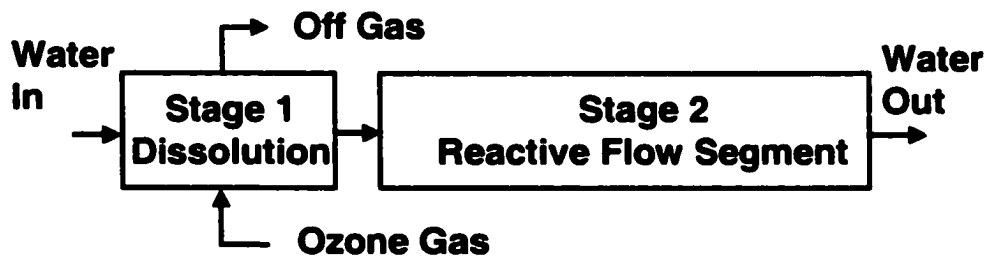
“Unfortunately, the characteristics that promote efficient gas-liquid mass transfer, particularly the desirability of intense agitation, lead to hydraulic characteristics that decrease disinfection efficiency (short-circuiting). Therefore, laboratory results on ozone inactivation of microorganisms are poor predictors of field performance, unless detailed aspects of field-scale hydraulics are considered.”

Ozone contactor design is further complicated by the uncertainty surrounding the potential role of agitation and direct contact with gaseous ozone on the intrinsic rate of microorganism inactivation.

How can this design problem be resolved? One solution approach is to modify existing fine bubble diffuser designs and to refine the engineering methods of analysis to better account for the hydrodynamic complexities in these types of contactors. This avenue has been explored to some extent by engineering researchers such as Henry and Freeman (1995) and Do-Quang and co-workers (2000a).

## 4.2 THE TWO-STAGE CONTACTOR DESIGN HYPOTHESIS

The hydrodynamic characteristics required for efficient microorganism inactivation are initial rapid mixing of the active chemical with the water followed by contact with the dissolved chemical in a vessel that is designed to minimize both back-mixing and micro-mixing. For an ozonation process in drinking water treatment, this hydrodynamic goal might best be achieved by separating the ozone gas-liquid mass transfer process from the microorganism inactivation process. It was hypothesized that such a two-stage ozonation process will provide optimal and predictable microorganism inactivation without compromising the requirement for good gas-liquid ozone transfer. The two-stage ozonation contactor design concept is illustrated in Figure 4-1. In the first stage, gaseous ozone is contacted with the flowing water and is rapidly dissolved using an in-line device such as a static mixer. Following off-gas separation, the microorganisms suspended in the water are contacted with dissolved ozone in a reactive flow segment for sufficient residence time to achieve the desired level of inactivation. The two processes are linked by the concentration of dissolved ozone in the water leaving the first stage and entering the second stage.



- > **Rapid Dissolution and Off-Gas Separation**
- > **Maximum micro-mixing**
- > **Mass transfer optimized**
- > **Dissolved Ozone Contact**
- > **Plug Flow**
- > **Segregated Flow**
- > **Microorganism Reduction Optimized**

Figure 4-1 Description of the two-stage ozone contactor design hypothesis.

In the two-stage ozone contactor design, the mass transfer and microorganism inactivation processes are de-coupled and can be optimized independently. Ozone mass transfer is optimized in the first stage by appropriate specification of the hydrodynamic conditions of gas-liquid contact. Microorganism inactivation is optimized in the second stage reactive flow segment by selection of a physical design that promotes plug flow residence time distribution behaviour. A two-stage design concept, in which one stage is optimized for mass transfer while the other is optimized for microorganism inactivation, was previously proposed in the literature (Finch and Smith 1991; Martin et al. 1992). The concept, however, has not been proven.

One of the important underlying assumptions of the two-stage design-hypothesis is that microorganism inactivation is determined solely by the conditions of dissolved ozone contact in the second stage. Most importantly, it is assumed that inactivation was independent of the hydrodynamics of gas-liquid contact in the first stage. As discussed in Chapter 4, the available literature regarding the effect of gas-liquid contact on microorganism inactivation is inconclusive. For the particular case of the encysted protozoa, like *Cryptosporidium* spp. or *Giardia* spp., virtually nothing was known regarding the importance of the gas-liquid contacting environment on inactivation by ozone.

### **4.3 RESEARCH OBJECTIVES**

The primary objective of the research program was to rigorously test the two-stage ozone contactor design hypothesis by experiment. The specific goals of the investigation were to:

1. design, build and test a small-scale continuous-flow ozonation system using an in-line static mixer for ozone dissolution;
2. determine the efficiency of inactivation of ozone resistant microorganisms in the experimental ozone contactor;
3. determine the effect of the hydrodynamic condition of gas-liquid contact within the static mixer on microorganism inactivation; and

4. establish the relationship between ozone gas-liquid mass transfer and microorganism inactivation in the experimental ozone contactor.

To determine if the findings generated were applicable to different microorganisms, the following three microorganisms were investigated:

1. spores of the aerobic bacterium *Bacillus subtilis*;
2. oocysts of *Cryptosporidium parvum*; and
3. cysts of *Giardia muris*.

Inactivation efficiency was to be assessed by comparing measured inactivation to that predicted by mathematical models of the contactor. These models incorporated both the hydrodynamics of the contactor and the kinetic models of microorganism inactivation. The effect of ozone on *C. parvum* oocysts and *G. muris* cysts has been studied extensively in laboratory batch reactors and is fairly well characterized. Because of the cost and logistical difficulties associated with conducting experiments with the encysted protozoa, the majority of the effort was concentrated on experimentation with the *B. subtilis* spores. A secondary objective of the thesis was to investigate the suitability of these spores as models for the ozone resistance of *C. parvum* oocysts.

## 5 EXPERIMENTAL APPROACH

### 5.1 CONCEPTUAL DESIGN OF AN EXPERIMENTAL OZONE STATIC MIXER CONTACTOR

A small-scale experimental ozone contactor was designed and constructed for the purpose of testing the two-stage ozone contactor hypothesis. The conceptual design of the experimental contactor and the key features that were important to the experimental design are described below. A simplified schematic of the experimental contactor is provided in Figure 5-1 below. A more complete description of the physical details of experimental contactor and related experimental procedures is found in Chapter 6.

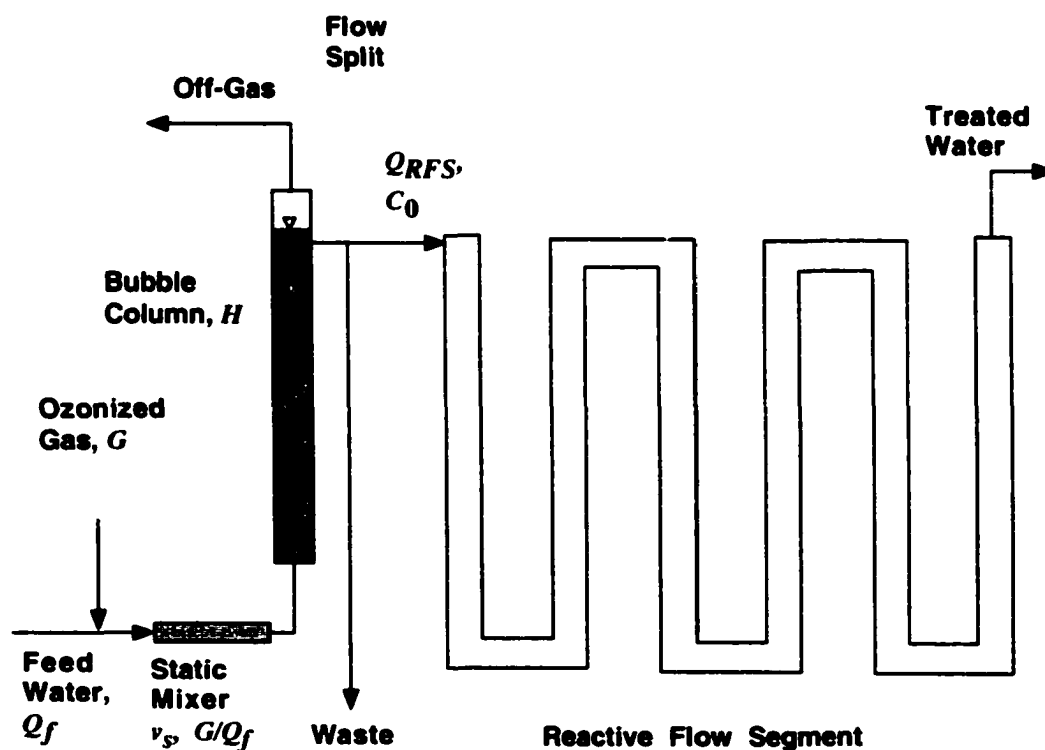
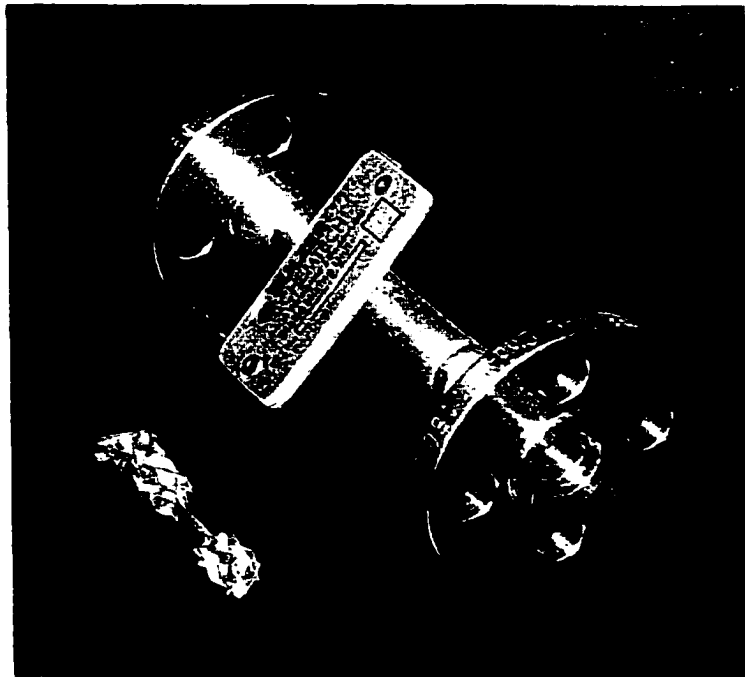


Figure 5-1 Simplified schematic of the experimental ozone static mixer contacting system.

The first stage of the experimental contactor was comprised of an in-line static mixer for initial contact between the ozonized gas and the flowing water, followed by a vertical bubble column for additional ozone dissolution and gas-liquid separation. A photograph of the static mixer, dismantled to show the mixing elements is provided in Figure 5-2. Although the duration of gas-liquid contact within the elements of the static mixer was short (less than 0.1 s), the hydrodynamic and liquid shear conditions promoted formation of fine ozone bubbles and resulted in rapid gas-liquid ozone mass transfer and dissolution. Fine bubbles generated in the static mixer were carried with the bulk liquid flow into the bottom of the bubble column where they rose with the liquid in a co-current flow pattern. Off-gas containing a residual of un-dissolved ozone accumulated above the liquid surface and was vented from the top of the column. The total duration of gas-liquid contact within the dissolution stage, including both the static mixer and bubble column, was typically less than 45 s.



**Figure 5-2** Photograph of the disassembled static mixer with internal mixing elements removed.

The water, now imparted with dissolved ozone, flowed from the top of the bubble column into the second stage reactive flow segment. At this point, ozone dissolution was complete and the ozone water mixer was in a well-mixed state due to the micro-mixing properties of the static mixer. With no requirements for additional gas-liquid mass transfer, the geometry of the reactive flow segment could, therefore, be selected solely on the basis of hydrodynamic conditions favourable to maximum microorganism inactivation. A long narrow pipe was selected as the geometry of choice to provide the following characteristics:

1. a total hydraulic residence time of up to 16 minutes;
2. a large length to diameter ratio to minimize the potential for flow short-circuiting and to provide a residence time distribution with plug-flow type characteristics; and
3. a diameter sufficiently large to minimize turbulence and micro-mixing.

The serpentine arrangement of the piping shown in Figure 5-1 was primarily for convenience. With this experimental contactor design, less than 5% of the hydraulic residence time was required for the task of ozone dissolution. The remaining 95% of the system hydraulic residence time, which was accounted for in the reactive flow segment, was dedicated to the microorganism inactivation function.

## **5.2 MANIPULATED EXPERIMENTAL VARIABLES**

The key manipulated experimental variables of the experimental ozone contactor and the nominal ranges of each are summarized in Table 5-1. The two variables governing the hydrodynamic conditions of gas-liquid contact within the static mixer were the superficial liquid velocity,  $v_s$ , and the gas-to-liquid volumetric flow rate ratio,  $G/Q_f$ . The superficial liquid velocity,  $v_s$ , was defined by the ratio of feed water volumetric flow rate,  $Q_f$ , and the internal empty pipe cross sectional area of the static mixer,  $A$ :

$$v_s = \frac{Q_f}{A} \quad \text{Equation 5-1}$$

The height of the bubble column,  $H$ , was introduced as an additional experimental variable that might impact the overall efficiency of gas-liquid mass transfer in the static mixer/bubble column system. The height of the column was varied between experiments by adding or removing vertical column sections.

Table 5-1 Manipulated variables in the experimental static mixer ozone contactor.

Variable	Symbol	Unit	Nominal Range
Feed Water Flow Rate	$Q_f$	L/min	7.5 to 15
Static Mixer Superficial Velocity	$v_s$	m/s	0.7 to 1.4
Gas to Liquid Volumetric Flow Rate Ratio @ 20°C and 1 atm	$G/Q_f$	%	1.2 to 4.1
Bubble Column Height	$H$	mm	45, 121, 225
Initial Ozone Concentration (at Reactive Flow Segment Inlet)	$C_0$	mg/L	0.1 to 1.2
Cumulative Theoretical Hydraulic Residence Time	$\tau$	min	4.5, 6, 12.2, 16

The conditions of dissolved ozone contact were determined primarily by the initial dissolved ozone concentration at the inlet to the reactive flow segment,  $C_0$ , and the hydraulic residence time in the reactive flow segment,  $\tau$ . For a given combination of water flow,  $Q_f$ , and  $G/Q_f$ , a desired  $C_0$  target was arrived at by adjusting the concentration

of ozone in the supplied ozone feed gas. Thereby,  $C_0$  could be maintained at a fixed target independent of the settings of  $Q_f$ ,  $v_s$ ,  $G/Q_f$  or  $H$ . The hydraulic residence time,  $\tau$ , was determined by the flow rate of water through the reactive flow segment and the length (and, therefore, volume) of the reactive flow segment. As indicated in Table 5.1, the length of the reactive flow segment and the total contact time could be varied between experiments as desired by adding or removing sections of piping.

### **5.3 INDEPENDENT CONTROL OF OZONE DISSOLUTION HYDRODYNAMICS AND DISSOLVED OZONE CONTACT**

The water flow leaving the top of the bubble column,  $Q_f$ , was split. One part,  $Q_{RFS}$ , was diverted to the reactive flow segment and the remainder was diverted to waste. Flow splitting is not a normal component of a functional water ozonation system but was incorporated into the experimental contactor to provide a measure of experimental flexibility. Most importantly, this feature enabled independent variation of the gas-liquid conditions within the static mixer and bubble column, and the conditions of dissolved ozone contact within the reactive flow segment. For example, to increase the efficiency of ozone dissolution, the feed water flow rate could be increased from 7.5 to 15 L/min. This would result in an increase of the superficial velocity in the static mixer from about 0.7 m/s to 1.4 m/s, with corresponding increases in the pressure drop and the rate of energy dissipation. By appropriate adjustment of the valve positions and the power level on the ozone generator, the water flow rate and initial ozone concentration at the inlet of the reactive flow segment could be maintained at the desired targets.

### **5.4 RESPONSE VARIABLES**

The primary response variables in the experimental study were the efficiency of ozone dissolution and the efficiency of microorganism inactivation. The efficiency of ozone dissolution was interpreted in terms of the ozone transfer efficiency ( $TE$ ). The  $TE$  measured the percent of ozone applied to the contactor with the feed gas that was actually transferred to the liquid. Because it is a direct measure of how efficiently the ozone is used, the  $TE$  is the performance parameter favoured by design engineers and is often used

as a design specification in ozone systems (Rakness et al. 1988). It should be noted here that the objective of the study was not to conduct a detailed study or a mechanistic modeling exercise of the mass transfer fundamentals in the static mixer system. The *TE* was intended to provide a simple means of assessing the mass transfer efficiency in the experimental ozone contactor.

Microorganism inactivation in the experimental static mixer contactor was determined in experiments in which prepared suspensions of microorganisms were seeded into the feed water while the unit was operate at a steady-state, continuous-flow ozonation condition. The level of inactivation was quantified by recovery and enumeration of live microorganisms in the feed and treated water streams. For *Bacillus subtilis* spores, the concentration of live microorganisms was determined by standard bacterial plate counts. For the encysted protozoa, *Cryptosporidium parvum* and *Giardia muris*, previously established animal infectivity assays were selected as the means of measuring microorganism viability.

The kinetics of inactivation of the microorganisms studied were established in batch ozone reactors. This information was combined with the measured ozonation and macro-mixing conditions within the experimental contactor to produce predictions of inactivation. Predicted inactivation was then compared to measured inactivation to assess the microorganism inactivation efficiency of the contactor. Ozonation conditions were determined by direct measurement of the dissolved ozone concentration profile and the residence time. Macro-mixing conditions were characterized by the residence time distribution and were measured in tracer dye experiments. Depending on the microorganism, the kinetic models of microorganism inactivation by ozone were either extracted from previously published studies, or were developed in a separate series of experiments in batch reactors. For *C. parvum*, the non-linear Horn-type kinetic model developed by Gyürék and co-workers (1999) for inactivation of oocysts in phosphate buffered ultrapure water served as the reference kinetic model. For *G. muris*, a modified version of a similar model reported by Finch and co-workers (1993b) was used as the reference. The kinetics of inactivation of *B. subtilis* spores by ozone were determined in series of batch-reactor experiments conducted as part of this study.

## **5.5 VARIABLE CONTROL**

Accurate comparison between microorganism inactivation observed in ozone studies is often hampered by differences in:

1. the species, strains or culture methods of the microorganisms;
2. the methods used to assess microorganism viability;
3. the characteristics of the test waters used; and
4. the methods used for measuring the ozone concentration and determining the exposure to dissolved ozone.

If these variables are not carefully controlled or adequately accounted for, extrapolation of bench-scale inactivation results to larger flow systems and determination of inactivation efficiency will be inaccurate. In this experimental study, the impact of these variables was eliminated or minimized by ensuring the sources of microorganisms, viability determination methods, and ozone measurement techniques used in the ozone contactor experiments corresponded, as much as possible, to those used in the reference batch reactor studies. For example, the same mouse infectivity assays and ozone measurement techniques used by others (Finch et al. 1993b; Gyürék et al. 1999; Li et al. 2001) to derive kinetic models for *C. parvum* and *G. muris* inactivation by ozone were used to measure inactivation of these microorganisms in the experimental static mixer contactor. Identical methods of spore culturing and enumeration were used for both batch reactor and static mixer contactor studies with *B. subtilis*. These measures ensured that the number of variables potentially affecting microorganism inactivation in the static mixer ozone contactor was reduced to one, namely, the hydrodynamics of mixing of the contactor.

## **5.6 SELECTION OF THE EXPERIMENTAL WATER SOURCE**

The batch reactor experiments used to develop the kinetic models for *C. parvum* (Gyürék et al. 1999; Li et al. 2001) and *G. muris* (Finch et al. 1993b) inactivation by ozone were carried out in prepared, phosphate-buffered ultrapure water. Operation of the experimental static mixer required quantities of water much greater than could be synthetically prepared in a normal laboratory. Building potable tap water was selected as

**a convenient and relatively high quality water source for all trials with the experimental contactor.**

## 6 EXPERIMENTAL MATERIALS AND METHODS

### 6.1 STATIC MIXER OZONE CONTACTOR MATERIALS AND METHODS

#### 6.1.1 Details of the Experimental Static Mixer Ozone Contactor

A detail schematic diagram of the experimental static mixer ozone contactor is provided in Figure 6-1. Physical details of the unit and of the experimental operation of the unit are provided in the following sections.

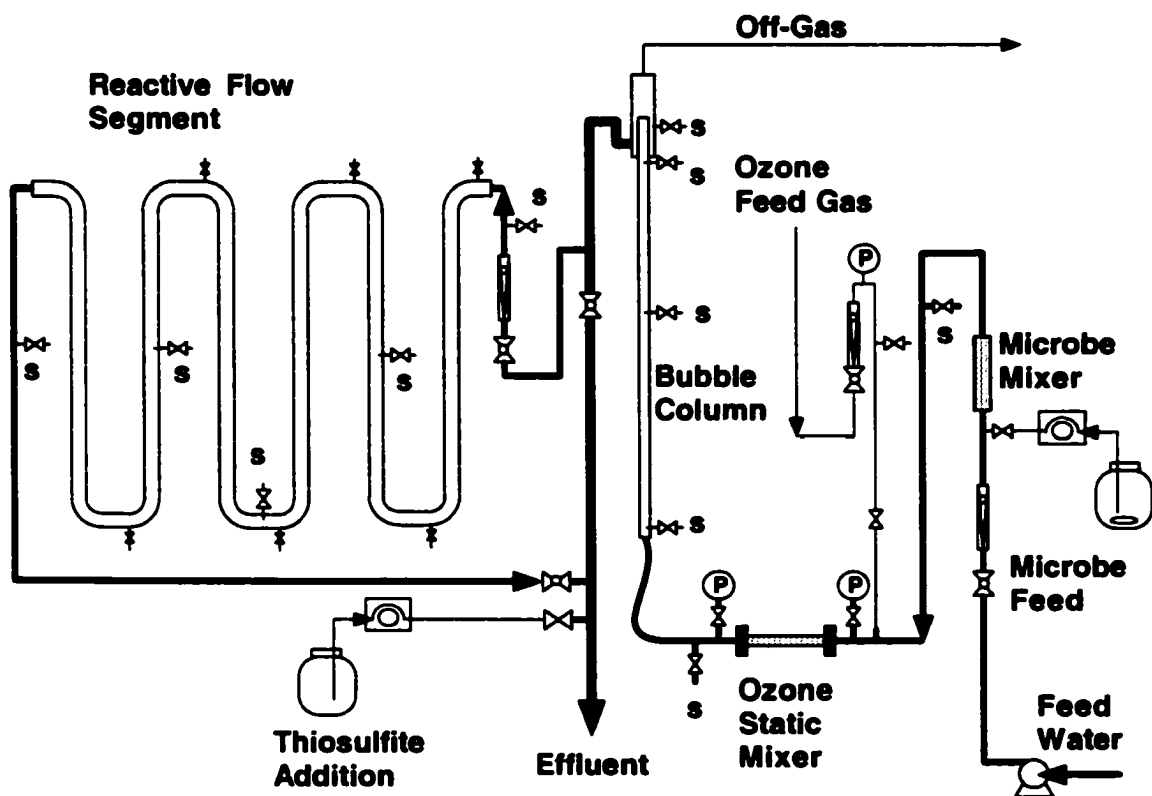


Figure 6-1 Detailed schematic of the experimental static mixer ozone contactor. Locations of liquid sampling points are indicated by the symbol "s".

For all experiments, the water source was tap water in room 219 of the Environmental Engineering Building at University of Alberta, Edmonton, AB. Tap water was supplied from the EPCOR Rossdale Water Treatment Plant in Edmonton. This plant

provides full conventional treatment including coagulation with alum and polymers, flocculation, settling, chlorination, dual media filtration and ammonia addition. Hot and cold tap water sources were blended to provide water at the desired experimental temperature to within  $\pm 1^\circ\text{C}$ . The combined water was passed through a set of activated carbon (F-400, Calgon Carbon, Pittsburgh, PA) columns to reduce the combined chlorine concentration from 2 mg/L to less than 0.2 mg/L. The chlorine-reduced water was then diverted to a 1000 L polyethylene storage tank. During experiments, water from the storage tank was pumped to the experimental static mixer contactor via a centrifugal pump. The flow was regulated by a ball valve and measured with an in-line flowmeter.

Ozonized gas was produced by passing extra-dry oxygen (Praxair, Edmonton, AB) through an air-cooled corona discharge generator (Doman Ozone, Edmonton, AB). Gas flow was regulated by an in-line rotameter equipped with a fine needle valve (Model P-03219-15, Cole Palmer, Niles, IL). Gas was introduced into the contacting system through a 3 mm ID Teflon<sup>®</sup> tube into the center of the feed water flow in the 19 mm ID polyvinyl chloride (PVC) pipe directly upstream of the static mixer. The water-gas mixture then flowed through a 15.7 mm ID Sulzer SMV static mixer fitted with three 15 mm corrugated-type structured stainless-steel elements. The arrangement of the static mixer elements within the static mixer spool piece is depicted in Figure 6-2. Including the space between the elements, the total internal mixing length and volume were 75 mm and 15 mL, respectively. The gas-liquid mixture leaving the static mixer flowed into the bottom of a 38 mm ID vertical bubble column via a 16 mm ID  $\times$  1 m section of clear polyvinyl chloride tubing. Off-gas was separated from the liquid at the top of the column by means of a circular overflow weir. The height of the column could be adjusted to 0.45 m, 1.2 m or 2.3 m by adding or removing column sections.

The flow of the gas-free, ozonated liquid from the weir was split. About 2 L/min was diverted to the reactive flow segment and the remainder was diverted to waste. This flow split was controlled by means of a regulating valve and an in-line flowmeter (Model P-324720-01, Cole Palmer) on the flow to the reactive flow segment. The reactive flow segment consisted of a 15 m length of 51 mm ID PVC, arranged in a serpentine fashion with six vertical sections of 2.2 m length each and six horizontal sections of 0.28 m each

connected with 90 degree elbow bends. The length of the reactive flow segment could be varied between experimental trials by adding or removing piping sections.

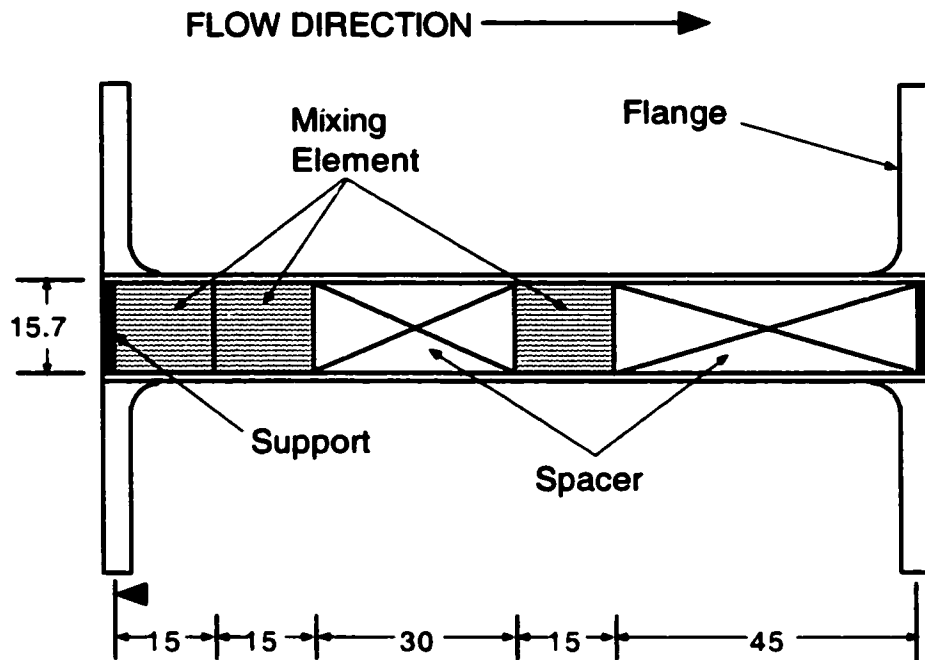


Figure 6-2 Detail of the internals of the Sulzer SMV static mixer. All dimensions are in mm.

A well-mixed suspension of microorganisms was seeded into the flowing feed water at a controlled rate using a variable speed peristaltic pump (Model 7553-70, Cole Palmer). Seeded microorganisms were blended with the flowing water by means of an in-line mixer (Model U-04669-92, Cole Palmer) located downstream of the microorganism addition point, but upstream of the ozone addition point and ozone static mixer. Capability for withdrawal of liquid samples was provided at various locations in the system as indicated in Figure 6-1. All sampling tubes and valves were constructed of Teflon<sup>®</sup> to minimize reaction with dissolved ozone, and were designed to withdraw the sample from the flowing liquid at a point located at distance from the inside of pipe

equivalent to 1/3 of the pipe diameter. Provision was also made for sampling of the ozonized feed gas and the off-gas from the top of the bubble column. All in-line flowmeters used for liquid flow measurement were calibrated by a timed collection and weight measurement and the calibrations were checked for each experimental trial. The pressure at the inlet and the outlet of the static mixer and at the outlet of feed gas rotameter was measure by pressure gauges. The feed gas rotameter was calibrated using a wet test meter (GCA/Precision Scientific, Chicago, IL). Gas flow was corrected for system pressure and temperature and reported in litres per minute (L/min) at 0°C and 1 atm.

The ozone in the effluent streams from the reactive flow segment and the bubble column was neutralized by continuous addition of sodium thiosulfite solution. For experiments with the human pathogenic organism *C. parvum*, the combined effluents were collected into a containment tank (not shown in Figure 6-1) and decontaminated by heating to 70°C and retaining that temperature for a minimum of one hour. Most of the system components were constructed of polyvinyl chloride (PVC) plastic to minimize reaction with ozone. The main sections of the bubble column and the reactive flow segment were fabricated of clear PVC to enable visual observation of mixing patterns during tracer experiments with methylene blue colored dye.

### 6.1.2 Ozone Transfer Efficiency Measurements

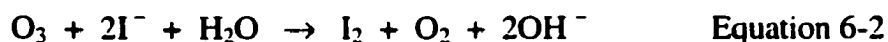
The following definition was use to calculate ozone transfer efficiency, *TE* (Langlais et al. 1991):

$$TE (\%) = \frac{Y_f - Y_o}{Y_f} \times 100\% \quad \text{Equation 6-1}$$

where  $Y_f$  and  $Y_o$  are the concentrations of ozone in the feed-gas and off-gas (in g/L), respectively. For the experimental static mixer ozone contactor,  $Y_f$  was the concentration of ozone in the gas from the ozone generator and  $Y_o$  was the concentration of ozone in the off-gas leaving the top of the bubble column. This transfer efficiency measurement,

therefore, incorporates the ozone transfer that occurs in the static mixer, the gas-liquid separator and any interconnecting piping and tubing.

The ozone concentrations in the feed-gas and in the off-gas were measured by the potassium iodide absorption method recommended by the International Ozone Association for determining gas-phase ozone concentrations (Masschelein et al. 1998). With the static mixer unit operating at steady-state, and after sufficient time was allowed to purge the gas headspace above the liquid at the top of the bubble column, the gas flow was diverted to the gas sampling apparatus depicted in Figure 6-3. The apparatus consisted of a gas-washing bottle filled with 300 mL of a solution of 5% reagent grade potassium iodide (Fisher Scientific Canada, Nepean, Ont.) prepared in de-ionized water. The sparging tube of the washing bottle was fitted with a drawn tip with a 0.5 mm diameter orifice that minimized back-pressure on the bubble column. The total volume of gas processed through the wash bottle was measured with a wet test meter (GCA/Precision Scientific). The ozone absorbed by the solution in the washing bottle rapidly reacts with iodide ion to liberate free iodine as follows:



After sampling was complete, the solution in the bubbler was acidified by addition of 10 mL of 1 N HCl solution (Fisher Scientific) and then titrated to a clear endpoint with 0.1 N certified grade sodium thiosulfate standard solution (Fisher Scientific) according to:



The volume of gas collected was corrected for ambient temperature, pressure and moisture content and reported in litres (L) of dry, ozone-free gas at NTP (0°C and 760 mmHg). The gas sample size for each analysis was between 1 and 2 L. The ozone concentration in the gas was calculated from the following equation:

$$Y = 24 \frac{N_{thio} V_{thio}}{V_g} \quad \text{Equation 6-4}$$

where  $N_{thio}$  is the normality of the thiosulfate titrant (0.1 N),  $V_{thio}$  is the volume of the thiosulfate titrant added (mL), and  $V_g$  is the total volume of the ozone gas collected in litres at NTP. The sample tubing used to collect the gas samples was composed of Teflon® PFA in order to minimize ozone gas decomposition.

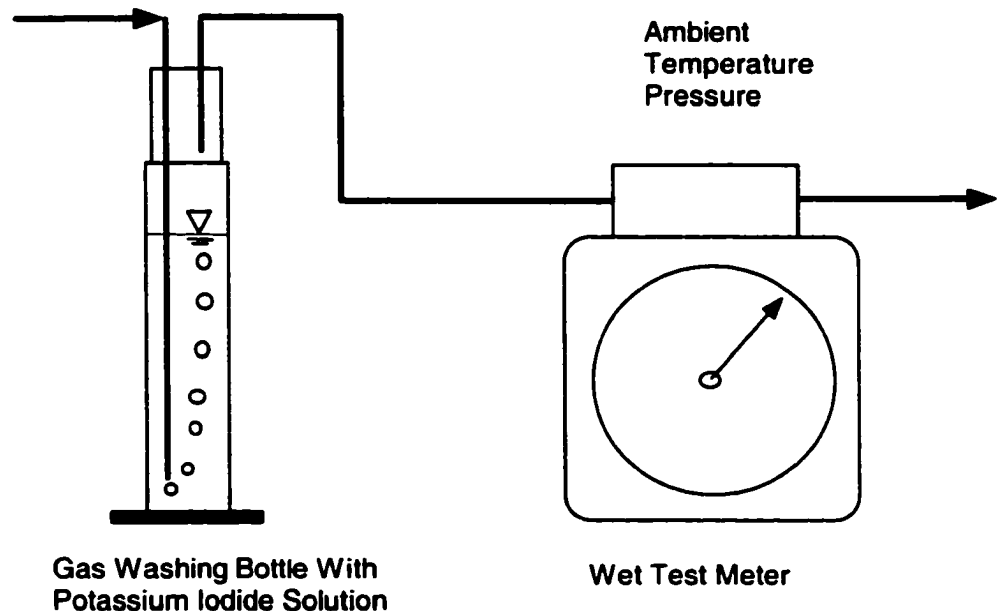


Figure 6-3 Apparatus used for sampling and determination of ozone concentration in static mixer ozone contactor feed gas and off gas.

### 6.1.3 Residence Time Distribution

The residence time distribution (RTD) was determined at each microorganism sampling point in the static mixer ozone contactor from the results of pulse-input tracer

tests conducted using methylene blue dye. For these tests, concentrated solutions (2 and 12.5 mg/L) of methylene blue (certified grade, Sigma Chemical Co., St. Louis, MO) were prepared in 5% glacial acetic acid (Fisher Scientific). With the static mixer contactor operating at a steady-state flow condition, between 10 and 20 mL of the concentrated dye solution was rapidly injected into the feed water at time equal to zero. A piece of 3 mm diameter Teflon® tubing was affixed to the end of a 60 mL plastic syringe to allow introduction of the tracer directly into the center of the 19 mm ID feed water pipe upstream of the microorganism in-line mixer. During the tracer experiments, the power to the ozone generator was shut off to avoid de-colorization of the dye by reaction with ozone. For each experiment, the dye concentration was monitored at the selected downstream location by diverting a side-stream of the flow through a 10 mm quartz spectrophotometric flow cell mounted inside a Hewlett Packard (Wilmington, DE) 8452A diode-array spectrophotometer. The absorbance at 652 nm was measured and recorded at 1 s intervals. The time required for the sample to reach and flush the flow cell was estimated to be 12 s.

The methods of classical residence time theory apply only for closed vessels. Deviations from the closed vessel conditions during tracer experiments can result in errors in the determination of mean residence time (Levenspiel and Turner 1970). The locations for downstream monitoring of the tracer dye concentration were, therefore, carefully chosen to ensure good radial mixing of the dye and adherence to the closed vessel requirements. For this reason, samples were withdrawn from locations where the liquid was well-mixed radially. To determine the RTD of the static mixer and bubble column combination, the dye concentration was monitored in the 7.7 mm ID sample pipe that connects outlet of the bubble column with the inlet of the reactive flow segment. For the RTD of the static mixer + bubble column + reactive flow segment combination, the dye concentration was monitored in the narrow 7.7 mm pipe at the exit of the reactive flow segment.

The normalized exit age distribution function,  $E(t)$ , at the downstream sampling location was estimated at each sampling instance according to:

$$E(t) = \frac{C_t(t)}{\int_0^{\infty} C dt} \equiv \frac{C_{avg,i}}{\sum_{i=0}^{i=t} C_{avg,i} \Delta t} \quad \text{Equation 6-5}$$

where  $C_t$  is the measured tracer absorbance at time  $t$ ,  $\Delta t$  is the sampling interval of 1 s and  $C_{avg,i}$  is the average dye absorbance at  $i = t$  given by:

$$C_{avg,i} = \frac{C_i - C_{i-1}}{2} \quad \text{Equation 6-6}$$

Tracer experiments were conducted in triplicate for each sample point.

#### 6.1.4 Microorganism Inactivation Experiments With *B. subtilis*

For all microorganism inactivation experiments, the static mixer contactor was operated at steady-state, with continuous addition of water, ozonized gas and microorganism suspension. For *B. subtilis* experiments, a quantity (30 to 60 mL) of prepared spore stock suspension was added to 6 L of distilled water in an 8 L plastic bottle together with a large, Teflon-coated magnetic stir bar. The bottle was sealed and shaken well to disperse the microorganisms, and then placed on a magnetic stir plate. The peristaltic pump speed was adjusted to provide a volumetric feed rate of the spore suspension of approximately 0.1 L/min. The volume of stock suspension and the suspension feed rate were chosen to provide a spore concentration of between  $2 \times 10^5$  and  $1 \times 10^6$  CFU/mL in the blended feed to the static mixer contactor.

Prior to the start of microorganism addition, the static mixer contactor was operated at the target steady-state ozonation condition for approximately 30 min to allow the ozone concentration in the water to stabilize. After this warm-up period, ozonation conditions were maintained constant and the microorganisms were continuously added to the feed for approximately 60 min. RTD analysis of the results of pulse tracer test experiments showed that 30 minutes was sufficient to allow the concentration at the exit

of the contactor to reach 98% of steady-state (the  $t_{98}$ ). Therefore, after 30 min of continuous microorganism addition, samples were collected from the static mixer feed and outlet, the inlet to the reactive flow segment and at four additional downstream locations in the reactive flow segment. Samples for spore enumeration (approximately 100 mL) were collected directly into bottles containing a 0.75 mL of 0.1 N certified sodium thiosulfate standard solution (Fisher Scientific), sufficient to neutralize the remaining dissolved ozone. Additional samples were collected for measurement of dissolved ozone, water temperature, pH and combined chlorine concentration. Samples for spore enumeration and dissolved ozone analysis were collected in triplicate. To avoid disturbance of steady-state conditions, sample collection started at the exit of reactive flow segment and proceeded progressively from downstream to upstream sample points. Procedures for enumeration of the spores in the collected samples by the membrane filtration method (see Section 6.3.2) were commenced immediately.

#### **6.1.5 Experiments With *C. parvum***

A purified suspension containing between  $2 \times 10^8$  and  $5 \times 10^8$  *C. parvum* oocysts in about 2 mL of Milli-Q<sup>®</sup> de-ionized water, prepared as described in Section 6.4.1, was added to a 4 L glass Erlenmeyer flask containing 3 L of deionized water. A large Teflon magnetic stir bar was added and stirring was commenced. Once the static mixer contactor was stabilized at the ozone target condition for 30 min, continuous addition of the oocyst suspension to the static mixer feed stream was started. The resulting concentration of oocysts in the feed stream was approximately  $1 \times 10^6$  oocysts/L.

After a time equal to the  $t_{98}$  had elapsed, samples were collected for recovery of oocysts and for dissolved ozone, temperature, pH and combined chlorine analysis. For oocyst recovery, 2 L each of the static mixer feed and outlet sample were collected into 2 L glass Erlenmeyer flasks into which 20 mL of a 0.1 N certified thiosulfate standard solution (Fisher Scientific) had been added. An 8 L sample of the outlet stream from the reactive flow segment was collected into two 4 L glass Erlenmeyer flasks into which 40 mL of a thiosulfate solution had been added. All sample flasks were gently stirred during sampling to ensure immediate neutralization of the dissolved ozone by the sodium thiosulfate.

The oocysts were recovered from the neutralized samples in the Erlenmeyer flasks by filtering the entire sample through a 47 mm polycarbonate track-etched membrane with a 0.8 micron pore size (Model K08CP04700, Osmonics, Minnetonka, MN) using a suction filtration apparatus. Oocysts were scraped and washed from the membrane using a rubber policeman and all the wash water was collected into 40 mL Teflon® lined plastic centrifuge tubes. Infectivity of the oocysts in the sample was determined using the neonatal CD-1 mouse model as described in Section 6.4.2.

#### **6.1.6 Experiments With *G. muris***

Experiments with *G. muris* cysts were similar to those with *C. parvum* except that larger samples (8 L versus 2 L) of the static mixer feed and outlet samples were collected. The feed suspension was prepared by adding between  $6 \times 10^6$  and  $13 \times 10^6$  cysts, prepared as described in Section 6.5.1, to 3 L of deionized water. The resulting cyst concentration in the feed water to the static mixer contactor was approximately  $1 \times 10^5$  oocysts/L. Cysts were recovered using the sample membrane filtration as describe for *C. parvum* oocysts in Section 6.1.5. Cyst recovery was enhanced by addition of a small amount 0.01% enzyme grade Tween 20 (Fisher Scientific) to the sample flasks during the rinse step. Infectivity of recovered cysts was determined using the latent period infectivity model in C3H/HeN mice as described in Section 6.5.3.

#### **6.1.7 Dissolved Ozone Measurement**

The inherent instability, reactivity and volatility of ozone make measurement in aqueous solution difficult, and different measurement techniques have yielded different results (Gordon et al. 1988). For this study, two measurement methods were used for aqueous-phase ozone concentration measurement; (1) direct ultraviolet (UV) absorbance and (2) the indigo trisulphonate colorimetric method. The UV method was selected as the primary measurement technique to allow for a direct comparison to the available kinetic models for inactivation of *C. parvum* (Gyürék et al. 1999) and *G. muris* (Finch et al. 1993b). These kinetic models were developed based on direct UV absorbance measurements of ozone at a wavelength of 260 nm and using the molar absorbance coefficient of  $3300 \text{ M}^{-1}\text{cm}^{-1}$  reported by Hart and co-workers (1983). The UV method

has the advantage that it directly measures a fundamental property of the ozone in solution, however it suffers from two major drawbacks. Firstly, it is vulnerable to interferences from the UV absorbance spectrums of other compounds that may be present in the water. Therefore, its use is limited to high quality waters that are relatively free from background interferences. Secondly, values for the molar absorbance of ozone in water at the wavelength range of 258 to 260 nm that have been reported in the literature range from 2900 to 3600 M<sup>-1</sup>cm<sup>-1</sup> (Gordon et al. 1988). To address the UV interference issue a colorimetric method, based on the reaction between ozone and the dye indigo trisulphonate, was developed by Bader and Hoigné (1981; 1982). The indigo method been accepted as the standard method for manual determination of ozone in natural waters by the International Ozone Association (Masschelein et al. 1998) and others (APHA AWWA WEF 1992). Therefore, parallel measurements of dissolved ozone were made using the indigo method to enable comparisons of the results of this study to other data sets.

For the direct UV measurements, the sampling tube on the static mixer apparatus and a 10 mm quartz cuvette were first rinsed thoroughly with sample. The cuvette was then filled with fresh sample and quickly placed into an Ultrospec 2000 (Pharmacia Biotech, Cambridge, UK) UV/visible spectrophotometer. The absorbance at 260 nm was immediately recorded. For low concentration ozone samples (less than 0.2 mg/L), a 50 mm quartz cuvette was used to increase method sensitivity. A reference blank was prepared by collecting a 200 mL sample of water from the outlet of the static mixer unit reactive flow segment, after several minutes of contact with dissolved ozone. The ozone in the sample was neutralized by addition of 0.20 mL of 1 M sodium formate solution (BDH Co., Toronto, Ont.) and the absorbance was measured at 260 nm. The ozone concentration in the sample, *C*, in mg/L was determined from the following equation:

$$C = [A_{260, \text{sample}} - A_{260, \text{reference}}] \times 14.45 \quad \text{Equation 6-7}$$

where  $A_{260, sample}$  is the absorbance of the sample and  $A_{260, reference}$  is the absorbance of the reference. The proportionality factor 14.45 is derived from the molar absorbance of 3300  $M^{-1}cm^{-1}$  and the molecular weight of ozone of 48,000  $mg \cdot mol^{-1}$ .

The standard method for determination of dissolved ozone by indigo trisulphonate (APHA AWWA WEF 1992; Bader and Hoigné 1981;1982) was used with some modification. A concentrated indigo trisulphonate stock solution was prepared by dissolving 0.770 g of 5,5'-7 indigosulfonic acid (Catalogue no. I-3007, Sigma Chemical Co.) and 1 mL of reagent grade concentrated phosphoric acid (Fisher Scientific) in de-ionized water up to 1 L. A working solution was then prepared by dissolving 100 mL of the stock solution, 11.5 mg of  $NaH_2PO_4 \cdot H_2O$  and 7 mL of concentrated phosphoric acid into de-ionized water up to 1 L. Ozonated water sample from the static mixer unit was allowed to flow into a 250 mL glass Erlenmeyer flask that had previously been made ozone demand-free. The end of the sampling tube was submerged below the surface of the liquid in the flask to minimize loss of ozone by evaporation. With the sample flowing, a 10 mL aliquot of the ozonated water was slowly withdrawn from the flask at from a point near the open end of the sampling tube using an Oxford Macroset pipette (Oxford Labware, St. Louis, MO). The pipette was fitted with a plastic tip that was previously made ozone demand-free (ODF). The aliquot was immediately dispensed into a vial containing 2, 5 or 10 mL of indigo reagent, with the tip of the pipette immersed below the liquid surface of the indigo reagent. For those samples in which combined chlorine was known to be present, an aliquot (0.100, 0.25 or 0.5 mL) of malonic acid reagent was added to the indigo reagent prior to sampling to mask potential interference. The malonic acid reagent was prepared by dissolving 5 g of reagent grade malonic acid (Fisher Scientific) up to 100 mL of de-ionized water. A reference blank was prepared by adding 10 mL of a sample of non-ozonated water from the feed tank of the static mixer contactor to the indigo reagent. The absorbance of the sample at 600 nm was measured on an Ultrospec 2000 UV/visible spectrophotometer using a 10 mm quartz cell. The ozone concentration,  $C$ , in mg/L was calculated according to the following equation:

$$C = \frac{(A_{600,blank} - A_{600,sample}) \cdot V_{total}}{f \cdot V_{sample}} \quad \text{Equation 6-8}$$

where  $A_{600,blank}$  and  $A_{600,sample}$  are the absorbances at 600 nm in a 10 mm cell for the blank and the sample, respectively, and  $V_{sample}$  and  $V_{total}$  are the volumes of original sample and the total volume of sample, indigo reagent and malonic acid in mL, respectively. The value of the sensitivity coefficient,  $f$ , used in this work was  $0.42 \text{ Lmg}^{-1} \text{ cm}^{-1}$  and is based on a molar absorbance coefficient of  $20\,000 \text{ M}^{-1} \text{ cm}^{-1}$  and stoichiometric reaction between ozone and indigo (Bader and Hoigné 1981).

## 6.2 BATCH REACTOR EXPERIMENTS

Microorganism inactivation experiments were conducted in well-stirred batch reactors using methods and materials very similar to those used by others to study the inactivation kinetics of *C. parvum* (Gyürék et al. 1999; Li et al. 2001) and *G. muris* (Finch et al. 1993b). The batch reactor apparatus is illustrated in Figure 6-4. The water matrix for experiments was either samples of water collected from the feed tank of the static mixer ozone contactor during experimental trials, or ozone demand-free phosphate buffer prepared in ultrapure de-ionized water (see Section 6.6.2 for preparation details). Suspensions of microorganisms were prepared in 200 mL of water matrix and then exposed to dissolved ozone in 250 mL Erlenmeyer reactor flasks. All material used in the batch reactor experiments, including glassware, stir bars and pipette tips, were made ozone demand-free (ODF) prior to use (Section 6.6.1).

For experiments with *B. subtilis*, an aliquot of prepared spore stock solution (see Section 6.3.1) was first diluted in an appropriate volume of the test water in a 50 mL plastic centrifuge tube. The contents of the tube were then mixed vigorously on a Maxi-Mix vortex mixer (Thermolyne Co., Dubuque, IO) at a high setting for 2 min to promote the break up of spores agglomerates. A 5 mL aliquot of the diluted, vortex-mixed spore suspension was then added to the test water in the reactor flask to provide a starting spore concentration of between  $1 \times 10^5$  and  $2 \times 10^6$  CFU/mL. For experiments with *C. parvum*, a suspension of purified and washed oocysts was prepared in about 0.5 mL of de-ionized

water in 5 mL plastic tube (see Section 6.4.1). The contents of the tube were vortex mixed at a high setting for 30 seconds and then transferred to the water in the reactor flask. The concentration of oocysts in the flask was  $5 \times 10^7$  oocysts/mL.

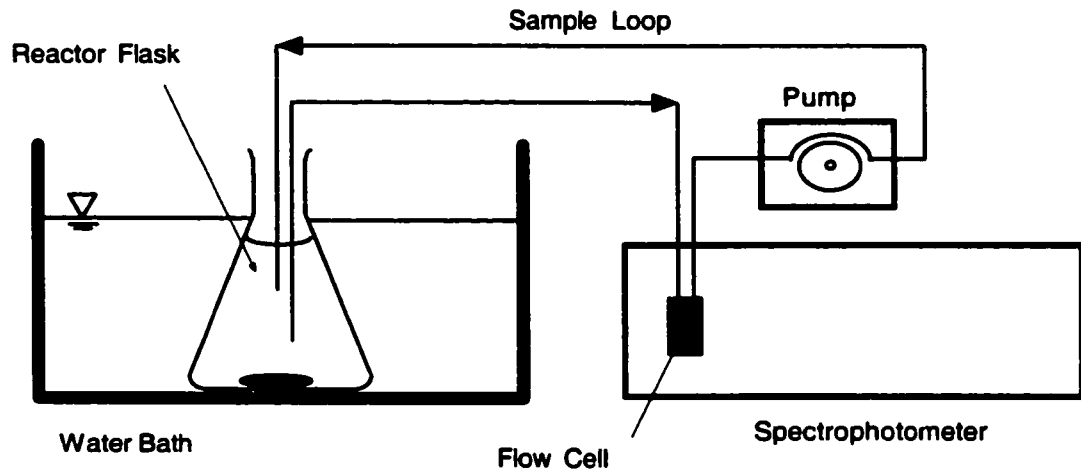


Figure 6-4 Apparatus used for microorganism inactivation experiments in well-mixed batch reactors with continuous dissolved ozone monitoring by UV absorbance.

Throughout the contact period, the microorganism suspension was continuously stirred by means of a Teflon<sup>®</sup>-coated magnetic stir bar. The reactor flask was immersed into a temperature-controlled water bath to control the reaction temperature to within  $\pm 0.5^\circ\text{C}$  of the specified target. Prior to ozone addition, the microorganism suspension was left in the water bath with stirring for 15 minutes to equilibrate to the experimental conditions. The temperature of the suspension was measured to make sure that the temperature was within  $\pm 0.5^\circ\text{C}$  of the target. Ozone stock solution was prepared by bubbling ozone gas through 300 mL of de-ionized water cooled to between 1 to  $4^\circ\text{C}$  in an ice chest. An aliquot of ozone stock solution was transferred to the stirred microorganism suspension in the reactor flask using a calibrated Oxford Macroset Pipette fitted with an ODF tip. The tip of the pipette was inserted just below the surface of the

suspension in the flask to minimize the loss of ozone by volatilization during the transfer. The concentration of ozone in the stock solution was determined both before and after the transfer by direct measurement of UV absorbance at 260 nm and assuming a molar absorption coefficient of  $3\,300\text{ M}^{-1}\text{cm}^{-1}$ . Absorbance measurements were made on an Ultrospec 2000 UV/visible spectrophotometer using a 10 mm quartz cuvette.

The dissolved ozone concentration in the suspension was monitored continuously by direct UV absorbance on a Hewlett Packard (Wilmington, DE) model 8452A diode-array spectrophotometer equipped with a 10 mm quartz continuous-flow cell. A molar absorbance coefficient of  $3\,300\text{ M}^{-1}\text{cm}^{-1}$  (Hart et al. 1983) was assumed. In addition to the UV measurement, samples were removed from the reactor flasks at intervals using an Oxford Macroset Pipette fitted with an ODF tip and analyzed using the indigo trisulphonate colorimetric method (Section 6.1.7). At the end of the prescribed contact time, 0.2 mL of 1 M reagent grade sodium formate solution (BDH Co.) was added to the flask to neutralize the remaining dissolved ozone.

For *B. subtilis* experiments, three 10 mL samples were removed from the flask for enumeration of viable spores by the membrane filtration method (Section 6.3.2). For *C. parvum* experiments, the contents of the reactor were transferred to a 250 mL plastic centrifuge tube and the oocysts recovered using the procedure described in Section 6.4.2. For each set of batch experiments, a control flask was established using the same procedures and conditions as the experimental flasks, but without addition of ozone.

### **6.3 BACILLUS SUBTILIS METHODS**

#### **6.3.1 Spore Production**

A sample of spores of *Bacillus subtilis* strain number 6633 was obtained from American Type Culture Collection (ATCC, Manassas, VA). A portion of the freeze-dried spore sample was added to nutrient broth and the broth culture was incubated for 1 to 2 days at 35°C to generate vegetative cells. For propagation of spores, 1 mL of the vegetative cell suspension was inoculated onto a layer of R2A agar in 1 L flasks along with a small amount (15 to 20 mL) of 0.05 M phosphate buffer (pH 6.0). After 14 to 16 days of incubation at 35°C, the spore suspension was collected from the agar and was

washed 3 times in ODF pH 8, 0.05 M phosphate buffer (4500 × g, 10 min). The suspension was then heated to 75°C in a water bath and maintained at this temperature for 20 min to kill any remaining vegetative cells. This spore suspension was then washed one more time in buffer, stored at 4°C and maintained as a mother stock. To generate daughter spore suspensions for experiments, the above process was repeated using a sample of the mother stock as starting material.

### **6.3.2 Enumeration**

Viable spores in experimental samples were enumerated using a membrane filtration method (Barbeau et al. 1997). Decimal dilution series of the experimental samples were prepared using 10 mL of aliquot and 90 mL of sterile peptone dilution water (APHA AWWA WEF 1992). For each analysis, 2 to 4 dilutions were filtered through pre-sterilized 47 mm × 0.45 micron membrane filters (part no. 66586, Gelman Sciences, Ann Arbor, MI) using a vacuum filtration apparatus. The filters were then placed on sterile trypticase soy broth saturated pads in Petri dishes. The dishes were placed in a dry air oven at 70 to 75°C for 20 minutes, to inactivate any vegetative cells, and then into a 35°C incubator. After 22 h to 24 h the plates were removed from the incubator and the number of colonies on each counted to determine the concentration of viable spores in the original sample. For each experimental sample, the entire enumeration procedure, including sample collection, preparation of the dilution series, and plating was done in triplicate. The number of viable spores in the original sample was reported as the log of colony-forming units (CFU) per mL based on geometric average of the triplicate plate counts.

## **6.4 CRYPTOSPORIDIUM PARVUM METHODS**

### **6.4.1 Oocyst Production**

*C. parvum* oocysts used in this study were originally obtained from Dr. Harley Moon (National Animal Disease Control center) and are known as the Iowa strain. Previously established methods of *C. parvum* oocyst production and purification from Holstein calves were used for the UV exposure experiments (Finch et al. 1994; Finch et

al. 1995; Finch et al. 1997). Calves, aged 2 to 4 days were infected with *C. parvum* oocysts and maintained on a diet of electrolyte solution. Feces collected from the calves at the onset of scouring were first passed through a series of sieves (400 to 75  $\mu\text{m}$ ). Oocysts were purified from the sieved feces by cesium chloride gradient centrifugation (Kilani and Sekla 1987). Recent work by others has demonstrated that purification using cesium chloride has no adverse effects on oocyst infectivity (Slifko et al. 2000). The calf diet of electrolyte solution reduced the lipid content of the feces and eliminated the need for the sucrose centrifugation pre-purification step that was used in previous work. Stock suspensions of purified oocysts were stored at 4°C in deionized water with antibiotics (100  $\mu\text{g}/\text{mL}$  streptomycin, 100  $\mu\text{g}/\text{mL}$  gentamicin, 100 U/mL penicillin) and 0.01% Tween 20 (Fisher Scientific).

#### **6.4.2 Determination of Oocyst Infectivity in CD-1 Neonatal Mice**

Neonatal mice have been shown to be good models for determining infectivity of *C. parvum* oocysts (Ernest et al. 1986). A mouse model using outbred neonatal CD-1 mice (Finch et al. 1993c) was used to evaluate infectivity of both fresh *C. parvum* oocysts and oocyst from ozonation experiments. Samples of oocysts suspended in water from ozonation experiments were centrifuged at 27,000  $\times g$  for 10 min at 4°C to concentrate the oocysts for inoculation into the neonatal CD-1 mice. The supernatant was aspirated and the cell pellet re-suspended in deionized water. Oocysts were counted in quadruplicate using a hemacytometer and appropriate dilutions prepared in deionized water for mouse infection. Breeding pairs of outbred CD-1 mice were obtained from the Charles River Breeding Laboratories (St. Constant, Quebec, Canada). The animals were given food and water *ad libitum* and were housed in cages with covers fitted with a 0.22  $\mu\text{m}$  filter in a specific pathogen-free (P-2 level) animal facility. Mice were inoculated intragastrically 5 days after birth with a known number of oocysts suspended in 50  $\mu\text{L}$  of deionized water. Intragastric inoculation was performed using a ball-point neonate feeding needle (24 gauge, Popper and Sons Inc.) attached to a tuberculin syringe. For each experimental sample, 2 to 4 dilutions of oocysts were prepared and cohorts of 5 to 10 mice were inoculated. Processing of the samples and inoculation of animals occurred within 24 h of experimental exposure to ozone.

The infectivity of the oocysts was determined 7 days after infection. The mice were killed by cervical dislocation and the large intestine (rectum to 30 mm anterior to the caecum) was removed and placed in 10 mL of ultrapure water from a Milli-Q® system water. The intestine was homogenized for 45 to 60 s in a Sorvall Omni-Mixer and the homogenate collected into a 15 mL polypropylene test tube. The suspension was centrifuged at  $2000 \times g$  for 15 min. The supernatant was then removed and the pellet was re-suspended in 10 mL of Milli-Q® water containing 0.01% Tween 20, and was centrifuged at  $2000 \times g$  for 15 min. After the second centrifugation, the supernatant was discarded and 20  $\mu\text{L}$  of the viscous pellet was removed and placed into a 6 mL polystyrene flow cytometer test tube fitted with a 35- $\mu\text{m}$  sieve (Becton Dickinson, Franklin Lakes, NJ). The intestinal homogenate was forced through the sieve by adding 400  $\mu\text{L}$  of 1% bovine serum albumen (BSA) in phosphate buffered saline (PBS)(Becton Dickinson). Samples were allowed to incubate for 15 min at room temperature to block non-specific absorption of the monoclonal antibody. One hundred microlitres of a 1:400 dilution of fluorescein labeled anti-*C. parvum* oocyst monoclonal antibody (ImmuCell) diluted in 1% BSA was subsequently added to each sample. The mixture was incubated at 37°C for 30 min.

The resulting suspension was examined for the presence of parasites on a FACScalibur flow cytometer (Becton Dickinson). Settings for the flow cytometer were as follows:

forward side scatter – photodiode voltage equivalent to E00, AmpGain 4.00;

side light scatter – photomultiplier voltage set to 402, AmpGain 4.00; and

FL1 - photomultiplier voltage set to 470.

All flow cytometric analyses were done at a high flow rate using PBS as the sheath fluid. Fifty-thousand events (parasite counts) were collected for each intestinal homogenate sample. Mice were scored as infected with *C. parvum* when the number of events segregating into a defined fluorescence region was greater than 1.25%. At regular intervals, flow cytometric results were confirmed using conventional microscopy methods. Daily negative controls were run in which the infectivity was checked in a

group of mice that were not exposed to oocysts. None of the negative control mice were positive for infection. A complete discussion of the flow cytometric procedures, including a discussion of the rationale for scoring mice as infected and a comparison to conventional microscopy, was presented by Neumann and co-workers (2000a, 2000b).

#### **6.4.3 Interpretation of *C. parvum* Infectivity Data with the Logistic Dose Response Model**

The proportion of mice positive for infection 7 days post-inoculation,  $P$ , was determined for each cohort using the previously described methods. The estimated number of infectious oocysts in the inoculum to each mouse,  $d$ , was then estimated using a logistic dose response model for *C. parvum* oocyst infectivity in the neonatal CD-1 mice. Logistic regression is appropriate for treatment of binary data (Neter et al. 1989). Logistic transformation of the binary infectivity results yield the logistic form of the dose-response model:

$$\ln\left[\frac{P}{1-P}\right] = \beta_0 + \beta_1 \log d \quad \text{Equation 6-9}$$

In Equation 6-9,  $P$  is the proportion of animals in a cohort that become infected subsequent to ingesting a specified live inoculum,  $d$ , of oocysts. The parameters of the logit model,  $\beta_0$  and  $\beta_1$ , were determined for the batch of oocysts used in the ozonation experiments in a series of oocyst dose-response experiments. Cohorts of 5 to 10 neonatal CD-1 mice were inoculated with levels of inoculums ranging from 25 to 200 oocysts per mouse. The number of animals positive for infection at each dose level was determined using the previously described methods. Parameters of the logit model were estimated from the results of the dose response experiments by maximizing the natural logarithm of the likelihood function,  $L$ , for binary data (Neter et al. 1989), given by:

$$\ln L = \sum_{i=1}^{\lambda} Y_i(\beta_0 + \beta_1 X_i) - \sum_{i=1}^{\lambda} \ln[1 + \exp(\beta_0 + \beta_1 X_i)] \quad \text{Equation 6-10}$$

In Equation 6-10, the subscripts  $i = 1, 2, \dots, \lambda$  represent each individual mouse used in the dose response experiment,  $X_i$  is the log (base 10) of the inoculum size for each mouse, and  $Y_i$  is the binary score (0 = not infected, 1 = positive) of each mouse after 7 days. The likelihood function was maximized and the model parameters estimated using the Solver function in Microsoft Excel 2000. Confidence intervals for the logit model parameters were calculated at the  $1-\alpha$  significance level by assuming that the errors of the model were normally distributed and determining the profile for maximum likelihood estimators given by:

$$\ln L_{1-\alpha}(\beta) \geq \ln L_{\max}(\beta) - \frac{1}{2} \chi_{p,\alpha}^2 \quad \text{Equation 6-11}$$

Here  $\beta_0$  and  $\beta_1$  are the logit response parameters,  $\chi_{p,\alpha}^2$  is the chi-squared distribution,  $\ln L(\beta)$  is the likelihood function for normally distributed errors and  $\ln L_{\max}(\beta)$  is the maximum of the  $\ln L$  (Seber and Wild 1989). Approximate 90% confidence intervals were calculated in Microsoft Excel 2000 by varying one parameter at time with the other set at the optimal estimate and satisfying the equality constraint of Equation 6-11.

#### 6.4.4 Characterization of Oocysts Used In Experiments

All oocysts used in this study were from a single batch of oocysts isolated from an infected Holstein calf between May 4 and 8, 2000. Oocysts were used in experiments between 18 and 75 days after isolation. Five dose-response trials were conducted with oocysts from this batch during this time period in order to determine the infectivity characteristics. Detailed information of these dose-response experiments was provided in Table A-1 of Appendix A. Information from the individual dose-response trials was pooled and the logit dose-response model (Equation 6-9) was fit to the pooled data using the maximum likelihood method (Equation 6-10). Because the dose-response

information was pooled, the logit model parameters generated represented the characteristics of the oocysts averaged over the life of the batch. The results of the pooled dose response analysis and the modeling are shown in Figure 6-5 below.

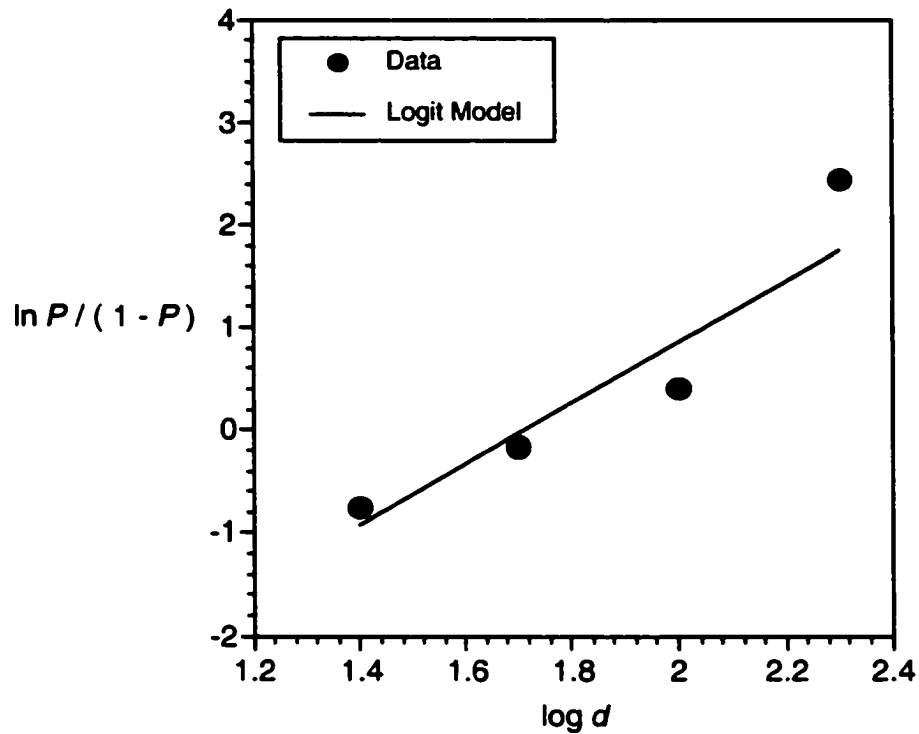


Figure 6-5 Dose-response of *Cryptosporidium parvum* oocysts used in experimental trials and maximum likelihood fit of logit dose-response model.

Best fit logit model parameters and the corresponding 90% confidence intervals were:

$$\beta_0 = -5.09 (-5.3, -4.8) \quad \text{and} \quad \beta_1 = 2.97 (2.8, 3.1)$$

The estimated oocyst dose required for 50% infection in the mice ( $ID_{50}$ ) were calculated from these parameters as follows:

$$ID_{50} = \text{antilog} (-\beta_0 / \beta_1) = 52.$$

In comparison, the  $ID_{50}$  of oocyst batches used to generate a kinetic model for inactivation by ozone at 22°C in earlier work ranged from 60 to 347 (Gyürék et al. 1999). Therefore, the oocysts used in this study were slightly more infectious than those used in the earlier work.

## **6.5 GIARDIA MURIS METHODS**

### **6.5.1 Cyst Production**

The strain of *G. muris* used in this study was originally isolated by Roberts-Thomson (1976) from a golden hamster. The parasite has been maintained in the laboratory since 1981 using bi-weekly passages in CD-1 or C3H/HeN mice. Methods for mouse inoculation and subsequent cyst collection and purification from mouse feces were adapted from those used previously (Belosevic and Faubert 1983; Finch et al. 1992; Labatiuk et al. 1991). Cysts for experiments were produced by inoculating groups of 8 to 11 week-old male C3H/HeN mice with purified suspensions of fresh cysts. Mice were inoculated by gastric intubation. Feces from the infected mice were collected over a 2 to 3 h period on each day of a one or two day period. Collection periods were somewhere between 4 and 28 days post-infection. To isolate cysts, the daily feces samples were emulsified in Milli-Q<sup>®</sup> water, layered on 1 M sucrose solution and then centrifuged for 15 min. at 400 × g at 4°C. After centrifugation, the cyst rich layer at the water-sucrose interface was carefully collected and then washed 3 to 4 times in Milli-Q<sup>®</sup> water by centrifugation at 600 × g for 10 min. Cyst concentration was then determined by hemocytometer count. Cysts for experiments were stored in Milli-Q water at 4°C and used within 72 h of collection.

### **6.5.2 Development of a Quantitative Infectivity Model in C3H/HeN Mice**

The pattern of *G. muris* cyst shedding in mice is characterized by a latent period, in which no or few cysts are observed in the feces. The latent period is followed by a phase of rapid increase in cyst output until a stable output of about 10<sup>6</sup> cysts per g of feces is reached, regardless of the size of infective inoculum (Belosevic and Faubert 1983; Belosevic et al. 1984). The feature that distinguishes the size of the infective

inoculum is the duration of the latent period and the temporal position of the rapid increase phase. In earlier work, the latent period was defined as the number of days post-infection until all of the mice in a cohort became positive for cysts in the feces (Labatiuk 1992). This method of defining latent period was found to be unsatisfactory because the assignment of positive mice is sensitive to limits of detection of individual cysts by microscopy. A new method was proposed in which the latent period is defined in terms of average cyst output from the cohort.

To determine the relationship between inoculum size and latent period, cohorts of five, 8 to 11 week old male C3H/HeN mice were infected with  $10^5$ ,  $10^4$ ,  $10^3$ ,  $10^2$ , or 10 cysts each in dose-response experiments. Cysts for the dose-response were collected and purified on the same day as infection. Mice were housed together, but were transferred to individual false bottom cages for 2 h each day post infection for feces collection. The wet feces sample collected from each mouse was weighed and cysts were recovered and purified using the previously described sucrose gradient centrifugation method. After centrifugation, the cysts were washed once in Milli-Q<sup>®</sup> water before counting on the hemocytometer. The average cyst output per gram of wet feces was determined for each cohort on successive post-infection days until cyst output was stable at about  $10^6$  cysts per gram of wet feces. The results of a typical dose-response experimental are shown in Figure 6-6.

The latent period (*LP*) in days, for each inoculum size was defined as the arithmetic average of the times to reach cyst outputs of  $10^3$ ,  $10^4$  and  $10^5$  cysts per g of wet feces. These times were interpolated directly from the cyst shedding curves of Figure 6-6. A relationship between latent period and size of infective inoculum was developed using information from three separate dose response experiments performed as part of this work, as well as information from similar experiments conducted by Labatiuk (1992) using identical cyst collection methods. Detailed information from these independent dose-response experiments was provided in Table A-2 of Appendix A. The dose-response relationship, shown in Figure 6-7, was found to be reproducible between different batches of cysts. The method of least-squares was used to fit the following empirical model equation to the data from all four dose-response experiments:

$$\log(d) = (-10.4 \pm 0.5) \log(LP) + (9.5 \pm 0.3)$$

Equation 6-12

In this model,  $d$  represented the number of infectious cysts in the mouse inoculum and  $LP$  was the latent period. In Equation 6-12, the model parameter values were shown together with the standard errors inside the brackets. Standard errors of the model parameters were determined by standard statistical techniques (Box et al. 1978).

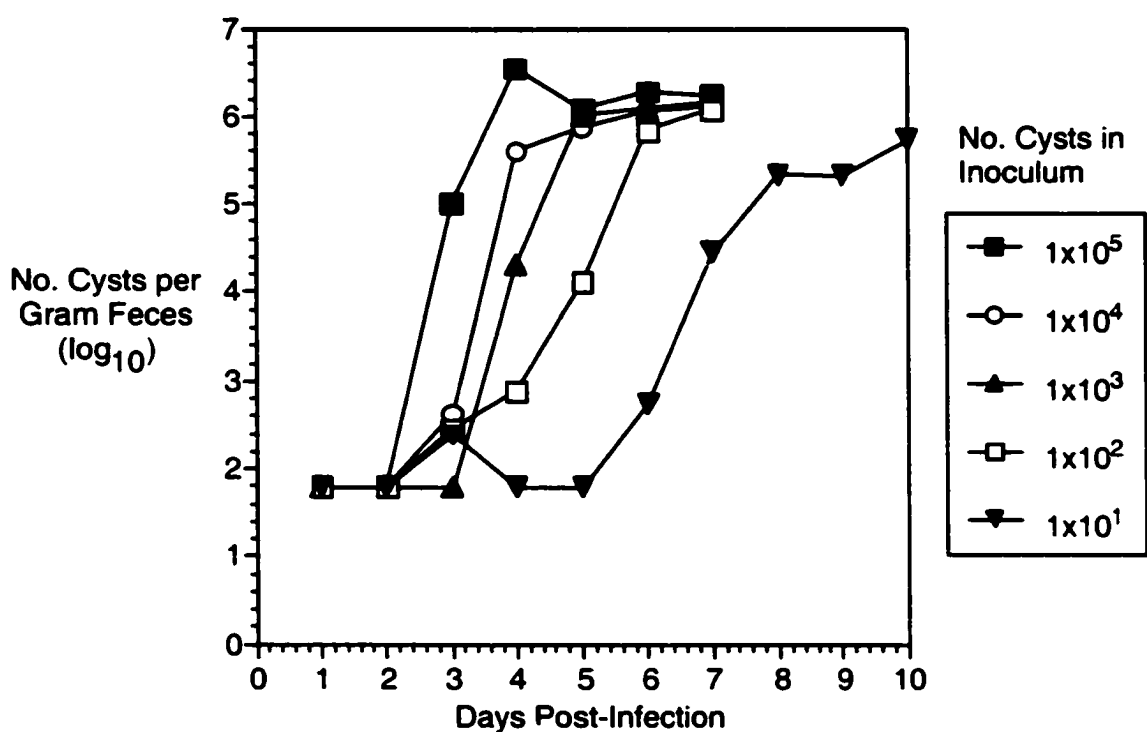


Figure 6-6 Pattern of cyst shedding in the feces of C3H/HeN mice infected with fresh *Giardia muris* cysts in a dose-response experiment.

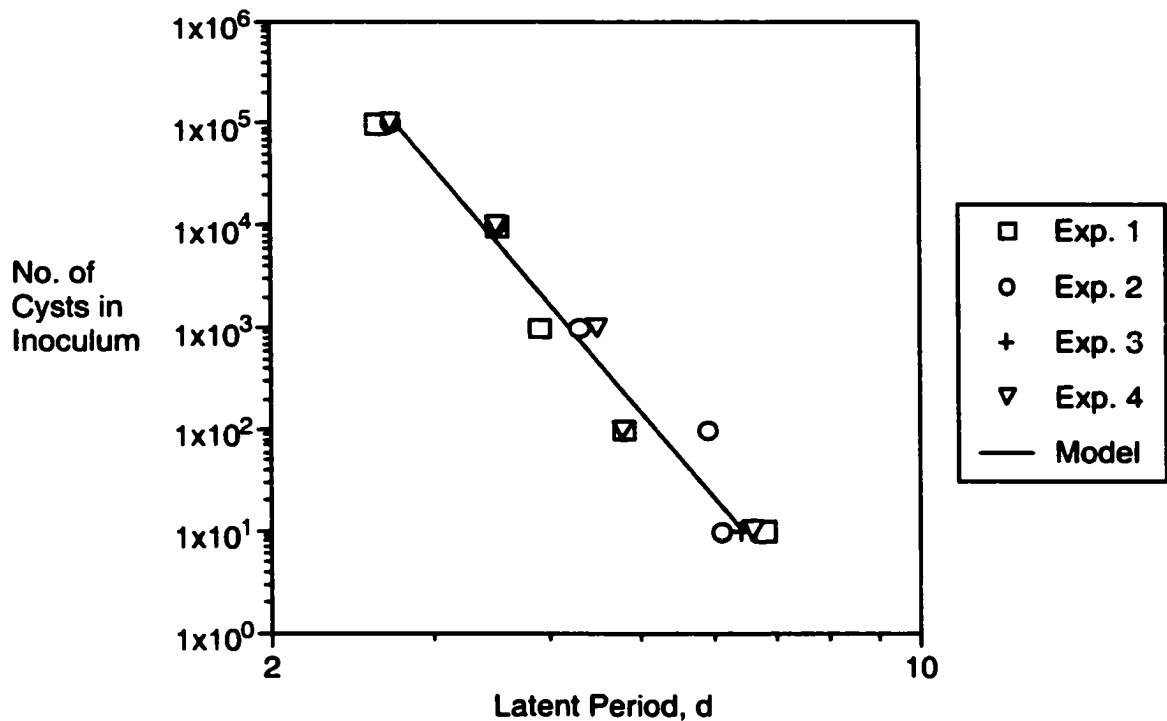


Figure 6-7 Latent period,  $LP$ , in the C3H/HeN mice as a function of the number of fresh *Giardia muris* cysts in the oral inoculum,  $d$ . Results from four dose response experiments are shown, including data from Labatiuk (1992) (indicated as Exp. 3).

### 6.5.3 Infectivity Analysis In Experimental Samples

Cysts from experimental samples were concentrated by centrifugation ( $800 \times g$  for 10 min at  $4^{\circ}\text{C}$ ). The supernatant was removed and the concentrated pellet was re-suspended in the remaining 2 to 3 mL of liquid using a glass Pasteur pipette. The cyst concentration was calculated from the average of a minimum of eight hemocytometer counts. For each experimental sample, 5 mice were inoculated with 0.2 mL of the concentrated suspension. Cyst production in the feces was monitored as described for the dose-response experiments and the latent period,  $LP$ , was determined in the same way. The number of infectious cysts in the inoculum to each mouse,  $d$ , was estimated from Equation 6-12.

## **6.6 MISCELLANEOUS PROCEDURES**

### **6.6.1 Ozone Demand-Free Materials**

All materials used in batch reactor trials or to analyze for dissolved ozone including flasks, stir bars and pipette tips, were made ozone demand-free (ODF) prior to use by soaking in a concentrated (approximately 20 mg/L) solution of ozone prepared in de-ionized water for at least 1 hour. After soaking, the ozone solution was drained, and the materials were covered with tin foil and placed in an air oven for 24 h at 80°C to remove any remaining moisture.

### **6.6.2 Ozone Demand-Free Phosphate Buffer**

The phosphate buffers at pH 6.0 and pH 8.0 used in the batch reactor experiments were prepared by dissolving appropriate amounts of reagent grade disodium hydrogen orthophosphate and potassium dihydrogen orthophosphate (BDH Co.) into de-ionized water from an Elga<sup>®</sup> Ultra-pure water system (Fisher Scientific). Buffer phosphate concentration was 0.05 M. The buffers were made ODF by bubbling ozonized gas through the prepared buffer, with stirring, until saturated with dissolved ozone at approximately 20 mg/L, and then letting stand for 1 h. The remaining ozone was removed by bringing the buffer to a boil for 10 minutes. After cooling, the pH was measured and recorded.

### **6.6.3 Measurement of Dissolved Combined Chlorine**

The concentration of combined chlorine in the chlorine-reduced tap water used in the static mixer contactor experiments was measured using the *N,N*-diethyl-*p*-phenylenediamine (DPD) colorimetric standard method (APHA AWWA WEF 1992) with Hach Permachem Reagent for DPD Total Chlorine (Cat. No. 14064-99, Hach Co., Loveland CO).

### **6.6.4 Measurement of pH and Temperature**

Water pH was measured on an accumet<sup>®</sup> Model 25 pH/Ion Meter (Fisher Scientific) that was calibrated daily using commercial buffers. Temperature was

measured using a calibrated thermocouple thermometer (Barnant Co., Model 600-1040, Barrington, IL).

## 6.7 CALCULATIONS

### 6.7.1 Mean Residence Time

At each sample location in the reactive flow segment, the mean residence time,  $t_m$  was calculated from the exit age distribution function,  $E(t)$ , using the method of moments described by Levenspiel (1972):

$$t_m = \int_0^{\infty} tE(t) dt \quad \text{Equation 6-13}$$

Equation 6-7 was solved numerically using the trapezoid rule with a step size of 1 s. Calculations were performed on a Microsoft Excel 2000 (Microsoft Co., Redmond, WA) spreadsheet program.

### 6.7.2 Average Concentration-Time Product

The microorganism inactivation measured for different levels of ozone treatment in the static mixer ozone contactor was interpreted using the product of the average ozone concentration and the effective contact time. The  $C_{avg}t_m$  in the reactive flow segment was estimated from an integrated average of the measured dissolved ozone concentration profile. A first-order ozone decomposition rate in the reactive flow segment was estimated by fitting the following equation to the measured ozone concentration profile:

$$C = C_0 \exp(-k_d t_m) \quad \text{Equation 6-14}$$

where  $C$  is the predicted dissolved ozone concentration at each sample location,  $C_0$  is the measured ozone concentration at the inlet of the reactive flow segment,  $t_m$  is the

arithmetic average of the measured mean residence times  $k_d$  the estimated first-order decomposition coefficient. An example of a typical dissolved ozone profile in the reactive flow segment, which was measured at 16°C is shown in Figure 6-8 along with the fit of Equation 6-14. Curve fitting of Equation 6-14 to the measured profiles was done using non-linear least squares regression and the Solver function in Excel 2000.

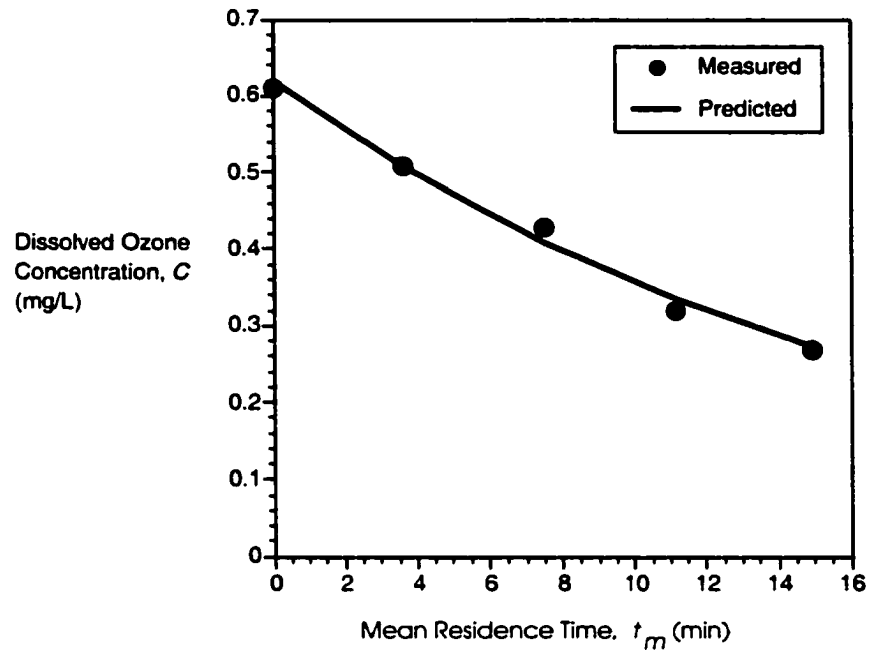


Figure 6-8 Typical ozone concentration profile in the reactive flow segment of the static mixer ozone contactor and fit of the first-order decomposition model. Experiment was conducted at 16°C using *Bacillus subtilis* spores.

An integrated average ozone concentration was then estimated for each sample point using the following equation (Langlais et al. 1991):

$$C_{avg} = \frac{C_0}{k_d t_m} [1 - \exp(-k_d t_m)] \quad \text{Equation 6-15}$$

The contribution of the bubble column to the total  $C_{avg}t_m$  was estimated using the following equation:

$$C_{avg}t_m = (C_{in} \times C_{out})^{1/2} t_m \quad \text{Equation 6-16}$$

where  $C_{in}$  and  $C_{out}$  are the concentration of dissolved ozone at the inlet and outlet of column, respectively, and  $t_m$  is the arithmetic average of the mean residence times determined in triplicate tracer experiments.

For batch reactor experiments, the  $C_{avg}t_b$  product was estimated in a similar way except that the batch sampling time,  $t_b$ , replaced the mean residence time,  $t_m$ , in Equations 6-14 and 6-15.  $C_0$  was the ozone concentration immediately after addition of the concentration ozone stock. An ozone decomposition profile in a typical batch experiment is shown in Figure 6-9.

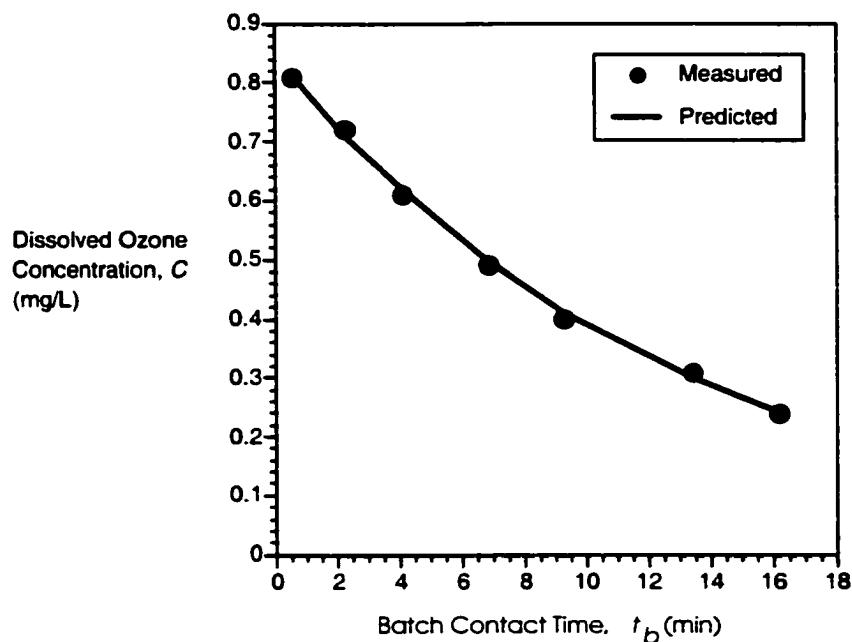


Figure 6-9 Typical ozone concentration profile in a batch reactor experiment and the fit of the first-order decomposition model. Experiment was conducted at 16°C using *Bacillus subtilis* spores.

### 6.7.3 Microorganism Reduction

Microorganism reduction by ozone in the static mixer contactor and in the batch reactors was interpreted in terms of the inactivation ratio,  $I$ , which was defined in log-units by the following equation:

$$I = -\log \frac{N}{N_0} \quad \text{Equation 6-17}$$

where  $N$  and  $N_0$  are the concentrations of live microorganisms in the water before and after the specified ozone treatment. The precise definition of  $N$  and  $N_0$  varied according to the microorganisms studied. For experimental trials with *B. subtilis* spores,  $N$  and  $N_0$  were determined directly from spore enumerations and were defined as follows:

$N_0$  = concentration of live spores in the static mixer contactor feed stream or prior to contact with ozone or in the batch reactor control flask (CFU/mL),  
and

$N$  = concentration of live spores after the specified contact with ozone in the static mixer contactor or in the batch reactor experimental flask (CFU/mL)

For triplicate plate counts ( $N_1$ ,  $N_2$  and  $N_3$ ) an average value of  $\log N$  was determined as follows:

$$(\log N)_{\text{avg}} = 1/3 [(\log N_1 + \log N_2 + \log N_3)] \quad \text{Equation 6-18}$$

The standard error of  $\log N$  and  $\log N_0$  and the Student t-distribution were used to construct 95% confidence intervals on the log inactivation ratio. The standard error, SE, of  $-\log N/N_0$  was determined as follows:

$$\text{SE} [-\log N/N_0] = \text{SE} [\log N_0] + [\text{SE} \log N] \quad \text{Equation 6-19}$$

The log inactivation ratio of the encysted protozoans was inferred from the outcomes of the infectivity analysis on the recovered cyst or oocyst samples. The inactivation ratio was estimated from:

$$I = -\log\left(\frac{N}{N_0}\right) = -\log\left(\frac{d}{d_0}\right) \quad \text{Equation 6-20}$$

where  $d$  and  $d_0$  were defined as:

$d$  = the estimated number of infectious cysts or oocysts in the inoculum to each mouse, and

$d_0$  = the total number of cysts or oocysts in the same inoculum as determined by hemocytometer count.

Standard errors and confidence intervals for the log inactivation ratio of the protozoa were not estimated because reported inactivation ratios were based on a single infectivity measurement.

## **7 KINETICS OF OZONE INACTIVATION OF *BACILLUS SUBTILIS* SPORES**

### **7.1 INTRODUCTION**

The efficiency of alternative ozone contactor designs for reduction of protozoan parasites, like *Cryptosporidium parvum*, is ideally evaluated by direct measurement. This is extremely difficult to do for ozone contactors in operation in drinking water facilities, because the concentration of *C. parvum* oocysts in the source water is usually several orders of magnitude below what is required for a meaningful assessment. One alternative is to evaluate a scale model of the contactor in seeding studies in which concentrated preparations of live parasites are introduced into the feed water. Seeded parasites are recovered from the treated water, typically by filtration, and the reduction in viability is determined by an appropriate method. Animal infectivity models are the most reliable means of determining the loss of viability of *C. parvum* oocysts exposed to ozone (See discussion in Chapter 2, Section 2.3.9). Using animal models, like the neonatal CD-1 mouse model for *C. parvum*, oral inocula on the order of  $10^4$  or  $10^5$  are required in order to determine levels of inactivation of 2 log-units or greater. This means that, even for a small-scale continuous-flow ozone contactor, like the experimental static mixer contactor described in Chapters 5 and 6, relatively large numbers of purified parasites, on the order of  $10^8$ , are required for meaningful challenge tests. The health and safety risks that must be considered further complicate such testing.

The task of evaluating an ozone contactor design would be greatly simplified if an appropriate model or surrogate microorganism was available. Cultured *Bacillus subtilis* spores have been proposed as a model organism to represent inactivation of *Cryptosporidium parvum* oocysts by ozone. Experience has shown that these aerobic bacterial spores are easy to culture and to enumerate. Moreover, preparations of these spores have been assigned a biosafety level classification of 1 by the American Type Culture Collection (ATCC). According to the material safety data sheet provided by ATCC, microbial cultures at this classification level are not “known to cause disease in healthy human adults or animals”. From health risk and ease of use perspectives, these spores are, therefore, potentially good model organisms. The final criterion to be

evaluated is how the resistance of these spores to ozone compares to that of *C. parvum* oocysts.

Published studies have suggested that the resistance to ozone of *B. subtilis* spores and *C. parvum* oocysts is similar. The investigations in these studies, however, were limited to a fairly narrow range of temperature range; 20 to 22°C in one case (Facile et al. 2000) and to 22.7°C in another (Owens et al. 2000). Another aspect that must be considered carefully in any seeding studies is that assessment of spore inactivation kinetics may be sensitive to bacterial strain, the methods used to culture, purify and enumerate spores, and to the protocols for carrying out the ozone exposures. The objectives of the study described in this chapter were to:

1. determine the ozone inactivation characteristics of a certain strain of *Bacillus subtilis* spores (ATCC 6633) using batch ozone reactors;
2. develop a kinetic model to describe spore inactivation by ozone over a range of temperature (3 to 22°C) and pH (6 to 8); and
3. use the kinetic model to compare spore inactivation by ozone at various temperatures and pH to that of *C. parvum* oocyst inactivation.

For objective 3, the kinetic model of *C. parvum* oocyst inactivation by ozone developed by Li and co-workers (2001) served as a basis for comparison. The model provides predictions of oocyst inactivation over a range of temperatures (1 to 35°C) and pH (6 to 8). To ensure the best comparison possible, the batch reactor protocols and ozone measurement techniques use by Li and co-workers (2001) were duplicated in this study with *B. subtilis* spores.

## **7.2 BATCH REACTOR OZONATION TRIALS**

### **7.2.1 Experimental Trials**

To elucidate the kinetics of inactivation of *B. subtilis* (ATCC 6633) spores, batch reactor ozonation experiments were carried out in ozone demand-free 0.05 M phosphate buffered laboratory water at two pH levels (6 and 8) and at three temperatures (3, 12 and 22°C). A minimum of eight batch reactor trials, spanning a range of dissolved ozone concentration (0.4 to 1.8 mg/L) and contact times (2 to 15 min), were completed at each

of the six pH and temperature combinations. Details of each experimental trial were provided in Tables B-1, B-2 and B-3 of Appendix B. The fifty batch ozonation trials listed in these tables were conducted in random order over the course of an eight-week period using a single stock preparation of spores that was stored at 4°C (Stock A). Randomization was done to ensure that the effect of gradual changes in the characteristics of the prepared spores on the subsequent analysis and modeling was minimized.

### **7.2.2 Determination of Dissolved Ozone Concentration**

Both the UV absorbance at 260 nm and the indigo trisulphonate methods were used to measure the dissolved ozone concentration in each batch reactor trial. The indigo-trisulphonate and direct UV absorbance methods are based on different operating principles. As a result, the ozone concentrations determined by the two methods were not the same. Data analysis and modeling, however, were based exclusively on measurement of ozone by the UV absorbance method. The justification for this was that Li and co-workers (2001) developed their kinetic model of *C. parvum* oocyst inactivation from a dataset that was derived from ozone concentrations determined strictly by direct UV absorbance. To maximize the integrity of the comparison between the results of this and the *C. parvum* study, parameters of the UV absorbance analytical procedure were matched. These parameters were (1) measurement wavelength of 260 nm, (2) specific molar absorbance of  $3\ 300\ \text{M}^{-1}\text{cm}^{-1}$  and (3) baseline absorbance correction according Equation 6-7.

### **7.2.3 Measured Spore Inactivation Curves**

Measured spore inactivation is plotted for each pH and temperature as a function of the integrated average dissolved ozone concentration - time product ( $C_{avg}t_b$ ) in Figures 7-1, 7-2 and 7-3. Each datum plotted in these figures was determined from the average spore enumeration of three samples extracted from a single ozonation reactor and three samples extracted from the corresponding control reactor. For a given temperature, spore inactivation was a non-linear function of the average dissolved ozone concentration-time product,  $C_{avg}t_b$ . Outcomes of trials with similar  $C_{avg}t_b$  products, but obtained with

different average dissolved ozone concentration,  $C_{avg}$ , and batch exposure time,  $t_b$ , were found to lie on the same inactivation curve. At each temperature, the spore inactivation curve was characterized by three distinct kinetic regions. At low  $C_{avg}t_b$ , a shoulder region was observed in which virtually no spore inactivation was measured. The shoulder region was followed by a region of rapid exponential decrease in viable spore concentration with increasing  $C_{avg}t_b$ . At higher  $C_{avg}t_b$  and inactivation levels, a tailing region was observed that was characterized by a much lower rate of spore inactivation. An increase in temperature had the effect of reducing the length of the shoulder region and increasing the slope and rate of inactivation in both the exponential and tailing regions.

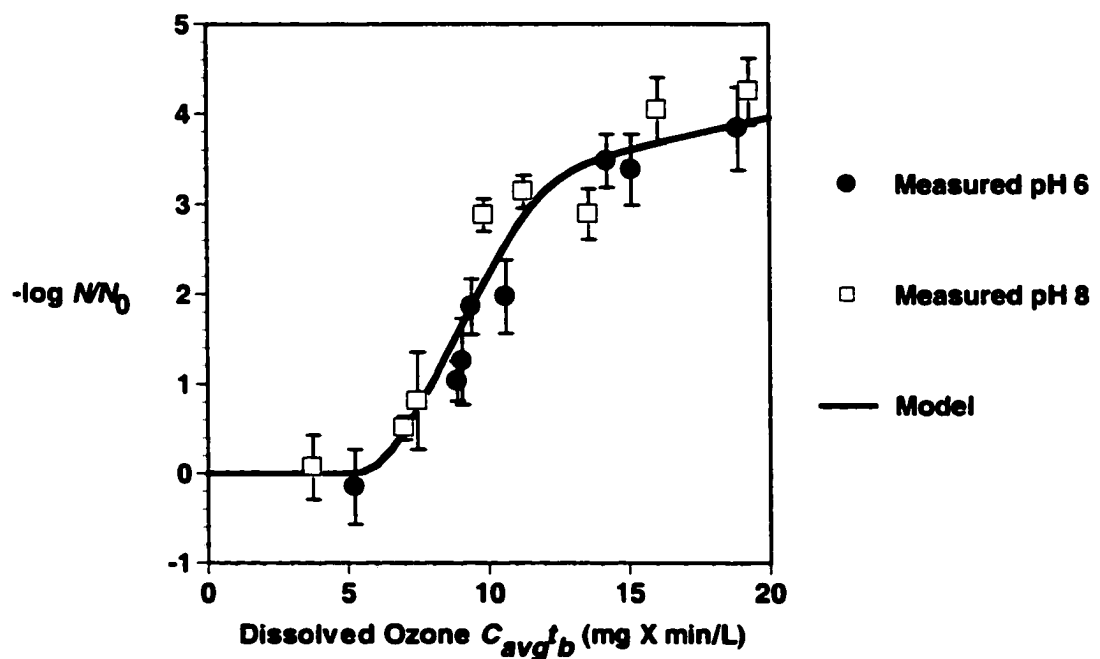


Figure 7-1 Ozone inactivation of *Bacillus subtilis* spores in ozone demand-free buffered laboratory water at 3°C.

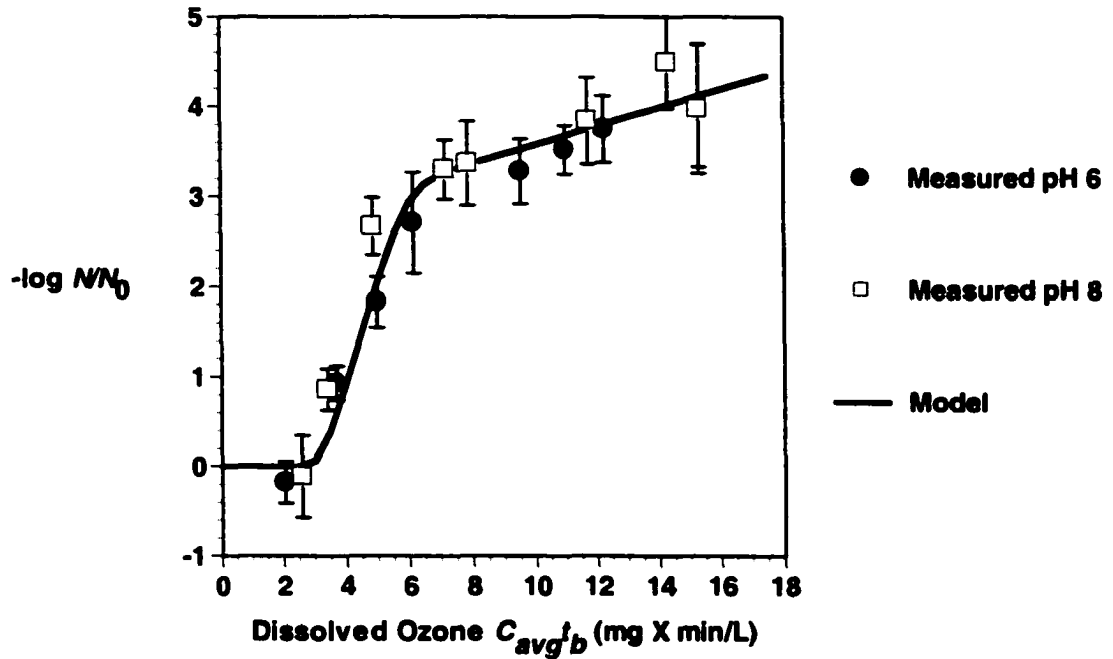


Figure 7-2 Ozone inactivation of *Bacillus subtilis* spores in ozone demand-free buffered laboratory water at 12°C.

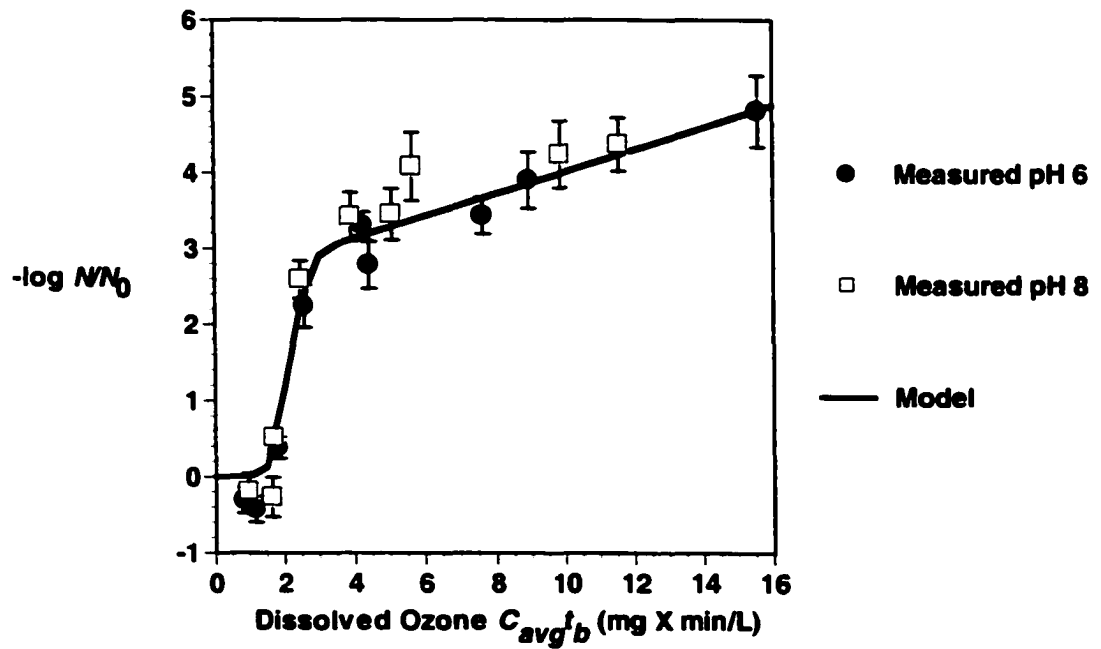


Figure 7-3 Ozone inactivation of *Bacillus subtilis* spores in ozone demand-free buffered laboratory water at 22°C.

Although poorly understood, tailing in the inactivation curves of bacterial spores and viruses exposed to various types of treatment is common (Cerf 1977; Hiatt 1964). Other investigators observed tailing phenomena in the survival curves of bacterial spores exposed to ozone but provided little explanation or discussion (Facile et al. 2000; Finch and Choe 1999). Tailing in the measured survival curves of *Vibrio cholerae* bacteria exposed to chlorine was attributed to the presence of a distinct sub-population of the bacteria that displayed increased resistance due to agglomeration and the presence a mucoid coating (Clark et al. 1994). The presence of agglomerated spore units that were much more difficult to completely inactivate than were the individual spores was suspected as the explanation for the tailing observed in the inactivation curves of Figures 7-1, 7-2 and 7-3. Microscopic observations of the experimental spore preparations suggested the presence of spore agglomerations that were bound to extra-cellular material or glycocalyx. Although the spore preparations were mixed vigorously prior to use in the experiments, specifically to promote break-up of agglomerates, it is unlikely that agglomerates were completely eliminated. Agglomerates were observed under the microscope even after the mixing procedure.

In several instances, the measured spore concentration in the experimental reactor at the lowest ozone exposures was greater than that measured in the untreated control reactor. This unexpected increase in viable spore concentration resulted in a small negative value for the reported log inactivation. This effect, which was most pronounced in the trials at 22°C (Figure 7-3), was possibly explained in terms of spore agglomerates. The hypothesis is that a mild ozone exposure was sufficient to decompose the extracellular material binding the spore agglomerates, but did not result in measurable inactivation of individual spores. Free viable spores were released into the medium, effectively increasing the number of colony-forming units (CFU).

## **7.3 KINETIC MODELING**

### **7.3.1 Development of a Two-Part Kinetic Model**

A kinetic model was developed to describe the ozone inactivation of *B. subtilis* spores measured in the batch reactor experiments. The main purpose of the model

development was to facilitate an unbiased comparison of the experimental spore inactivation kinetics to the ozone inactivation kinetics of *C. parvum* oocysts previously determined by Li and co-workers (2001). The sigmoid shape of the experimental spore inactivation curves plotted in Figures 7-1, 7-2 and 7-3 indicated that spore inactivation could not be described adequately with a simple first-order Chick-Watson rate law. The multi-phase nature of the observed inactivation curves suggested a more complex inactivation mechanism or heterogeneity of the spore population. In preliminary attempts, none of the literature kinetic models described in Table 2-4 were found to adequately describe the sigmoid form of the observed spore inactivation curves. No one model was capable of describing both the observed shoulder and tailing phenomena.

A two-part kinetic model was proposed to describe observed spore inactivation by ozone. In this model, the shoulder and exponential regions of the inactivation curve reflected inactivation of individual spores, freely suspended in the water matrix. The consistent presence of the initial shoulder in the inactivation curves at the different temperatures and pH was an indication of an inactivation mechanism that was based on cumulative damage (Hiatt 1964). The multi-target model (Table 2-4) was, therefore, used to mathematically describe inactivation of individual spores by a cumulative damage mechanism. A separate first-order rate term was then added to the mathematical formulation to account for the more gradual inactivation of agglomerated spore units. A similar modeling approach was used to describe inactivation of free and particle-associated coliform bacteria by ultraviolet light in wastewater (Emerick et al. 2000). The formulation of the proposed model was:

$$N = N_{0,i} \left[ 1 - (1 - e^{-k_i C t})^{n_i} \right] + N_{0,a} e^{-k_a C t} \quad \text{Equation 7-1}$$

The first term of this equation represented inactivation of individual spores,  $N_i$ , according to the multi-target model, and the second term represents inactivation of agglomerated

spore units,  $N_a$ , by a simple first-order process. The variables were defined as follows;  $N$  was the total number of live CFU after a given dissolved ozone  $Ct$  exposure,  $N_{0,i}$  and  $N_{0,a}$  were the initial number of CFU due to individual spores and agglomerated spore units, respectively,  $n_c$  was the number of targets that must be hit in order to inactivate an individual spore, and  $k_i$  and  $k_a$  were rate constants. Implicit in the model formulation was the assumption that the rates of inactivation were first-order with respect to the number of targets in the individual spores and the number of agglomerated spore units, and first-order with respect to ozone concentration. The number of live microorganisms of both types was, therefore, proportional to the simple  $Ct$  product, which, in the batch reactor experiments, was given by the integrated average  $C_{avg}t_b$ .

Another parameter that was specified in order to complete the model was the number ratio of the two spore subpopulations. The value of this ratio was given by the parameter,  $r$ , which was defined as follows:

$$r = \frac{N_{0,a}}{N_{0,i} + N_{0,a}} \quad \text{Equation 7-2}$$

The number of critical targets,  $n_c$  and the fraction of agglomerated units,  $r$ , were properties of the spore population and were not likely to be functions of temperature.

### 7.3.2 Modeling Temperature Dependence

Temperature dependence of the spore inactivation kinetics was, therefore, modeled in terms of temperature dependence of the rate constants,  $k_i$  and  $k_a$ . According to Arrhenius activation energy theory (Levenspiel 1972), temperature dependence of kinetic rate constants is given by:

$$\frac{k_1}{k_2} = \exp\left[-\frac{E_A}{R}\left(\frac{1}{T_1} - \frac{1}{T_2}\right)\right] \quad \text{Equation 7-3}$$

where  $E_A$  is the activation energy of the reaction,  $R$  is the universal gas constant and  $k_1$  and  $k_2$  are the values of the rate constant at the respective absolute temperatures  $T_1$  and  $T_2$ . Equation 7-3 may be re-written as:

$$\frac{k_1}{k_2} = \theta^{T_1 - T_2} \quad \text{Equation 7-4}$$

where the temperature coefficient,  $\theta$ , is given by  $\exp(E_A/RT_1T_2)$ . Over a sufficiently small temperature range,  $\theta$ , can be assumed to be constant. Using this approach, the temperature dependence of the two rate constants in Equation 7-1 were mathematically described as follows:

$$k_{i,T} = k_{i,12} \theta_i^{T-12} \quad \text{Equation 7-5}$$

and

$$k_{a,T} = k_{a,12} \theta_a^{T-12} \quad \text{Equation 7-6}$$

The reference temperature in Equations 7-5 and 7-6 was 12°C, the approximate midpoint of the experimental range.

### 7.3.3 Model Regression to Experimental Data

Best-fit parameters of the kinetic model were estimated by simultaneous regression of Equations 7-1, 7-2, 7-5 and 7-6 to the datasets of Figures 7-1, 7-2 and 7-3. The criteria for best fit was minimization of the sum of the squares of the residuals described as follows:

$$\min \sum \left[ \log \left( \frac{N}{N_0} \right)_{\text{model}} - \log \left( \frac{N}{N_0} \right)_{\text{measured}} \right]^2 \quad \text{Equation 7-7}$$

Least-square computations were performed in a Microsoft Excel 2000 spreadsheet using the Solver function with the Newton search method selected and the convergence tolerance set to 0.0001.

The kinetic model was found to provide a good fit to the observed experimental outcomes at each of the three experimental temperatures. Best-fit model parameters are summarized in Table 7-1. Inactivation curves predicted by the model are compared to the batch reactor experimental results in Figures 7-1, 7-2 and 7-3. Direct comparisons of the model-predicted and measured inactivation are provided in Figures 7-4, 7-5 and 7-6. The 45° diagonal solid lines in these figures represented a perfect model fit to the data. Model prediction errors were given by:

$$\varepsilon_i = \log \left( \frac{N}{N_0} \right)_{\text{predicted}} - \log \left( \frac{N}{N_0} \right)_{\text{measured}} \quad \text{Equation 7-8}$$

When all the errors at each temperature and pH were grouped together and plotted as a frequency histogram, the errors were found to approximate a random normal distribution (Figure 7-8). The mean value of the grouped prediction error,  $\bar{\varepsilon}_i$ , was -0.04 log units and when tested using the Student t-distribution was found to be not statistically different than zero at the 95% confidence level (Table 7-2). The assumptions of least-squares regression were, therefore, adequately fulfilled.

The activation energies reported in Table 7-1 were estimated from the best-fit values of the temperature coefficients  $\theta_i$  and  $\theta_a$ , and Equation 7-3. The magnitude of the activation energies provides some insight into the processes underlying microorganism inactivation. For example, the activation energy of individual spores,  $E_{A,i} = 49$  kJ/mole, was very close to the activation energy reported for inactivation of *C. parvum* oocysts by

ozone of 51.7 kJ/mole (Li et al. 2001). This is consistent with the contention that a similar rate-limiting step governed inactivation of individual spores and oocysts. On the other hand, the activation energy for inactivation of the agglomerated spore units,  $E_{A,i} = 28$  kJ/mole, was only half that of individual spores. This is an indication that inactivation of agglomerated spores was controlled by a different physical or chemical process than inactivation of individual spores or oocysts.

Table 7-1 Best-fit parameters of the *Bacillus subtilis* spore inactivation kinetic model as determined by least-squares regression.

Parameter	Physical Significance	Best-Fit Value	Units
$k_i$	Rate constant for inactivation of free spores	2.8	L mg <sup>-1</sup> min <sup>-1</sup>
$\theta_i$	Temperature coefficient for inactivation of free spores	1.08	none
$k_a$	Rate constant for inactivation of resistant agglomerated spore units	0.23	L mg <sup>-1</sup> min <sup>-1</sup>
$\theta_a$	Temperature coefficient for inactivation agglomerated spore units	1.04	none
$n_c$	Number of targets for inactivation of free spores	8500	number
$r$	Fraction of agglomerated spore units in the total population	0.003	none
$E_{A,i}$	Estimated Arrhenius activation energy for free spores	49	kJ mol <sup>-1</sup>
$E_{A,a}$	Estimated Arrhenius activation energy for agglomerated spore units	28	kJ mol <sup>-1</sup>

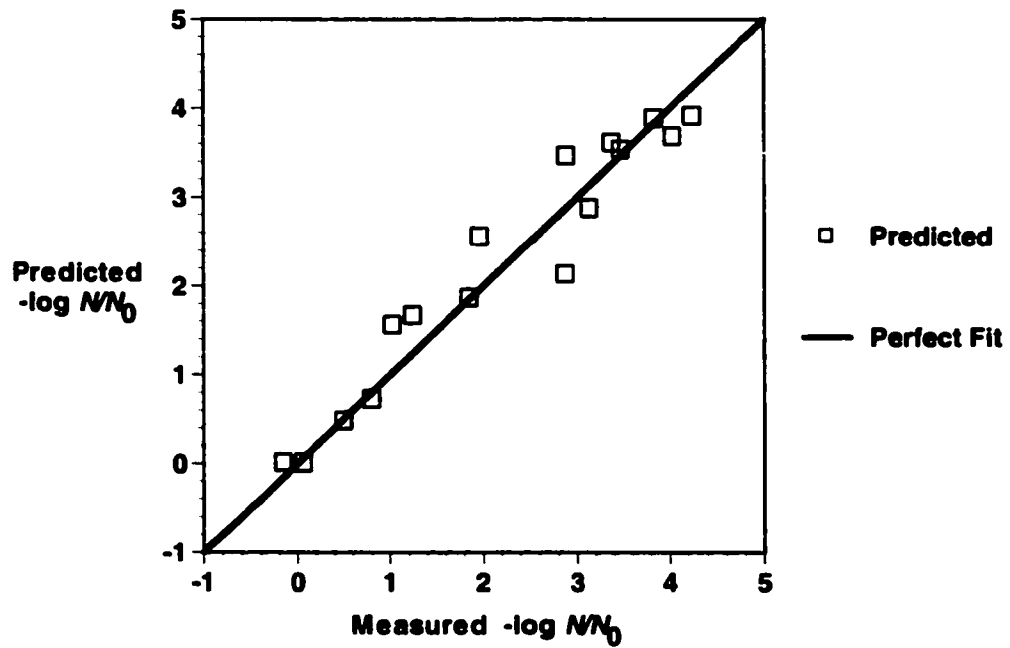


Figure 7-4 Comparison of model-predicted and measured inactivation of *Bacillus subtilis* spores at 3°C.

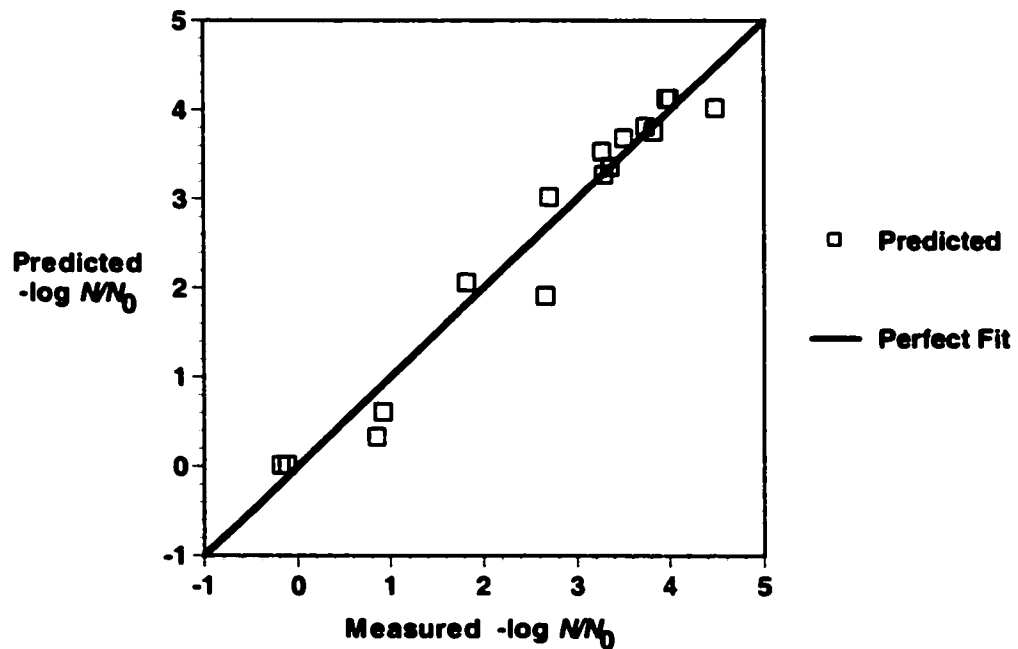


Figure 7-5 Comparison of model-predicted and measured inactivation of *Bacillus subtilis* spores at 12°C.

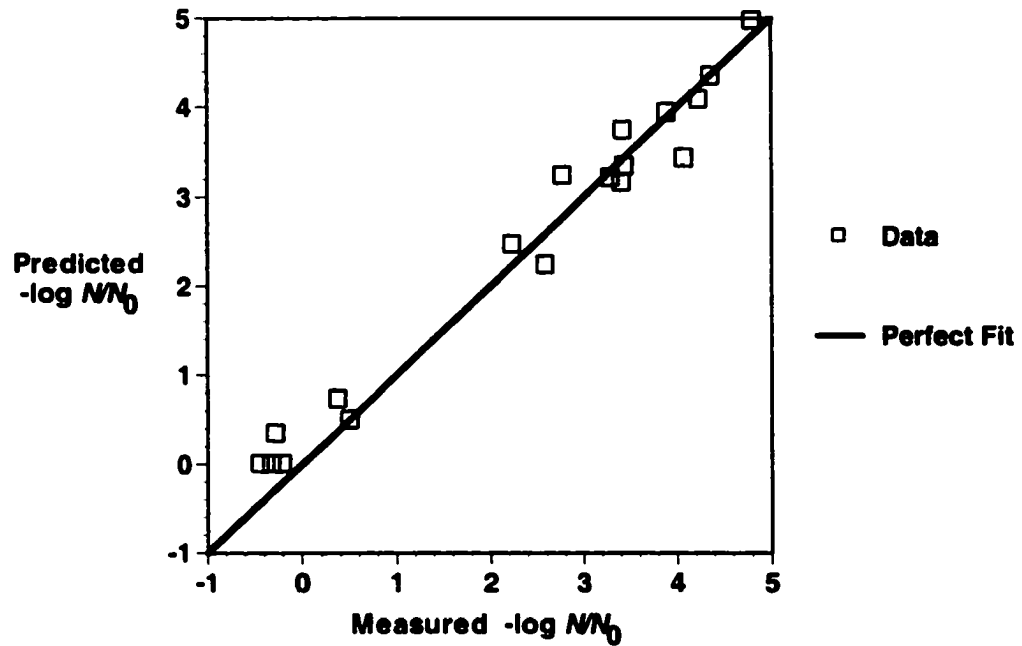


Figure 7-6 Comparison of model-predicted and measured inactivation of *Bacillus subtilis* spores at 22°C.

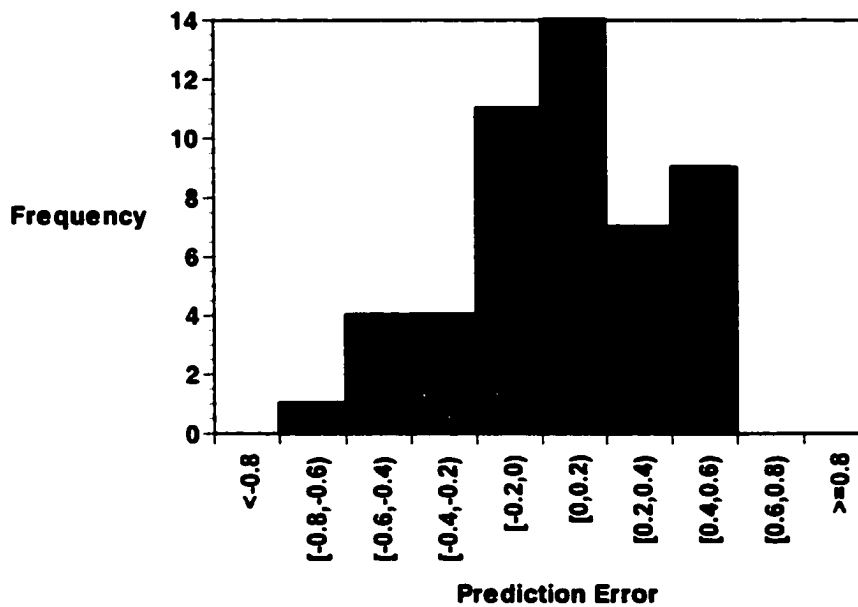


Figure 7-7 Histogram of the *Bacillus subtilis* ozone inactivation kinetic model prediction errors.

#### 7.4 EFFECT OF pH ON SPORE INACTIVATION

The stability of aqueous molecular ozone is known to be a strongly dependent on pH, however, it is less clear to what extent pH affects the intrinsic rate of microorganism inactivation by ozone. Published studies differ in the reported effect of pH on microorganism inactivation by ozone (Farooq et al. 1977a; Roy et al. 1981a). In Figures 7-1, 7-2 and 7-3 the effect of pH on ozone stability in the batch reactors was accounted for by representing inactivation in terms of the ozone  $C_{avg}t_b$  product, in which the integrated average ozone concentration,  $C_{avg}$ , was calculated using Equation 6-15. This representation assumes that, for a given temperature, spore inactivation was determined by the integrated dissolved ozone exposure only, and that the rate of reaction between dissolved ozone and the microorganisms was independent of either pH or the rate of ozone decomposition. A cursory examination of the inactivation curves in Figures 7-1, 7-2 and 7-3 suggests that spore inactivation was only slightly greater at pH 8 than at pH 6 for an equivalent  $C_{avg}t_m$ , and that this assumption thus was true.

The pH effect was more closely investigated by examination of the mean prediction errors,  $\bar{\epsilon}_i$ , of the kinetic model for each temperature and pH (Table 7-2). According to the signs on the computed values of  $\bar{\epsilon}_i$ , the model tended to over-predict inactivation at pH 6 and to under-predict inactivation at pH 8. The effect was consistent at each temperature. When grouped by pH, the magnitude of the mean prediction errors were computed to be + 0.2 and - 0.2 log-units at pH 6 and pH 8, respectively, and these were statistically different than zero at the 95% confidence level. Spore inactivation at pH 8 was, on average, 0.4 log-units greater than at pH 6. It was concluded that, between pH 6 and 8, pH had a statistically significant but relatively minor effect on inactivation of these spores. For kinetic model development, therefore, no distinction was made between pH, and experimental outcomes at both pH 6 and 8 were combined into a single dataset.

Table 7-2 Analysis of the *Bacillus subtilis* kinetic model prediction errors at each pH and temperature level.

Temp. °C	pH	Mean Error $\bar{\epsilon}_i$	n	s	$t_{\alpha/2}$	<sup>1</sup> 95% Confidence Limits on Mean Error $\bar{\epsilon}_i \pm t_{\alpha/2} \frac{s}{\sqrt{n}}$	<sup>2</sup> Statistical Significance at 95% Level?
3	6	0.3	8	0.2	2.4	0.1, 0.4	Yes
12	6	0.2	8	0.2	2.4	0.0, 0.3	Yes
22	6	0.3	9	0.2	2.3	0.1, 0.4	Yes
ALL	6	0.2	25	0.2	2.1	0.1, 0.3	Yes
3	8	-0.2	8	0.4	2.4	0.5, -0.1	No
12	8	-0.2	8	0.2	2.4	-0.02, 0.3	No
22	8	-0.1	9	0.3	2.3	-0.1, 0.3	No
ALL	8	-0.2	25	0.3	2.1	-0.3, -0.01,	Yes
ALL	ALL	0.04	50	0.3	2.0	-0.05, -0.1,	No

<sup>1</sup>Confidence limits were determined using the two-tailed Student t distribution with  $\alpha/2 = 0.025$

<sup>2</sup>Statistical significance was determined by comparing the measured mean error to zero. Significance was rejected if 95% confidence interval included zero.

## 7.5 COMPARISON TO OTHER STUDIES

The ozone inactivation characteristics of *B. subtilis* spores determined in this study differed somewhat from what has been reported by others. Facile and co-workers (2000) conducted a detailed study of the kinetics of *B. subtilis* spore inactivation by ozone using batch reactors and phosphate-buffered laboratory water. Working at 22°C and with the same strain of *B. subtilis* spores (ATCC 6633) used in the present study, they reported that the Hom kinetic model provided an adequate description of spore inactivation by ozone. They seem to have ignored, however, the lack of fit of the Hom model in the shoulder region of the observed inactivation curves. If they had investigated lower temperatures, Facile and co-workers (2000) may have discovered a more pronounced shoulder region in the spore inactivation curves and found that the Hom model provided a much poorer fit. In the present study, the size of the shoulder region was found to increase substantially as the temperature was decreased from 22°C to 3°C (Figures 7-1, 7-2 and 7-3). In the preliminary modeling work, the Hom model was found to provide a poor fit to the observed shoulder, especially at the lower temperatures, and was abandoned. The multi-target model, on the other hand, was found to adequately describe the shoulder at each experimental temperature.

According to the kinetic model developed in this study, a dissolved ozone  $Ct$  of 2.4 mg×min/L was required to provide 2 log-unit inactivation of spores at 22°C, and at either pH 6 or 8 (Figure 7-8). Facile and co-workers (2000) reported a comparable  $Ct$  product (3.2 mg×min/L) for 2 log-units inactivation of *B. subtilis* spores at pH 6.3 and 22°C. At pH 8.2, however, they reported a much greater  $Ct$  product requirement (6.3 mg×min/L) for the same level of inactivation. From the experimental information provided in their published work, it was not clear if these researchers appropriately accounted for the decomposition of ozone in these estimated  $Ct$  requirements. Ozone is much less stable at pH 8.2 than at pH 6.3. This may help explain why these researchers reported a significant pH effect on the ozone inactivation of the *B. subtilis* spores, while no such effect was observed in the present study. Using similar batch reactor protocols and within the same pH range (6 to 8), others reported that the effect of pH on inactivation of *C. parvum* oocysts by ozone was not significant (Gyürék et al. 1999; Li et al. 2001).

Owens and co-workers (2000) reported on the inactivation of an unidentified strain of *B. subtilis* spores seeded into a pilot-scale ozone bubble-column contactor. In natural water from the Ohio River, the  $Ct$  product required for 2 log-units inactivation was estimated to be 18 mg×min/L at 22.7°C. This  $Ct$  product is considerably greater than that reported in either this study or by Facile and co-workers. Such discrepancies in the inactivation requirements for *B. subtilis* spores reported from different studies might be attributed to differences in the experimental material and methods used. Spore sensitivity to ozone is potentially affected by the strain of bacterium and the procedures used for propagation of vegetative cells, sporulation, purification and enumeration of viable spores. Unfortunately, Owens and co-workers did not report these details in their work. The importance of method consistency and quality control when using spores as model organisms is emphasized.

## **7.6 COMPARISON TO *CRYPTOSPORIDIUM PARVUM***

Comparisons of the model-predicted ozone inactivation curves for *B. subtilis* spores and for *C. parvum* oocysts for three different temperatures (3, 12 and 22°C) are provided in Figures 7-8, 7-9 and 7-10. The *B. subtilis* curves were produced using the kinetic model developed in Section 7-3 with the parameters listed in Table 7-1. The *C. parvum* curves were produced using the temperature-corrected incomplete gamma Hom kinetic model previously reported by Li and co-workers (2001). Model inputs used in these simulations are indicated in the captions of each figure. For *B. subtilis* spores, the choice of initial ozone concentration,  $C_0$ , and first-order decomposition,  $k_d$ , rate was not important because inactivation was determined by the  $C_{avg}t_b$  product. On the other hand, different combinations of  $C_0$  and  $k_d$  will have a minor effect on predicted *C. parvum* inactivation because inactivation is proportional to  $C_{avg}^{0.70}t_b^{0.73}$  (Gyürék et al. 1999; Li et al. 2001).

A perfect model microorganism would share comparable ozone resistance to the pathogen of interest over the entire spectrum of ozone exposure conditions likely to be encountered in practice. Clearly, the spores of *B. subtilis* investigated in this study did not fulfill this criterion (Figures 7-8, 7-9 and 7-10). In particular, the shapes of the inactivation curves of the two microorganisms differed considerably. The curvi-linear  $C.$

*parvum* oocyst inactivation curve predicted by the Li and co-workers (2001) model contrasted sharply with the sigmoid inactivation curve of the *B. subtilis* spores. Because identical batch reactor protocols were used in both studies, it must be concluded that the observed differences in the inactivation curves were due solely to differences in the action of dissolved ozone on the microorganisms.

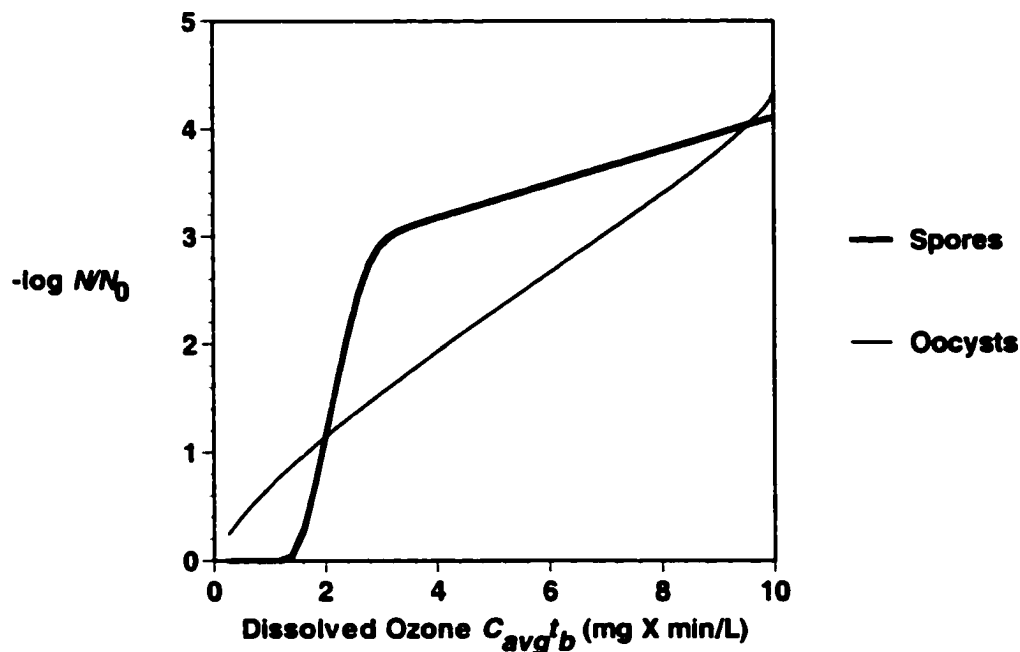


Figure 7-8 Comparison of model-predicted ozone inactivation curves of *Bacillus subtilis* ATCC 6633 spores and *Cryptosporidium parvum* oocysts at 22°C and pH 6 to 8. Model simulations were based on the following ozonation conditions:  $C_0 = 1$  mg/L,  $k_d = 0.1$  mg/L,  $t_b =$  various.

The different shapes of the inactivation curves of the two microorganisms complicated attempts at one-to-one comparison of inactivation. At low  $Ct$ , oocyst inactivation was greater than spore inactivation, mainly because of the shoulder region of the spore inactivation curve. At approximately 1 log-unit inactivation, the inactivation curves intersected and spore and oocyst inactivation requirements were approximately equal. As  $Ct$  was increased, however, spore and oocyst inactivation diverged rapidly. At

the highest  $Ct$  levels, spore inactivation exceeded oocyst inactivation by as much as two to three log-units. The same pattern was observed at each temperature, however the difference between spore and oocyst inactivation at high  $Ct$  was greatest at the lowest temperature (Figure 7-10). For this reason, direct inference of *C. parvum* oocyst inactivation capability of an ozone contactor, based on *B. subtilis* spore inactivation measured in challenge experiments, must be done with care.

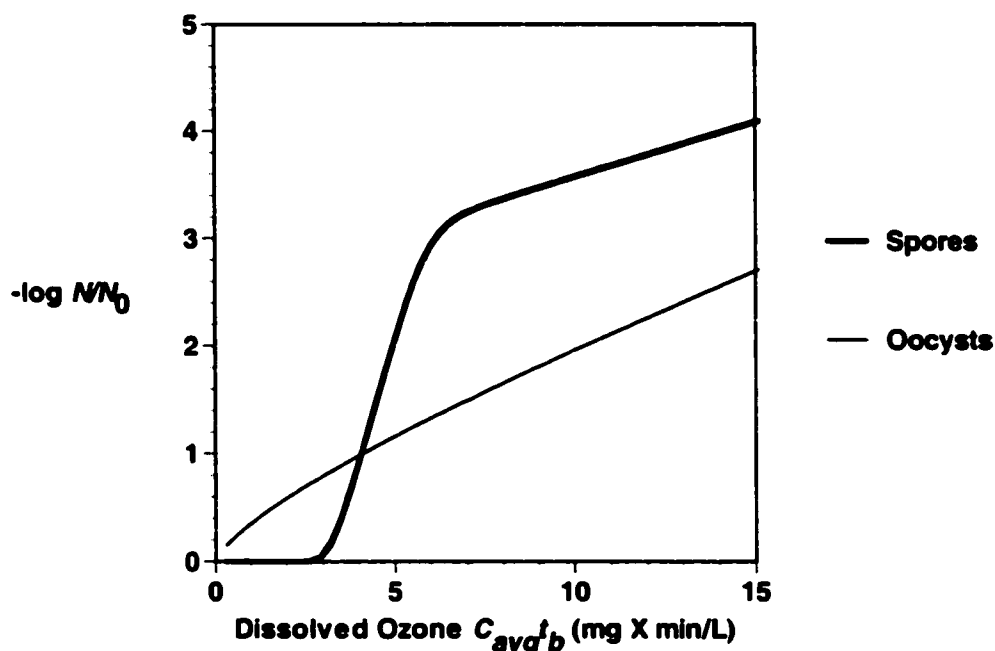


Figure 7-9 Comparison of model-predicted ozone inactivation curves of *Bacillus subtilis* ATCC 6633 spores and *Cryptosporidium parvum* oocysts at 12°C and pH 6 to 8. Model simulations were based on the following ozonation conditions:  $C_0 = 1.25$  mg/L,  $k_d = 0.05$  mg/L,  $t_b =$  various.

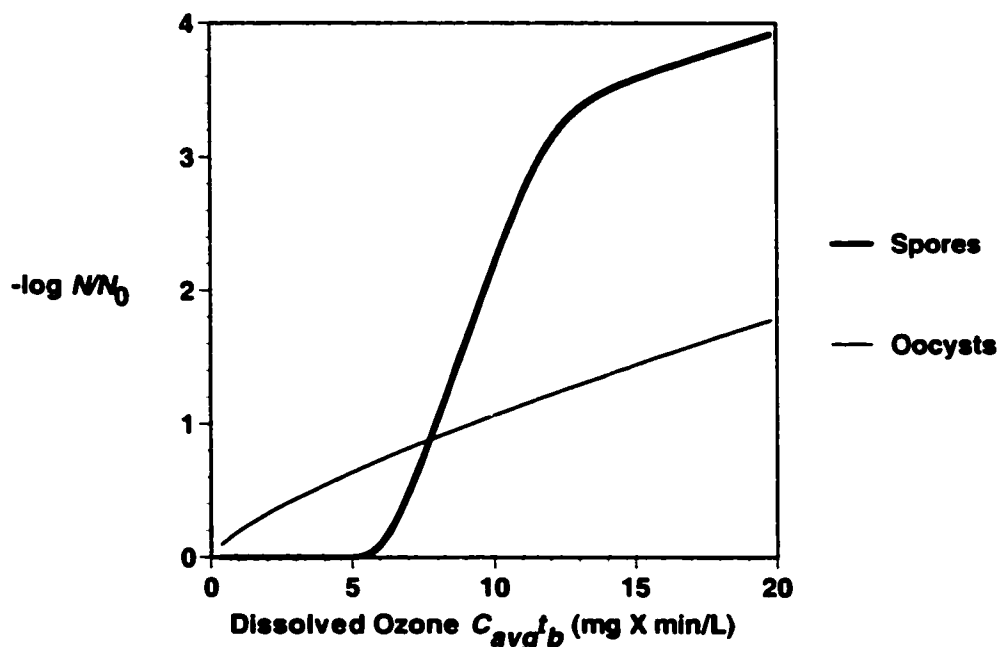


Figure 7-10 Comparison of model-predicted ozone inactivation curves of *Bacillus subtilis* ATCC 6633 spores and *Cryptosporidium parvum* oocysts at 3°C and pH 6 to 8. Model simulations were based on the following ozonation conditions:  $C_0 = 1.50$  mg/L,  $k_d = 0.05$  mg/L.

## 7.7 COMPARISON OF OZONE MEASUREMENT METHODS

The previous kinetic analysis was based on measurement of the dissolved ozone concentration in the batch reactors by the direct UV absorbance method. It was noted earlier that, in each batch reactor trial dissolved ozone concentration was also determined by the indigo trisulphonate colorimetric technique. The data set collected (Tables B-1, B-2 and B-3 of Appendix B) provided an excellent opportunity to compare the two analytical methods. Each of the batch reactor trials was carried out in ODF phosphate-buffered laboratory water. In this clean aqueous matrix, the potential sources of interference with the measurement of ozone by UV absorbance at 260 nm were few. The amount of background UV absorbance at 260 nm was low relative to the absorbance of ozone, and the change in background before and after ozone exposure was negligible. A

comparison of the two measurement methods, in terms of the ratio of the integrated average ozone concentration determined by the indigo method versus that determined by direct UV absorbance is presented in Figure 7-11. In the 50 batch reactor trials, the measurement ratio was observed to range from as low as 0.96 to as high as 1.35. The mean value was 1.17 with a relative standard deviation of 7%. The scatter plot at the top of Figure 7-11 and the histograms below it suggest that the ratio was randomly distributed and was independent of both ozone concentration and pH.

In this relatively clean aqueous system, therefore, ozone measurement by indigo was, on average, 17% greater than that measured by direct UV absorbance. This offset, which appeared to be constant in these batch reactor experiments, was probably related to the assumptions regarding the molar absorption coefficients used in the respective methods. The molar absorbance coefficient of  $3\,300\text{ M}^{-1}\text{cm}^{-1}$  used in the UV absorbance method was based on the published experimental work of Hart and co-workers (1983). The value of  $20\,000\text{ M}^{-1}\text{cm}^{-1}$  at 600 nm used with the indigo trisulphonate method was originally determined by Bader and Hoigné (Bader and Hoigné 1981) and is the currently recommended standard (APHA AWWA WEF 1992). There is, however, some degree of uncertainty associated with both of these values. According to Gordon and co-workers (1988), various molar absorption coefficients have been reported in the literature for aqueous molecular ozone. A recent study suggested that the molar absorption coefficient for determination of ozone by the indigo trisulphonate method might vary by up to 25%, depending on the source of the commercial indigo reagent (Gordon et al. 2000).

When making comparisons between different ozone studies or datasets, therefore, due consideration must be given to the methods used to measure dissolved ozone concentration. Differences in the methods used could very easily result in systematic bias when comparing inactivation of different microorganisms in similar contacting systems, or when comparing microorganism inactivation measured in two different ozone contacting systems. The comparison between ozone inactivation of *C. parvum* oocysts and *B. subtilis* spores presented in this chapter was free from this type of bias because identical ozone measurement methods were used to develop the respective kinetic models. The importance of ozone measurement method in such comparisons will be revisited in subsequent chapters of this thesis.

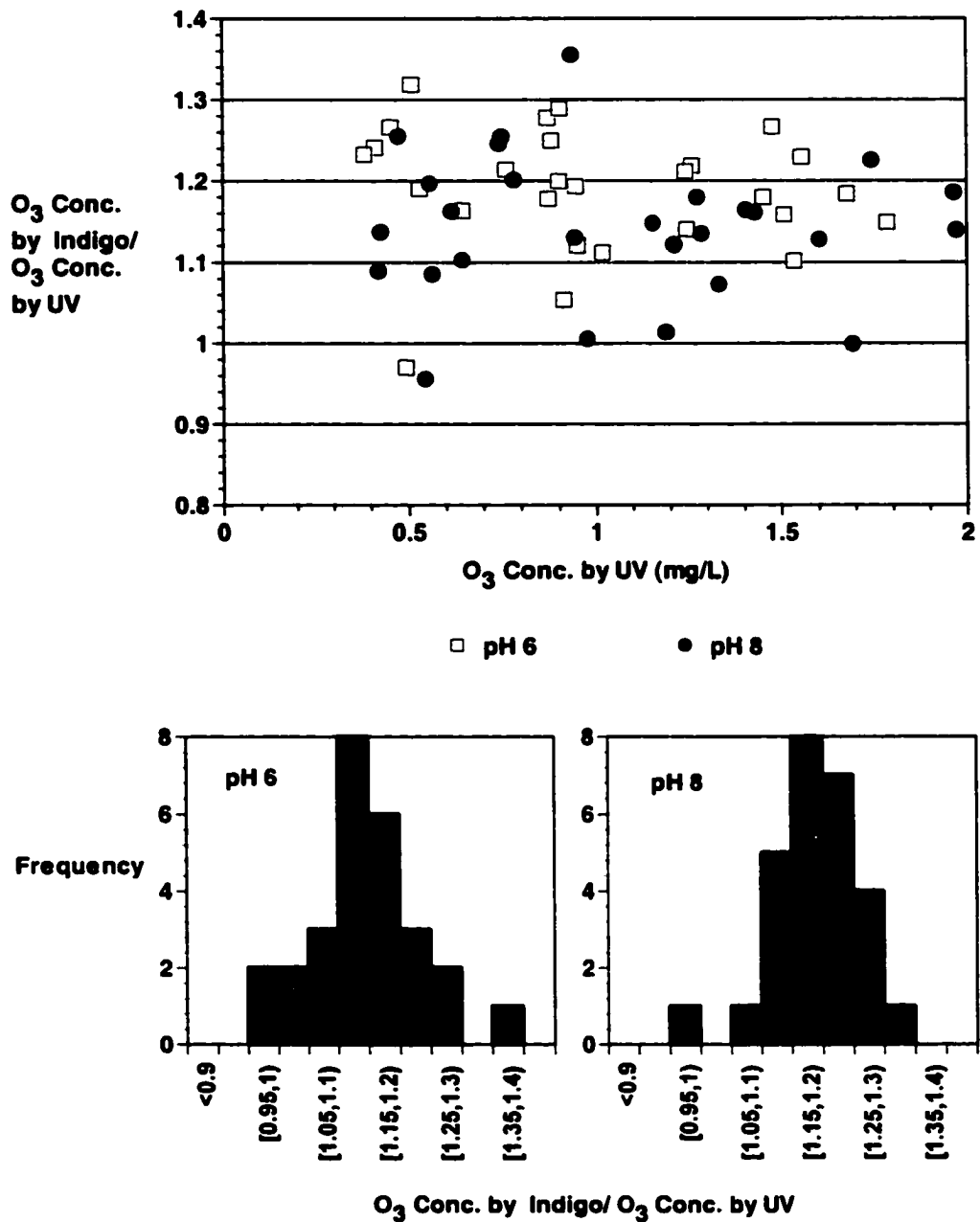


Figure 7-11 Ratio of the average dissolved ozone concentration in the *Bacillus subtilis* spore batch reactor experiments as determined by the indigo trisulphonate method and the direct UV absorbance method. TOP: Ratio is shown as a function of the dissolved ozone concentration and pH. BOTTOM: Histograms of the ratio at each pH.

## **7.8 SUMMARY OF BATCH REACTOR EXPERIMENTS WITH *BACILLUS SUBTILIS* SPORES**

A kinetic model was developed that predicts ozone inactivation of the strain of *B. subtilis* spores used in this study. The model was valid from 3 to 22°C and from pH 6 to 8. Direct inference of *C. parvum* inactivation from measured spore inactivation was not recommended due to gross differences in the shapes of the inactivation curves of the respective microorganisms. *B. subtilis* spores may still potentially serve as model organisms for evaluation of the hydrodynamic efficiency of ozone contactor designs. By comparing the measured spore inactivation in an ozone contactor for a given ozonation condition to the spore inactivation predicted by batch reactor studies, the hydrodynamic efficiency of the contactor can be assessed. Problems such as flow short-circuiting and excessive back-mixing can, potentially, be detected and resolved. If the challenge tests are conducted over a range of ozonation conditions, the strength of the analysis will improve. The intrinsic kinetics of inactivation of the experimental spores must, of course, be fairly well characterized in batch reactors. The added caveat is that the experimental methods, including spore methods and ozone measurement, must be carefully duplicated between the batch reactors and the experimental contactor. This approach to contactor evaluation using *B. subtilis* spores was demonstrated in experiments with the experimental static mixer ozone contactor described in Chapter 9.

## 8 OZONE TRANSFER EFFICIENCY

### 8.1 INTRODUCTION

Static mixers are useful for dispersion and dissolution of gases into liquids because the hydrodynamic conditions within the mixer elements promote generation of fine gas bubbles and high mass transfer rates. Available literature suggests that ozone gas-liquid mass transfer efficiency in static mixers is governed by hydrodynamic variables such as the superficial liquid velocity,  $v_s$ , pressure drop and the gas-to-liquid volumetric flow rate ratio,  $G/Q_f$  (Martin et al. 1992; Richards and Fleischman 1975; Zhu et al. 1989b). The objective of the experiments described in this chapter was to determine the factors that affected ozone mass transfer efficiency in the experimental static mixer contactor. The information developed was used in subsequent chapters to help study the relationship between ozone mass transfer efficiency and microorganism reduction in the static mixer contactor.

### 8.2 EXPERIMENTAL SYSTEM AND VARIABLES

The components of the experimental static mixer system that were part of the transfer efficiency study, the important experimental variables and the relevant sampling locations are summarized in Figure 8-1. The manipulated hydrodynamic variables were the superficial liquid velocity within the static mixer,  $v_s$ , and the gas-liquid volumetric flow rate ratio,  $G/Q_f$ . The height of the bubble column,  $H$ , was included as third manipulated variable. Ozone transfer efficiency determination was based on the measurement of ozone concentration in the feed gas,  $Y_f$ , and in the off-gas leaving the top of the bubble column,  $Y_o$ , and was calculated according to Equation 6-1. This measure of transfer efficiency included ozone dissolution that occurred within the mixing elements and spaces of the static mixer itself (see Figure 6-2), as well as any additional dissolution that occurred as the bubbles formed in the mixer rose in the bubble column. It also included any ozone dissolution that occurred in the 1 m length of 16 mm ID connecting tubing between the outlet of the static mixer and the bubble column.

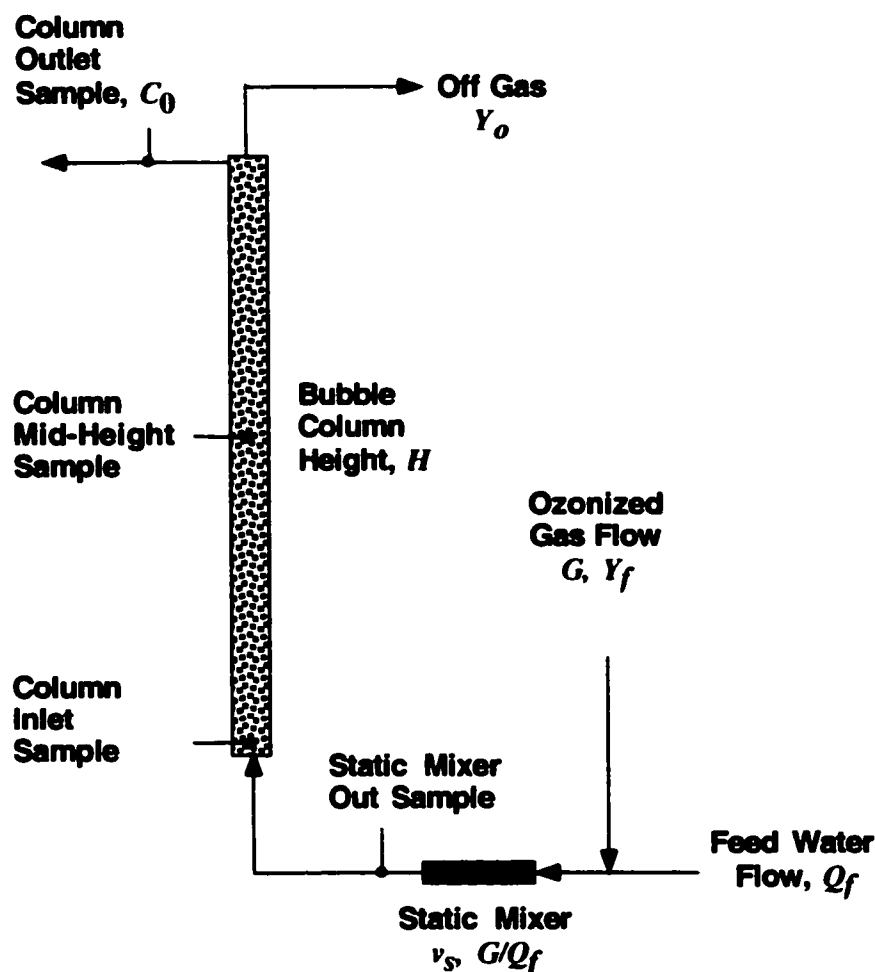


Figure 8-1 Manipulated and response variables in the ozone transfer efficiency experiments.

### 8.3 PRELIMINARY EXPERIMENTS

Detailed experimental information on each of the 31 transfer efficiency trials that were completed as part of this study was provided in Table C-1 of Appendix C. With the exception of trials 27 and 28, all trials were conducted at constant feed water temperature of  $16 \pm 1^\circ\text{C}$ . Trials 27 and 28 were conducted at a feed water temperature of  $7^\circ\text{C}$ . A set of preliminary experiments was carried out at a fixed feed water flow rate and with the bubble column adjusted to the maximum height of 2.3 m (Trials 1 thru 8 in Table C-1). At constant hydrodynamic conditions within the static mixer (i.e.  $v_s$  and  $G/Q_f$ ), transfer

efficiency was found to be essentially independent of both the feed gas ozone concentration,  $Y_f$ , the applied ozone concentration,  $C_a$ , and the dissolved ozone concentration at the outlet of the column,  $C_0$  (Table 8-1). The most significant finding was that operation of the static mixer contactor at a lower  $G/Q_f$  resulted in substantially greater transfer efficiency, regardless of the dissolved ozone concentration. The results of these preliminary trials were used as the basis for a designed experiment on ozone transfer efficiency.

Table 8-1 Results of preliminary ozone transfer efficiency trials with the experimental static mixer contactor.

Trial	$v_s$	$G/Q_f$	$Y_f$	$C_a$	$C_0$	TE
	m/s	%	g/L	mg/L	mg/L	%
1	0.93	4.3	47	2.0	1.6	80.2
2	0.93	4.4	86	3.7	3.0	80.9
3	0.93	4.3	10	0.4	0.4	77.9
4	0.93	4.3	71	2.4	2.8	78.3
5	0.93	1.3	90	0.9	1.0	92.2
6	1.04	1.2	104	1.1	1.6	92.7
7	1.04	1.2	20	0.2	0.2	93.8
8	1.04	1.2	104	1.1	0.9	93.2

#### 8.4 TRANSFER EFFICIENCY DESIGNED EXPERIMENT

A factorial experiment was designed to quantitatively evaluate the impact of hydrodynamic conditions within the experimental static mixer contactor, given by  $v_s$  and  $G/Q_f$ , on transfer efficiency. One of the advantages of a static mixer is that the

dissolution of ozone is very rapid and takes place within a very short contact time. Rapid dissolution in the static mixer reduces the need for the large two-phase contacting chambers of conventional fine-bubble diffuser contactors. The dissolved ozone profile measured in the static mixer and bubble column of the experimental contactor (Figure 8-2) indicated that development of the dissolved ozone concentration was mostly complete by the time the two-phase mixture entered the bottom of the bubble column. A considerable fraction of the ozone transfer appears to have occurred in the 1 m section of 16 mm ID tubing that connected the outlet of the static mixer to the inlet of the bubble column. This raised the question of the importance of the bubble column to overall ozone gas-liquid mass transfer and dissolution. To explore this question, the height of the bubble column,  $H$ , was included as a third factor in the experimental design.

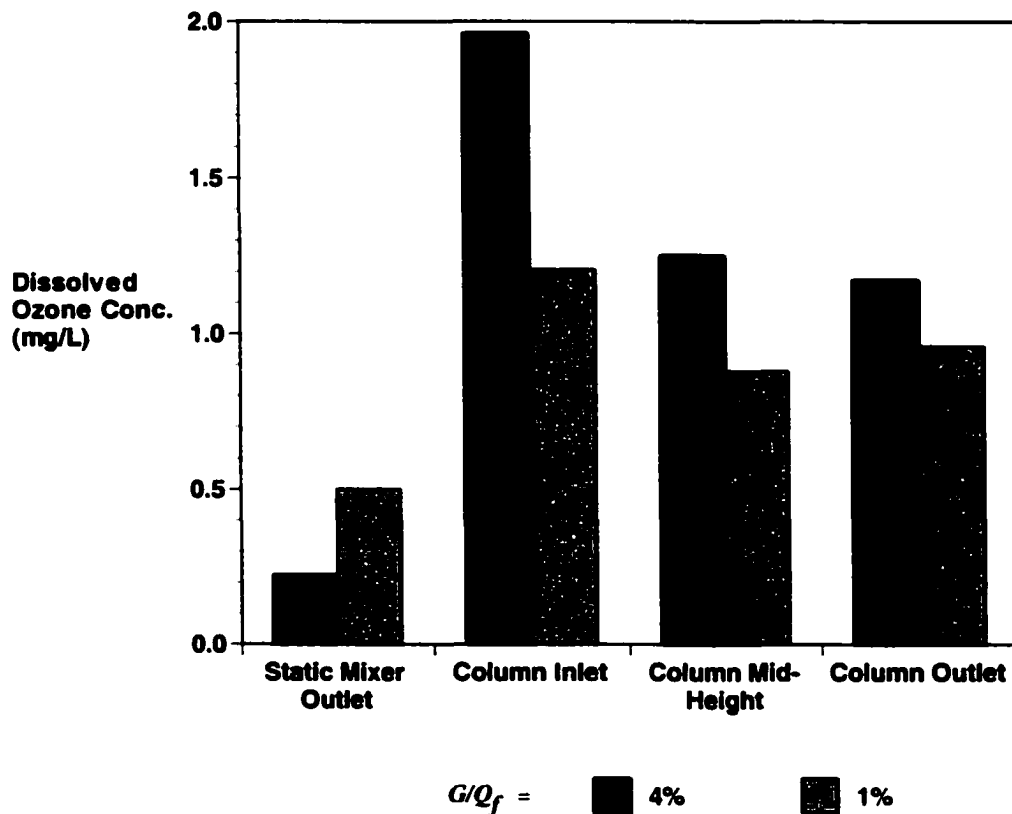


Figure 8-2 Typical dissolved ozone profiles in the static mixer ozone contactor bubble column at high and low  $G/Q_f$  settings. The static mixer superficial velocity,  $v_s$ , was constant at 0.9 m/s.

A two-level, three-factor full-factorial experiment was designed to investigate the potential effects of the three factors ( $v_s$ ,  $G/Q_f$  and  $H$ ) on ozone transfer efficiency and any possible interactions. The high (+1) and low (-1) target levels for each of the factors are provided in Table 8-2. In factorial experimental design, the magnitude of the manipulated variables are often normalized to a range of between -1 and +1 and are expressed in coded units as follows (Box et al. 1978):

$$\text{Coded Value} = 2 \left[ \frac{\text{Real Measured Value} - \text{Low Target Value (-1)}}{\text{High Target Value (+1)} - \text{Low Target Value (-1)}} \right] - 1 \quad \text{Equation 8-1}$$

The outcomes of the experimental design trials are summarized in Table 8-3. The coded values the factors shown in Table 8-3 were adjusted for the actual conditions achieved during the experimental trial. The experimental trials shown in Table 8-3 were carried out in random order to minimize the effects of day-to-day variations in uncontrolled variables such as water quality and ozone generator operation.

Table 8-2 Settings of the transfer efficiency designed experiment factors in real and coded units.

<b>Variable</b>	<b>Low Level</b>	<b>Medium Level</b>	<b>High Level</b>
<b>Coded Unit</b>	-1	0	+1
$v_s$ , m/s	0.7	0	1.3
$G/Q_f$ , %	1.2	2.7	4.1
$H$ , m	0.45	1.4	2.3

**Table 8-3** Results of ozone transfer efficiency factorial designed experiment on the experimental static mixer contactor.

Trial	Factor Values in Coded Units			Response Variables	
	$v_s$	$G/Q_f$	$H$	$TE$	$C_0$
				%	mg/L
16	-1.04	-1.02	-1	76.1	1.2
20	-1.15	-0.98	1	88.7	1.2
11	-1.21	1.22	-1	66.3	0.8
29	-0.94	0.85	1	77.4	0.8
17	0.04	-1.01	-1	86.7	1.0
31	-0.36	-0.88	-0.16	87.1	1.2
22	0.04	-1.01	1	93.0	1.1
15	0.04	0.95	-1	73.7	0.5
21	0.04	0.99	1	82.0	0.8
25	1.28	-1.02	-1	90.3	1.0
26	1.13	-0.99	-0.16	91.8	1.2
24	1.18	-1.01	1	93.8	1.3
10	1.10	-0.03	-1	81.3	1.0
23	1.18	-0.02	1	88.1	1.0
12	-0.16	0.05	-0.16	80.6	1.1
19	-0.09	0.00	-0.16	82.0	0.8
18	-0.08	-0.01	-0.16	80.7	0.9

Although the transfer efficiency was the primary response variable, the value of the ozone concentration at the outlet of bubble column,  $C_0$ , was also provided for information purposes. For each experimental setting of  $v_s$  and  $G/Q_f$ , the objective was to maintain  $C_0$  at approximately 1 mg/L by appropriate adjustment of the feed gas ozone

concentration. During the experiments,  $C_0$ , varied between 0.5 and 1.3 mg/L. Based on the outcomes of the preliminary trials (Table 8-1), this variation in dissolved ozone concentration was not expected to have a significant effect on transfer efficiency. Also, during the course of the experiment, it became clear that it was not possible to maintain stable operation of the contactor at the target test condition of high (+1)  $v_s$  and high (+1)  $G/Q_f$ . A target condition of high (+1)  $v_s$  and intermediate (0)  $G/Q_f$  was, therefore, substituted. As a result, the resulting factorial experiment was less than perfectly balanced.

## 8.5 TRANSFER EFFICIENCY MODELING

To interpret the outcomes of the designed experiment in Table 8-3, an empirical mathematical model of the following general linear polynomial form was regressed to the experimental data:

$$TE = a_0 + a_1x_1 + a_2x_2 + a_3x_3 + a_{11}x_1^2 + a_{22}x_2^2 + a_{33}x_3^2 + a_{12}x_1x_2 + a_{13}x_1x_3 + a_{23}x_2x_3 + a_{123}x_1x_2x_3 \quad \text{Equation 8-2}$$

In this equation, the generic variables  $x_1$ ,  $x_2$ ,  $x_3$  represented the normalized coded values of the experimental variables  $v_s$ ,  $G/Q_f$  and  $H$ . Model coefficients,  $a_0$ ,  $a_1$  ...etc., were computed by multiple linear regression of Equation 8-2 to the data of Table 8-3 using least squares minimization criteria. Computations were done on a Microsoft Excel 2000 spreadsheet program using the Solver function. Several linear models with different combinations of the terms shown in Equation 8-2 were tested using regression analysis. Analysis of variance (ANOVA) was used to test the significance of each model. The significance of model terms was determined by comparing the computed coefficient value to zero in a hypothesis test. Terms were rejected if the probability of a type I error, indicated by the  $p$ -value computed for that parameter, was greater than 0.05.

Of the various linear model forms explored, the following model was found to provide the best fit to the data:

$$TE = 83.2 + 3.9v_s' - 6.1(G/Q_f)' + 4.1H' - 1.8v_s'^2 + 1.8v_s'(G/Q_f)'H' \quad \text{Equation 8-3}$$

The prime (') in Equation 8-3 signifies that the value of each manipulated variable was in coded units as defined by Equation 8-1. ANOVA results for this model are summarized and presented in Table 8-4 below.

**Table 8-4** Analysis of variance (ANOVA) results for the transfer efficiency model least-squares linear regression.

Source of Variation	Degrees of freedom	Sum of Squares	Mean Square	F-statistic	p-value
Model	5	878	176	126	$2.5 \times 10^{-9}$
Error	11	15.3	1.4		
Total	16	893			

Model Term	Coefficient	Standard Error	p-value
Y-intercept	83.2	0.43	$8.3 \times 10^{-21}$
$v_s$	3.9	0.37	$3.9 \times 10^{-7}$
$G/Q_f$	-6.1	0.38	$4.7 \times 10^{-9}$
$H$	4.2	0.35	$1.2 \times 10^{-7}$
$v_s^2$	-1.8	0.45	0.002
$v_s \times G/Q_f \times H$	1.8	0.47	0.003

**Notes:** Computation of standard error, sums of squares, mean square and p-values were done using the regression option in the Analysis Tool Pak of Microsoft Excel 2000.

The large value of the computed  $F$  statistic ( $F = 126$ ) compared to value required for significance at the 99.9% level ( $F > 9.6$ ) is indicative of the significance of the regressed model. The computed  $p$ -values demonstrated that each model term was significantly different than zero at the 95% confidence level ( $p < 0.05$ ). Comparison of model-predicted and measured transfer efficiency indicated a good overall fit to the data (Figure 8-3).

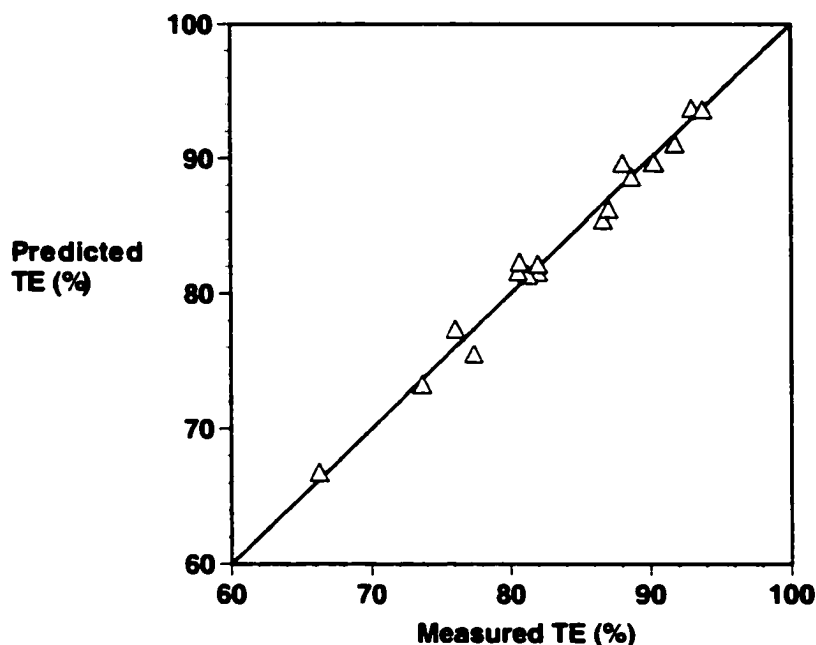


Figure 8-3 Comparison of model-predicted and measured ozone transfer efficiency. The 45 degree diagonal line represents a perfect model fit.

## 8.6 MODEL PREDICTIONS

As expected, the hydrodynamic conditions within the static mixer, determined by the superficial velocity,  $v_s$ , and the gas-liquid volumetric flow rate ratio,  $G/Q_f$ , were found to have significant effects on ozone transfer efficiency. Transfer efficiency was greatest when  $v_s$  was highest and  $G/Q_f$  was lowest. Transfer efficiency was also improved by increasing column height under all hydrodynamic conditions within the

static mixer. Increasing column height increased both the duration of contact between gas bubbles and the water, and the pressure of the total gas pressure in the static mixer. An increase in either of these factors was intuitively expected to result in an increase in the amount of ozone transferred to the liquid phase. The significance of the 3-factor term ( $v_s \times G/Q_f \times H$ ) in the model suggested variable interactions that were not necessarily intuitive. The empirical transfer efficiency model of Equation 8-3 and these interactions were investigated further by examining plots of selected model predictions such as those provided in Figure 8-4.

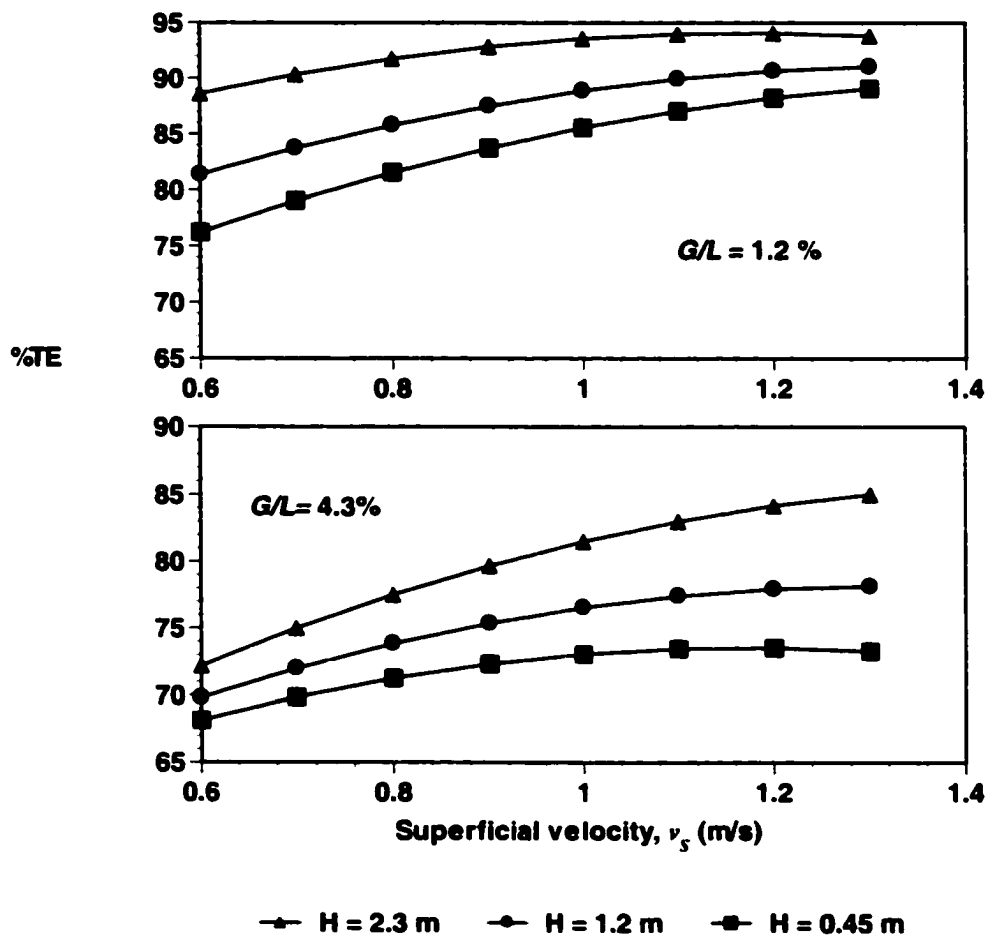


Figure 8-4 Examples of transfer efficiency model predictions. Effect of superficial velocity,  $v_s$ , within the static mixer and bubble column height,  $H$ , on transfer efficiency at two  $G/Q_f$  levels.

The plots of Figure 8-4 suggest that the importance of column height to transfer efficiency was related to the hydrodynamic conditions within the static mixer. For example, at high  $v_s$  and low  $G/Q_f$  (top of Figure 8-4), ozone dissolution within the static mixer was efficient and most of the transfer occurred within the mixer itself. At this condition, the effect of the bubble column was relatively small. A five-fold increase in the height of the separator from 0.45 m to 2.3 m produced only a 4 percent increase in transfer efficiency. At low  $v_s$ , and still at a low  $G/Q_f$ , where the mass transfer and dissolution within the static mixer was less efficient, a much larger (~11%) percent increase in transfer efficiency was realized by making the column taller. Interestingly, at a high  $G/Q_f$  condition (bottom of Figure 8-4) the effect was reversed. The column height had the least impact at the lowest velocities, where efficiency was lowest, and the most impact at higher velocities and efficiency.

## 8.7 EFFECT OF WATER TEMPERATURE

The factorial designed experiment was carried out at a constant water temperature of  $16 \pm 1^\circ\text{C}$ . To determine to the magnitude of the effect of a decrease in temperature on the transfer efficiency in the static mixer, two trials were conducted at a lower temperature of  $7^\circ\text{C}$ . The results of these trials are summarized in Table 8.5 together with the results of three other trials conducted at  $16^\circ\text{C}$  and at the same settings of  $v_s$ ,  $G/Q_f$  and  $H$ . The decrease in water temperature of  $9^\circ\text{C}$  resulted in only a modest increase in transfer efficiency of about 1.9%. Based on the principles of gas-liquid mass transfer, this reduction in water temperature may have affected ozone transfer efficiency in the static mixer system in several ways, and was, therefore, the outcome was difficult to predict. On the one hand, ozone gas solubility, which is governed by Henry's law, dictates that the equilibrium driving for mass transfer,  $C^* - C$ , was greater at  $7^\circ\text{C}$  than at  $22^\circ\text{C}$ . On the other hand, diffusion rates generally decrease with temperature, therefore, the rate of diffusion through the liquid-film, described by rate coefficient,  $k_L$ , in Equation 2-1, would have been lower at  $7^\circ\text{C}$  than at  $22^\circ\text{C}$ . In addition, the change in water viscosity with temperature may have influenced the formation and size of the ozone bubbles and the thickness of the liquid film in more complex ways. The outcomes of the low temperature trials suggest, in the static mixer system, that the solubility and other

mass transfer rate mechanisms balanced each other, resulting in overall transfer efficiency that was relatively insensitive to temperature.

Table 8-5 Effect of water temperature on ozone transfer efficiency in the static mixer contactor.

Trial	Temp.	Factor Values			Measured Transfer Efficiency, <i>TE</i>
		$v_s$	$G/Q_f$	$H$	
	°C	m/s	%	m	%
12	16	0.93	2.72	1.4	80.6
18	16	0.95	2.63	1.4	80.7
19	16	0.95	2.65	1.4	82.0
27	7	0.96	2.65	1.4	82.8
28	7	0.96	2.65	1.4	83.2

## 8.8 DISCUSSION

Engineers often prefer ozone transfer efficiency (*TE*) for specifying and measuring performance of ozone dissolution systems (Rakness et al. 1988). Although this parameter can be used to compare the efficiency and economics of ozone use between different types of contactors, it provides little information regarding the mechanisms that govern the gas-liquid mass transfer process. For example, a taller column may have resulted in better ozone transfer efficiency either through increased duration of bubble contact or increased gas pressure. By itself, the transfer efficiency measurement provided no insight into which physical factor was more important. Researchers who have conducted detailed mechanistic studies of ozone mass transfer, such as Zhou and Smith (2000) and Roustan and co-workers (1996), prefer to use of the

overall mass transfer coefficient,  $k_L a$ , of Lewis and Whitman two-film theory. The primary purpose of the analysis presented in this chapter, however, was to develop a mathematical tool that could be used to predict the ozone transfer efficiency in the experimental static mixer contactor under a limited set of well-defined operating conditions. For this purpose, the empirical approach was considered sufficient. A detailed mechanistic study of the gas-liquid ozone mass transfer based on available mass transfer theories, though interesting to consider, was beyond the intended scope of the work.

The empirical modeling analysis provided useful insights into optimization of ozone dissolution in a static mixer contacting system. The finding that transfer efficiency increased with superficial velocity and decreased with increasing gas-liquid flow rate ratio was consistent with what has been reported by other researchers for ozone dissolution in static mixing systems (Martin et al. 1992; Richards and Fleischman 1975; Zhu et al. 1989b). In mechanically stirred ozone contactors, the overall mass transfer coefficient,  $k_L a$ , has been observed to be directly proportional to the power input or rate of energy dissipation (Langlais et al. 1991). In a static mixer, the rate of energy dissipation is directly proportional to the fluid pressure drop and flowrate, which is, in turn proportional to the superficial velocity (supporting data in Table C-1 of Appendix C). The measured superficial velocity effect in the experimental static mixer was, therefore, expected.

Better transfer efficiency at lower  $G/Q_f$  may be explained in terms of either a hydrodynamic effect or a concentration effect. In the hydrodynamic explanation, lower  $G/Q_f$  resulted in the formation of smaller gas bubbles with greater specific surface area and better mass transfer properties. Smaller bubbles were qualitatively observed at lower  $G/Q_f$ , but this observation was not confirmed by quantitative bubble size measurement. At lower  $G/Q_f$ , a higher concentration of ozone in the ozonized feed gas was required in order to maintain the same applied ozone dose and dissolved ozone concentration. The equilibrium dissolved ozone concentration,  $C^*$ , and the driving force for ozone mass transfer,  $C^* - C$ , were consequently higher at lower  $G/Q_f$ . According to two-film theory (Equation 2-1), this should have resulted in a higher overall mass transfer rate,  $M$ . With the experimental static mixer system, however, it was difficult to determine to what

extent these two potential mechanisms influenced transfer efficiency because the variables  $G/Q_f$ ,  $Y_f$  and  $C_0$  were not independent. The settings of any two of these variables determined the level of the third. Nevertheless, for a fixed dissolved ozone concentration in the bubble column outlet, the most efficient operation was at a low  $G/Q_f$  and high feed gas ozone concentration,  $Y_f$ . Better transfer efficiency at low gas flows is an advantage of static mixers because it means that these devices can be effectively integrated with modern, high-concentration ozone generators. In comparison, conventional fine bubble diffusion systems are limited by the requirement of sufficient volumetric gas flow to ensure adequate gas-liquid mixing and ozone dissolution (Shulz et al. 1995).

In previous experimental studies involving static mixers (Martin et al. 1992; Richards and Fleischman 1975; Zhu et al. 1989b), the ozone transfer efficiency was reported for the overall contacting system only and not for the individual system components. Addition of the bubble column height as an experimental variable in the present study provided new insight into the contribution of the various components of a static mixer dissolution system for ozone. Difficulty in collecting a representative gas sample prevented direct determination of transfer efficiency within the static mixer itself. The dissolved ozone concentration, however, increased between the outlet of the static mixer and the inlet of the bubble column (Figure 8-1). This meant that dissolution was far from complete at the outlet of the static mixer and that significant additional ozone dissolution occurred within the 0.7 s and 1.5 s hydraulic residence time in the connecting tubing between the static mixer outlet and the bubble column inlet. The transfer efficiency model further demonstrated that additional ozone mass transfer occurred within the bubble column, even at optimum conditions within the static mixer.

To truly optimize static mixer systems for ozone dissolution, equipment designers need to consider the contribution of the various system components, including the static mixer itself, the static mixer outlet piping and any downstream contact vessels. Designers also need to consider how these components work together to provide the best ozone dissolution. In particular, the role of the piping at the exit of the static mixer should be considered carefully. A more detailed investigation than the empirical study

presented in this Chapter, however, would be required in order to better understand the mechanisms dominating ozone gas-liquid mass transfer in the static mixer contactor.

## **9 INACTIVATION OF *BACILLUS SUBTILIS* SPORES IN THE STATIC MIXER CONTACTOR**

### **9.1 INTRODUCTION**

Mass transfer in gas-liquid systems is often dominated by hydrodynamic considerations. The study in Chapter 8 demonstrated how the static mixer liquid velocity,  $v_s$ , and the gas-liquid flow rate ratio,  $G/Q_f$ , dictated ozone transfer efficiency in the experimental contactor. An ozone contacting system designed for microorganism reduction, however, involves both gas-liquid mass transfer and the reaction between ozone and the microorganisms. The question addressed in this chapter was: to what extent does the hydrodynamic environment within the static mixer influence the intrinsic kinetics of microorganism inactivation by ozone? Of particular interest was to determine if microorganism inactivation was affected by the hydrodynamic conditions of gas-liquid contact within the static mixer.

### **9.2 EXPERIMENTAL DESIGN**

In this experimental study, cultured *Bacillus subtilis* (ATCC 6633) spores were used as indicators of microorganism reduction efficiency in challenge tests. In Chapter 7, the ozone resistance and inactivation kinetics of this strain of spores was characterized. It was concluded that these microorganisms were useful for evaluation of the efficiency of microorganism reduction in ozone contacting systems. A factorial experiment was designed using the experimental static mixer contactor in which the hydrodynamic conditions within the static mixer were varied by adjusting the settings of  $v_s$  and  $G/Q_f$ . Target conditions for the 2-level, 2-factor design are provided in Table 9-1. By exploiting the independent flow adjustment capability of the experimental contactor, the conditions of dissolved ozone contact in the reactive flow segment (RFS) were maintained approximately constant while experimental settings of  $v_s$  and  $G/Q_f$  were varied. For example, the flow rate in the reactive flow segment was maintained at a nominal setting of 2 L/min regardless of the setting of  $v_s$ . The dissolved ozone concentration at the inlet to the reactive flow segment,  $C_0$ , was adjusted to between 0.9 and 1.1 mg/L for each setting of  $v_s$  and  $G/Q_f$  by manipulating the ozone concentration in

the feed gas. All spore challenge trials were done using the shortest bubble column configuration ( $H = 0.45$  m) and at a target water temperature of 16°C. The ozone transfer efficiency at each operating condition was estimated using the empirical transfer efficiency model developed in Chapter 8.

Table 9-1 Target experimental conditions for the factorial designed experiment on the effect of static mixer hydrodynamic conditions on *Bacillus subtilis* spore inactivation.

Target Experimental Setting	$v_s$ m/s	$G/Q_f$ %	$^1C_0$ mg/L	RFS Flow Rate L/min
1	0.6	1.2	0.9 to 1.1	2.0
2	0.6	2.6	0.9 to 1.1	2.0
3	1.4	1.2	0.9 to 1.1	2.0
4	1.4	2.6	0.9 to 1.1	2.0

<sup>1</sup>Dissolved ozone concentration at inlet to reactive flow segment (RFS)

### 9.3 RESIDENCE TIME DISTRIBUTION

#### 9.3.1 Determination of the Mean Residence Times

Microorganism inactivation measured at different locations in the static mixer contactor was interpreted in terms of the cumulative dissolved ozone  $C_{avg}t_m$  product. To permit a rigorous analysis, precise knowledge of the mean residence time,  $t_m$ , at each microorganism sampling location was required. The mean residence time was carefully determined for each microorganism sampling location by way of pulse tracer tests with methylene blue dye. Examples of the exit age distribution,  $E(t)$ , measured at the outlet of the bubble column for two different feed water flow rates and  $G/Q_f$ , were provided in Figure 9-1. These flow rates corresponded to the target settings of the superficial

velocity,  $v_s$ , in Table 9-1. The value of  $G/Q_f$  was found to have little impact on the measured  $E(t)$  and  $t_m$  for the bubble column. Examples of the exit age distributions measured at each of the sampling locations in the reactive flow segment for a fixed flow rate of 2 L/min were shown in Figure 9-2. Each tracer test was repeated in either duplicate or triplicate and the mean residence time,  $t_m$ , was calculated using Equation 6-13. The calculated  $t_m$  values for each replicated tracer test are provided in Table 9-2. For the reactive flow segment, the relative standard deviation of replicated  $t_m$  determinations ranged from 1.2 to 4.5%. Exit age distributions and calculated  $t_m$  values were, therefore, considered reproducible.

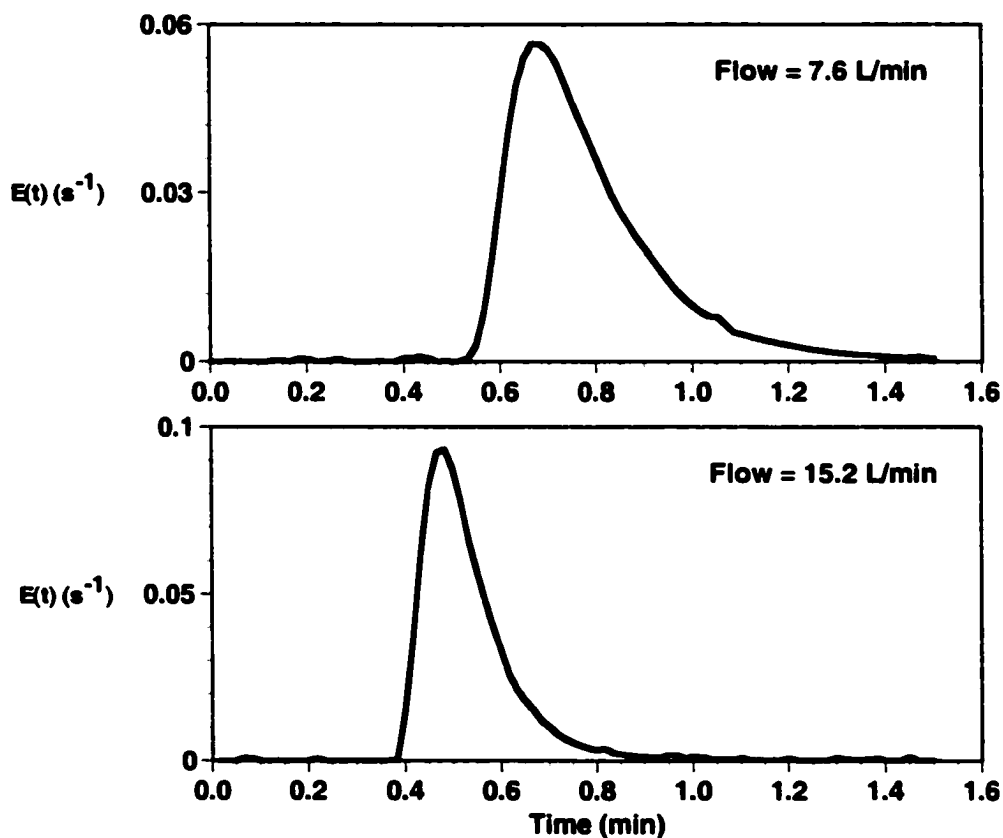


Figure 9-1 Examples of the exit age distribution,  $E(t)$ , measured at the outlet of the bubble column for the two experimental feed water flow rates.

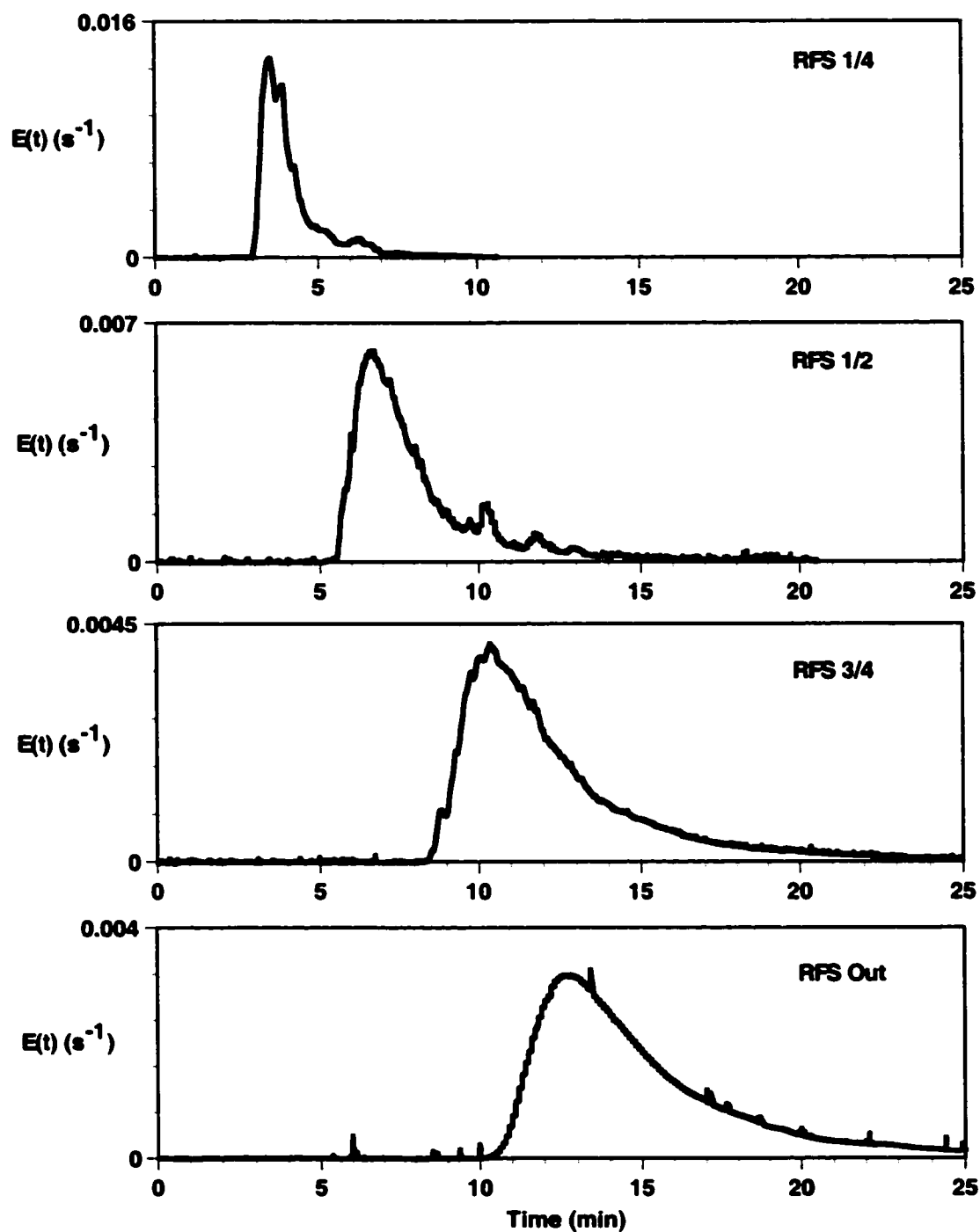


Figure 9-2 Examples of the exit age distribution,  $E(t)$ , measured at four different locations in the reactive flow segment (RFS) for a flow rate of 2 L/min.

Table 9-2 Summarized results of replicate residence time determinations at microorganism sampling locations in the experimental static mixer ozone contactor.

Location	Water Flow Rate, $Q_f$ L/min	$G/Q_f$ %	Mean Residence Time, $t_m$ (min)				$t_{10} / t_m$			
			1	2	3	Avg.	1	2	3	Avg
Column Out	7.5	1.2	0.63	0.72	na	0.68	0.68	0.69	na	0.69
Column Out	7.5	2.6	0.68	0.75	na	0.72	0.66	0.64	na	0.65
Column Out	15.2	1.2	0.40	0.57	na	0.49	0.65	0.70	na	0.68
Column Out	15.2	2.6	0.45	0.42	na	0.44	0.58	0.57	na	0.58
<sup>1</sup> RFS ¼	2	na	4.5	4.3	4.5	4.4	0.83	0.78	0.83	0.81
<sup>1</sup> RFS ½	2	na	8.0	8.6	8.6	8.4	0.75	0.73	0.75	0.74
<sup>1</sup> RFS ¾	2	na	12.2	11.9	12.1	12.1	0.77	0.79	0.78	0.78
<sup>1</sup> RFS Out	2	na	16.0	15.5	16.5	16.0	0.80	0.77	0.82	0.80

<sup>1</sup>Measured at a bubble column flow rate of 7.6 L/min.

na = not applicable (single-phase flow in reactive flow segment)

### 9.3.2 Effect of the Residence Time Distribution on Ozone Decomposition

For each spore challenge experiment, the average  $t_m$  values reported in Table 9-2 were integrated with the measured dissolved ozone concentration profile and the average  $C_{avg}t$  products at each sampling location according to Equations 6-14 and 6-15. This calculation of  $C_{avg}t_m$  assumed that, in terms of the ozone decomposition reaction, the

deviation from perfect plug flow behaviour in the contactor was negligible. Perfect plug flow, however, is an abstraction that is generally not achieved in practice. The measured  $E(t)$  curves of Figure 9-1 and Figure 9-2, were closer to streamline or laminar flow than perfect plug flow (Nauman and Buffham 1983). The colored dye used in the tracer tests permitted visual examination of the flow pattern within the contactor during the tracer tests. Observations of the radial dye concentration profile were consistent with a laminar-type flow pattern. Further, the estimated Reynold's number in the reactive flow segment of approximately 800 was more closely associated with laminar flow than fully developed turbulent flow in pipes (Daugherty and Franzini 1977).

To test if the observed deviation from perfect plug flow in the static mixer contactor had a significant impact on ozone decomposition, a series of segregated flow analysis calculations were performed. Equation 3-13 and Equation 6-15 were combined to yield the following segregated flow analysis expression for the estimated ozone  $C_{avg}t_m$  in a non-ideal flow contactor:

$$C_{avg}t_m = \int_{t=0}^{t=\infty} \left[ \frac{C_0}{k_d} (1 - \exp(-k_d t)) \right]_{\text{batch}} E(t) dt \quad \text{Equation 9-1}$$

Using the measured  $E(t)$  in Figure 9-2 and reasonable estimates of the first-order ozone decomposition rate,  $k_d$ , (0.02 to 0.04  $\text{min}^{-1}$ ) the  $C_{avg}t_m$  product calculated using the plug flow assumption (Equation 6-15) was found to be within 5% of that determined using the segregated flow analysis (Equation 9-1). For determination of the dissolved ozone  $C_{avg}t_m$  products in the experimental ozone contactor, the assumption of plug flow, therefore, was considered to be sufficiently accurate.

#### 9.4 FACTORIAL EXPERIMENT RESULTS

The  $2 \times 2$  factorial design described in Table 9-1 was completely replicated for a total of eight *B. subtilis* challenge experiments, two at each of the four static mixer hydrodynamic conditions. A summary of the ozonation conditions actually achieved in

each of the eight challenge experiments is provided in Table 9-3. Complete information for each experiment, including ozonation conditions and spore enumeration information, is provided in Tables D-1, D-2 and D-3 of Appendix D.

Table 9-3 Experimental conditions for *Bacillus subtilis* spore inactivation experiments in the experimental static mixer ozone contactor.

Trial	$v_s$	$G/Q_f$	$^1C_0$	$^2k_d$	$^3TE$	$^4M$	$^5Temp.$	$^6$ Inactivation in the static mixer
	m/s	%	mg/L	min <sup>-1</sup>	%	mg/min	°C	log-units
34	0.63	1.3	1.22	0.039	77	9.8	16.6	0.30 ± 0.5
38	0.59	1.3	1.22	0.018	75	9.5	15.6	0.07 ± 0.2
35	1.34	2.5	0.88	0.016	82	15.0	16.0	0.01 ± 0.1
39	1.38	2.4	0.98	0.037	82	17.5	15.4	-0.03 ± 0.2
36	1.37	1.2	1.34	0.030	89	23	16.3	0.01 ± 0.5
40	1.40	1.2	0.83	0.032	89	14.7	16.4	0.11 ± 0.4
37	0.55	3.2	1.16	0.023	70	8.3	16.4	0.04 ± 0.2
41	0.69	2.5	1.47	0.039	75	12.4	16.4	0.03 ± 0.4

<sup>1</sup>Ozone concentration measured at the inlet of the RFS.

<sup>2</sup>Estimated 1<sup>st</sup> order ozone decomposition constant in the RFS.

<sup>3</sup>Ozone transfer efficiency estimated from an empirical model.

<sup>4</sup>Ozone mass transfer rate based on measured  $Q_f$  and measured  $C_0$  values.

<sup>5</sup>Average of water temperature measured at inlet to static mixer and outlet of reactive flow segment.

<sup>6</sup>Mean and ± 95% confidence interval shown.

For each trial, ozone mass transfer was characterized by the transfer efficiency,  $TE$ , and the overall rate of mass transfer,  $M$ , in mass per unit time. The ozone transfer efficiency values listed in Table 9-3 were calculated using the empirical model described in Chapter 8 (Equation 8-3) with the height of the bubble column,  $H$ , set equal to 0.45 m. The mass transfer per unit time was estimated as the product of the feed water flowrate,  $Q_f$ , and the ozone residual at the outlet of the bubble column,  $C_0$ . The last column in Table 9-3 shows the spore inactivation within the static mixer itself. This was determined from measurement of viable spore concentrations in the feed and at the outlet of the static mixer.

#### 9.4.1 Selection of Dissolved Ozone Measurement Method

Spore inactivation measured in duplicate challenge experiments is plotted as a function of the dissolved ozone  $C_{avg}t_m$  product in the contactor Figure 9-3. Plots were shown for each of the four experimental static mixer hydrodynamic conditions. The  $C_{avg}t_m$  upon which these plotted inactivation curves were based were derived from dissolved ozone analysis by the indigo trisulphonate colorimetric method. Similar inactivation curves, but based on dissolved ozone analysis by the UV absorbance method, were shown in Figure 9-4. Reproducibility of the measured inactivation curves based on the indigo trisulphonate method was found to be superior. The variation associated with the UV absorbance method was believed to have been the result of background interference arising from the presence of UV absorbing compounds in the tap water that served as the water source in these experiments. The indigo trisulphonate method was less sensitive to the presence of UV absorbing compounds because the spectrophotometric measurement was made at 600 nm, in the visible light range.

Further evidence of background interference was provided by the ratio of the ozone concentrations determined by the two methods. During the *B. subtilis* spore challenge experiments, the ratio of the ozone concentration measured by the indigo trisulphonate method to that measured by the UV absorbance method varied from 1.0 to 1.7. In the batch reactor trials of Chapter 7, which were carried in phosphate-buffered laboratory water with little background interference, the range of this ratio 0.95 to 1.35 (see Section 7.7). Further, these challenge experiments with *B. subtilis* spores were

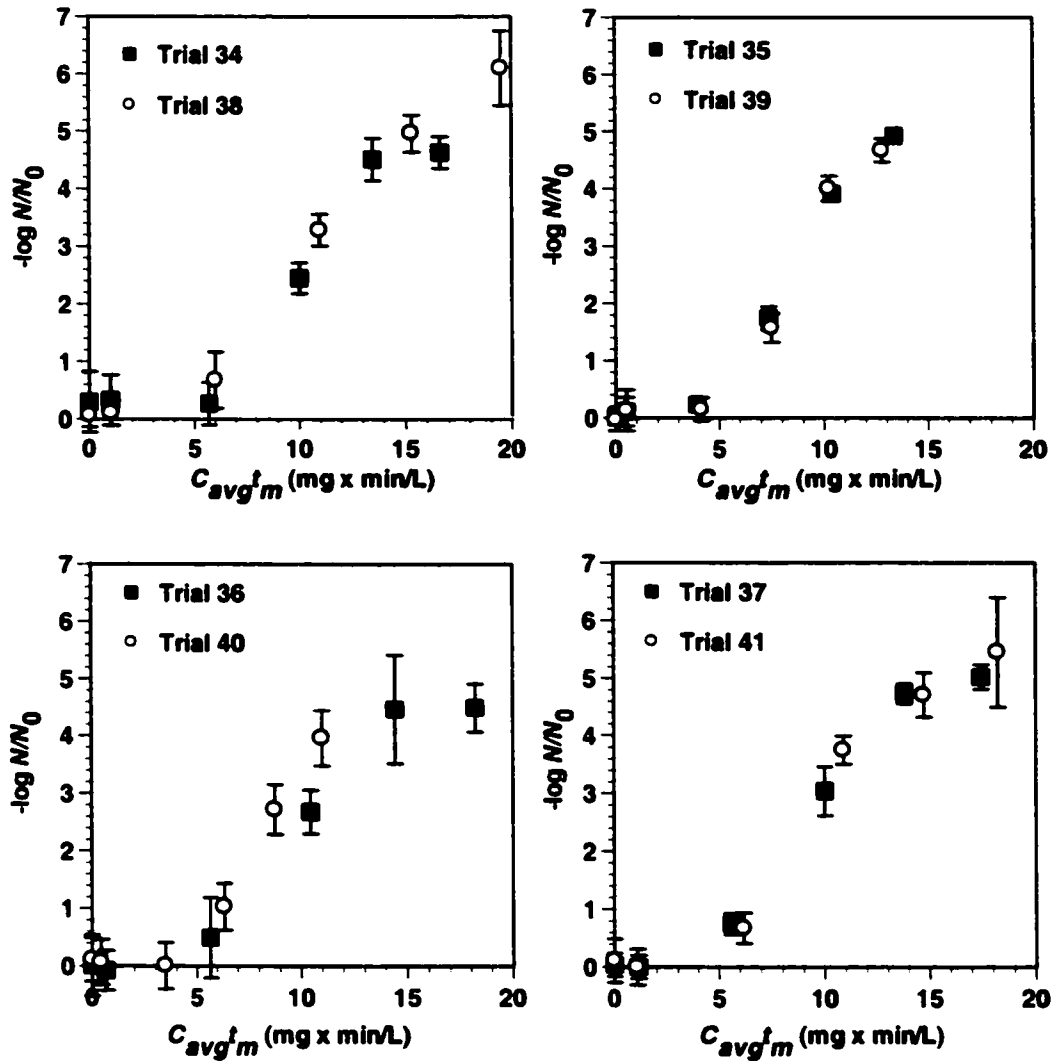


Figure 9-3 Results of duplicate challenge trials with *Bacillus subtilis* spores at different static mixer hydrodynamic conditions based on ozone concentration determined using the indigo trisulphonate measurement method.

carried out relatively early in the experimental period, and the baseline correction for the UV absorbance method described by Equation 6-7 was not used. (The correction was used in the batch reactor trials of Chapter 7 and was later adopted in the static mixer contactor experiments with *C. parvum* and *G. muris*.) For these reasons, results of the challenge experiments with *B. subtilis* spores were interpreted based on ozone measurement by the indigo trisulphonate method.

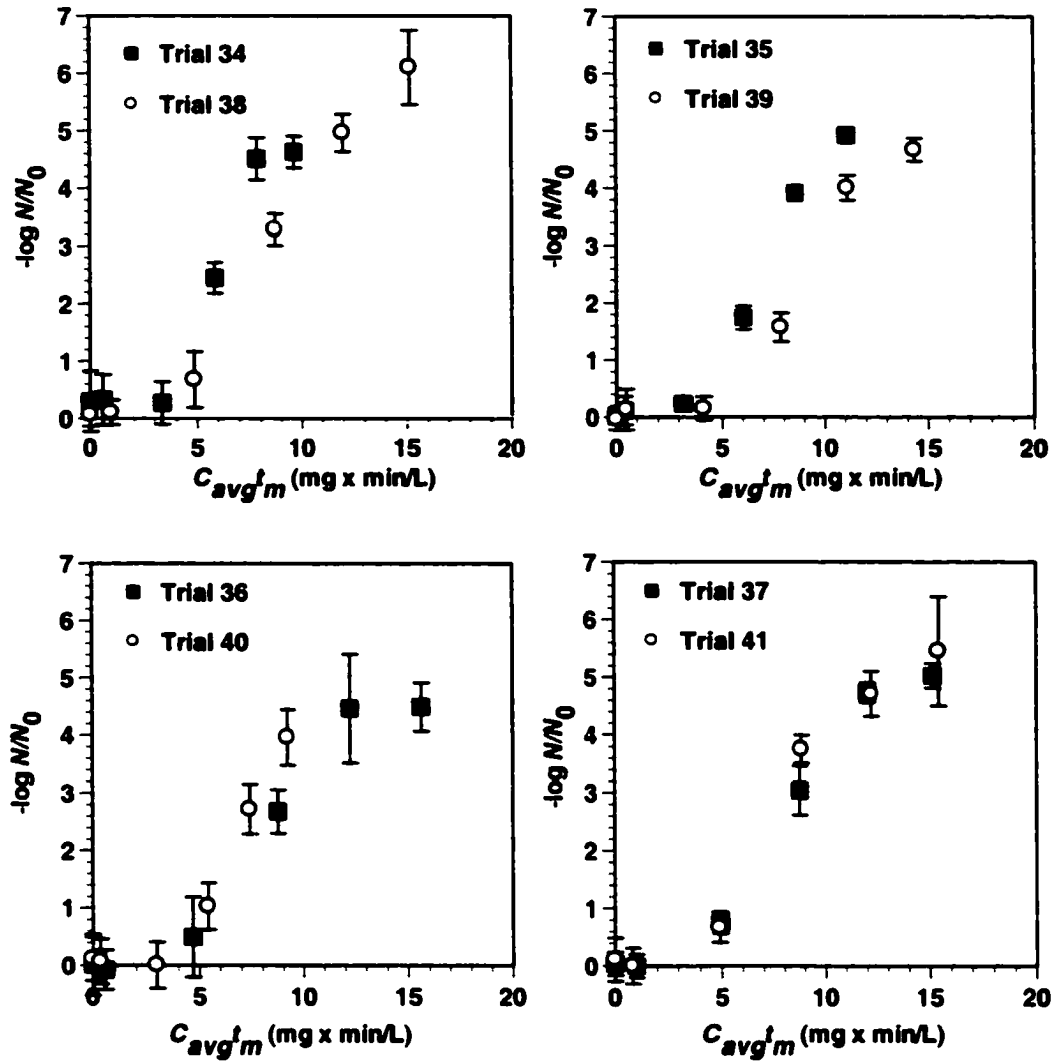


Figure 9-4 Results of duplicate challenge trials with *Bacillus subtilis* spores at different static mixer hydrodynamic conditions based on ozone concentration determined using the UV absorbance measurement method.

## 9.5 EFFECT OF STATIC MIXER HYDRODYNAMICS

### 9.5.1 Proposed Mechanisms for Enhanced Inactivation

Contact within the static mixer may have potentially enhanced microorganism inactivation by ozone by several mechanisms. For example, the relatively high liquid

shear stresses within the static mixer that promoted high rates of mass transfer may have also cause sufficient physical damage to the microorganism cell wall and resulted in *direct* loss of viability. If ozone was present, shear stress induced weakening of the cell wall and membrane may have resulted in increased permeability, rapid penetration of ozone to the inactivation sites within the cell, and rapid loss of viability. Or, as proposed by Zhu and co-workers (1989a) the enhanced mass transfer regime within the static mixer may have resulted in a significant increase in the rate of reaction between ozone and the cell wall. As suggested by the gas bubble theory of Farooq and others (1977a; 1978) and Ahmad and Farooq (1984), an enhanced reaction rate of inactivation may also have been promoted by the increased gas-liquid surface area within the static mixer.

Initial contact with ozone within the static mixer may have also altered the integrity or permeability of the microorganism cell wall or membrane without causing immediate loss of viability. Such a change in the cell wall or membrane induced by the static mixer could have resulted in an increased rate of inactivation by subsequent contact with dissolved ozone. In the experimental static mixer contactor, this indirect effect would have been manifested in the inactivation curves of Figure 9-3. If this proposed indirect hydrodynamic effect were significant, the resulting inactivation curves would have been a function of the static hydrodynamic parameters such as  $v_s$  and  $G/Q_f$ .

### **9.5.2 Evidence for a Direct Effect: Spore Inactivation in the Static Mixer**

One or more of these mechanisms, acting in isolation or in combination, may have resulted in a direct and measurable loss of viability within the static mixer itself. Given the very brief contact time within the mixer of less than 1 s and the resistance to ozone demonstrated by the spores in batch reactor studies, a measurable loss of microorganism viability at the outlet of the static mixer would have been interpreted as a *direct* effect. The measured log inactivation across the static mixer reported in Table 9-3 suggested that very little direct loss of viability occurred in the experimental contactor, even at the highest superficial velocities. On average, the measured inactivation within the static mixer itself in the eight trials was only 0.07 log-units. A hypothesis test based on a two-tailed Student t-distribution indicated that this level of average inactivation was not statistically different from zero at the 95% level (probability of a type I error,  $p =$

0.1). Further, the 90<sup>th</sup> percentile of the distribution of the measured inactivation within the static mixer, was found to overlap the origin (Figure 9-5).

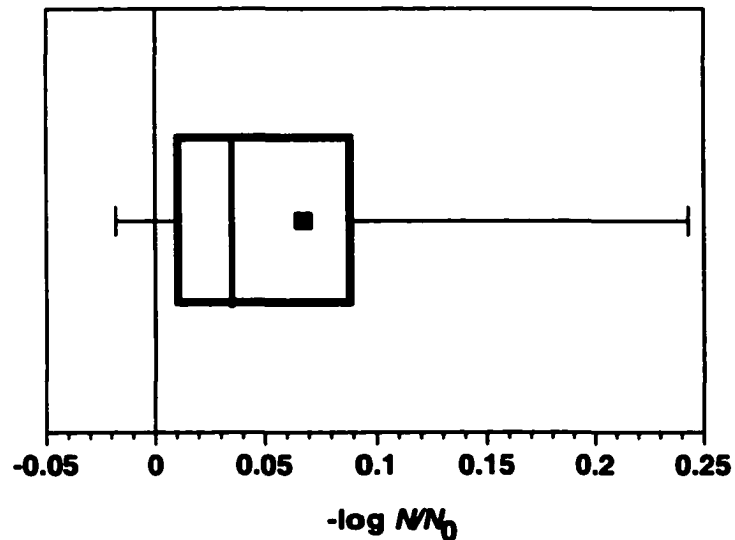


Figure 9-5 Box and whisker diagram of measured *Bacillus subtilis* spore inactivation across the static mixer itself. From left to right, lines represent 90%, 25%, median, 25% and 90% percentile boundaries, respectively. The square symbol represents the mean.

### 9.5.3 Evidence for an Indirect Effect: Spore Inactivation in the Reactive Flow Segment

The results of the eight challenge experiments with *B. subtilis* spores at different static mixer hydrodynamic conditions, are plotted together in Figure 9-6. On first examination, there appeared to be no discernable difference between the inactivation curves determined at the various combinations of  $v_s$  and  $G/Q_f$ . The sigmoid shape of the ozone inactivation curve observed with this strain of spores in the batch reactor trials was also apparent in the inactivation curves generated in the static mixer. The characteristics of the curve, such as size of the shoulder region and slope of the exponential and tailing regions, were independent of the settings of  $v_s$  and  $G/Q_f$ .

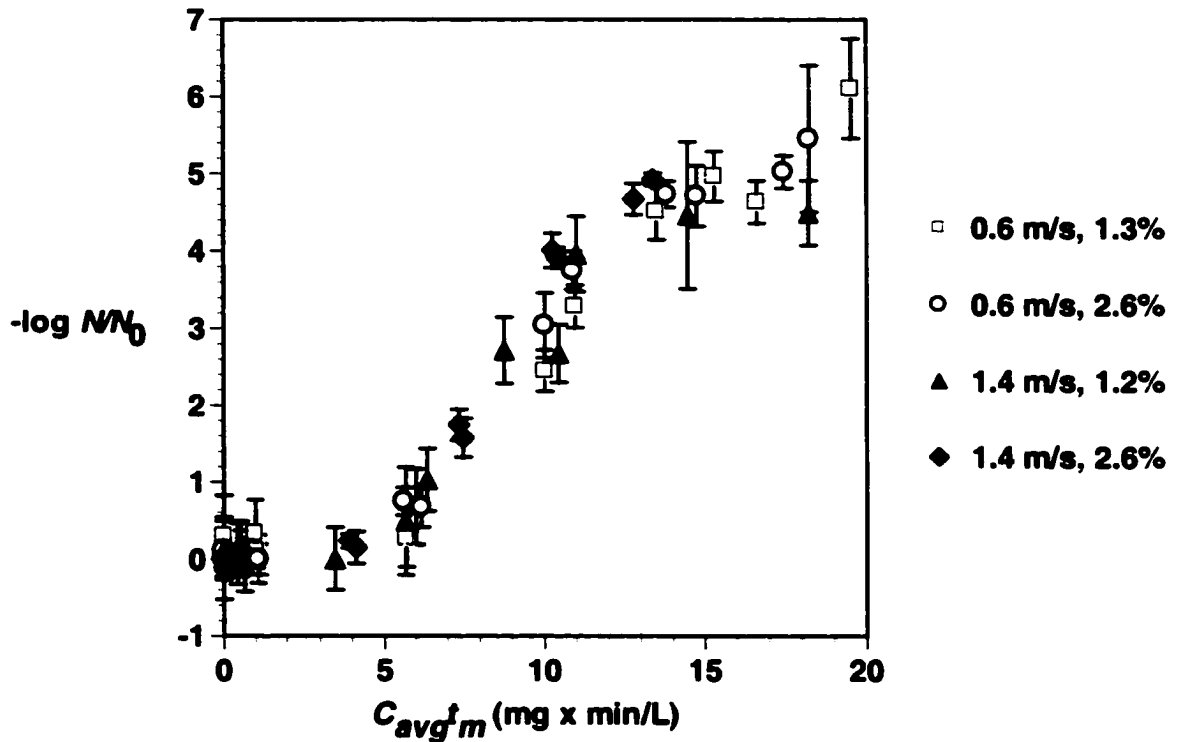


Figure 9-6 Effect of hydrodynamic conditions within the static mixer on the *Bacillus subtilis* spore inactivation curve in the static mixer ozone contactor. The different symbols represent different combinations of the superficial velocity,  $v_s$ , and gas-liquid flow rate ratio,  $G/Q_f$ , in the static mixer.

To more closely examine the potential effect of static mixer hydrodynamic conditions, the inactivation measured at each of the four hydrodynamic conditions was compared to the average inactivation determined for all sets of hydrodynamic conditions. Average inactivation was determined by fitting Equation 7-1 to the combined dataset of Figure 9-6 using linear least-squares regression. Recall from Chapter 7 that Equation 7-1 was used to model the spore inactivation kinetics determined in batch ozone reactors. The best-fit average inactivation curve is shown in Figure 9-7. Model prediction errors, given by

$$\varepsilon_i = \log\left(\frac{N}{N_0}\right)_{\text{predicted}} - \log\left(\frac{N}{N_0}\right)_{\text{measured}} \quad \text{Equation 9-2}$$

were then determined for each experimental condition. The values of  $\varepsilon_i$  are plotted for each hydrodynamic condition in Figure 9-8.

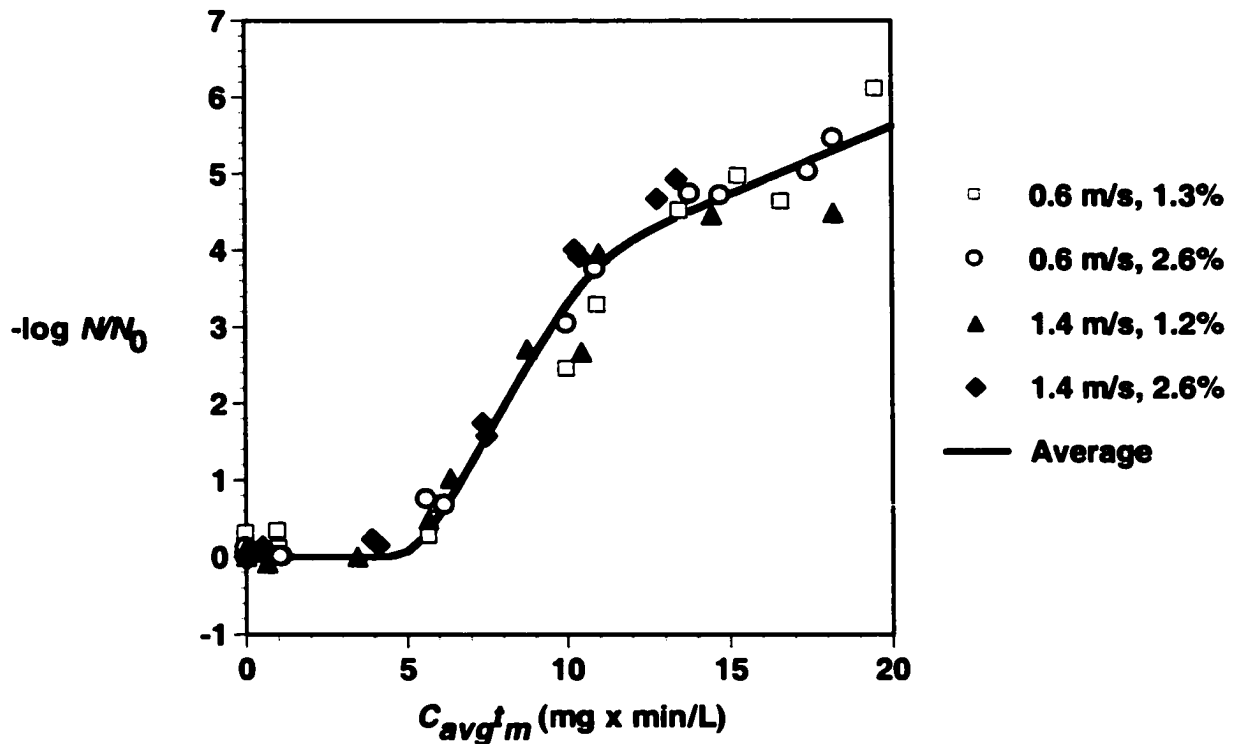


Figure 9-7 Best-fit curve of *Bacillus subtilis* spore inactivation in the experimental static mixer contactor. Best-fit model parameters of Equation 7-1 are:  $k_i = 1.7$ ,  $k_a = 0.41$ ,  $n_c = 9800$ ,  $r = 0.0089$ . Error bars shown in Figure 9-6 have been removed for clarity.

Errors were distributed between -1.0 and +1.0 log-units with mean values,  $\bar{\varepsilon}_i$ , ranging from -0.3 to +0.1 log-units (Figure 9-8). In only one case ( $v_s = 1.4$  m/s,  $G/Q_f = 2.5\%$ ) were the residuals consistently greater than or less than zero and was the mean error,  $\bar{\varepsilon}_i$ , statistically different than zero (based on a Student t-test). In this case, the mean and maximum absolute values of the error were only -0.3 log-units and -0.5 log-units, respectively. Based on this examination of the errors, it was concluded that

inactivation curves generated under the different static mixer hydrodynamic conditions were not substantially different from the average curve and from each other. Moreover, for the conditions investigated in the static mixer contactor, spore inactivation was essentially independent of the mass transfer performance of the system as indicated by the transfer efficiency,  $TE$ , and the overall rate of mass transfer,  $M$  (Table 9-3).

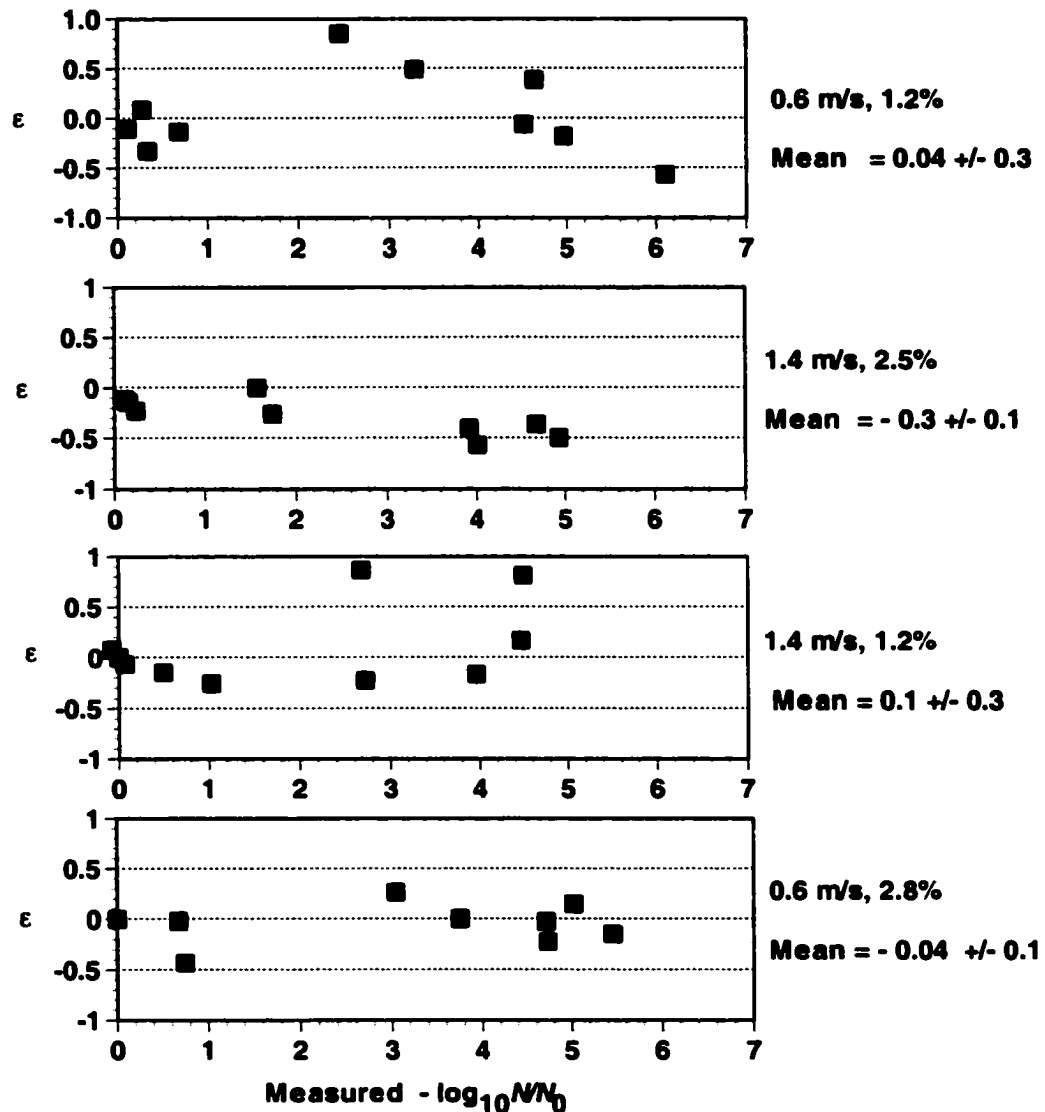


Figure 9-8 Effect of static mixer hydrodynamic conditions ( $v_s$  and  $G/Q_f$ ) on prediction errors of the average *Bacillus subtilis* spore inactivation model. The mean error and the 95% confidence interval of the mean error are shown.

## 9.6 COMPARISON TO BATCH REACTORS

### 9.6.1 Experimental Conditions for Generation of the Batch Reactor Inactivation Curves

Spore inactivation measured in the static mixer contactor, at all hydrodynamic conditions, is compared to spore inactivation measured in batch reactors in Figure 9-9.

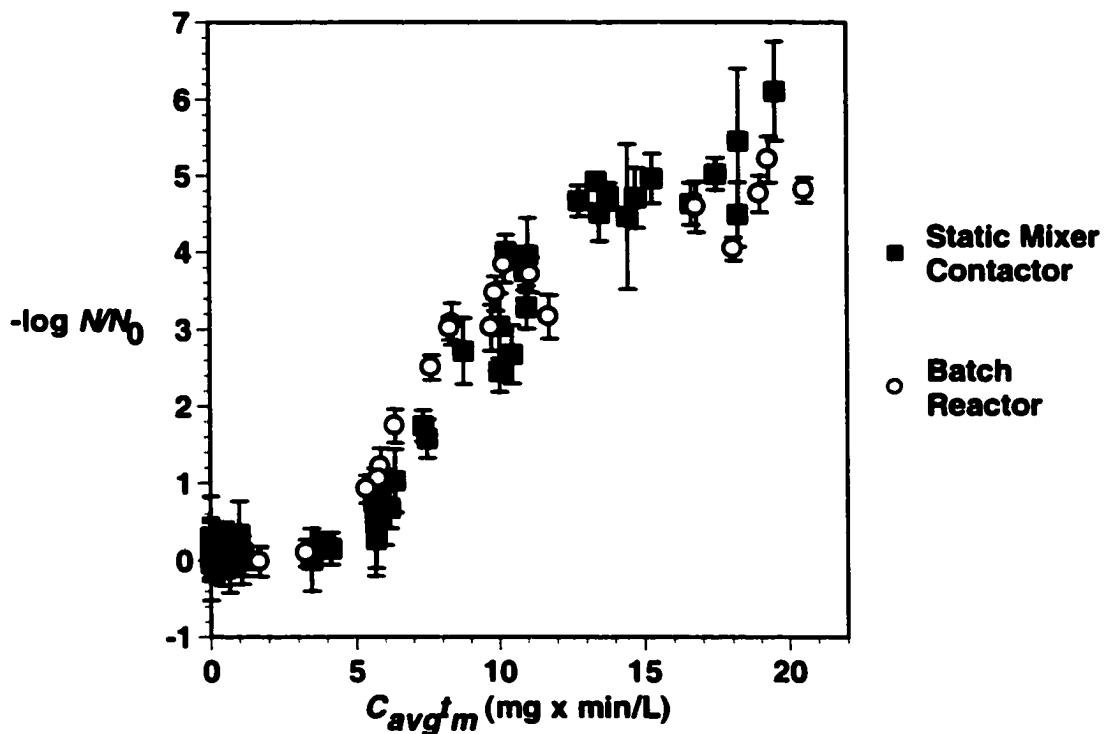


Figure 9-9 Comparison between *Bacillus subtilis* spore inactivation measured in the static mixer contactor, under all hydrodynamic conditions, and *Bacillus subtilis* spore inactivation measured in batch reactors at 16°C.

To minimize the potential effect of extraneous variables on this comparison, care was taken to ensure that the methods and materials used in these batch reactor trials matched those of the static mixer contactor experiments as much as possible. Spores from the same stock preparations (batches B and C) were used in both sets of experiments. Samples of water were collected from the feed tank of the static mixer contactor on each

experimental day. These were combined, stored at 4°C for no longer than 4 weeks, and then used as the matrix water in the batch reactor experiments. Both batch reactor and static mixer trials were conducted at  $16.0 \pm 1^\circ\text{C}$ . In both cases, results were interpreted based on dissolved ozone concentration measured using the indigo trisulphonate method. Average dissolved ozone concentrations ranged from approximately 0.6 to 2.1 mg/L in the batch reactor experiments and from approximately 0.8 to 1.2 mg/L in the static mixer contactor experiments. Complete details of the batch reactor experiments are provided in Table D-4 of Appendix D.

### **9.6.2 Modeling of the Batch Reactor Inactivation Curve**

A cursory examination of Figure 9-9 suggested little difference in the spore inactivation curves measured in the two different ozone contactor configurations. To better compare the inactivation curves, an empirical model was developed to describe the inactivation curve observed in the batch reactor experiments. Once again, the *B. subtilis* spore inactivation model of Equation 7-1 was chosen to represent the batch reactor data and the best fit was determined using least-squares regression. The best-fit model is shown in Figure 9-10. Model-predicted spore inactivation in the batch reactors and the static mixer contactor were compared in Figure 9-11. The model comparison revealed that, although the inactivation curves were similar, they were not identical. At  $C_{avg}t_m$  levels between approximately 5 and 9 mg×min/L, inactivation in the batch reactors exceeded that of the static mixer contactor by almost 1 log-unit. At  $C_{avg}t_m$  greater than approximately 12 mg×min/L, the reverse was true.

### **9.6.3 Interpretation of the Tailing Region as Spore Agglomeration**

Spore inactivation curves measured in the static mixer contactor and in the batch reactors were remarkably similar (Figure 9-9 and 9-11), though not identical. Approximately equivalent inactivation was achieved in each contactor configuration at the same dissolved ozone  $Ct$  product. There was little evidence to suggest that initial gas-liquid mixing within the static mixer increased the intrinsic rate of rate of microorganism inactivation by ozone, compared to exposure to dissolved ozone only and with gentle mixing in batch reactors. Spore inactivation was, therefore, determined primarily by the

conditions of contact with dissolved ozone, and was independent of the conditions of gas-liquid contact. One exception to this was an apparent reduction in the tailing effect at high  $Ct$  in the static mixer contactor. This was indicated by the fact that the computed value of the inactivation rate constant of the agglomerated spore units,  $k_a$ , for the static mixer contactor was approximately 40% higher than for the batch reactors.

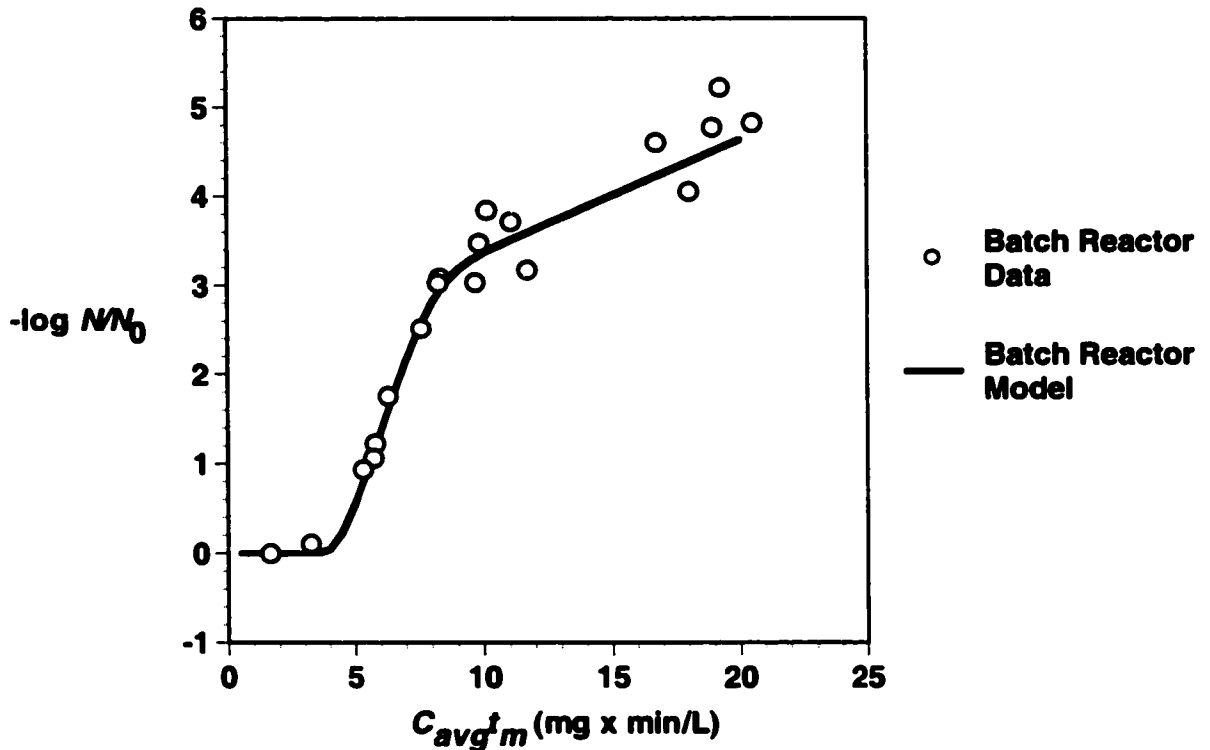


Figure 9-10 Linear regression fit of the *Bacillus subtilis* spore inactivation model (Equation 7-1) to spore inactivation measured in the batch reactor ozonation trials. Best-fit model parameters are:  $k_i = 2.0$ ,  $k_a = 0.29$ ,  $n_c = 7000$ ,  $r = 0.0074$ .

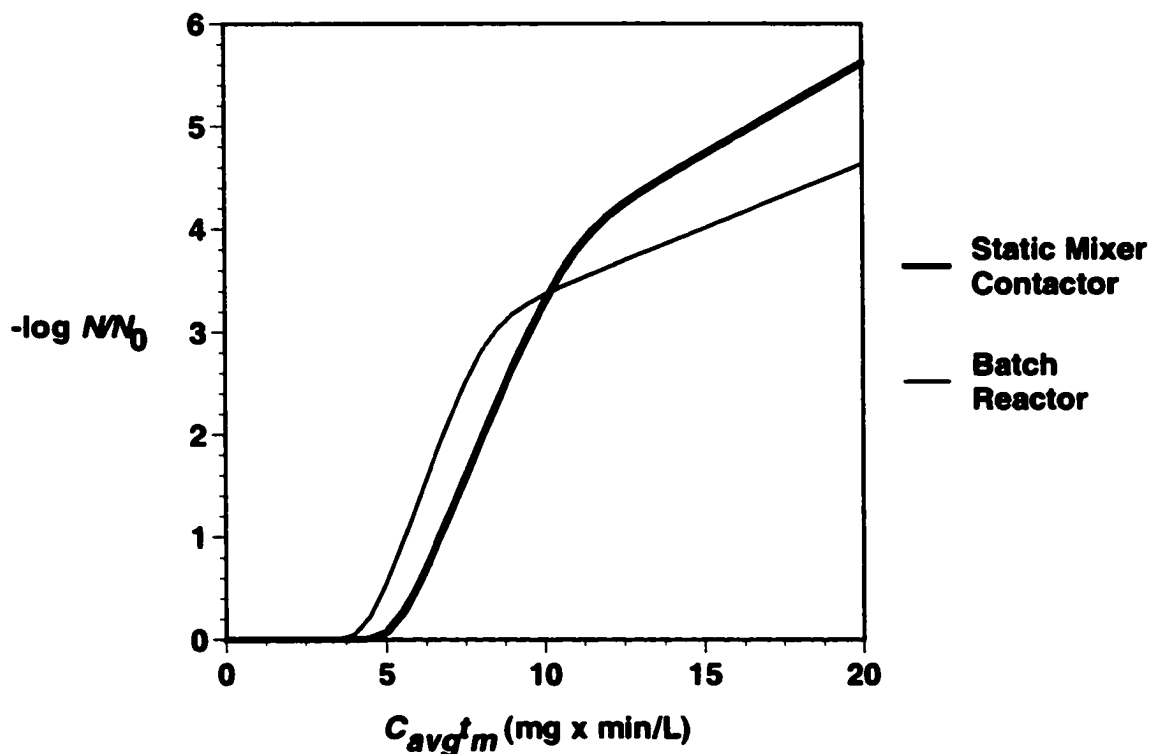


Figure 9-11 Comparison between *Bacillus subtilis* spore inactivation measured in the static mixer contactor, under all hydrodynamic conditions, and spore inactivation measured in batch reactors at 16°C using best-fit models. Best-fit parameters of the static mixer contactor model are:  $k_i = 1.7$ ,  $k_a = 0.41$ ,  $n_c = 9800$ ,  $r = 0.0089$ . Best-fit parameters of the batch reactor model are:  $k_i = 2.0$ ,  $k_a = 0.29$ ,  $n_c = 7000$ ,  $r = 0.0074$ .

In Chapter 8, it was postulated that tailing in the observed spore inactivation curves was due to spore agglomeration. An alternative explanation is that the tailing was caused by spore population heterogeneity and the presence of a sub-population of spores with greater resistance to ozone. The difference in tail inactivation rates between the static mixer contactor and the batch reactors is more consistent with the agglomeration hypothesis than the heterogeneity hypothesis. In both batch reactor and static mixer contactor experiments, spore preparations were mixed vigorously prior to use in experiments to promote break-up of spore agglomerates. The persistence of the tail in the batch reactor inactivation curves was evidence that this procedure reduced, but did

not eliminate, agglomerates. In the static mixer contactor experiments, agglomerates were exposed to additional shear stress within the static mixer itself. This might have promoted more efficient break-up of spore agglomerates and might have accounted for the observed increased in inactivation rate in the tail region. If tailing was due to heterogeneity alone, the degree of vigorous mixing and shear stress experienced by the spores would likely have had no effect on the observed inactivation curves and one would expect no differences in the tailing regions of the inactivation curves measured in the two reactor configurations.

The cause of the tailing in the spore inactivation curves was not confirmed in this work, but could likely be determined through further experimental research. If it were shown that tailing in the inactivation curves was due to the presence of agglomerates that were present in the spore preparations as hypothesized, then one might argue that the static mixer effect, and perhaps the tailing effect itself, was an experimental artifact.

#### 9.6.4 Interpretation with Segregated Flow Analysis

The deviation between the spore inactivation curves generated in the batch reactor and the static mixer contactor in the exponential region of the inactivation curve (at lower  $C_{avg}t$ ) was interpreted in terms of the hydrodynamic efficiency of the reactive flow segment. The residence time distribution and deviation from plug flow may have accounted for the lower spore inactivation measured in the static mixer contactor compared to the batch reactors. In terms of hydrodynamic efficiency, batch reactors are identical to perfect plug flow reactors (Levenspiel 1972). To test the plausibility of this hypothesis, a series of segregated flow analysis computer simulations were done. The spore inactivation model of Equation 7-1 was combined with the general expression for segregated flow analysis given by Equation 3-13 to yield the following expression:

$$\frac{N}{N_0} = \int_{i=0}^{\infty} \left\{ \frac{N_{0,i} \left[ 1 - (1 - e^{-k_i C t})^{n_i} \right] + N_{0,a} e^{-k_a C t}}{N_0} \right\} E(t) dt \quad \text{Equation 9-3}$$

The measured exit age distributions,  $E(t)$ , of Figure 9-2 and the best-fit parameters of batch spore inactivation model of Figure 9-10 were substituted into in Equation 9-3. The resulting equation was solved numerically on a Microsoft Excel 2000 spreadsheet using the trapezoid rule with a step size of 1 s. The results of two simulations at mean residence times,  $t_m$ , of 8.2 min and 15.5 min are summarized in Table 9-4. The first simulation was done at a shorter residence time and at an ozonation condition in the exponential region of the spore inactivation curve. The second simulation was done a longer residence time and at an ozonation condition in the tailing region of the spore inactivation curve.

The results of the first simulation case are consistent with the residence time distribution explanation for lower spore inactivation in the static mixer contactor in the exponential region of the inactivation curves. For identical initial ozone conditions, inactivation determined by segregated flow analysis was about 1 log-unit lower than that predicted for batch or perfect plug flow conditions, and was within 0.1 log-unit of average measured inactivation in the static mixer contactor. The reason for this was that, in the exponential region of the inactivation curve, spore inactivation was very sensitive to residence time. Those spores that spent less time in the contactor had a much greater likelihood of survival and exerted a disproportionate effect on the overall log inactivation of the entire population. This residence time effect was much lower in the second simulation because spore inactivation was much less sensitive to residence time in the tailing region of the inactivation curve. Here, spore inactivation predicted by segregated flow analysis was almost identical to that predicted for batch or perfect plug flow conditions, but was less than the measured inactivation in the static mixer contactor. This is consistent with the spore agglomeration explanation for the reduced tailing in the spore inactivation curve that was observed in the static mixer contactor.

Table 9-4 Comparison of model-predicted *Bacillus subtilis* spore inactivation in batch reactors and in the experimental static mixer ozone contactor.

Simulation Case	<sup>1</sup> Batch/Plug Flow Model	<sup>2</sup> Segregated Flow Analysis	<sup>3</sup> Static Mixer Measured
$C_0 = 1 \text{ mg/L}$ $k_d = 0.03 \text{ min}^{-1}$ $t_m = 8.2 \text{ min}$ $C_{avg}t_m = 7.3 \text{ mg}\times\text{min/L}$	2.4	1.5	1.4
$C_0 = 1 \text{ mg/L}$ $k_d = 0.03 \text{ min}^{-1}$ $t_m = 15.5 \text{ min}$ $C_{avg}t_m = 12.4 \text{ mg}\times\text{min/L}$	3.7	3.6	4.2

<sup>1</sup>Based on batch reactor analysis with the following best-fit model parameters of Equation 7-1:  $k_i = 2.0$ ,  $k_a = 0.29$ ,  $n_c = 7000$ ,  $r = 0.0074$ .

<sup>2</sup>Based on segregated flow analysis using the exit age distributions described in Figure 9-2 and the following best-fit model parameters of Equation 7-1:  $k_i = 2.0$ ,  $k_a = 0.29$ ,  $n_c = 7000$ ,  $r = 0.0074$ .

<sup>3</sup>Based on batch reactor analysis and the following best-fit model parameters of Equation 7-1:  $k_i = 1.7$ ,  $k_a = 0.41$ ,  $n_c = 9800$ ,  $r = 0.0089$ .

## **9.7 SUMMARY OF *B. SUBTILIS* SPORE EXPERIMENTS**

A previous study reported that reduction of *E. coli* by ozone in a static mixer system was determined primarily by the mass transfer rate of ozone into water (Zhu et al. 1989a). Another study suggested that decreasing the velocity in a static mixer improved the reduction of heterotrophic plate count (HPC) and coliform bacteria (Bonnard et al. 1999). The weakness of these earlier experimental studies with static mixers was that the conditions of gas-liquid contact were coupled to the conditions of dissolved ozone contact. This may have confounded interpretation of the experimental results with respect to the effect of the static mixer on microorganism inactivation. The unique design and flexibility of the experimental static mixer contactor used in the present study enabled a careful investigation of the role of the static mixer on *B. subtilis* spore inactivation by ozone. Most importantly, the experimental design permitted the effects of static mixer hydrodynamics, and ozone gas-liquid mass transfer, to be separated from those of dissolved ozone contact.

Other than a modest reduction in tailing at high inactivation levels, which might have been an experimental artifact, there was little evidence to suggest that *B. subtilis* spore inactivation was influenced by the hydrodynamic conditions within the static mixer. After accounting for the residence time distribution in the reactive flow segment, spore inactivation in the static mixer contactor was equivalent to that measured in the batch reactors when compared on the basis of the dissolved ozone *Ct* product. Spore inactivation, therefore, was determined primarily by contact with dissolved ozone contact and the residence time distribution. Vigorous initial gas-liquid mixing in the static mixer provided no apparent enhancement of the rate of spore inactivation rate by ozone when compared to contact with dissolved ozone with gentle mixing in batch reactors. In the static mixer, spore inactivation was independent of either the ozone transfer efficiency or the mass transfer rate, as long as the amount of ozone transferred was sufficient to establish the required dissolved ozone residual.

## 10 INACTIVATION OF *CRYPTOSPORIDIUM PARVUM* IN THE STATIC MIXER CONTACTOR

### 10.1 INTRODUCTION

As discussed in the literature review of Chapter 2, the effect of aqueous ozone on *C. parvum* oocysts has been extensively studied. The most comprehensive studies have been limited to investigations of the kinetics of inactivation in laboratory-scale well-mixed batch reactors (Gyürék et al. 1999; Li et al. 2001), semi-batch reactors (Rennecker et al. 1999) or continuous-flow, reactors (Oppenheimer et al. 2000). There are few published experimental studies that have explored the potential impact of ozone gas-liquid contactor design on *C. parvum* inactivation, and these have been limited in scope (Owens et al. 2000; States et al. 2000). The results of the experimental study presented in Chapter 9 demonstrated that inactivation of spores of the bacterium *Bacillus subtilis* in a static mixer contactor was determined primarily by contact with dissolved ozone. The intrinsic rate of spore inactivation was unaffected by the hydrodynamic conditions of gas-liquid contact within the mixing elements of the static mixer. One objective of the experimental study presented in this chapter was to determine if this conclusion extends to the encysted protozoan parasite *Cryptosporidium parvum*. A second objective was to rigorously test the two-stage ozone contactor design hypothesis put forward in Chapter 4 by assessing the *C. parvum* inactivation efficiency in the experimental static mixer contactor.

Inactivation of seeded *C. parvum* oocysts was measured in a series of carefully controlled challenge experiments with the experimental static mixer contactor. The efficiency of oocyst inactivation was assessed by comparing measured inactivation to predictions of inactivation that were generated by integrating basic hydrodynamic models of the macro-mixing pattern with a published kinetic model of *C. parvum* oocyst inactivation by ozone at 22°C. It was recognized at the outset that the success of this comparison would depend greatly on the influence of extraneous or nuisance variables.

Strict quality control measures were implemented to ensure that the influence of these variables was minimized.

## **10.2 EXPERIMENTAL DESIGN**

### **10.2.1 Static Mixer Contactor Challenge Experiments**

Nine challenge experiments with *C. parvum* oocysts were completed with the experimental static mixer ozone contactor. For each experiment, the bubble column height,  $H$ , was maintained of 0.45 m to minimize contact time within the bubble column. The feed water temperature was regulated to  $22 \pm 1^\circ\text{C}$ , the temperature for which the published kinetic model of *C. parvum* inactivation by ozone was developed (Gyürék et al. 1999). Most of the experimental trials (seven of nine) were done at approximately constant hydrodynamic conditions within the static mixer. The superficial liquid velocity,  $v_s$ , and the gas-liquid flow rate ratio,  $G/Q_f$ , were maintained at 0.6 m/s and between 1.2% and 1.6%, respectively. Two additional experimental trials were completed at  $v_s$  of 1.4 m/s to investigate the potential effect of static mixer hydrodynamic conditions on oocyst inactivation. Using the flow splitting feature of the experimental contactor, the flow rate through the reactive flow segment,  $Q_{RFS}$ , was maintained at approximately 2 L/min, independent of the static mixer superficial velocity,  $v_s$ . In each experimental trial, the power level on the ozone generator was adjusted such that the ozone concentration at the inlet of the reactive flow segment,  $C_0$ , was between 0.5 and 0.6 mg/L. Different experimental  $C_{avg}t_m$  conditions were obtained by adjusting the length of the reactive flow segment to provide total contact times of approximately 4, 8 and 16 min.

To assess the level of oocyst inactivation in the contactor, samples of the reactive flow segment outlet water were collected for oocyst recovery using the membrane filtration method and subsequent infectivity analysis with the CD-1 neonatal mouse assay. In each trial, a sample of the contactor feed water, after seeding of oocysts but prior to ozone addition, was also collected for oocyst recovery and infectivity analysis. This sample served as quality control, the purpose being to ensure that the infectivity of the oocysts seeded into the feed water was within the normal range for prepared oocysts.

To determine the extent of direct oocyst inactivation within the static mixer itself, an additional sample was collected from the outlet of the static mixer in five of the nine trials. A single control trial was done using oxygen gas in place of ozonized gas and with 16 min total contact time to confirm that oocyst inactivation was due solely to exposure to ozone.

### **10.2.2 Batch Reactor Experiments**

As a quality control measure, a series of batch reactor experiments were completed in parallel with the static mixer contactor challenges. The primary purpose of these batch reactor experiments was to validate the use of the literature inactivation kinetic model and to investigate the possibility of oocyst batch or water matrix effects on the kinetics of oocyst inactivation. Samples of water were collected from the feed tank of the static mixer contactor during experimental days. For each batch reactor experiment, a preparation of parasites was taken from the same batch of oocysts used in the static mixer contactor experiments. The parasites were suspended in 200 mL of the contactor water in the 250 mL batch reactors flasks, equilibrated to 22°C, and then exposed to controlled doses of dissolved ozone according to the procedures described in Section 6-2. The experimental temperature of 22°C was chosen to correspond to the target temperature of the static mixer contactor experiments and to the temperature for which the published kinetic model of *C. parvum* inactivation by ozone was developed (Gyürék et al. 1999). Batch reactor experiments were typically conducted on the same day or at least during the same week as the static mixer contactor experiments to ensure that the properties of the parasites and the water used were representative of those used in the static mixer contactor experiments.

## **10.3 CONTACTOR MODELING**

### **10.3.1 Basic Approach**

To assess microorganism reduction efficiency in the static mixer contactor, measured oocyst inactivation was compared to that predicted by mathematical models. Two approaches were used to model inactivation in the static mixer contactor; plug flow

analysis (PFA) and segregated flow analysis (SFA). Both approaches assumed that the rate of oocyst inactivation at any point in the contactor was determined by the concentration of dissolved ozone and the intrinsic oocyst inactivation kinetics. The two modeling approaches differed only in how the residence time distribution of the contactor was considered. In plug flow analysis, the contactor was assumed to behave as a perfect plug flow reactor. Segregated flow analysis is a chemical reaction engineering technique in which batch reaction kinetics are integrated with residence time distribution information to estimate conversion in a non-ideal flow reactor (Levenspiel 1972). Segregated flow analysis has been used by others to model microorganism reduction by chlorine in water and wastewater treatment (Haas 1988; Lawler and Singer 1993; Trussell and Chao 1977) and is an integral component of the integrated disinfection design framework (IDDF) approach to analysis of microorganism reduction in drinking water treatment (Bellamy et al. 2000). Recall from Chapter 3 the general equation for segregated flow analysis is:

$$\frac{N}{N_0} = \int_{t=0}^{t=\infty} \left( \frac{N}{N_0} \right)_{\text{batch}} E(t) dt \quad \text{Equation 3-13}$$

where  $N/N_0$  is the estimated inactivation ratio in the continuous-flow contactor,  $(N/N_0)_{\text{batch}}$  is the inactivation ratio in a batch reactor, and  $E(t)$  is the exit age distribution of the contactor.

### 10.3.2 Kinetic Model of *C. parvum* Oocyst Inactivation

The rate of *C. parvum* oocyst inactivation by dissolved ozone was interpreted using the Hom kinetic model of Gyürék and co-workers (1999) for 22°C. Li and co-workers (2001) later expanded the model to incorporate the effect of water temperature from 1°C to 35°C. The temperature dependence was not relevant in this analysis because all experiments, both in the static mixer contactor and in the batch reactors, were carried at  $22 \pm 1^\circ\text{C}$ . Although the first-order Chick-Watson model has been used to model *C. parvum* inactivation by ozone, Gyürék and co-workers (1999) reported that the non-linear

Hom model provided a statistically superior fit to their dataset. The Hom kinetic model they used was presented in Chapter 3 and is repeated below in differential and logarithm base 10 integrated forms:

$$\text{Differential form:} \quad \frac{dN}{dt} = -k_H m N C^n t^{m-1} \quad \text{Equation 3-1}$$

$$\text{Integrated form:} \quad -\log \frac{N}{N_0} = k'_H C^n t^m \quad \text{Equation 3-2}$$

Note that  $k'_H = k_H/\ln(10)$  corrects for conversion to base 10 logarithm from the base  $e$  natural logarithm.

Equation 3-2 is only strictly applicable if the dissolved ozone concentration,  $C$ , is constant. In the experiments with *B. subtilis* spores at 16°C (Chapter 9), the dissolved ozone concentration decreased by between 27% and 47% from the inlet to the outlet of the reactive flow segment in the experimental static mixer contactor. To account for this large reduction in ozone concentration in the reactive flow segment, the expression for first-order ozone decomposition,  $C = C_0 \exp(-k_d t)$ , was inserted into Equation 3-2. The resulting expression was identical to Equation 2-11 for batch reactors:

$$-\log \frac{N}{N_0} = k'_H C_0^n \int_0^t [\exp(-k_d t)]^n t^m dt \quad \text{Equation 2-11}$$

Equation 2-11 was solved exactly using the incomplete gamma function to yield the incomplete gamma Hom formulation (Gyürék and Finch 1998; Haas and Joffe 1994), previously presented in Chapter 3:

$$-\log \frac{N}{N_0} = \frac{mk'_H C_0}{(nk_d)^m} \gamma(m, nk_d t) \quad m > 0, nk_d t \geq 0 \quad \text{Equation 3-6}$$

where  $\gamma(m, nk_d t)$  is the incomplete gamma function. Using batch reactors with Iowa strain oocysts suspended in ozone demand-free phosphate buffered lab water at 22°C, Gyürék and co-workers (1999) determined the following best-fit values for the parameters of the incomplete gamma-Hom kinetic model:  $k'_H = 0.68 \text{ min}^{-1}$ ,  $n = 0.70$  and  $m = 0.73$ . In their experiments, Gyürék and co-workers measured dissolved ozone using direct UV absorbance at 260 nm with a molar extinction coefficient of  $3\,300 \text{ M}^{-1} \text{ cm}^{-1}$ , and measured *C. parvum* oocyst infectivity reduction using a neonatal CD-1 mouse model. Using statistical techniques that were well-suited to multi-parametric non-linear regression, they estimated that the 90% confidence range on the model predictions was approximately  $\pm 0.7$  log-units over the range of conditions investigated.

### 10.3.3 Predicted Inactivation in the Reactive Flow Segment

*C. parvum* oocyst inactivation in the reactive flow segment was estimated by both plug flow analysis and segregated flow analysis. For plug flow analysis,  $C_0$  in Equation 3-6 was set equal to the dissolved ozone concentration at the inlet of the reactive flow segment. The first-order ozone decomposition rate constant,  $k_d$ , represented the rate of ozone decomposition within the reactive flow segment. For each experimental trial,  $C_0$  and  $k_d$  were estimated by least-squares regression of Equation 6-14 to the measured ozone concentration profile in the reactive flow segment. An example of this regression was provided in Figure 6-8. The time variable,  $t$ , used in all of these calculations was the average mean residence time,  $t_m$ , previously determined at various points along the reactive flow segment in pulse tracer tests (Table 9-2).

For segregated flow analysis, the incomplete gamma Hom kinetic expression for *C. parvum* oocyst inactivation by ozone with first-order ozone decomposition (Equation 3-6) was substituted into the general expression for segregated flow analysis (Equation 3-13) to yield the following expression:

$$\frac{N}{N_0} = \int_{t=0}^{t=\infty} \text{anti log} \left( \frac{-mk'_H C_0^n}{(nk_d)^m} \gamma(m, nk_d t) \right) E(t) dt \quad \text{Equation 3-15}$$

$C_0$  and  $k_d$  in Equation 3-15 were determined in the same manner as described above for plug flow analysis. The exit age distribution,  $E(t)$ , at each point along the reactive flow segment was determined in pulse tracer tests (Figure 9-2). Equation 3-15 was solved numerically on a Microsoft Excel 2000 computer spreadsheet program using the trapezoidal rule with a step size six of 1 s in the time variable,  $t$ . Numerical solution of Equation 3-15 provided the inactivation ratio,  $N/N_0$ , at the exit of the contactor. This was then converted to log inactivation by computing the base 10 logarithm.

#### 10.3.4 Predicted Inactivation in the Bubble Column

Although most of the oocyst inactivation was expected to occur in the reactive flow segment, a small, but not negligible, amount was also expected to occur during the initial period of gas-liquid contact within the bubble column. The dissolved ozone profile within the bubble column at the lower  $G/Q_f$  settings was observed to be relatively flat (See Figure 8-1). Inactivation within the bubble column was, therefore, estimated by assuming constant dissolved ozone concentration and perfect plug flow. The geometric mean of the ozone concentration in the bubble column,  $C_{avg}$ , was estimated using Equation 6-16 and the average mean residence time,  $t_m$ , was determined from pulse tracer tests and the residence time distribution analysis (Table 9-2). Using these values for  $C$  and  $t$ , the estimated level of inactivation in the bubble column was calculated using Equation 3-2. Inactivation calculated for the reactive flow segment, by either the plug flow analysis or the segregated flow analysis procedures describe above, was added to the inactivation calculated for the bubble column to yield the estimated net inactivation at the outlet of the reactive flow segment.

## 10.4 RESULTS OF CHALLENGE EXPERIMENTS

### 10.4.1 Ozonation Conditions

A summary of the ozonation conditions for each of the nine *C. parvum* oocyst challenge experiments with the static mixer contactor is provided in Table 10-1. Full details of the ozonation and other operating conditions for each of these experiments are provided in Tables E-1 and E-2 of Appendix E. Due to the very short residence time within the static mixer (less than 0.2 s), the  $C_{avg}t_m$  to which the oocysts were exposed at the outlet of the static mixer was considered to be essentially zero. The measured experimental  $C_{avg}t_m$  in the bubble column was limited to between 0.25 and 0.52 mg×min/L. In comparison, the cumulative  $C_{avg}t_m$  at the reactive flow segment outlet ranged from 1.9 to 6.8 mg×min/L, depending on the contact time. The majority of the oocyst inactivation, therefore, was expected to take place within the reactive flow segment.

To maintain internal consistency, all modeling calculations and interpretations of experimental work discussed in this Chapter were based on ozone concentration determined by UV absorbance at 260 nm. All  $C_{avg}t_m$  values in Table 10-1 are based on measurement of dissolved ozone by UV absorbance at 260 nm rather than by the indigo trisulphonate method, even though both methods were used. UV absorbance at 260 nm was selected as the basis for comparison primarily because Gyürék and co-workers (1999) used this method exclusively in their batch reactor experiments. To improve the accuracy of the UV absorbance for measurement of dissolved ozone in the GAC-filtered tap water, the baseline correction technique described by Equation 6-7 was implemented for the *C. parvum* challenge experiments. As a result, the variability of the UV absorbance method was reduced relative to the experiments with *B. subtilis* spores described in Chapter 9. In the *C. parvum* experiments the ratio of ozone concentration determined by the indigo trisulphonate method to that determined by the UV absorbance method ranged from 1.1 to 1.5 with an average of 1.3 (data in Tables E-1 and E-2 of Appendix E). With the *B. subtilis* trials, this ratio varied from 1.0 to 1.7.

Table 10-1 Summary of ozonation conditions for the *Cryptosporidium parvum* challenge experiments in the static mixer contactor. All ozone concentrations are based on measurements by UV absorbance at 260 nm.

Trial	$v_s$	$G/Q_f$	$^1TE$	$^2M$	Bubble Column			Reactive Flow Segment				Cum. $^7C_{avg}t_m$
					$^3C_{avg}$	$^4t_m$	$C_{avg}t_m$	$^5C_0$	$^4t_m$	$^6k_d$	$C_{avg}t_m$	
	m/s	%	%	mg/min	mg/L	min	mg× min/L	mg/L	min	min <sup>-1</sup>	mg× min/L	mg× min/L
43	0.63	1.26	74	3.6	0.60	0.73	0.44	0.50	15	0.055	5.08	5.5
44	0.64	1.23	74	4.0	0.56	0.71	0.40	0.53	15	0.037	6.12	6.5
45	0.68	1.18	76	5.7	0.78	0.67	0.52	0.73	7.4	0.047	4.57	5.1
46	0.64	1.24	74	4.3	0.62	0.71	0.44	0.57	7.4	0.059	3.45	3.9
47	0.65	1.22	75	4.7	0.66	0.70	0.46	0.62	15	0.055	6.35	6.8
48	1.12	1.57	84	7.5	0.59	0.55	0.32	0.57	3.7	0.028	1.96	2.3
49	0.64	1.24	74	4.0	0.60	0.71	0.43	0.54	3.6	0.070	1.72	2.2
50	0.64	1.24	74	4.1	0.58	0.71	0.41	0.55	3.7	0.091	1.66	2.1
51	1.38	1.56	86	8.2	0.56	0.45	0.25	0.51	3.6	0.075	1.59	1.9
C	0.60	1.26	na	na	0	0.7	0	0	15	0	0	0

<sup>1</sup> Ozone transfer efficiency estimated from an empirical model

<sup>2</sup> Ozone mass transfer rate based on measured  $Q_f$  and measured  $C_0$  values

<sup>3</sup> Geometric average of ozone concentration at inlet and outlet of bubble column

<sup>4</sup> Mean residence time determined from residence time distribution

<sup>5</sup> Ozone concentration at inlet of RFS estimated from best-fit of 1<sup>st</sup> order kinetic model to measured ozone profile in RFS

<sup>6</sup> 1<sup>st</sup> order ozone decomposition rate constant estimated from best-fit of 1<sup>st</sup> order kinetic model to measured ozone profile in the RFS

C = control run with no ozone added

na = not applicable

#### **10.4.2 *C. parvum* Inactivation Measured by the CD-1 Neonatal Mouse Model**

Oocyst inactivation results measured with the CD-1 neonatal mouse model are provided in Table 10-2. Additional details pertaining to the infectivity analysis with mouse model are provided in Table E-3 of Appendix E. Recovery of sufficient numbers of oocysts for infectivity analysis in the *C. parvum* challenge experiments required collection of the entire 2 L/min flow of water leaving the reactive flow segment. For this reason, oocyst inactivation was measured only at the outlet of the reactive flow segment in each experimental trial. In the *B. subtilis* spore challenge experiments, in contrast, samples were collected for spore viability determination from four different points along the length of the reactive flow segment. The difficulty and expense of conducting the challenges with live *C. parvum* oocysts limited the number of experimental challenges that could be completed with these parasites. As a consequence, the *C. parvum* dataset was much less extensive than that for *B. subtilis*.

Oocyst inactivation measured in the contactor feed samples, prior to any ozone exposure, ranged from -0.7 to +0.6 log-units with a mean of 0.05 log-units. This range of variation in infectivity of the control samples as determined by the CD-1 neonatal mouse assay is similar to that reported in a previous study on UV inactivation of *C. parvum* oocysts (Craik et al. 2001). Most importantly, the average inactivation in the contactor feed determined from the results of all nine trials was close to zero. In the single no ozone control trial, no loss of infectivity was observed between the feed and the outlet of the contactor. There was little evidence to suggest that inactivation measured in the experimental ozonation trials was due to anything other than contact with ozone.

For experimental trial 44, the infectivity result was reported as greater than the numerical value indicated in Table 10-2. In this particular trial, a single infection was observed in the cohort that received an inoculum of 10 000 oocysts per mouse, but no infections were observed in the cohort that received an inoculum of 100 000 oocysts per mouse. This unusual result was interpreted by setting the number of infections in the higher inoculum equal to one, and then calculating the log inactivation for both inocula. The infectivity reduction was then reported as greater than the arithmetic average of these

two calculated results. All other infectivity results were interpreted in a straightforward manner.

Table 10-2 Measured and model-predicted *Cryptosporidium parvum* oocyst inactivation in the experimental static mixer ozone contactor.

Trial	Model Predicted			Measured		
	Column Out	Cumulative at RFS Out		Feed	Static Mixer Out	RFS Out
		PFA	SFA			
43	0.4	2.8	2.7	-0.2	-0.3	3.1
44	0.4	3.1	3.0	-0.2	-0.2	> 3.3
45	0.4	2.6	2.5	-0.5	0.3	3.1
46	0.4	2.1	2.0	-0.7	1.0	2.3
47	0.4	3.2	3.1	0.5	0.1	3.4
48	0.3	1.4	1.4	0.6	nd	1.5
49	0.4	1.4	1.4	0.2	nd	1.7
50	0.4	1.4	1.4	0.2	nd	2.0
51	0.3	1.3	1.2	0.1	nd	1.5
Control	0	0	0	0.5	nd	0.4

nd = not done

#### 10.4.3 Measured *C. parvum* Oocyst Inactivation Curve

Measured oocyst inactivation was plotted as a function of the cumulative dissolved ozone  $C_{avg}t_m$  product in the static mixer contactor in Figure 10-1. The plotted values at the  $x$ -axis origin represent inactivation measured at the outlet of the static mixer where, because of the extremely short residence time, the  $C_{avg}t_m$  product was essentially zero. As expected, inactivation was found to increase proportionately with  $C_{avg}t_m$ . The polynomial trendline shown along with the experimental data in Figure 10-1 suggested

that the relationship between inactivation and  $C_{avg}t_m$  was not first-order. Best-fit values of the trendline parameters were determined using non-linear least squares regression. Calculations were performed in a Microsoft Excel 2000 spreadsheet using the solver tool. The best-fit value of the  $C_{avg}t_m$  exponent of 0.6 was relatively close to the values of the exponent parameters ( $n = 0.70$  and  $m = 0.73$ ) of the Hom kinetic model reported by Gyürék and co-workers (1999). This finding tends to support the use of a non-linear Hom-type kinetic model to describe oocyst inactivation rather than a first-order Chick-Watson kinetic model preferred by other researchers (Oppenheimer et al. 2000; Rennecker et al. 1999).

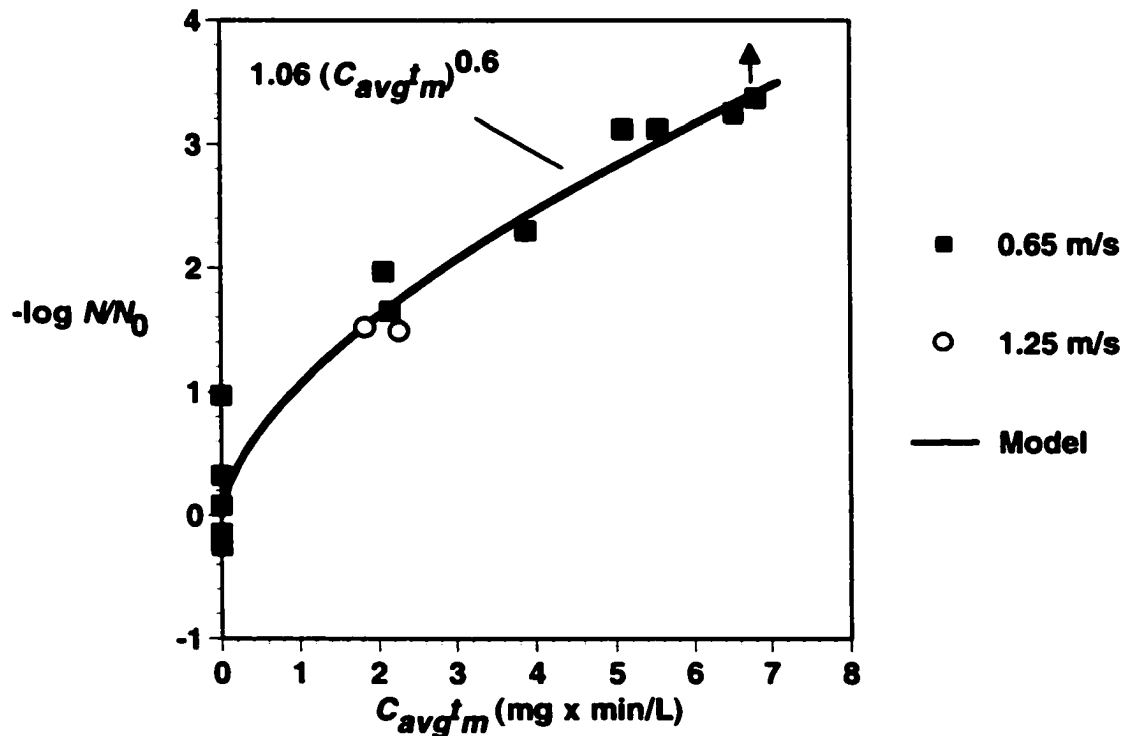


Figure 10-1 Measured inactivation of *Cryptosporidium parvum* oocysts in the experimental static mixer ozone contactor. The arrow indicates that the measured inactivation was beyond the level of detection of the infectivity analysis for this datum.

## **10.5 EFFECT OF STATIC MIXER HYDRODYNAMIC CONDITIONS ON *C. PARVUM* INACTIVATION**

### **10.5.1 Direct Effect on *C. parvum* Inactivation**

In trials 43 through 47, the mean measured oocyst inactivation in the feed and static mixer outlet streams was 0.06 log-units and 0.19 log-units, respectively (columns 5 and 6 of Table 10-2). The difference in mean inactivation between the feed and the static mixer outlet streams was, therefore, only 0.13 log-units. The distributions of the measured values, illustrated in the box and whisker diagram of Figure 10-2 were found to overlap the origin considerably. This was an indication that inactivation in neither the feed nor static mixer streams was significantly different than zero. In these five trials, the inactivation measurements in the feed and static mixer outlet streams were paired results. The distribution of the paired differences was also shown (SMX Out – SMX In) in the Figure 10-2. This distribution of this result also significantly overlapped the origin. A two-tailed hypothesis test based on the Student t-distribution confirmed that the mean paired difference in inactivation was not statistically different than zero at the 95% confidence level ( $p = 0.55$ ). Given such a large value of the computed  $p$  statistic, it was concluded with a considerable degree of statistical confidence that the small amount of direct inactivation of oocysts that was measured between the inlet and outlet of the static mixer was not significant.

### **10.5.2 Indirect Effect on *C. parvum* Inactivation**

Both predicted ozone transfer efficiency,  $TE$ , and the measured ozone mass transfer rate,  $M$ , increased considerably for the two trials conducted at the higher static mixer superficial velocity (trials 48 and 51 in Table 10-1). Given that the dissolved  $G/Q_f$  ratio and the dissolved ozone concentration,  $C_0$ , were unchanged, the increase in transfer efficiency and mass transfer rate in these two trials was probably related to increased gas-liquid mixing intensity within the static mixer and decreased bubble size. Oocyst inactivation, on the other hand, was essentially unchanged when compared on the basis of dissolved ozone  $C_{avg}t_m$  (Figure 10-1). This finding supports the notion that oocyst inactivation in the experimental static mixer contactor was determined primarily by

contact with dissolved ozone and was unaffected by the hydrodynamic conditions within the static mixer. Further, inactivation was independent of both the ozone mass transfer efficiency and mass transfer rate in the static mixer contactor.

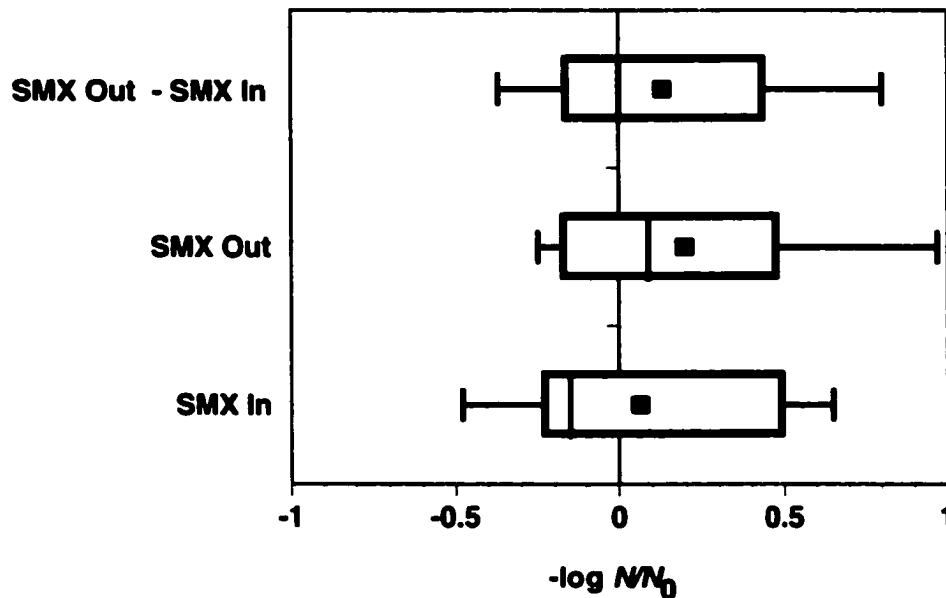


Figure 10-2 Box and whisker diagram of measured *Cryptosporidium parvum* inactivation measured directly at the inlet and outlet of the static mixer. From left to right, lines represent 90%, 25%, median, 25% and 90% percentile boundaries, respectively. The square symbol represents the mean.

## **10.6 VALIDATION OF THE BATCH KINETIC MODEL**

### **10.6.1 Importance of Validation**

Gyürék and co-workers (1999) conducted their experiments in pH 6 to 8 phosphate-buffered ultrapure water using eight different batches of Iowa strain oocysts that were isolated from the feces of Holstein calves. One of the potential weaknesses of the contactor modeling analysis was that this kinetic model might not have adequately represented the rate of inactivation of the oocysts used in the static mixer contactor experiments. Relatively little is known about how oocyst strain, isolation procedure, age and storage conditions affect *C. parvum* resistance to ozone, nor to what extent water composition and quality affect the inactivation kinetics. These variables, therefore, represent potential sources of error in the modeling analysis.

One study reported that the kinetics of inactivation by ozone of different strains of *C. parvum* oocysts were significantly different (Rennecker et al. 1999). The single batch of oocysts used in the static mixer contactor experiments, therefore, were derived from the same Iowa strain as used by Gyürék and co-workers (1999) and were isolated from a Holstein calf using similar procedures. Another recent study reported that for turbidity less than 10 NTU and pH between 6.5 and 8.2 the rate of *C. parvum* inactivation by ozone was not significantly affected by water quality (Oppenheimer et al. 2000). The large volumes of water required in the static mixer contactor experiments prohibited the use of ultrapure water. A good quality, low turbidity, building tap water at pH 7.5 to 8.1 that was additionally treated with granular activated carbon filtration was used as convenient substitute source (Section 6.1.1). Therefore, neither experimental water matrix nor oocyst batch was expected to have a significant effect on ozone inactivation kinetics. In order to remove any uncertainty regarding the modeling analysis, it was, nevertheless, important to verify this expectation.

### **10.6.2 *C. parvum* Inactivation in Batch Reactors Versus Kinetic Model-Prediction**

Seven batch reactor experiments were completed using the same batch of oocysts and the same water as used in the static mixer challenge experiments. Other than water matrix and oocyst batch, all other experimental procedures were identical to those used

by Gyürék and co-workers (1999). These procedures included; the reactor type (batch), water temperature ( $22 \pm 1^\circ\text{C}$ ), ozone determination by UV absorbance at 260 nm with a molar absorbance coefficient of  $3\,300\ \text{M}^{-1}\ \text{cm}^{-1}$ , and oocyst infectivity determination by the neonatal CD-1 mouse model. Details of the batch reactor experiments are provided in Tables E-4 and E-5 of Appendix E. Oocyst inactivation measured in these batch reactor experiments is compared to that predicted by the Hom kinetic model of Gyürék and co-workers (1999) in Figure 10-3. Model predictions were generated by inserting the experimental batch reactor ozonation conditions, given by  $C_0$ ,  $k_d$  and  $t_b$  (Table E-4) into the incomplete gamma-Hom model formulation (Equation 3-6). The central diagonal line in Figure 10-3 represents perfect model fit. The outer diagonal lines in Figure 10-3 represent the approximate error bounds of the Hom kinetic, estimated by Gyürék and co-workers (1999) to be  $\pm 0.7$  log-units at the 90% confidence level.

### 10.6.3 Error Analysis

In 6 out of the 7 experiments, measured inactivation was within the approximate error bounds of the kinetic model. Moreover, the mean prediction error,  $\bar{\varepsilon}$ , was only 0.03 log-units. (Prediction errors,  $\varepsilon_i$ , were defined using Equation 7-8.) Although a hypothesis test based on the two-tailed Student t-distribution indicated that this mean error was not significantly different from zero at the 95% confidence level ( $p = 0.95$ ), the prediction errors were not randomly distributed, indicating possible lack-of-fit. To test for the significance of this lack-of-fit, a straight line (not shown in Figure 10-3) was regressed through the data points using least-squares criteria. The 95% confidence intervals of the slope and y-intercept of this line, computed using least-squares criteria and the regression tool in Microsoft Excel 2000, were  $1.4 \pm 1.2$  and  $-1.0 \pm 2.9$ , respectively. The computed parameters of this model-fit line, therefore, were not statistically different from the unity slope and zero y-intercept of the perfect fit line. It was thus concluded that, on average, the kinetic model of Gyürék and co-workers (1999) neither overestimated nor underestimated *C. parvum* inactivation. There may have been some degree of lack of fit, however, the statistical evidence was not sufficient to establish true lack of fit.

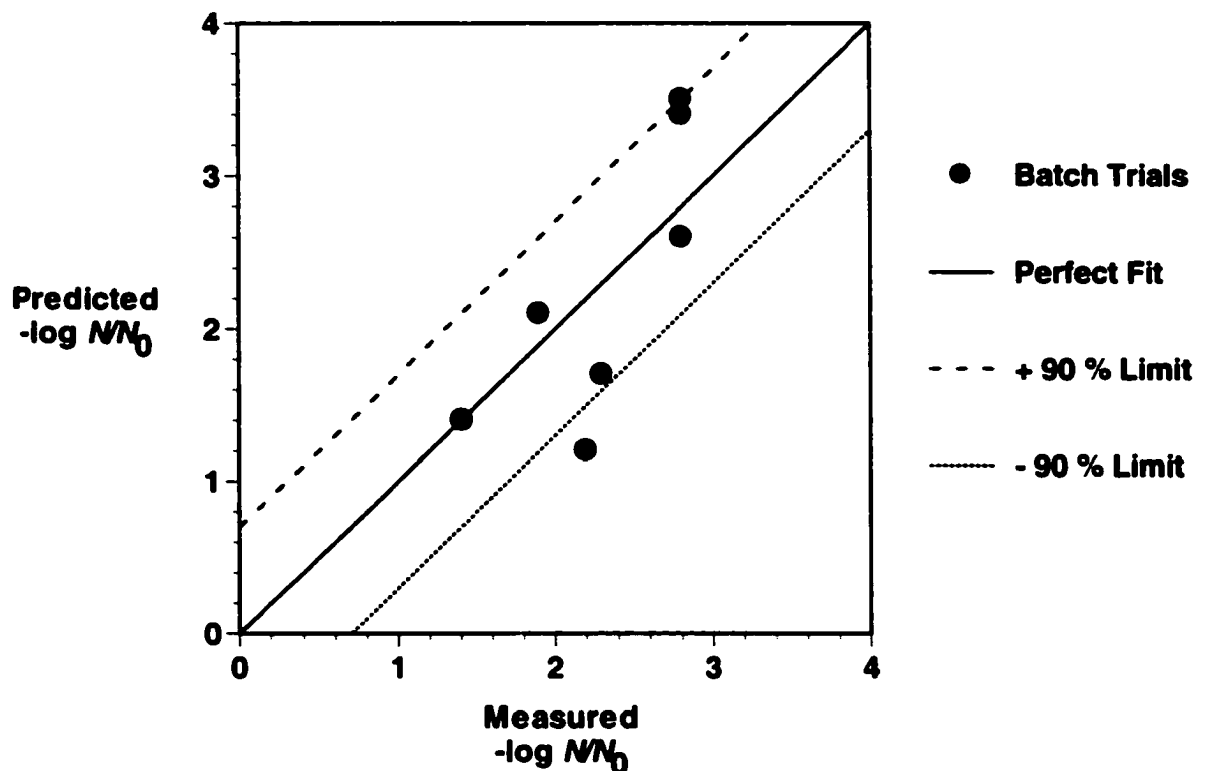


Figure 10-3 Comparison of model-predicted and measured batch reactor inactivation of the *Cryptosporidium parvum* oocysts used in the static mixer contactor experiments

## 10.7 RESULTS OF MODELING ANALYSIS

### 10.7.1 Model Predictions

Predictions of *C. parvum* inactivation for each of the experimental ozonation conditions summarized in Table 10-1 are provided in Table 10-2. Inactivation predicted at the outlet of bubble column is provided in column 2. Predictions of net inactivation at the outlet of the reactive flow segment are provided in columns 3 and 4, based on plug flow analysis and segregated flow analysis, respectively. The inactivation curve of *C. parvum* by ozone was previously observed to be non-linear with respect to  $C_{avg}t_m$ , (Figure 10-1). Because of this non-linearity in oocyst response to ozone, the additive correction

was, therefore, not exact. The magnitude of the error introduced, however, was expected to be minor because inactivation in the bubble column was limited to 0.4 log-units.

### **10.7.2 Comparison between Plug Flow Analysis (PFA) and Segregated Flow Analysis (PFA)**

According to the modeling analysis, the residence time distribution in the reactive flow segment had little influence on oocyst inactivation. Predictions of oocyst inactivation based on the assumption of perfect plug flow were within 0.1 log-unit of those generated using segregated flow analysis and the measured exit age distribution (Table 10-2). This was true regardless of the experimental residence time or  $C_{avg}t_m$  product. Close agreement between the plug flow and segregated flow predictions was the first indication that the two-stage design of the contactor was conducive to very efficient inactivation of *C. parvum*. That is, based solely on knowledge of the exit age distribution,  $E(t)$ , inactivation in the experimental contactor was expected to approach that of a perfect plug flow contactor.

The segregated flow analysis computations did not consider the potential effect of the degree of fluid segregation or extent of micro-mixing that exists in the contactor. One of the conclusions of the theoretical analysis of Chapter 3 was that, for the case of *C. parvum* inactivation by ozone with first-order ozone decomposition, the degree of segregation in a contactor might have an important effect on inactivation. Strictly speaking, segregated flow analysis provides only an upper bound on predicted inactivation (Figures 3-2, 3-3 and 3-4). Measured inactivation in a contactor that was closer to a micro-mixed condition might be considerably lower than that predicted on the assumption of a segregated fluid. It was further argued in Chapter 3 that, on the basis of segregation number, a typical ozone contactor is more likely to approximate a micro-mixed state with respect to ozone. The experimental results suggest that the degree of segregation did not have a significant effect on *C. parvum* inactivation in the static mixer contactor. Indeed, measured inactivation exceeded that predicted by segregated flow analysis (Figure 10-4). A possible explanation is that the residence time distribution of the contactor was sufficiently close to that of perfect plug flow such that the degree of segregation had little influence on the level of inactivation. According to reaction

engineering theory, the degree of segregation becomes unimportant for most reacting systems as the residence time distribution behaviour approaches that of perfect plug flow (Levenspiel 1972; Nauman and Buffham 1983). A second explanation is that the theory of micro-mixing and segregation as applied to dissolved homogeneous chemical reactants, like ozone, does not apply equally to microorganisms like *C. parvum*.

### 10.7.3 Comparison to Measured Inactivation

Model-predicted inactivation at the outlet of the reactive flow segment is plotted against measured inactivation in Figure 10-4. The 45 degree diagonal line in this figure represents a perfect model fit. The upper and lower diagonal lines represent the approximate 90% confidence bounds of the kinetic model of  $\pm 0.7$  log-units (Gyürék et al. 1999). A series of data points lying exactly on, or evenly distributed about the perfect fit line would indicate that inactivation was equivalent to the theoretical maximum predicted for a perfect plug contactor. In a hydrodynamic and mixing sense, the contactor would be considered perfectly efficient in terms of microorganism reduction for this range of ozonation conditions. A series of data points lying above the line would suggest the impact of deviations from perfect plug-flow residence time distribution behaviour and would indicate less than perfectly efficient performance.

The outcomes of each of the nine challenge experiments with the static mixer contactor were found to lie below the 45 degree diagonal line of perfect fit, but within the approximate 90% confidence band of the kinetic model predictions. Using the definition of error given by Equation 7-8, the calculated mean prediction error,  $\bar{\epsilon}_i$ , of the contactor model was determined to be -0.3 log-units. In other words, measured inactivation was actually greater than the theoretical maximum of perfect plug flow by, on average, 0.3 log-units. Although the individual results were within the approximate prediction intervals of the model, a hypothesis test based on a two-tailed Student t-distribution revealed that this computed mean error of 0.3 log-units was statistically significant at the 95% confidence level ( $p = 0.0007$ ).

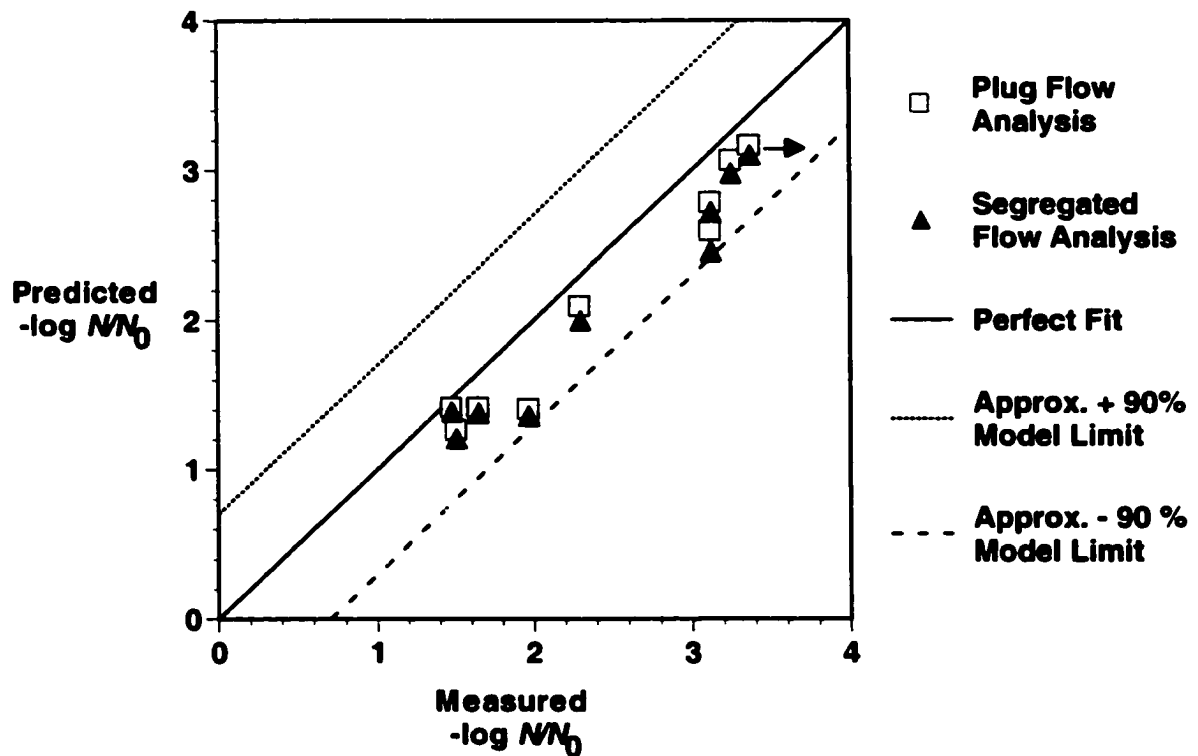


Figure 10-4 Comparison of model-predicted and measured *Cryptosporidium parvum* oocyst inactivation at the outlet of the reactive flow segment in the experimental study static mixer contactor. The arrow indicates that the measured inactivation was beyond the level of detection of the infectivity analysis for this datum.

Attempts to rationally explain the 0.3 log-unit mean prediction error were inconclusive. The batch kinetic model validation exercise described in Section 10-6 helped to rule out explanations related to oocyst batch or water matrix effects. Unidentified sources of bias in determination of the  $C_{avg}t_m$  products may have also accounted for the mean error. A relatively small systematic error in determination of  $C_{avg}t_m$  would be required to generate the observed prediction error. For example, a consistent error in the estimation of the  $C_{avg}t_m$  of only 0.13  $\text{mg}\times\text{min}/\text{L}$ , equivalent to about 2% to 6% of the experimental  $C_{avg}t_m$  values, would have been sufficient to generate a 0.3 log-unit prediction error in inactivation (Figure 10-1). A third explanation for the

offset was that the rate of oocyst inactivation was indeed enhanced by virtue of the conditions of initial gas-liquid contact within the static mixer. However, as noted earlier, doubling of the superficial velocity in the static mixer had no apparent effect on oocyst inactivation in the reactive flow segment (Figure 10-1). Given this inconsistency and the relatively small magnitude of the prediction error of 0.3 log-units, it is difficult to conclude that significant kinetic enhancement occurred.

#### 10.7.4 Comparison to *B. subtilis* Inactivation

*C. parvum* oocyst inactivation in the experimental static mixer contactor exceeded predictions based on the assumption of perfect plug flow over the full range of experimental  $C_{avg}t_m$  conditions. Recall from Chapter 9, that *B. subtilis* spore inactivation in the experimental static mixer contactor was approximately 1 log-unit less than that predicted based on perfect plug flow at intermediate  $C_{avg}t_m$  values. What accounted for this apparent difference in inactivation performance of these two microorganisms in the experimental static mixer contactor? The explanation is related to the different shapes of the inactivation curves of the two microorganisms.

The contrast between the sigmoid shape of the spore inactivation curve and curvilinear shape of the oocyst inactivation curve was depicted in Figure 7-4, 7-5 and 7-6 of Chapter 7. Most importantly, the slope of the exponential region of the spore inactivation near the middle of the experimental  $Ct$  range was much steeper than the slope of the *C. parvum* oocyst inactivation curve. In Chapter 9, it was explained that inactivation of spores in a continuous flow contactor would tend to be sensitive to the residence time distribution because of the steep slope of the inactivation curve in this  $Ct$  region. This point was demonstrated mathematically using segregated flow analysis and was supported by experimental measurements in the static mixer contactor. Segregated flow analysis using the same residence time distributions showed that *C. parvum* oocyst inactivation was considerably less sensitive to the residence time distribution than was spore inactivation. Again, this was supported by the results of challenge experiments with oocysts. This point is important when considering use of model organisms for evaluating the efficiency of ozone contactors. The appropriateness of a particular

microorganism will depend not only on the overall level or resistance to ozone, but on the shape of the inactivation curve as well.

## **10.8 SUMMARY OF *CRYPTOSPORIDIUM PARVUM* EXPERIMENTS**

The results of the *C. parvum* challenge experiments described in this chapter suggest that, for the hydrodynamic and ozonation conditions investigated, inactivation of *C. parvum* in the experimental static mixer contactor was determined primarily by contact with dissolved ozone. There was little evidence to suggest that the intrinsic rate of oocyst inactivation by dissolved ozone was significantly enhanced by initial gas-liquid contact in the static mixer. If any such enhancement occurred, it was limited to less than 0.3 log-unit. The two-stage contactor hypothesis presented in Chapter 4 was demonstrated. Based on segregated flow analysis modeling, the residence time distribution in the static mixer contactor was predicted to have little effect on *C. parvum* inactivation. Contactor performance, in terms of microorganism inactivation, was expected to be approach that of a perfect plug flow contactor. This expectation was confirmed by direct measurement of *C. parvum* inactivation at the outlet of the reactive flow segment. Efficient *C. parvum* inactivation was therefore achieved in the continuous-flow ozone dissolution and contacting system. Ozone was rapidly dissolved with the static mixer and hydrodynamically efficient dissolved ozone contact was achieved in the reactive flow segment.

## 11 INACTIVATION OF *GIARDIA MURIS* IN THE STATIC MIXER CONTACTOR

### 11.1 INTRODUCTION

In the experiments described in Chapters 9 and 10, *Bacillus subtilis* spores and *Cryptosporidium parvum* oocysts were found to be largely unaffected by the hydrodynamic and gas-liquid contacting environment that existed within the static mixer. The objective of the experimental study described in this chapter was to determine if these conclusions could be extended to *Giardia* spp. cysts. The effect of static mixer hydrodynamics on *G. muris* was determined using the same approach that was previously described for *B. subtilis* cysts and *C. parvum* oocysts. Challenge experiments with *G. muris* cysts were conducted in the experimental static mixer contactor in which the static mixer hydrodynamic conditions were varied independently from the conditions of dissolved ozone contact in the reactive flow segment.

### 11.2 EXPERIMENTAL DESIGN

A total of six challenge experiments were completed with *G. muris*. For each, the short bubble column configuration ( $H = 0.45$  m) was employed and the feed water temperature was regulated to 22°C. Experiments were carried out at nominal static mixer superficial velocities,  $v_s$ , of either 0.5 m/s or 1.4 m/s while maintaining approximately constant dissolved ozone conditions. Because *G. muris* oocysts are considerably more sensitive to the effects of ozone, much lower target ozone exposures were used in the *G. muris* challenges compared to those used in the *C. parvum* oocyst challenges. The objective was to ensure that cyst inactivation remained within measurable limits. The length of the reactive flow segment was reduced to provide a total contact time of approximately 3.7 minutes, and the target ozone concentration range was decreased from about 0.6 mg/L to 0.1 mg/L. In each experiment, samples of water were collected from the feed (after cyst addition but prior to ozone addition), the static mixer outlet and the reactive flow segment outlet for cyst recovery and infectivity analysis with the C3H/HeN mouse latent period model.

## 11.3 CONTACTOR MODELING

### 11.3.1 *G. muris* Kinetic Model

Finch and co-workers (1993b) published a non-linear Hom kinetic model that described the inactivation of *G. muris* by ozone. The mathematical form of the model was the following:

$$-\log \frac{N}{N_0} = k'_H C^n t^m \quad \text{Equation 3-2}$$

The Finch and co-worker kinetic model was developed from a very limited dataset of experimental batch reactor ozonation trials with *G. muris* cysts. To develop a more robust kinetic model, the data from the Finch and co-worker study was combined with information from additional reactor ozonation experiments with *G. muris* extracted from the doctoral thesis of Charles Labatiuk (1992), who was one of the Finch co-workers. The relevant information regarding the batch reactor ozonation experimental trials extracted from the Labatiuk thesis and used for model development is summarized in Table F-4 of Appendix F.

The Finch and co-worker (1993b) and Labatiuk (1992) studies were selected mainly because the strain of *G. muris* cysts used was the same as in this study, and inactivation was assessed using a similar infectivity assay based on latent period of infection in C3H/HeN mice. The Labatiuk thesis contains information on numerous batch reactor ozonation experiments with *G. muris* that were conducted in various different natural water matrices and at various temperature and pH conditions. Only those trials for which certain experimental conditions were comparable to those of the static mixer challenge experiments were selected for examination. These experimental conditions were, namely, a matrix of phosphate buffered ultrapure water, a temperature of 22°C and near neutral pH (6.7 to 7.6). For this analysis, the Hom kinetic model of Equation 3-2 was simplified by assuming that values of the exponent parameters  $n$  and  $m$  were equal. With this assumption, inactivation became a non-first order function of the

simple  $Ct$  product, that is, a function of  $(Ct)^n$ . Using non-linear regression with least-squares minimization criteria, the best fit parameters of Equation 3-29 were determined to be  $k'_H = 3.3$  and  $n = m = 0.18$ . The fit of the model to the combined Finch and co-worker and Labatiuk datasets is shown in Figure 11-1. The resulting inactivation curve was found to deviate significantly from linearity. Cyst inactivation was very rapid initially, but quickly diminished with a pronounced tailing effect. A small fraction of the cyst population ( $<0.1\%$ ) appeared to exhibit resistance to extended ozone exposure.

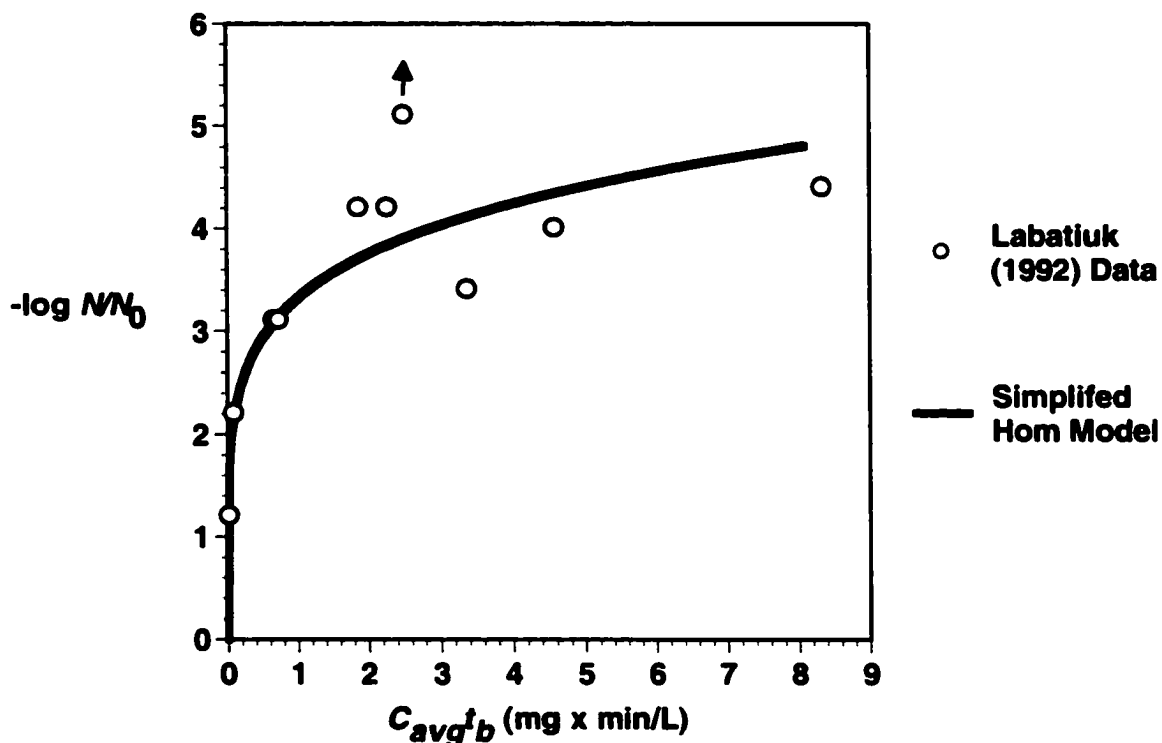


Figure 11-1 Inactivation of *Giardia muris* by ozone in batch reactors as determined by latent period infectivity analysis in C3H/HeN mice. Data is from Labatiuk (1992). Arrows indicate that the outcome was beyond the detection limit of the infectivity assay.

### 11.3.2 A Simplified Contactor Modeling Approach

A simpler approach was used to model inactivation of *G. muris* in the experimental static mixer contactor than was used for *C. parvum*. For *G. muris*, the entire static mixer contactor, including both the bubble column and the reactive flow segment, was treated as a single ideal plug flow unit. The rationale for the simpler modeling approach was as follows. In Chapter 10, it was explained that two-stage modeling approach used for *C. parvum* was inexact for non-linear kinetics, however, the error introduced was expected to be minor because little inactivation was expected in the bubble column. Based on the simplified *G. muris* kinetic model and the non-linear inactivation curve of Figure 11-1, much of the cyst inactivation was expected to take place very rapidly and in the bubble column, even at the lower ozone concentrations employed. Relatively less inactivation was expected to occur in the reactive flow segment of the experimental contactor. Simple addition of the computed inactivation in both segments, as was done for *C. parvum*, would have resulted in serious errors in the case of *G. muris*.

To estimate the net *G. muris* inactivation in the contactor for a given experimental ozonation condition, an integrated average  $C_{avg}t_m$  was first determined by combining the contributions of the bubble column and the reactive flow segment. The  $C_{avg}t_m$  in each of these sections was computed as described for the previous challenge experiments with *B. subtilis* spores and *C. parvum* oocysts. The average  $C_{avg}t_m$  thus determined was substituted directly in the simplified Hom kinetic model of Equation 3-2 (with  $m=n$ ) and the log inactivation calculated.

## 11.4 CHALLENGE EXPERIMENT RESULTS

Ozonation conditions for each of the challenge experiments with *G. muris* cysts are summarized in Table 11-1. Further details of the ozonation and other operating conditions of the *G. muris* challenge experiments are provided in Tables F-1 and F-2 of Appendix F. The ozone conditions selected for analysis were those based on measurement of dissolved ozone by the UV absorbance method. The justification for this decision was identical to that described for analysis of the *C. parvum* challenge experiments in Chapter 10. That is, the dataset used to develop the batch kinetic model

of *G. muris* inactivation by ozone was based on ozone measurements by UV absorbance at 260 nm with a molar absorbance coefficient of 3 300 M<sup>-1</sup>cm<sup>-1</sup> (Labatiuk, 1992). Cyst inactivation measured using the C3H/HeN mouse latent period model was summarized for each trial in Table 11-2. Information regarding determination of cyst inactivation using the C3H/HeN mouse latent period model is provided in Table F-3 of Appendix F. Model-predicted inactivation determined for the experimental ozonation conditions is also provided in Table 11-2. As expected, most of the cyst inactivation within the static mixer contactor was predicted to occur within the bubble column.

Table 11-1 Summary of ozonation conditions for the *Giardia muris* challenge experiments with the experimental static mixer contactor. All ozone concentrations are based on measurements by UV absorbance at 260 nm.

Trial	$v_s$	$G/Q_f$	<sup>1</sup> TE	<sup>2</sup> M	Bubble Column			Reactive Flow Segment				Total
					$C_{avg}$	$t_m$	$C_{avg}t_m$	$C_0$	$t_m$	$k_d$	$C_{avg}t_m$	$C_{avg}t_m$
	m/s	%	%	mg/L	mg/L	min	mg× min/L	mg/L	min	min <sup>-1</sup>	mg× min/L	mg× min/L
54	0.46	1.70	71	0.44	0.11	1.21	0.13	0.08	3.7	0.15	0.23	0.37
55	1.15	1.50	86	1.00	0.08	0.60	0.05	0.07	3.6	0.18	0.20	0.25
56	0.39	1.98	68	0.49	0.13	1.31	0.17	0.11	3.7	0.10	0.33	0.51
57	1.32	1.30	89	1.36	0.10	0.51	0.05	0.09	3.6	0.13	0.26	0.31
58	0.43	1.80	69	0.36	0.09	1.25	0.11	0.07	3.6	0.23	0.18	0.28
59	1.33	1.36	88	0.96	0.08	0.51	0.04	0.06	3.7	0.20	0.16	0.20

<sup>1</sup>Ozone transfer efficiency was estimated from an empirical model

<sup>2</sup>Ozone mass transfer rate based on measured  $Q_f$  and measured  $C_0$  values

Table 11-2 Measured and model-predicted *Giardia muris* cyst inactivation in the experimental static mixer ozone contactor. All values are in log-units.

Trial	PFA Model Predicted		Measured		
	Bubble Column Out	RFS Out	Feed	Static Mixer Out	RFS Out
54	2.3	2.8	0.18	-0.22	-0.23
55	2.0	2.6	-0.22	-0.32	> 2.2
56	2.4	3.0	-0.36	-0.11	1.5
57	2.0	2.7	-0.39	-0.73	1.3
58	2.3	2.7	-0.5	-0.04	> 3.0
59	1.9	2.5	-0.49	-0.72	> 3.4
Control	0	0	-0.19	-0.20	0.63

### 11.5 CYST INACTIVATION WITHIN THE STATIC MIXER

A box and whisker diagram of cyst inactivation measured in the feed and outlet of the static mixer is shown in Figure 11-2. Counter to expectations, a slight increase in infectivity (i.e. negative inactivation) was observed in the cysts present in both the feed and static mixer outlet streams. Average inactivation levels were -0.2 log-units and -0.4 log-units in the feed and static mixer outlet, respectively. This may have reflected a slight increase in the infectivity of the cyst preparations used in experiments relative to those used to develop the latent period dose-response model (Figure 6-7). Because the measured inactivation in the static mixer feed and outlet streams represented paired data, the difference between these results was calculated for each experimental trial. The mean of these paired differences was determined to be only 0.1 log units. Therefore, even though the average measured inactivation in the static mixer feed and outlet stream may

have differed from zero, the change in inactivation was not significantly different from zero. It was concluded, therefore, that no measurable inactivation occurred within the static mixer itself. This was true at both low and high superficial velocities within the static mixer.

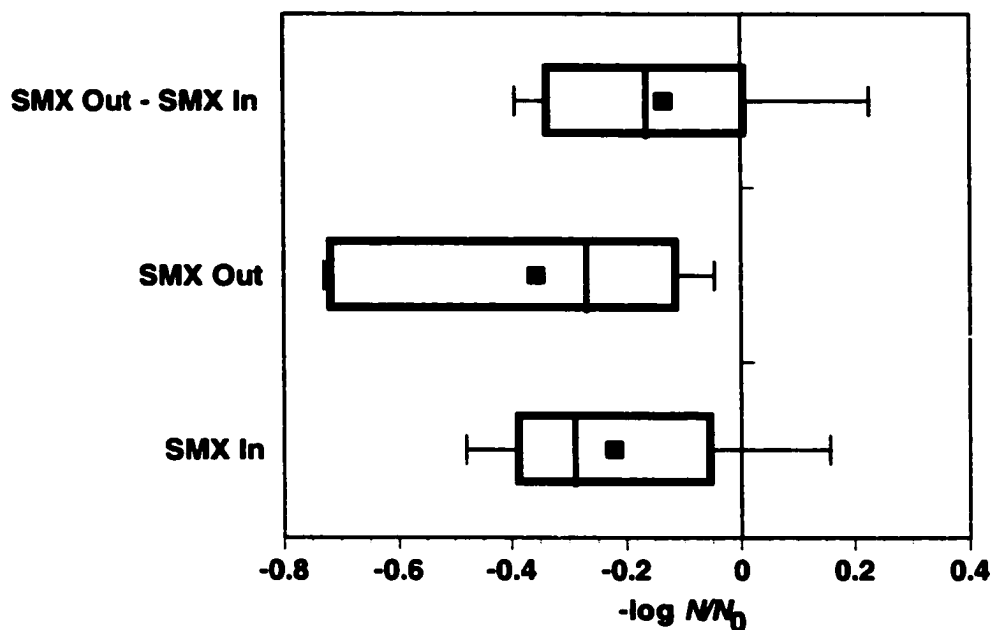


Figure 11-2 Box and whisker diagram of measured *Giardia muris* inactivation at the inlet at outlet of the static mixer. From left to right, lines represent 90%, 25%, median, 25% and 90% percentile boundaries, respectively. The square symbol represents the mean.

## 11.6 COMPARISON TO MODEL PREDICTIONS

*G. muris* cyst inactivation is plotted as a function of the measured dissolved ozone  $C_{avg}t_m$  product in static mixer contactor in Figure 11-3. Predictions of the simplified Hom model are also plotted in Figure 11-3 for comparison purposes. Precise interpretation of the results was made difficult by the rather large amount of variability in the outcomes of the infectivity analysis. One of the limitations of the *G. muris* challenge experiments was

the relatively low recovery of cysts from the outlet of the reactive flow segment. Cyst recoveries measured at the outlet of the reactive flow segment ranged from as low as 0.2% to as high as 19% (Table F-3, Appendix F). In comparison, *C. parvum* recoveries were consistently higher, at between 6 and 67% (Table E-3, Appendix E). In the experiment in which cyst recovery was only 0.2% (Trial 54), essentially no cyst inactivation was observed at the outlet of the reactive flow segment. If those cysts that were inactivated by ozone were less likely to be recovered in the sample filtration procedure, then this would have introduced a bias into the measured inactivation result. This would explain the unusually low inactivation result of Trial 54. Such low recoveries significantly reduce the confidence in the experimental result. A modification to the cyst concentration procedure that resulted in better cyst recovery was introduced in Trials 57, 58 and 59. In these trials, the 8 L samples of water that were collected from each sampling point were split into two 4 L portions and each portion was filtered through a single PCTE filter. In addition, a small amount of Tween 20, a surfactant, was added to improve the recovery of cysts from the PCTE filter. Based on infectivity analysis of the feed samples in these trials (Table F-3, Appendix F), there was no evidence that these procedures had an adverse effect on the infectivity of the cysts.

A second difficulty of the *G. muris* analysis was posed by the fact that in three of the trials (Trials 55, 58 and 59) the measured inactivation was beyond the limits of detection of the infectivity assay. As an approximate and conservative analysis, the average inactivation of all trials was estimated by setting the outcomes of these trials at the detection limit. Because of the very low cyst recovery, the result of Trial 54 was excluded from this analysis. The estimated average inactivation of the five remaining experimental trials was 2.3 log units. For the range of experimental  $C_{avg}t_m$  products (approximately 0.2 to 0.5 mg×min/L), the simplified Hom model predicted between 2.5 log-units and 2.9 log-units inactivation. The average measured inactivation, therefore, was not considerably different from that predicted using the simplified Hom model and assuming perfect plug flow. The result also agrees well with the ozone resistance of *G. muris* cysts reported by others in the literature. For example, the  $Ct$  product required for 2 log-units of inactivation at 25°C and pH 7 in batch reactors was estimated to be 0.27 mg×min/L (Wickramanayake et al. 1984b). It may be concluded, though tentatively, that

cyst inactivation was unaffected by the hydrodynamic conditions within the static mixer, the transfer efficiency and overall mass transfer rate.

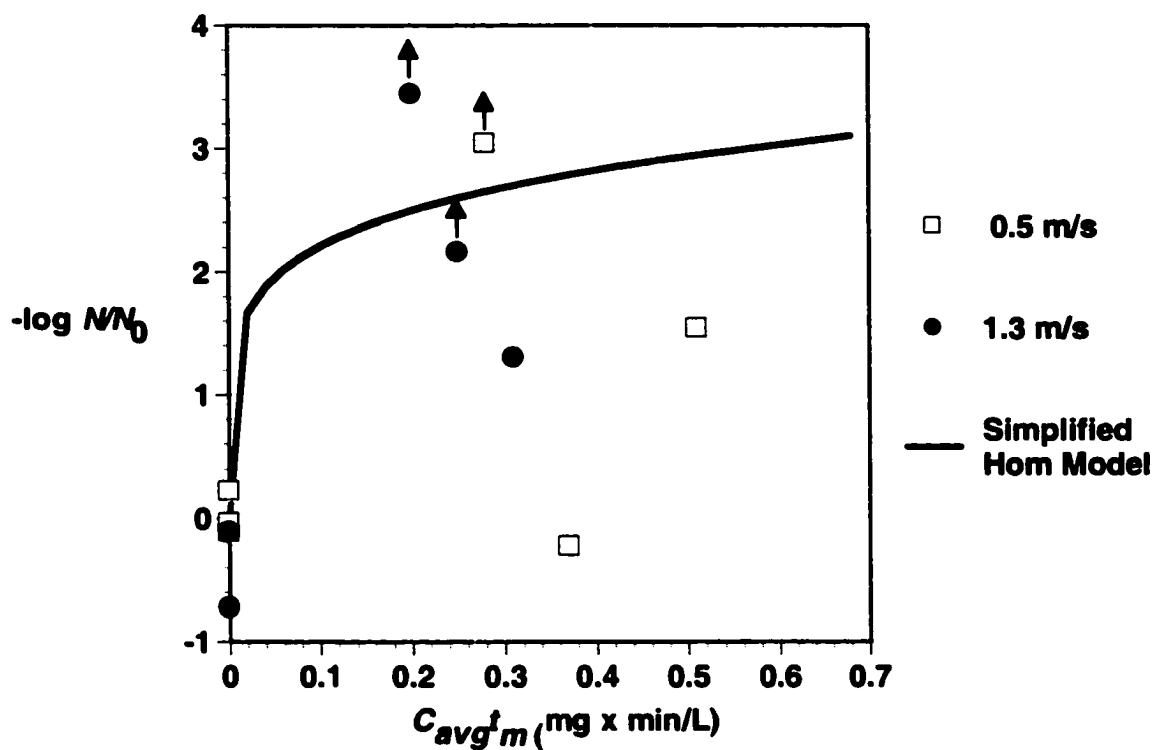


Figure 11-3 Inactivation of *Giardia muris* in the experimental static mixer ozone contactor at different superficial velocities,  $v_s$ , in the static mixer. The solid line represents predictions of the simplified Hom batch kinetic model. Arrows indicate outcomes were beyond the detection limit of the infectivity assay.

### 11.7 SUMMARY OF *GIARDIA MURIS* EXPERIMENTS

The finding that little or no inactivation of *B. subtilis* spores or *C. parvum* oocysts resulted from direct gas-liquid contact within the static mixer was also found to apply to *G. muris* cysts. This finding was interesting because *G. muris* cysts are known to be less robust than *C. parvum* oocysts. Compared to *C. parvum* oocysts, *Giardia* spp. cysts are

less resistant to chemical oxidants used in water treatment, including chlorine compounds (Table 2-1) and ozone (Table 2-5 and Table 2-6). In addition, *Giardia* spp. cysts are not as resistant to physical stresses as are *C. parvum* oocysts. For example, freezing at  $-6^{\circ}\text{C}$  for 4 days resulted in greater than 99.8% loss of *G. muris* cyst viability (Wickramanayake et al. 1985), while only 80% of *C. parvum* oocysts were killed by freezing at  $-22^{\circ}\text{C}$  (Robertson et al. 1992). Anecdotal evidence in the author's laboratory suggested that vigorous mixing on a vortex mixer resulted in reduced counts and lysis of cysts in *G. muris* preparations. For this reason, the vigorous mixing of *G. muris* preparations was strictly avoided. *C. parvum* oocysts, on the other hand, were found to be insensitive to this mixing procedure and the procedure was routinely employed to thoroughly mix *C. parvum* suspensions.

Given the variability in the infectivity analyses, the low cyst recovery, and the number of outcomes that were above the detection limit, it was not possible to state categorically whether or not initial gas-liquid contact within the static mixer affected *G. muris* inactivation by dissolved ozone in the reactive flow segment.

## 12 DISCUSSION AND SUMMARY

### 12.1 THE PROBLEM STATEMENT REVISITED

Ozonation is a technology for reduction of the protozoan parasite *Cryptosporidium parvum* in drinking water treatment. The effect of dissolved ozone on oocysts of *C. parvum* has now been well established and several studies have elucidated and modeled the kinetics of the rate of inactivation of oocysts by ozone in controlled laboratory environments (Gyürék et al. 1999; Li et al. 2001; Oppenheimer et al. 2000; Rennecker et al. 1999). There are several unanswered questions regarding the effect of ozone on oocysts. Some of these are listed below:

- What is the mechanism by which ozone inactivates or reduces the infectivity of individual oocysts?
- How does water quality affect oocyst inactivation kinetics?
- What are the impacts of oocyst strain, source and age on susceptibility to ozone?
- Will environmental oocysts behave similarly to the preparations that have been used in the published kinetic studies?
- How can the differences between the results obtained in the different laboratory studies be rationalized into reliable design criteria that can be used by the water treatment industry to guide facility design?

These questions will undoubtedly be answered by ongoing laboratory research. In this thesis project, they were put aside in order to concentrate on a different problem. The research question describing that problem was: How can the knowledge of *C. parvum* inactivation kinetics by ozone that has been accumulated in the laboratory be applied to the problem of designing efficient ozone contactors?

Although ozone contactors have been used in the water and wastewater treatment industry for many years and for different purposes, only a few studies have specifically addressed the problem of optimizing ozone contactor hydrodynamic design for reduction of resistant microorganisms, and these have been largely theoretical (Do-Quang et al.

2000b; Roustan et al. 1991). Application of ozone in water treatment facilities has been dominated by a single contactor design, namely the multi-chamber, fine bubble diffuser contactor illustrated in Figure 2-2. One of the reasons this design has been favoured, is, as noted in the review by Langlais and co-authors (1991), it is both familiar and proven. Conventional fine-bubble diffuser contactors, however, which consist of arrays of diffusers in large contact basins, have been designed primarily for ozone mass transfer. In addition, rigorous design procedures and approaches based on fundamental engineering science have been slow to emerge. Empirical design rules, such as the US EPA Ct design criteria described in the Guidance Manual to the Surface Water Treatment Rule (Malcolm Pirnie Inc. and HDR Engineering Inc. 1991) have dominated design practice.

The theoretical analysis described in Chapter 3 demonstrated that the mixing regime within an ozone contactor will have an important effect on the level of *C. parvum* reduction. For ozone contactors, efficient inactivation will be promoted mainly by ensuring residence time behaviour that approaches that of perfect plug flow. Several engineering studies demonstrated that this hydrodynamic regime is difficult to achieve in a conventional fine bubble diffusers (Bellamy 1995; Do-Quang et al. 2000a; Henry and Freeman 1995; Martin et al. 1995). One of the limiting factors is that the operations of gas-liquid contact for ozone dissolution, and dissolved ozone contact for inactivation of microorganisms are constrained to take place in same contacting vessel. As part of this thesis, therefore, a two-stage contactor concept, in which ozone dissolution and microorganism reduction processes are treated as separate unit operations, was proposed as a ozone contactor design alternative.

The theoretical analysis and the two-stage contactor concept relied on the assumption that the process of inactivation of oocysts by ozone can be treated much like a chemical reaction between two dissolved reactants. Ozone contactor analysis was, therefore, amenable to treatment using the chemical reaction engineering concepts of residence time distribution and fluid segregation. Further, it was assumed that inactivation kinetic models developed in batch reactors, such as the *C. parvum* ozone kinetic model developed by Gyürék and co-workers (2001) and Li and co-workers (2001), can be used to predict microorganism inactivation by ozone in full-scale

contactors. But was it safe to assume that oocysts and ozone behaved as dissolved reactants in continuous-flow systems? Consider that in a 1 mg/L solution of ozone, about 1 million ozone molecules occupy a volume equal to that occupied by a single 5  $\mu\text{m}$  diameter, spherical *C. parvum* oocyst particle (see calculation in Appendix G). Moreover, the roles of gaseous ozone and the intensity of gas-liquid mixing on microorganism inactivation were uncertain. Some researchers suggested that reduction of yeast and bacteria was improved by promoting gas-liquid contact (Ahmad and Farooq 1984; Farooq et al. 1977a; Farooq et al. 1978) or intense mixing (Masschelein 1982b). Others argued that bacterial inactivation was determined by primarily dissolved ozone (Finch and Smith 1991; Scaccia and Rosen 1978). Very little was known regarding the effect of gas-liquid mixing on inactivation of *C. parvum* oocysts or, indeed, on the mechanism of *C. parvum* inactivation by dissolved ozone.

The research objectives were first to demonstrate that efficient microorganism inactivation, of *C. parvum* oocysts in particular, could be achieved in a two-stage ozone contactor using a static mixer for gas-liquid mass transfer and rapid dissolution. The approach taken was to design and build an experimental static mixer contactor, and to measure inactivation of *C. parvum* oocysts and other microorganisms in carefully controlled challenge experiments. Static mixers create an intense hydrodynamic environment that not only promotes rapid ozone gas-liquid mass transfer, but may also enhance the rate of ozone inactivation of microorganisms (Bonnard et al. 1999; Zhu et al. 1989a). The second objective was, therefore, to investigate the effect of the hydrodynamic conditions of gas-liquid contact within the static mixer on microorganism inactivation. The intended goal was to understand the impact of the static mixer on microorganisms and to better define the role of this device for improving the reduction of microorganisms in an ozone contacting system.

## 12.2 FACTORS THAT DETERMINED MICROORGANISM INACTIVATION IN THE STATIC MIXER CONTACTOR

### 12.2.1 Effect of Turbulent Mixing on Mass Transfer and Microorganisms

In the experimental static mixer contactor, the seeded microorganisms were exposed to two extremes of hydrodynamic conditions of contact with ozone. The first phase involved very brief, but vigorous turbulent mixing with both gaseous and dissolved ozone within the mixing elements of the static mixer itself. In the second phase, the microorganisms were exposed to dissolved ozone under gentle mixing conditions within the reactive flow segment. The concept of the velocity gradient,  $G$ , and energy dissipation rate,  $\epsilon$ , have been used to quantify the intensity of turbulence in mixing processes in water treatment (Amirtharajah and O'Melia 1990). These concepts have been applied to the case of static mixers employed for mixing coagulation chemicals (Schulgen et al. 1996). Values of these hydrodynamic parameters were calculated for the experimental static mixer and are provided in Table 12-1. Details of the calculations are provided in Appendix H.

Table 12-1 Estimated hydrodynamic conditions within the static mixer.

Superficial Velocity $v_s$ (m/s)	<sup>1</sup> Contact Time (s)	<sup>2</sup> Pressure Drop $\Delta p$ (kPa)	Velocity Gradient $G$ (s <sup>-1</sup> )	Rate of Energy Dissipation $\epsilon$ (J/kg·s)	Kolmogoroff Mixing Scale $\eta$ ( $\mu\text{m}$ )
0.6	0.075	6	9,200	80	10
1.4	0.032	32	32,000	1000	5

<sup>1</sup>Contact time within the mixing elements of the static mixer.

<sup>2</sup>Estimated pressure drop based on measurement made during experiments.

The evidence from the experimental studies was that the level of turbulent shear stress induced by the velocity gradients within the static mixer was not sufficient to cause damage that resulted in a direct lethal affect. Nor was there any evidence that a brief initial exposure within the static mixer altered the integrity of these microorganisms and their resistance to dissolved ozone. This finding applied to all three microorganisms investigated, *B. subtilis* spores, *C. parvum* oocysts or *G. muris* cysts. With *G. muris* cysts, the evidence of an indirect effect was not conclusive due to poor cyst recovery and variation in the experimental outcomes, but a strong effect was indicated. At the two levels of static mixer superficial velocities,  $v_s$ , that were investigated, the microorganisms were exposed to estimated G values of 9 200 and 32 000  $s^{-1}$  and energy dissipation rates,  $e$ , of 80 and 1 000  $J/(kg \cdot s)$ . In comparison, G values for in-line mixers used for rapid mixing of coagulation chemicals in water treatment processes are typically between 3 000 and 5 000  $s^{-1}$  (Amirtharajah and O'Melia 1990). Kastanek and co-authors (1993) listed values of energy dissipation rates,  $e$ , determined for various types of gas-liquid mixing equipment, including bubble columns and stirred vessels, that were between 1.5 and 11  $J/(kg \cdot s)$ . The turbulent mixing conditions experienced by the microorganisms in this study were considerably greater than what would likely be encountered in water treatment practice.

The Kolmogoroff mixing length,  $\eta$ , is another parameter used in turbulent mixing theory to describe the scale of turbulence. The mixing length provides an estimate of the size of the smallest turbulent eddies that can be expected for a given energy dissipation rate. Given the estimated sizes of  $\eta$  in Table 12-1, it is evident why the mass transfer rates in static mixer systems are much more rapid than in bubble diffusers. Bubbles generated in conventional porous diffusers are the order of a few hundred  $\mu m$  or much greater (Zhou and Smith 2000). In the experimental static mixer, bubbles of this size would have been susceptible to size reduction by the shear stress induced by the comparatively small turbulent eddies that were established. Most microorganisms in drinking water, however, are much smaller than the bubbles generated by porous diffusers. *C. parvum* oocysts are approximately 3 to 5  $\mu m$  in size, and *G. muris* cysts are about 8 to 12  $\mu m$  in size. *B. subtilis* spores are even smaller, at about 1  $\mu m$  or less. Turbulent eddies of 5 and 10  $\mu m$  size (Table 12-1) are sufficient to generate very fine

bubbles and high gas-liquid mass transfer rates, but are not small enough to transmit turbulent shear stress to spores, and are probably not small enough to do to a significant extent for cysts and oocysts. In light of these estimates of the scale of turbulence, it is not surprising that brief contact within the static mixer did not result in direct physical damage to these microorganisms. Moreover, it is not likely that the intensity of mixing in conventional gas-liquid contacting equipment used in water treatment would be sufficient to cause physical damage to these types of microorganisms.

### **12.2.2 Relationship Between Mass Transfer and Microorganism Reduction**

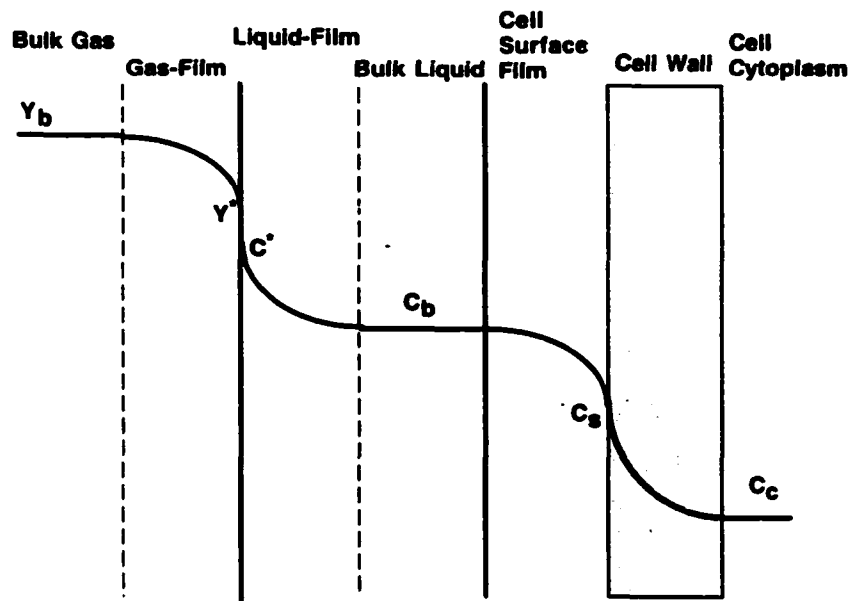
Zhu and co-workers (1989a) reported significant inactivation of *E. coli* in a static mixer system with a residence time of between 2 and 6 seconds. They further concluded from their experiments that the rate of *E. coli* inactivation was controlled primarily by the rate of gas-liquid mass transfer. Results obtained with the microorganisms used in the investigations described in this thesis suggested otherwise. It was demonstrated that inactivation of *B. subtilis* spores, *C. parvum* oocysts and *G. muris* cysts within the static mixer, was independent of both the mass transfer efficiency and the overall mass transfer rate. The rapid development of a dissolved ozone concentration in the static mixer and the bubble column (Figure 8-2) was indicative of the high rate of ozone gas-liquid mass transfer in the experimental ozone contactor. Measurable dissolved ozone concentrations were developed in the very brief (< 0.1 s) residence time within the static mixer. Most of the gaseous ozone was dissolved by the time the flowing water reached the inlet of the bubble column, after less than 3 s of total contact time. Despite the rapid mass transfer rate, there was no evidence of inactivation within the static mixer itself or of improved inactivation with subsequent dissolved ozone contact for any of the microorganisms studied.

The discrepancy between the results of this study and that of Zhu and co-workers (1989a) can be explained in terms of the relative rates of gas-liquid mass transfer, ozone reaction in solution and the microorganism inactivation processes. It is a well-established principle of chemical reaction engineering that, if the reaction between a dissolved gas and soluble substrate is sufficiently fast, the rate of gas-liquid mass transfer will control the overall rate of reaction in a heterogeneous gas-liquid reaction system. If, on the other

hand, the reaction is very slow, then the rate is determined by kinetics alone and mass transfer resistance has a little effect (Levenspiel, 1972). The principle can be extended to the case of the reaction between ozone and microorganisms. For a microorganism to be inactivated by ozone in a gas-liquid contactor, the ozone must first be transported from the bulk gas-phase to the bulk liquid-phase by diffusion through both gas and liquid films. The ozone must then diffuse through another film to the surface of the microorganism. The ozone then diffuses through the cell wall, spore coat or (oo)cyst wall, to the points of lethal effect, which may be targets within the protoplasm of the cell such as the cellular DNA. A recent study using SYTO-9<sup>®</sup> vital dyes suggested found that reduction of infectivity of oocysts exposed to ozone correlated with changes in permeability of the oocyst wall (Gyürék et al. 2001). This suggests that the sites of lethal effect with the oocysts, are structural constituents of the oocyst wall itself and not components of the protoplasm. Either way, the ozone must first diffuse through the oocyst wall to the critical sites. This multi-step, mass transfer-inactivation process is depicted at the top of Figure 12-1.

If the reactions at the sites of lethal effect within the cell interior or cell wall were very fast relative to the diffusion rates through the gas, liquid or cell wall films, mass transfer would tend to dominate the overall rate of microorganism inactivation. In this case, faster mass transfer, in either the gas or liquid phase, promoted by higher turbulent mixing levels would tend to result in greater microorganism inactivation in a given contacting volume. Similarly if the rate of ozone decomposition within the liquid was very fast, such that gas-liquid mass transfer was required to maintain the concentration of dissolved ozone in the bulk liquid, then the gas-liquid mass transfer rate would be seen to control inactivation. This may explain the findings of Zhu and co-workers (1989a) with *E. coli*. At the ozone concentrations used in their work, the time frame required for log levels inactivation of vegetative *E. coli* bacteria is on the order of a few seconds (Hunt and Marinas 1997; Zhou and Smith 1994) which is approximately the same time scale required for gas-liquid mass transfer. In addition, Zhu and co-workers (1989a) were exploring a wastewater system in which the rate of ozone decomposition was probably much greater than in the treated drinking water use in the presented study.

**CASE 1: TWO-PHASE MASS TRANSFER LIMITED**



**CASE 2: SINGLE-PHASE MICROORGANISM LIMITED**

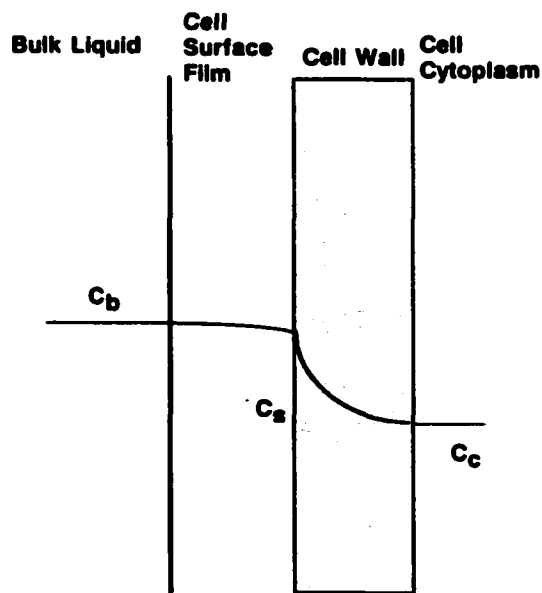


Figure 12-1 Depiction of ozone concentration profiles in microorganism inactivation processes for two physical cases.

As a result, the rates of microorganism inactivation and ozone decomposition were very fast relative to the gas-liquid mass transfer rate. Inactivation and decomposition occurred as quickly as the ozone was transferred from the gas to the liquid phase. In contrast, the time required for inactivation of the microorganisms used in the present study was much longer, on the order of minutes. This explains why no inactivation of these microorganisms was observed within the static mixer, despite the rapid gas-liquid mass transfer. A measurable effect of ozone on these microorganisms required extended contact with dissolved ozone in the reactive flow segment, after ozone dissolution was complete. As long as a sufficient dissolved ozone concentration was developed in the static mixer and bubble column, the overall rate of inactivation was unaffected by the gas-liquid mass transfer rate. The relatively low rate of ozone decomposition in the drinking water decreased the necessity for continuous gas-liquid mass transfer that would otherwise be required in order to maintain the required dissolved ozone concentration.

### **12.2.3 Effect of Dissolved Ozone and Mixing**

Microorganism inactivation in the experimental static mixer contactor was a function of the dissolved ozone concentration and residence time distribution. This was demonstrated conclusively for *B. subtilis* spores and *C. parvum* oocysts. In each of the challenges experiments with the static mixer contactor, the Reynold's number was constant at value of approximately 800. The seeded microorganisms were, therefore, exposed to dissolved ozone mostly under laminar flow conditions and with very little turbulent mixing or dissipation of energy. In comparison, the microorganisms in the batch reactor experiments were probably exposed to a greater mixing intensity by virtue of the magnetic stir bar (Note: mixing intensity in the batch reactors was not measured). The difference in mixing regimes, however, had no apparent effect on microorganism inactivation by the dissolved ozone. Both spore inactivation and oocyst inactivation in the contactor were accurately predicted based on kinetic models determined in well-stirred batch reactors. In the case of *B. subtilis* spores, the discrepancy between inactivation in the contactor and the batch reactors at intermediate  $C_{avg}t_b$  was explained in terms of a residence time effect. No such explanations were required for the case of *parvum* oocysts, because no discrepancy was observed.

These results suggest that the rate of microorganism inactivation in the reactive flow segment of the experimental contactor was not limited by the rate of mass transfer from the bulk liquid to the surface of the spores or oocysts. Rather, the rate of inactivation was controlled by processes that occurred within the spore or oocyst, such as diffusion through the cell wall or reaction at the sites of lethal effect. The scenario of a microorganism limited rate process is depicted at the bottom of Figure 12-1. In this figure, the concentration of dissolved ozone at the surface of the oocyst,  $C_s$ , is essentially the same as the concentration in the bulk liquid,  $C_b$ . The rate of inactivation is determined by the concentration of ozone in the bulk liquid. Two important points are illustrated by the comparison between microorganism inactivation in the contactor and the batch reactors. First, kinetic models of *B. subtilis* spore and *C. parvum* oocyst inactivation by ozone that were developed in well-stirred batch reactors should be valid for prediction of the rate of microorganism reduction in reactive flow segments in full-scale water treatment processes. Second, efforts to increase the rate of spore or oocyst inactivation by increasing the degree of turbulent mixing beyond that required for replacement of the ozone consumed in the inactivation reaction are not likely to be successful. These points will likely hold for any microorganism that has similar, or greater, resistance to ozone than *B. subtilis* spores or *C. parvum* oocysts.

### 12.3 ENGINEERING SIGNIFICANCE

Based on the experimental investigations and the previous discussion, it follows that, to achieve the most effective inactivation of ozone resistant pathogenic microorganisms like *C. parvum*, ozone contactors should be designed to create the optimum conditions for contact with dissolved ozone. These are:

1. generation of a sufficient dissolved ozone concentration; and
2. a residence time distribution behaviour that approaches that of perfect plug flow.

The role of the static mixer in improving microorganism inactivation, therefore, is primarily to serve as a means for rapidly and efficiently dissolving the gaseous ozone. Once the ozone is dissolved and the off-gas separated, efficient microorganism inactivation can be realized by contact with dissolved ozone in a well-designed reactive

flow segment. When integrated into a two-stage contactor design, static mixers can, therefore, be effectively exploited to achieve efficient microorganism reduction. The fact that inactivation of *B. subtilis* spores and *C. parvum* oocysts in the static mixer contactor was nearly equivalent to that of a perfect plug flow contactor, demonstrated this point. Other gas-liquid contacting devices that provide rapid dispersal and dissolution of ozone, such as venturi injectors, may potentially perform the same role as static mixers in the two-stage contactor design.

From a process design perspective, another advantage of a two-stage ozone contactor based on a static mixer is that the mass transfer process is decoupled from the microorganism inactivation process. In the experimental investigations, ozone transfer efficiency in the static mixer contactor was demonstrated to be independent of microorganism inactivation. The same level of inactivation was achieved at either high or low ozone mass transfer efficiency provided that the conditions of dissolved ozone contact were the same. In conventional fine bubble-diffuser contactors, a relatively large physical volume is required for ozone dissolution. Economic and space constraints often dictate that mass transfer and dissolved ozone contact be carried out in the same vessel. If the contactor consists of both gas dispersion basins and reactive flow basins, the situation may be improved to some degree, however the physical design of the latter will still be dictated by the design of the former. A much smaller residence time will be required for ozone dissolution with a static mixer, therefore, it may be much easier to consider the design of the ozone contactor as two distinct unit operations. By separating the contactor into ozone dissolution and dissolved ozone contact unit operations, design flexibility will be increased and both operations can be optimized independently. In a full-scale static mixer contactor, mass transfer requirements, economics of ozone generation and pressure drop restrictions will dictate the design of the ozone dissolution unit operation. The design of the dissolved ozone contacting unit operation, the reactive flow segment, will be dictated primarily by the microorganism inactivation requirements. The two unit operations will be linked by the dissolved ozone concentration.

## 12.4 APPLICATION AT LARGER SCALES

The two-stage ozone contactor design was demonstrated in the laboratory using a relatively small-scale model contactor. Another potential advantage of the two-stage design is the potential for straightforward and reliable scale-up. Separation of ozone dissolution and dissolved ozone contact into two unit operations means that the hydrodynamic design of the reactive flow segment need not be restricted by gas-liquid mass transfer requirements. For the reactive flow segment, the primary scale-up variables are the mean residence time and the residence time distribution. The reactive flow segment must provide sufficient contact time with a residence time that approaches plug flow, and with little opportunity for flow short-circuiting. The simulations of Chapter 3 suggested that a macro-mixing regime that was equivalent to 20 CFSTRs in series (i.e.  $J = 20$ ) was adequate for efficient inactivation of *C. parvum*. At  $J$  values of less than 10, the *C. parvum* inactivation was sensitive to the value of  $J$  and degree of back-mixing in the contactor.

The few published studies on the dispersal and dissolution of the ozone in static mixer systems suggest that mass transfer in static mixers can be modeled in terms of physical variables (Grosz-Röll et al. 1982; Martin and Galey 1994; Richards and Fleischman 1975). In principle, therefore, ozone mass transfer in static mixers is scale-able. Proprietary information on mixer performance developed by the manufacturers of static mixer equipment may also be available to aid in scale-up. As a parenthetical note, the manufacturer of the static mixer used in this experimental work, Sulzer, was able to provide estimates of the ozone mass transfer efficiency for various sizes and configurations of the SMV static mixer. Static mixers themselves have a relatively small construction footprint, and are amenable to modular installations. This feature may facilitate applications in water treatment facilities treating large volumes of water. In side-stream injection, ozonized gas is contacted with only a fraction of the total water flow in the treatment plant in a static mixer. This side-stream is then combined with the main water flow. This design option can be exploited for scale-up of static mixer installations and to address issues of turndown ratio.

Examples of the application of static mixers for dissolution of ozone in water treatment are available. Chandrakanth and co-workers (2000) described an evaluation of static mixers in water treatment plants at both pilot- and full-scale. Four examples of full-scale installations of static mixers for ozone dissolution in water treatment plants in the UK were used as part of the study, though few details were provided. According to the authors, these ozonation installations were intended primarily for oxidation of pesticides. Martin and co-workers (1995) described a  $84 \times 10^6$  L/d installation that used side-stream injection of ozone with static mixers. In 2000, the Greater Vancouver Regional District (GVRD) commissioned an ozonation facility at their Coquitlam location (Reil 2001). The facility was comprised of a unique side-stream ozone injection system that made use of static mixers. The duration of gas-liquid contact was less than 12 seconds, including off-gas separation. Ozonated water flowed into a 3 m ID  $\times$  1000 m long stainless steel pipeline contactor that provided 10 minutes of contact time between microorganisms and the ozonated water.

This GVRD system was remarkably similar in concept to the two-stage contactor design described in Figure 4-1 and, unlike previous ozone static mixer installations, was designed primarily to provide protection against *C. parvum*. No hydrodynamic characterization or microorganism inactivation assessments were done (at least to the author's knowledge). The hydrodynamic performance of the GVRD contactor was, therefore, estimated based on the physical dimensions and operating conditions. Details of these calculations were provided in Appendix I. The Reynolds number in the pipeline was calculated to be approximately  $5 \times 10^6$ , which indicates fully-developed turbulent flow. Using information provided for turbulent flow in pipes (Levenspiel 1972), the dispersion number of the pipeline was estimated to be  $1 \times 10^3$  or equivalent to 80 CFSTRs in series (i.e.  $J = 80$ ). The hydrodynamic performance of this contactor for *C. parvum* inactivation was, therefore, likely to approach that of a perfect plug flow contactor and very efficient inactivation was expected. The GVRD ozone contactor demonstrated the feasibility of the two-stage ozone contactor design concept at full-scale with a real-world example. The design challenge in most situations will be to determine how to integrate a pipe-line contactor, or one with equivalent hydrodynamic performance, into a treatment facility given head loss, space and economic constraints.

## 13 CONCLUSIONS

Static mixers have been proposed, and have been used to a limited extent, as alternatives to conventional fine bubble diffusers contactors for dissolution of ozone in drinking water. An experimental investigation was carried out to help determine how static mixers can be employed to improve the ozonation process for the particular case of reduction of pathogenic microorganisms like *Giardia lamblia* and *Cryptosporidium parvum*. Static mixers have also been proposed as a means of enhancing the rate of microorganism inactivation by ozone, though no work had been done to test this hypothesis against encysted parasites like *G. lamblia* or *C. parvum*. A theoretical analysis demonstrated that inactivation of *C. parvum* in a continuous flow dissolved ozone contactor will be maximized by improving the approach to plug flow and by minimizing micro-mixing. An experimental study involving a small-scale static mixer ozone contactor was carried out to investigate these questions. The main conclusions of the study are listed below.

1. Static mixers can be employed to improve the design of ozone contactors for the reduction of pathogenic microorganisms in drinking water treatment. The main role of the static mixer is to serve as a means for rapidly and efficiently dissolving ozone into the water. By integrating a static mixer into a two-stage ozone contactor design that consists of an ozone dissolution stage followed by dissolve ozone contact stage, an ozone contactor can be designed to mimic a perfect plug flow contactor. Very efficient inactivation of *Cryptosporidium parvum* can, thereby, be achieved. This approach to contactor design represents an improvement over conventional fine bubble diffuser ozone contactors.
2. There was no evidence that measurable inactivation of *Bacillus subtilis* spores, *Cryptosporidium parvum* oocysts and *Giardia muris* cysts occurred within the static mixer itself. Nor was there evidence that inactivation of these microorganisms by dissolved ozone was improved or hindered, or affected in any way, by initial vigorous

mixing and gas-liquid contact within the static mixer. Inactivation was determined exclusively by the conditions of contact with dissolved ozone, namely the dissolved ozone concentration, the mean residence time and the residence time distribution.

3. In the experimental contactor, there was no evidence that inactivation of *C. parvum* oocysts and *B. subtilis* spores was controlled by mixing or mass transfer. This includes mass transfer of ozone between the gas and liquid phases, or between the bulk liquid phase and the oocyst or spore surface. This finding supports the use of kinetic models of microorganism inactivation developed in small, well-stirred batch reactors for predicting inactivation in full-scale water treatment processes.
4. The efficiency of ozone dissolution in a static mixer ozone contactor was determined by the hydrodynamic conditions of gas-liquid contact, including the superficial velocity and the gas-liquid flow rate ratio. Dissolution efficiency was greatest at the highest velocities and the lowest gas-liquid flow rate ratio tested. Ozone dissolution, however, was not complete in the static mixer. Additional ozone transfer occurred in the piping and a bubble column downstream of the static mixer. For true optimization of the ozone dissolution unit operation, these components of the contactor should be considered in conjunction with the static mixer during system design.
5. Spores of the aerobic bacterium *B. subtilis* may serve as useful indicators of the efficiency of an ozone contactor for microorganism reduction. A kinetic model of spore inactivation by ozone, which was applicable at temperatures ranging from 3 to 22°C, and at pH between 6 and 8, was developed. Spore inactivation was found to be only slightly dependent on pH. Although the spores shared a similar resistance to ozone as *C. parvum* oocysts, the shape of the inactivation curves of the two microorganisms differed considerably. It is not recommended that inactivation of *C. parvum* oocysts be inferred directly from measured inactivation of *B. subtilis* spores.

## 14 RECOMMENDATIONS

In terms of engineering design, the following recommendations are made:

1. In order to optimize conditions for inactivation of *Cryptosporidium parvum*, ozone contactor design effort should be concentrated on aspects of contact with dissolved ozone. Most importantly, contactors should be designed to maximize the approach to plug flow. A two-stage ozone contactor design, using static mixers or other devices for rapid and efficient dissolution of ozone, is a recommended alternative to conventional fine bubble diffuser contacting basins. There is no reason to believe that increasing the intensity of mixing in an ozone contactor will improve the rates of inactivation. Such measures may, in fact, serve to decrease performance if they contribute to back-mixing or micro-mixing and are not recommended.
2. If static mixers are selected as the means for ozone dissolution, designers should consider the contribution of other components of the ozone contactor to ozone transfer efficiency. This includes the piping at the exit of the static mixer, and any downstream contacting vessel in which additional gas-liquid contact takes place.

In terms of future research, the following recommendations are made:

3. This study focused primarily on the effects of the static mixer and the hydrodynamics of gas-liquid contact on microorganism inactivation by ozone. Ozone system design may be subject additional constraints that are related to other components of the water of other treatment objectives. Future research work should be directed at determining how the hydrodynamics within the static mixer affects aspects such as formation of ozonation by products such as bromate and aldehydes, and decomposition of natural organic matter and formation of assimilable organic carbon (AOC).
4. The extremely rapid mass transfer properties of the static mixer may provide advantages for other beneficial uses of ozone in water treatment for which mass

transfer rates are important. These include oxidation and destruction of organic micro-pollutants, oxidation chlorination process by-product pre-cursors and enhanced coagulation. Research investigations into the use of static mixers for improving conversion or reaction selectivity is recommended.

5. Relatively few studies have been published in which the ozone dissolution in static mixers has been investigated from the point of the view of mass transfer theory. The work in Chapter 8 of this thesis was mostly empirical in nature. One of the conclusions, however, was that other components of the contacting system contribute significantly to overall mass transfer efficiency. Further fundamental work should be done better understand the mass transfer that occurs within the static mixer and in the various downstream system components. One approach might be to use laser doppler anemometry to characterize the bubble size distributions within the static mixer as has been used by others to study conventional bubble columns (Zhou and Smith 2000).

## 15 REFERENCES

- Ahmad, M. and S. Farooq. 1984. Influence of Bubble Sizes on Ozone Solubility Utilization and Disinfection. *Water Science and Technology*, 17:1081-1090.
- Amirtharajah, A. and C.R. O'Melia. 1990. Coagulation Processes: Destablization, Mixing and Flocculation. In *Water Quality and Treatment*. Edited by F. Pontius. 1194 pp. McGraw-Hill, New York, NY.
- Amy, G., C. Douville, B. Daw, J. Sohn, C. Galey, D. Gatel and J. Cavard. 2000. Bromate Formation Under Ozonation Conditions to Inactivate *Cryptosporidium*. *Water Science and Technology*, 41(7):61-66.
- APHA AWWA WEF. 1992. *Standard Methods for the Examination of Water and Wastewater*. 18th edition. Edited by Greenberg, A. E., Clesceri, L. S. and Eaton, A. D. American Public Health Association, Washington, DC.
- Bader, H. and J. Hoigné. 1981. Determination of Ozone in Water by the Indigo Method. *Water Research*, 15:449-456.
- Bader, H. and J. Hoigné. 1982. Determination of Ozone in Water by the Indigo Method: A Submitted Standard Method. *Ozone: Science and Engineering*, 4:169-176.
- Barbeau, B., L. Boulos, R. Desjardins, J. Coallier, M. Prévost, M. and D. Duchesne. 1997. A Modified Method for the Enumeration of Aerobic Spore-Forming Bacteria. *Canadian Journal of Microbiology*, 43(10):976-980.
- Bellamy, W. 1995. *Full-Scale Ozone Contactor Study*. AWWA Research Foundation and the American Water Works Association, Denver, CO, 198 p.

- Bellamy, W., K. Carlson, D. Pier, J. Ducoste and M. Carlson. 2000. Determining Disinfection Needs. *Journal of the American Water Works Association*, 92(5):44-52.
- Bellamy, W., G.R. Finch, C.N. Haas and J. Oxenford. 1997. *The Integrated Disinfection Design Framework for Potable Water Disinfection*. AWWA Research Foundation and the American Water Works Association, Denver, CO, 68 p.
- Belosevic, M. and G.M. Faubert. 1983. *Giardia muris*: Correlation Between Oral Dosage, Course of Infection, and Trophozoite Distribution in the Mouse Small Intestine. *Experimental Parasitology*, 56:93-100.
- Belosevic, M., G.M. Faubert, E. Skamene and J.D. MacLean. 1984. Susceptibility and Resistance of Inbred Mice to *Giardia muris*. *Infection and Immunity*, 44:282-286.
- Black, E.K., G.R. Finch, R. Taghi-Kilani and M. Belosevic. 1996. Comparison of Assays for *Cryptosporidium parvum* oocysts Viability After Chemical Disinfection. *FEMS Microbiology Letters*, 135:187-189.
- Bonnard, R., C. Adrien, C. de Traversay and F. Luck. 1999. Static Mixer as a Disinfectant Process? In *Proceedings of the 14th Ozone World Congress*, Volume 2. International Ozone Association, Stamford, CT, pp. 251-261.
- Botzenhart, K., G.M. Tarcson and M. Ostruschka. 1993. Inactivation of Bacteria and Coliphages by Ozone and Chlorine Dioxide in a Continuous Flow Reactor. *Water Science and Technology*, 27(3-4):363-370.
- Bourne, J., R., J. Lenzner and S. Petrozzi. 1992. Micromixing in Static Mixers. An Experimental Study. *Ind Eng Chem Res*, 31(4):1216-1222.

- Box, G.E.P., W.G. Hunter and J.S. Hunter. 1978. *Statistics for Experimenters*. John Wiley & Sons, New York, NY, 653 p.
- Broadwater, W.T., R.C. Hoehn and P.H. King. 1973. Sensitivity of Three Selected Bacterial Species to Ozone. *Applied Microbiology*, 26(3):391-393.
- Bukhari, Z., T.M. Hargy, J.R. Bolton, B. Dussert and J.L. Clancy. 1999. Medium-Pressure UV for Oocyst Inactivation. *Journal of the American Water Works Association*, 91(3):86-94.
- Bukhari, Z., M.M. Marshall, D.G. Korich, C.R. Fricker, H.V. Smith, J. Rosen and J.L. Clancy. 2000. Comparison of *Cryptosporidium parvum* Viability and Infectivity Assays Following Ozone Treatment of Oocysts. *Applied and Environmental Microbiology*, 66(10):4598.
- Burleson, G.R., T.M. Murray and M. Pollard. 1975. Inactivation of Viruses and Bacteria by Ozone, With and Without Sonication. *Applied Microbiology*, 29(3):340-344.
- Campbell, A.T., L.J. Robertson, R. Anderson, H.V. Smith and J.F.W. Parker. 1997. Viability of *Cryptosporidium* Oocysts: Assessment Following Disinfection with Ozone. In *Proceedings of the International Symposium on Waterborne Cryptosporidium*, American Water Works Association, Denver, CO. pp 97-102.
- Cerf, O. 1977. A Review: Tailing of Survival Curves of Bacterial Spores. *Journal of Applied Bacteriology*, 42:1-19.
- Chandrakanth, M., M. Prévost, G. Finch, S. Craik and J. Leparc. 2000. Evaluation of Static Mixers at Bench- and Pilot-scale for Enhanced Ozone Dissolution and Inactivation of *Bacillus subtilis* in Water Treatment. In *Proceedings of the American Water Works Association 2000 Annual Conference*. American Water Works Association. Denver, CO.

- Chauret, C., K. Nolan, P. Chen, S. Springthorpe and S. Sattar. 1998. Aging of *Cryptosporidium parvum* Oocysts in River Water and Their Susceptibility to Disinfection by Chlorine and Monochloramine. *Canadian Journal of Microbiology*, 44(12):1154-1160.
- Chelkowska, K., D. Grasso, I. Fábíán and G. Gordon. 1992. Numerical Simulations of Aqueous Ozone Decomposition: Comparison of Mechanisms. *Ozone: Science and Engineering*, 14(1):33-49.
- Chick, H. 1908. An Investigation of the Laws of Disinfection. *Journal of Hygiene (Cambridge)*, 8:92-158.
- Choe, K. 1998. Ozone Inactivation of *Bacillus cereus* Spores in Ozone Demand Free Water. Master of Science Thesis, University of Alberta, Edmonton, Alberta, 84 p.
- Clark, D.P. 1999. New Insights into Human Cryptosporidiosis. *Clinical Microbiology Reviews*, 12(4):554-563.
- Clark, R.M., E.W. Rice, B.K. Pierce, C.H. Johnson and K.R. Fox. 1994. Effect of Aggregation on *Vibrio cholerae* Inactivation. *Journal of Environmental Engineering*, 120(4):875-887.
- Coffey, B.M. and J.T. Gramith. 1994. Demonstration-Scale Evaluation of Ozone Disinfection Calculation Methods. In *IOA, Pan American Committee Meeting*. International Ozone Association, Stamford, CT.
- Coin, L., C. Gomella, C. Hannoun and J.-C. Trimoreau. 1967. Inactivation par l'Ozone du Virus de la Poliomyélite Présent dans les Eaux. *La Presse Médicale*, 75(38):1883-1884.

- Coin, L., C. Hannoun and C. Gomella. 1964. Inactivation par l'Ozone du Virus de la Poliomyélite Présent dans les Eaux. *La Presse Médicale*, 72(37):2153-2156.
- Cox, F.E.G. 1993. *Modern Parasitology*. 2 nd edition. Blackwell Scientific Publications. Oxford, UK, 276 p.
- Craik, S.A., G.R. Finch, J.R. Bolton and M. Belosevic. 2000. Inactivation of *Giardia muris* Cysts Using Medium-Pressure Ultraviolet Radiation in Filtered Drinking Water. *Water Research*, 34(18):4325-4332.
- Craik, S.A., G.R. Finch, J.R. Bolton and M. Belosevic. 2001. Inactivation of *Cryptosporidium parvum* Cysts Using Medium-Pressure Ultraviolet Radiation in Filtered Drinking Water. *Water Research*, 35(6):1387-1398.
- Craun, G.F. 1990. Waterborne Giardiasis. In *Giardiasis*. Edited by E. A. Meyer. Volume 3, Elsevier, Amsterdam, pp. 267-293.
- Craun, G.F., S.A. Hubbs, F. Frost, R.L. Calderon and S.H. Via. 1998. Waterborne Outbreaks of Cryptosporidiosis. *Journal of the American Water Works Association*, 90(9):81-91.
- Crawford, F.G. and S.H. Vermund. 1988. Human Cryptosporidiosis. *CRC Critical Reviews in Microbiology*, 16(2):113-159.
- Current, W.L. and L.S. Garcia. 1991. Cryptosporidiosis. *Clinical Microbiology Reviews*, 4(3):325-358.
- Dahi, E. 1976. Physicochemical Aspects of Disinfection of Water by Means of Ultrasound and Ozone. *Water Research*, 10:677-684.

- Dahi, E. and E. Lund. 1980. Steady State Disinfection of Water by Ozone and Sonozone. *Ozone: Science and Engineering*, 2:13-23.
- D'Antonio, R.G., R.E. Winn, J.P. Taylor, T.L. Gustafson, W.L. Current, M.M. Rhodes, G.W.J. Gary and R.A. Zajac. 1985. A Waterborne Outbreak of Cryptosporidiosis in Normal Hosts. *Annals of Internal Medicine*, 103(6):886-888.
- Daugherty, R.L. and J.B. Franzini. 1977. *Fluid Mechanics With Engineering Applications*. McGraw-Hill, New York, NY, 564 p.
- Davidson, R.A. 1990. Treatment of Giardiasis: The North American Perspective. In *Giardiasis* Volume 3. Edited by E. A. Meyer. Elsevier, Amsterdam, pp. 325-334.
- de Graaf, D.C., E. Vanopdenbosch, L.M. Ortega Mora, H. Abbassi and J.E. Peeters. 1999. A Review of the Importance of Cryptosporidiosis in Farm Animals. *International Journal For Parasitology*, 29(8):1269-1287.
- de Traversay, C., J. Baron, C. Adrien, P. Brasseur and J.-C. Joret. 1999. Inactivation of *Cryptosporidium parvum* with Ozone and Ozone Hydrogen Peroxide. In *Proceedings of the 14th Ozone World Congress Dearborn* Volume 1, International Ozone Association, Stamford, CT, pp. 13-19.
- Di Giovanni, G.D., F.H. Hashemi, N.J. Shaw, F.A. Abrams, M.W. LeChevallier and M. Abbaszadegan. 1999. Detection of Infectious *Cryptosporidium parvum* Oocysts in Surface and Filter Backwash Water Samples by Immunomagnetic Separation and Integrated Cell Culture-PCR. *Applied and Environmental Microbiology*, 65(8):3427-3432.
- Do-Quang, Z., C.C. Ramirez and M. Roustan. 2000a. Influence of Geometrical Characteristics and Operating Conditions on the Effectiveness of Ozone

- Contacting in Fine-Bubbles Conventional Diffusion Reactors. *Ozone: Science and Engineering*, 22(4):369-378.
- Do-Quang, Z., M. Roustan and J.P. Duguet. 2000b. Mathematical Modeling of Theoretical *Cryptosporidium* Inactivation in Full-Scale Ozonation Reactors. *Ozone: Science and Engineering*, 22(1):99-111.
- DuPont, H.L., C.L. Chappell, C.R. Sterling, P.C. Okhuysen, J.B. Rose and W. Jakubowski. 1995. The Infectivity of *Cryptosporidium parvum* in Healthy Volunteers. *New England Journal of Medicine*, 332(13):855-859.
- Emerick, R.W., F.J. Loge, T. Ginn and J.L. Darby. 2000. Modeling the Inactivation of Particle-Associated Coliform Bacteria. *Water Environment Research*, 72(4):432-438.
- Ernest, J.A., B.L. Blagburn, D.S. Lindsay and W.L. Current. 1986. Infection Dynamics of *Cryptosporidium parvum* (Apicomplexa: Cryptosporiidae) in Neonatal Mice (*Mus musculus*). *Journal of Parasitology*, 72(5):796-798.
- Facile, N., B. Barbeau, M. Prevost and B. Koudjonou. 2000. Evaluating Bacterial Aerobic Spores as a Surrogate for *Giardia* and *Cryptosporidium* Inactivation by Ozone. *Water Research*, 34(12):3238-3246.
- Farooq, S., E.S.K. Chian and R.S. Engelbrecht. 1977a. Basic Concepts in Disinfection with Ozone. *Journal of the Water Pollution Control Federation*, 49:1818-1831.
- Farooq, S., R.S. Engelbrecht and E.S.K. Chian. 1978. Process Considerations in Design of Ozone Contactor for Disinfection. *Journal of the Environmental Engineering Division, Proceedings of the American Society of Civil Engineering*, 104(E5):835-847.

- Farooq, S., R.S. Englebrecht and E.S.K. Chian. 1977b. Influence of Temperature and U.V. Light on Disinfection With Ozone. *Water Research*, 11:737-741.
- Fayer, R. editor. 1997. *Cryptosporidium and Cryptosporidiosis*. CRC Press, Inc., Boca Raton, FL, 251 p.
- Fayer, R., J.M. Trout and M.C. Jenkins. 1998. Infectivity of *Cryptosporidium parvum* Oocysts Stored in Water at Environmental Temperatures. *Journal of Parasitology*, 84(6):1165-1169.
- Feely, D.E., D.V. Holberton and S.L. Erlandsen. 1990. The Biology of *Giardia*. In *Giardiasis* Volume 3. Edited by E. A. Meyer. Elsevier, Amsterdam, pp. 11-49
- Fetner, R.H. and R.S. Ingols. 1956. A Comparison of the Bactericidal Activity of Ozone and Chlorine Against *Escherichia coli* at 1°C. *Journal of General Microbiology*, 15:381-385.
- Filice, F.P. 1952. Studies on the Cytology and Life History of a *Giardia* from the Laboratory Rat. *University of California Publications in Zoology*, 57:53-146.
- Finch, G.R. and E.K. Black. 1994. Chemical Inactivation of *Cryptosporidium parvum* in Drinking Water. In *Critical Issues in Water and Wastewater Treatment, Proceedings of the 1994 National Conference on Environmental Engineering*. Edited by J. N. Ryan and M. Edwards. American Society of Civil Engineers. New York, NY. pp. 42-49.
- Finch, G.R., E.K. Black, L. Gyürék and M. Belosevic. 1993a. Ozone Inactivation of *Cryptosporidium parvum* in Demand-Free Phosphate Buffer Determined by In Vitro Excystation and Animal Infectivity. *Applied and Environmental Microbiology*, 59(12):4203-4210.

- Finch, G.R., E.K. Black, L. Gyürék and M. Belosevic. 1994. *Ozone Disinfection of Giardia and Cryptosporidium*. AWWA Research Foundation and the American Water Works Association, Denver, CO, 56 p.
- Finch, G.R., E.K. Black and L.L. Gyürék. 1995. Ozone and Chlorine Inactivation of *Cryptosporidium*. In *Proceedings of the American Water Works Association Water Quality Technology Conference*. American Water Works Association, Denver, CO, pp. 1303-1318.
- Finch, G.R., E.K. Black, C.W. Labatiuk, L. Gyürék and M. Belosevic. 1993b. Comparison of *Giardia lamblia* and *Giardia muris* Cyst Inactivation by Ozone. *Applied and Environmental Microbiology*, 59(11):3674-3680.
- Finch, G.R. and K. Choe. 1999. Using *Bacillus* Spores as a Surrogate for Ozone Inactivation of *Cryptosporidium*. In *Proceedings of the 14th Ozone World Congress*, Volume 1. International Ozone Association, Stamford, CT, pp. 35-42.
- Finch, G.R., C.W. Daniels, E.K. Black, F.W. Schaefer, III and M. Belosevic. 1993c. Dose-Response of *Cryptosporidium parvum* in Outbred, Neonatal CD-1 Mice. *Applied and Environmental Microbiology*, 59(11):3661-3665.
- Finch, G.R. and N. Fairbairn. 1991. Comparative Inactivation of Poliovirus Type 3 and MS2 Coliphage in Demand-Free Buffer Using Ozone. *Applied and Environmental Microbiology*, 57(11):3121-3126.
- Finch, G.R., L.L. Gyürék, L.R.J. Liyanage and M. Belosevic. 1997. *Effect of Various Disinfection Methods on the Inactivation of Cryptosporidium*. AWWA Research Foundation and the American Water Works Association, Denver, CO, 66 p.

- Finch, G.R., C.W. Labatiuk, R.D. Helmer and M. Belosevic. 1992. *Ozone and Ozone-Peroxide Disinfection of Giardia and Viruses*. AWWA Research Foundation and the American Water Works Association, Denver, CO, 120 p.
- Finch, G.R. and H. Li. 1999. Inactivation of *Cryptosporidium* at 1°C using Ozone or Chlorine Dioxide. *Ozone: Science and Engineering*, 21(5):477-486.
- Finch, G.R. and D.W. Smith. 1991. Pilot-Scale Evaluation of the Effects of Mixing on Ozone Disinfection of *Escherichia coli* in a Semi-Batch Stirred Tank Reactor. *Ozone: Science and Engineering*, 13(5):593-605.
- Finch, G.R., D.W. Smith and M.E. Stiles. 1988. Dose-Response of *Escherichia coli* in Ozone Demand-Free Phosphate Buffer. *Water Research*, 22(12):1563-1570.
- Garber, L.P., M.D. Salman, H.S. Hurd, T. Keefe and J.L. Schlater. 1994. Potential risk factors for *Cryptosporidium* infection in dairy calves. *Journal of the American Veterinary Medical Association*, 205(1):86-91.
- Gard, S. 1957. Chemical Inactivation of Viruses. In *CIBA Foundation Symposium on the Nature of Viruses*. Edited by G. E. W. Wolstenholme and E. C. P. Millar. J. & A. Churchill Ltd., London, pp. 123-146.
- Glaze, W.H. 1987. Drinking-Water Treatment with Ozone. *Environmental Science and Technology*, 21(3):224-230.
- Glaze, W.H. 1990. Chemical Oxidation. In *Water Quality and Treatment*, Fourth Edition. Edited by F. W. Pontius. McGraw-Hill, New York, NY, pp. 747-779
- Goepfert, J.M., W.M. Spira and H.U. Kim. 1972. *Bacillus cereus*: Food Poisoning Organism. A Review. *J. Milk Food Technol.*, 35(4):213-227.

- Gordon, G., R.D. Guaw, M. Yuko, B. Walters and B. Bubnis. 2000. Using Indigo Absorbance to Calculate the Indigo Sensitivity Coefficient. *Journal of the American Water Works Association*, 92(12):96-107.
- Gordon, G., G.E. Pacey, W.J. Cooper and R.G. Rice. 1988. Current State-of-the-Art Measurements of Ozone in the Gas Phase and in Solution. *Ozone: Science and Engineering*, 10:353-366.
- Grasso, D. and W.J. Weber. 1989. Mathematical Interpretation of Aqueous-Phase Ozone Decomposition Rates. *Journal of Environmental Engineering*, 115(3):541-559.
- Grosz-Röll, F., J. Bättig and F. Moser. 1982. Gas/Liquid Mass Transfer With Static Mixer Units. In *Fourth European Conference on Mixing*. BHRA Fluid Engineering, Cranfield, Bedford, England, pp. 225-236.
- Gyürek, L.L. and G.R. Finch. 1998. Modeling Water Treatment Chemical Disinfection Kinetics. *Journal of Environmental Engineering*, 124(9):783-793.
- Gyürek, L.L., G.R. Finch and M. Belosevic. 1997. Modeling Chlorine Inactivation Requirements of *Cryptosporidium parvum* Oocysts. *Journal of Environmental Engineering*, 123(9):865-875.
- Gyürek, L.L., H. Li, M. Belosevic and G.R. Finch. 1999. Ozone Inactivation Kinetics of *Cryptosporidium parvum* in Phosphate Buffer. *Journal of Environmental Engineering*, 125(10):913-924.
- Gyürek, L.L., N.F. Nuemman, G.R. Finch and M. Belosevic. 2001. Comparison Between Animal Infectivity and Nucleic Acid Staining for Determination of Viability of Ozone-Inactivated *Cryptosporidium parvum* Oocysts. *Ozone: Science and Engineering*, 23(1):1-13.

- Haas, C.N. 1980. A Mechanistic Kinetic Model for Chlorine Disinfection. *Environmental Science and Technology*, 14(3):339-340.
- Haas, C.N. 1981. Rational Approaches in the Analysis of Chemical Disinfection Kinetics. In *Chemistry in Water Reuse*. Edited by W. J. Cooper. Volume 1. Ann Arbor Science, Ann Arbor, MI, pp. 381-399.
- Haas, C.N. 1988. Micromixing and Dispersion in Chlorine Contact Chambers. *Environmental Technology Letters*, 9:35-44.
- Haas, C.N. 1990. Disinfection. In *Water Quality and Treatment*, Fourth Edition. Edited by F. Pontius. McGraw-Hill, New York, NY, pp. 877-932.
- Haas, C.N., C.S. Crockett, J.B. Rose, C.P. Gerba and A.M. Fazil. 1996. Assessing the Risk Posed by Oocysts in Drinking Water. *Journal of the American Water Works Association*, 88(9):131-136.
- Haas, C.N., M.S. Heath, J. Jacangelo, J. Joffe, U. Anmangandla, J.C. Hornberger and J. Glicker. 1995. *Development and Validation of Rational Design Methods of Disinfection*. AWWA Research Foundation and the American Water Works Association, Denver, CO, 43 p.
- Haas, C.N. and B. Heller. 1990. Kinetics of Inactivation of *Giardia lamblia* by Free Chlorine. *Water Research*, 24(2):233-238.
- Haas, C.N. and J. Joffe. 1994. Disinfection Under Dynamic Conditions - Modification of Hom Model for Decay. *Environmental Science and Technology*, 28(7):1367-1369.

- Haas, C.N., J. Joffe, M. Heath, J. Jacangelo and U. Anmangandla. 1998. Predicting Disinfection Performance in Continuous Flow Systems From Batch Disinfection Kinetics. *Water Science and Technology*, 38(6):171-179.
- Haas, C.N. and S.B. Karra. 1984a. Kinetics of Microbial Inactivation by Chlorine - I. Review of Results in Demand-free Systems. *Water Research*, 18(11):1443-1449.
- Haas, C.N. and S.B. Karra. 1984b. Kinetics of Microbial Inactivation by Chlorine - II. Kinetics in the Presence of Chlorine Demand. *Water Research*, 18(11):1451-1454.
- Hall, R.M. and M.D. Sobsey. 1993. Inactivation of Hepatitis A Virus And MS2 By Ozone And Ozone-Hydrogen Peroxide In Buffered Water. *Water Science and Technology*, 27(3/4):371-378.
- Hamelin, C. and Y.S. Chung. 1974. Optimal Conditions for Mutagenesis by Ozone in *Escherichia coli* K12. *Mutation Research*, 24:271-279.
- Harakeh, M. and M. Butler. 1984. Inactivation of Human Rotavirus, SA11 and Other Enteric Viruses in Effluent by Disinfectants. *Journal of Hygiene (Cambridge)*, 93:157-163.
- Harakeh, M.S. and M. Butler. 1985. Factors Influencing the Ozone Inactivation of Enteric Viruses in Effluent. *Ozone: Science and Engineering*, 6:235-243.
- Harris, J.R. and F. Petry. 1999. *Cryptosporidium parvum*: Structural Components of the Oocyst Wall. *Journal of Parasitology*, 85(5):839-849.
- Hart, E.J., K. Sehested and J. Holcman. 1983. Molar Absorptivities of Ultraviolet and Visible Bands of Ozone in Aqueous Solutions. *Analytical Chemistry*, 55:46-49.

- Heathcote, G.R. and B.E. Drage. 1995. Development of an ozone disinfection contactor using a physical scale model. *Ozone: Sci. Eng.*, 17(1):15-24.
- Heindel, H.L., S.A. Hardy, A. Amirtharajah and M.J. Arrowood. 1999. Disinfection of *Cryptosporidium parvum* With Static Mixers. In *Proceedings of the American Water Works Association Water Quality and Technology Conference*. American Water Works Foundation, Denver, CO.
- Henry, D.J. and E.M. Freeman. 1995. Finite Element Analysis and T-10 Optimization of Ozone Contactors. *Ozone Science And Engineering*, 17(6):587-606.
- Herbold, K., B. Flehmig and K. Botzenhart. 1989. Comparison of Ozone Inactivation, in Flowing Water, of Hepatitis A Virus, Poliovirus 1 and Indicator Organisms. *Applied and Environmental Microbiology*, 55(11):2949-2953.
- Hiatt, C.W. 1964. Kinetics of the Inactivation of Viruses. *Bacteriological Reviews*, 28(2):150-163.
- Hijnen, W.A.M., F.A.P. Houtepen, W.M.H. van der Speld and D. van der Kooij. 1997. Spores of Sulphite-Reducing Clostridia: a Surrogate Parameter for Assessing the Effects of Water Treatment Processes on Protozoan (Oo)Cysts? In *Proceedings of the International Symposium on Waterborne Cryptosporidium*, Edited by C. R. Fricker, J. L. Clancy and P. A. Rochelle. American Water Works Association, Denver, CO, pp. 115-125.
- Hirata, T., D. Chikuma, A. Shimura, A. Hashimoto, N. Motoyoma, K. Takahashi, T. Moniwa, M. Kaneko, S. Siato and S. Maede. 2000. Effects of Ozonation and Chlorination on Viability and Infectivity of *Cryptosporidium parvum* Oocysts. *Water Science and Technology*, 41(7):39-46.

- Hoff, J.C. 1986. *Inactivation of Microbial Agents by Chemical Disinfectants*. Water Engineering Research Laboratory, U. S. Environmental Protection Agency, Cincinnati, OH.
- Hoff, J.C., E.W. Rice and F.W. Schaefer, III. 1985. Comparison of Animal Infectivity and Excystation as Measures of *Giardia muris* Cyst Inactivation by Chlorine. *Applied and Environmental Microbiology*, 50(4):1115-1117.
- Hoigné. 1988. The Chemistry of Ozone in Water. In *Process Technologies for Water Treatment*. Edited by S. Stucki. Plenum Press, New York, NY, pp. 121-143.
- Hoigné, J. and H. Bader. 1975. Ozonation of Water: Role of Hydroxyl Radicals as Oxidizing Intermediates. *Science*, 190(4216):782-784.
- Hoigné, J. and H. Bader. 1983a. Rate Constants of Reactions of Ozone with Organic and Inorganic Compounds in Water - I. Non-Dissociating Organic Compounds. *Water Research*, 17(1):173-183.
- Hoigné, J. and H. Bader. 1983b. Rate Constants of Reactions of Ozone with Organic and Inorganic Compounds in Water - II. Dissociating Organic Compounds. *Water Research*, 17(1):185-194.
- Hoigné, J. and H. Bader. 1994. Characterization of Water Quality Criteria for Ozonation Processes. Part II: Lifetime of Added Ozone. *Ozone: Science and Engineering*, 16(2):121-134.
- Hoigné, J., H. Bader, W.R. Haag and J. Staehelin. 1985. Rate Constants of Reactions of Ozone with Organic and Inorganic Compounds in Water - III. Inorganic Compounds and Radicals. *Water Research*, 19(8):993-1004.

- Hom, L.W. 1972. Kinetics of Chlorine Disinfection in an Ecosystem. *Journal of the Sanitary Engineering Division, Proceedings of the American Society of Civil Engineering*, 98(SA1):183-193.
- Hunt, N., K. and B. Mariñas, J. 1999. Inactivation of *Escherichia coli* with Ozone: Chemical and Inactivation Kinetics. *Water Research*, 33(11):2633-2641.
- Hunt, N.K. and B.J. Marinas. 1997. Kinetics of *Escherichia coli* Inactivation with Ozone. *Water Research*, 31(6):1355-1362.
- Ishizaki, K., K. Sawadaishi, K. Miura and N. Shinriki. 1987. Effect of Ozone on Plasmid DNA of *Escherichia coli* *In Situ*. *Water Research*, 21(7):823-827.
- Ishizaki, K., N. Shinriki and H. Matsuyama. 1986. Inactivation of *Bacillus* Spores by Gaseous Ozone. *Journal of Applied Bacteriology*, 60(67-72)
- Islam, A. 1990. Giardiasis in Developing Countries. In *Giardiasis*, Volume 3. Edited by E. A. Meyer., Elsevier, Amsterdam, pp. 235-266.
- Jacangelo, J.G., S.S. Adham and J. Lainé. 1995. Mechanism of *Cryptosporidium*, *Giardia* and MS2 Virus Removal by MF and UF. *Journal of the American Water Works Association*, 87(9):107-121.
- Jarroll, E.L., Jr, A.K. Bingham and E.A. Meyer. 1981. Effect of Chlorine on *Giardia lamblia* Cyst Viability. *Applied and Environmental Microbiology*, 41(2):483-487.
- Jarroll, E.L., Jr., A.K. Bingham and E.A. Meyer. 1980. *Giardia* Cyst Destruction: Effectiveness of Six Small-Quantity Water Disinfection Methods. *American Journal of Tropical Medicine and Hygiene*, 29(1):8-11.

- Joost, R.D., L.A. Jackson and L.J. Bollyky. 1989. Optimization of Ozone Contactors for Drinking Water Disinfection. In *Proceedings of the Ninth Ozone World Congress, Volume 2*. Edited by L. J. Bollyky. International Ozone Association, Stamford CT, pp. 551-561.
- Kanjo, Y., I. Kimata, M. Iseki, S. Miyanaga, H. Okada, C. Banno, M. Matsumoto and Y. Shimada. 2000. Inactivation of *Cryptosporidium spp.* Oocysts with Ozone and Ultraviolet Irradiation Evaluated by In Vitro Excystation and Animal Infectivity. *Water Science and Technology*, 41(7):119-125.
- Kastanek, F., J. Zahradnik, J. Kratochvil and J. Cermak. 1993. *Chemical Reactors for Gas-Liquid Systems*. Ellis Horwood, New York, NY, 406 p.
- Katzenelson, E., B. Kletter and H.I. Shuval. 1974. Inactivation Kinetics of Viruses and Bacteria by Use of Ozone. *Journal of the American Water Works Association*, 66(12):725-729.
- Katzenelson, E., G. Koerner, N. Biedermann, M. Peleg and H.I. Shuval. 1979. Measurement of the Inactivation Kinetics of Poliovirus by Ozone in a Fast Flow Mixer. *Applied and Environmental Microbiology*, 37(4):715-718.
- Kilani, R.T. and L. Sekla. 1987. Purification of *Cryptosporidium* Oocysts and Sporozoites by Cesium Chloride and Percoll Gradients. *American Journal of Tropical Medicine and Hygiene*, 36:505-508.
- Kim, C.K., D.M. Gentile and O.J. Sproul. 1980. Mechanism of Ozone Inactivation of Bacteriophage f2. *Applied and Environmental Microbiology*, 39(1):210-218.
- Kimball, A.W. 1953. The Fitting of Multi-Hit Survival Curves. *Biometrics*, 9:201-211.

- Korich, D.G., J.R. Mead, M.S. Madore, N.A. Sinclair and C.R. Sterling. 1990. Effects of Ozone, Chlorine Dioxide, Chlorine and Monochloramine on *Cryptosporidium parvum* Oocyst Viability. *Applied and Environmental Microbiology*, 56(5):1423-1428.
- Kramer, M.H., B.L. Herwaldt, G.F. Craun, R.L. Calderon and D.D. Juranek. 1996. Waterborne Disease: 1993 and 1994. *Journal of the American Water Works Association*, 88(3):66-80.
- Kuo, C.K. and F. Yocum. 1982. Mass Transfer of Ozone into Aqueous Systems. In *Handbook of Ozone Technology and Applications, Volume 1*. Edited by R. G. Rice and A. Netzer. Ann Arbor Science Publishers, Ann Arbor, MI, pp. 105-141.
- Labatiuk, C.W. 1992. Ozone and Ozone-Hydrogen Peroxide Inactivation of *Giardia*. PhD Thesis, University of Alberta, Edmonton, AB, 247 p.
- Labatiuk, C.W., M. Belosevic and G.R. Finch. 1992a. Evaluation of High Level Ozone Inactivation of *Giardia muris* Using an Animal Infectivity Model. *Ozone: Science and Engineering*, 14(1):1-12.
- Labatiuk, C.W., M. Belosevic and G.R. Finch. 1992b. Factors Influencing the Infectivity of *Giardia muris* Cysts Following Ozone Inactivation in Laboratory and Natural Waters. *Water Research*, 26(6):733-743.
- Labatiuk, C.W., M. Belosevic and G.R. Finch. 1994. Inactivation of *Giardia muris* Using Ozone and Ozone-Hydrogen Peroxide. *Ozone: Science and Engineering*, 16(1):67-78.
- Labatiuk, C.W., F.W. Schaefer, III, G.R. Finch and M. Belosevic. 1991. Comparison of Animal Infectivity, Excystation and Fluorogenic Dye as Measures of *Giardia*

*muris* Cyst Inactivation by Ozone. *Applied and Environmental Microbiology*, 57(11):3187-3192.

Langlais, B., D. Perrine, J.C. Joret and J.P. Chenu. 1990. The C.T Value Concept for Evaluation of Disinfection Process Efficiency; Particular Case of Ozonation for Inactivation of Some Protozoan: Free Living Amoeba and *Cryptosporidium*. In *New Developments: Ozone in Water and Wastewater Treatment. Proceedings of the International Ozone Association Spring Conference* International Ozone Association, Stamford, CT.

Langlais, B., D.A. Reckhow and D.R. Brink editor. 1991. *Ozone in Water Treatment: Application and Engineering*. Lewis Publishers, Inc., Chelsea, MI, 569 p.

Lawler, D.F. and P.C. Singer. 1993. Analyzing Disinfection Kinetics and Reactor Design: A Conceptual Approach Versus the SWTR. *Journal of the American Water Works Association*, 85(11):67-76.

Le Paulouë, J. and B. Langlais. 1999. State-Of-The-Art of Ozonation in France. *Ozone: Science and Engineering*, 21(2):153-162.

Le Sauze, N., A. Laplanche, N. Martin and G. Martin. 1993. Modeling of Ozone Transfer in a Bubble Column. *Water Research*, 27(6):1071-1083.

Leahy, J.G., A.J. Rubin and O.J. Sproul. 1987. Inactivation of *Giardia muris* Cysts by Free Chlorine. *Applied and Environmental Microbiology*, 53(7):1448-1453.

LeChevallier, M.W. and W.D. Norton. 1995. *Giardia* and *Cryptosporidium* in Raw And Finished Water. *Journal of the American Water Works Association*, 87(9):54-68.

- LeChevallier, M.W., W.D. Norton and R.G. Lee. 1991a. Occurrence of *Giardia* and *Cryptosporidium* spp. in Surface Water Supplies. *Applied and Environmental Microbiology*, 57(9):2610-2616.
- LeChevallier, M.W., W.D. Norton and R.G. Lee. 1991b. Occurrence of *Giardia* and *Cryptosporidium* spp. in Surface Water Supplies. *Applied and Environmental Microbiology*, 57(9):2610-6.
- LeChevallier, M.W., W.D. Norton, J.E. Siegel and M. Abbaszadegan. 1995. Evaluation of the Immunofluorescence Procedure for Detection of *Giardia* Cysts and *Cryptosporidium* Oocysts in Water. *Applied and Environmental Microbiology*, 61(2):690-697.
- Lev, O. and S. Regli. 1992a. Evaluation of Ozone Disinfection Systems: Characteristic Concentration *C*. *Journal of Environmental Engineering*, 118(4):477-494.
- Lev, O. and S. Regli. 1992b. Evaluation of Ozone Disinfection Systems: Characteristic Time *T*. *Journal of Environmental Engineering*, 118(2):268-285.
- Levenspiel, O. 1972. *Chemical Reaction Engineering*. Second edition. John Wiley & Sons Inc., New York, NY, 578 p.
- Levenspiel, O. and J.C.R. Turner. 1970. The Interpretation of Residence Time Distributions. *Chemical Engineering Science*, 25:1605-1609.
- Li, H., L.L. Gyürék, G.R. Finch, D.W. Smith and M. Belosovic. 2001. Effect of Temperature on Ozone Inactivation of *Cryptosporidium parvum* in Oxidant Demand-Free Phosphate Buffer. *Journal of Environmental Engineering*, 127(5):456-467.

- Logsdon, G.S. 1988. Comparison of Some Filtration Processes Appropriate for *Giardia* Cyst Removal. In *Advances in Giardia Research*. Edited by P. M. Wallis and B. R. Hammond. University of Calgary Press, Calgary, AB, pp. 95-102.
- MacKenzie, W.R., N.J. Hoxie, M.E. Proctor, M.S. Gradus, K.A. Blair, D.E. Peterson, J.J. Kazmierczak, D.G. Addiss, K.R. Fox, J.B. Rose and J.P. Davis. 1994. A Massive Outbreak in Milwaukee of *Cryptosporidium* Infection Transmitted Through the Public Water Supply. *New England Journal of Medicine*, 331(3):161-167.
- Majumdar, B., W.H. Ceckler and O.J. Sproul. 1973. Inactivation of Poliovirus in Water by Ozonation. *Journal of the Water Pollution Control Federation*, 45(12):2433-2443.
- Malcolm Pirnie Inc. and HDR Engineering Inc. 1991. *Guidance Manual for Compliance with the Filtration and Disinfection Requirements for Public Water Systems Using Surface Water Sources*. American Water Works Association. Denver, CO.
- Mariñas, B., J., L. Sun and M. Aieta, E. 1993. Modeling Hydrodynamics and Ozone Residual Distribution in a Pilot-Scale Ozone Bubble-Diffuser Contactor. *Journal of the American Water Works Association*, 85(3):90-99.
- Marshall, M.M., D. Naumovitz, Y. Ortega and C.R. Sterling. 1997. Waterborne Protozoan Pathogens. *Clinical Microbiology Reviews*, 10(1):67-85.
- Martin, N., M. Benezet-Toulze, C. Laplace, M. Faivre and B. Langlais. 1992. Design and Efficiency of Ozone Contactors for Disinfection. *Ozone: Science and Engineering*, 14(5):391-405.
- Martin, N., V. Boisdon, A. Laplanche and P. Uhlig. 1995. Modelization of Industrial Ozonation Tanks: A Useful Tool for the Design of 2000s Ozone Contactor. *Water Supply*, 13(2):57-74.

- Martin, N. and C. Galey. 1994. Use of Static Mixer for Oxidation and Disinfection by Ozone. *Ozone Science and Engineering*, 16(6):455-473.
- Masschelein, W., G. Fransolet and J. Genot. 1975. Techniques for Dispersing and Dissolving Ozone in Water /Part 1. *Water and Sewage Works* 122(12):57-60.
- Masschelein, W., G. Fransolet and J. Genot. 1976. Techniques for Dispersing and Dissolving Ozone in Water / Part 2. *Water and Sewage Works*, 123(1):34-60.
- Masschelein, W.J. 1982a. Contacting of Ozone with Water and Contactor Offgas Treatment. In *Handbook of Ozone Technology and Applications, Volume 1*, Edited by R. G. Rice and A. Netzer. Ann Arbor Science Publishers, Ann Arbor, MI, pp. 143-224.
- Masschelein, W.J. 1982b. The Direct Action of Dispersed Ozonized Gas Bubbles. In *Ozonation Manual for Water and Wastewater Treatment*. Edited by W. J. Masschelein. John Wiley & Sons, New York, NY, pp. 93-95.
- Masschelein, W.J., L. Blauch, E. Thieben, J. Bell and A. Reading. 1998. Ozone Science and Engineering Special Issue on Quality Assurance in Ozone Practice (1998). *Ozone: Science and Engineering*, 20(6):443-487.
- Medema, G.J., F.M. Schets, P.F.M. Teunis and A.H. Havelaar. 1998. Sedimentation of Free and Attached *Cryptosporidium* Oocysts and *Giardia* Cysts in Water. *Applied and Environmental Microbiology*, 64(11):4460-4466.
- Mehta, Y.M., C.E. George and C.H. Kuo. 1989. Mass Transfer and Selectivity of Ozone Reactions. *Canadian Journal of Chemical Engineering*, 67:118-126.

- Meyer, E.A. 1990a. Introduction. In *Giardiasis*. Edited by E. A. Meyer. Volume 3. Elsevier, Amsterdam, pp. 1-9.
- Meyer, E.A. 1990b. Taxonomy and Nomenclature. In *Giardiasis*. Edited by E. A. Meyer. Volume 3. Elsevier, Amsterdam, pp. 51-60.
- Morgan, U.M., L.H. Xiao, R. Fayer, A.A. Lal and R.C.A. Thompson. 1999. Variation in *Cryptosporidium*: Towards a Taxonomic Revision of the Genus. *International Journal For Parasitology*, 29(11):1733-1751.
- Morooka, S., K. Ikemizu and Y. Kato. 1979. The Decomposition of Ozone in Aqueous Solution. *International Chemical Engineering*, 19(4):650-654.
- Myers, K.J., A. Bakker and D. Ryan. 1997. Avoid Agitation by Selecting Static Mixers. *Chemical Engineering Progress*, 93(6):28-38.
- Nauman, E.B. and B.A. Buffham. 1983. *Mixing in Continuous Flow Systems*. John Wiley and Sons, New York, NY, 271 p.
- Neter, J., W. Wasserman and M.H. Kutner. 1989. *Applied Linear Regression Models, Second Edition*. Irwin, Boston, MA, 667 p.
- Neumann, N.F., L.L. Gyürék, G.R. Finch and M. Belosevic. 2000. Intact *Cryptosporidium parvum* Oocysts Isolated After In Vitro Excystation are Infectious to Neonatal Mice. *FEMS Microbiology Letters*, 186(1):331-336.
- Nieminski, E.C. 1990. Ozone Contactor Hydraulic Considerations in Meeting 'CT' Disinfection Requirements. *Ozone: Science and Engineering*, 12(2):133-143.
- Nieminski, E.C. and W.D. Bellamy. 1998. Application of Pathogen Surrogates to Improve Treatment Plant Performance. In *Proceedings of the American Water*

*Works Association Water Quality Technology Conference. American Water Works Association, Denver, CO.*

Nieminski, E.C. and S.M. Bradford. 1991. Impact of Ozone Treatment on Selected Microbiological Parameters. *Ozone: Science and Engineering*, 13(2):127-145.

Nieminski, E.C., F.W. Schaefer, III and J.E. Ongerth. 1995. Comparison of two methods for detection of Giardia cysts and Cryptosporidium oocysts in water. *Applied and Environmental Microbiology*, 61(5):1714-1719.

Nime, F.A., J.D. Burek, D.L. Page, M.A. Holscher and J.H. Yardley. 1976. Acute Enterocolitis in a Human Being Infected with the Protozoan *Cryptosporidium*. *Gastroenterology*, 70:592-598.

Oke, N.J., D.W. Smith and H. Zhou. 1998. An Empirical Analysis of Ozone Decay Kinetics in Natural Waters. *Ozone: Science and Engineering*, 20:361-379.

Okun, D.A. 1996. From Cholera to Cancer to Cryptosporidiosis. *Journal of Environmental Engineering*, 122(6):453-458.

Olson, M.E., N.J. Guselle, R.M. O. Handley, M.L. Swift, T.A. McAllister, M.D. Jelinski and D.W. Morck. 1997. *Giardia* and *Cryptosporidium* in Dairy Calves in British Columbia. *Canadian Veterinary Journal*, 38(11):703-706.

Ongerth, J.E. 1989. *Giardia* Cyst Concentrations in River Water. *Journal of the American Water Works Association*, 81(9):81-86.

Ongerth, J.E. 1990. Evaluation of Treatment for Removing *Giardia* Cysts. *Journal of the American Water Works Association*, 82(6):85-96.

- Ongerth, J.E. and J.P. Pecoraro. 1995. Removing *Cryptosporidium* Using Multimedia Filters. *Journal of the American Water Works Association*, 87(12):83-89.
- Ongerth, J.E. and H.H. Stibbs. 1987. Identification of *Cryptosporidium* Oocysts in River Water. *Applied and Environmental Microbiology*, 53(4):672-676.
- Oppenheimer, J.A., E.M. Aieta, R.R. Trussell, J.G. Jacangelo and I.N. Najm. 2000. *Evaluation of Cryptosporidium Inactivation in Natural Waters*. AWWA Research Foundation and the American Water Works Association, Denver, CO, 197 p.
- Overbeck, P.K. 2000. WQA Ozone Task Force - An Update. *Ozone News*, 28(3):19-22.
- Owens, J.H., R.J. Miltner, E.W. Rice, C.H. Johnson, D.R. Dahling, F.W. Schaefer and H.M. Shukairy. 2000. Pilot-scale ozone inactivation of *Cryptosporidium* and other microorganisms in natural water. *Ozone: Science and Engineering*, 22(5):501-517.
- Owens, J.H., R.J. Miltner, F.W. Schaefer, III and E.W. Rice. 1994. Pilot-Scale Ozone Inactivation of *Cryptosporidium*. *Journal of Eukaryotic Microbiology*, 41(5):S56-S57.
- Owens, J.H., R.J. Miltner, F.W. Schaefer, III and E.W. Rice. 1995. Pilot-Scale Ozone Inactivation of *Cryptosporidium* and *Giardia*. In *Proceedings of the American Water Works Association Water Quality Technology Conference*. American Water Works Association, Denver, CO, pp. 1319-1328.
- Parker, J.F.W., G.F. Greaves and H.V. Smith. 1993. The Effect of Ozone on the Viability of *Cryptosporidium parvum* Oocysts and a Comparison of Experimental Methods. *Water Science and Technology*, 27(3-4):93-96.

- Patania, N.L., J.G. Jacangelo, L. Cummings, A. Wilczak, K. Riley and J. Oppenheimer. 1995. *Optimization of Filtration for Cyst Removal*. AWWA Research Foundation and American Water Works Association, Denver, CO, 158 p.
- Peeters, J.E., E.A. Mazás, W.J. Masschelein, I.V. Martinez de Maturana and E. Debacker. 1989. Effect of Disinfection of Drinking Water with Ozone or Chlorine Dioxide on Survival of *Cryptosporidium parvum* Oocysts. *Applied and Environmental Microbiology*, 55(6):1519-1522.
- Perrine, D., P. Georges and B. Langlais. 1990. Efficacité de l'Ozonation des Eaux sur l'Inactivation des Oocystes de *Cryptosporidium*. *Bulletin de l'Academie Nationale de Medecine*, 174(6):845-850.
- Plummer, J.D., J.K. Edzwald and M.B. Kelley. 1995. Removing *Cryptosporidium* by Dissolved-air Flotation. *Journal of the American Water Works Association*, 87(9):85-95.
- Rader, R.G., M. Mutsakis, F. Grosz-Roell and W. Maugweiler. 1989. Better Absorption? Try a Static Mixer. *Chemical Engineering*, 96(7):137-142.
- Rakness, K.L., R.C. Renner, B.A. Hegg and A.G. Hill, IV. 1988. Practical Design Model for Calculating Bubble Diffuser Contactor Ozone Transfer Efficiency. *Ozone: Science and Engineering*, 10(2):173-214.
- Ransome, M.E., T.N. Whitmore and E.G. Carrington. 1993. Effect of Disinfectants on the Viability of *Cryptosporidium parvum* Oocysts. *Water Supply*, 11(1):75-89.
- Reddy, S., R. Joost and J. Heckler. 1997. Ozone Contactor Hydrodynamics. *Ozone: Science and Engineering*, 19(4):307-321.

- Reduker, D.W., C.A. Speer and J.A. Blixt. 1985. Ultrastructural Changes in the Oocyst Wall During Excystation of *Cryptosporidium parvum* (Apicomplexa; Eucoccidiorida). *Canadian Journal of Zoology*, 63:1892-1896.
- Reil, D. 2001. *Overcoming Unique Design and Commissioning Challenges at GVRD Ozone Treatment Facilities*. Vancouver, BC: BC Hydro.
- Rendtorff, R.C. 1954. The Experimental Transmission of Human Intestinal Protozoan Parasites. II. *Giardia lamblia* Cysts Given in Capsules. *American Journal of Hygiene*, 59:209-220.
- Rennecker, J.L., B.J. Mariñas, J.H. Owens and E.W. Rice. 1999. Inactivation of *Cryptosporidium parvum* Oocysts With Ozone. *Water Research*, 33(11):2481-2488.
- Rice, E.W., K.R. Fox, R.J. Miltner, D.A. Lytle and C.M. Johnson. 1996. Evaluating Plant Performance with Endospores. *Journal of the American Water Works Association*, 88(9):122-130.
- Rice, R.G. 1999. Ozone in the United States of America -- State-Of-The-Art. *Ozone: Science and Engineering*, 21(2):99-118.
- Richard, Y. 1994. Ozone Demand Water Test. *Ozone: Science and Engineering*, 16(4):355-365.
- Richards, D.A. and M. Fleischman. 1975. Ozone Transfer to Aqueous Systems in a Static Mixer. In *Proceedings of the Second International Symposium on Ozone Technology*. Edited by R. G. Rice, P. Pichet and M.-A. Vicent. International Ozone Association, Stamford, CT, pp. 57-70.

- Riesser, V.N., J.R. Perrich, E.B. Silver and J.R. McCammon. 1977. Possible Mechanisms for Poliovirus Inactivation by Ozone. In *Forum on Ozone Disinfection*. Edited by E. G. Fochtman, R. G. Rice and M. F. Browning. International Ozone Institute, Cleveland, OH, pp. 186-192.
- Roach, P.D., M.E. Olson, G. Whitley and P.M. Wallis. 1993. Waterborne *Giardia* Cysts and *Cryptosporidium* Oocysts in the Yukon, Canada. *Applied and Environmental Microbiology*, 59(1):67-73.
- Robertson, L.J., A.T. Campbell and H.V. Smith. 1992. Survival of *Cryptosporidium parvum* Oocysts Under Various Environmental Pressures. *Applied and Environmental Microbiology*, 58(11):3494-3500.
- Roberts-Thomson, I.C., D.P. Stevens, A.A.F. Mahmoud and K.S. Warren. 1976. Giardiasis in the Mouse: An Animal Model. *Gastroenterology*, 71:57-61.
- Rochelle, P.A., D.M. Ferguson, T.J. Handojo, R. De Leon, M.H. Stewart and R.L. Wolfe. 1997. An Assay Combining Cell Culture with Reverse Transcriptase PCR to Detect and Determine the Infectivity of Waterborne *Cryptosporidium parvum*. *Applied and Environmental Microbiology*, 63(5):2029-2037.
- Rose, J.B., C.P. Gerba and W. Jakubowski. 1991a. Survey of Potable Water Supplies for *Cryptosporidium* and *Giardia*. *Environmental Science and Technology*, 25(8):1393-1400.
- Rose, J.B., C.N. Haas and S. Regli. 1991b. Risk Assessment and Control of Waterborne Giardiasis. *American Journal of Public Health*, 81(6):709-713.
- Roth, J.A. and D.E. Sullivan. 1983. Kinetics of Ozone Decomposition in Water. *Ozone: Science and Engineering*, 5(1):37-49.

- Roustan, M., C. Beck, C. Wable, J.P. Duguet and J. Mallevalle. 1993. Modelling Hydraulics Of Ozone Contactors. *Ozone: Science and Engineering*, 15:213-226.
- Roustan, M., H. Debellefontaine, Z. Do Quang and J.P. Duguet. 1998. Development of a Method for the Determination of Ozone Demand of a Water. *Ozone: Science and Engineering*, 20(6):513-520.
- Roustan, M., J.P. Duguet, B. Brette, E. Brodard and J. Mallevalle. 1987. Mass Balance Analysis of Ozone in Conventional Bubble Contactors. *Ozone: Science and Engineering*, 9(3):289-297.
- Roustan, M., Z. Stambolieva, J.P. Duguet, O. Wable and J. Mallevalle. 1991. Influence of Hydrodynamics on *Giardia* Cyst Inactivation by Ozone. Study by Kinetics and by "CT" Approach. *Ozone: Science and Engineering*, 13(4):451-462.
- Roustan, M., R.Y. Wang and D. Wolbert. 1996. Modeling Hydrodynamics And Mass Transfer Parameters In A Continuous Ozone Bubble Column. *Ozone: Science and Engineering*, 18(2):99-115.
- Roy, D., E.S.K. Chian and R.S. Engelbrecht. 1981a. Kinetics of Enteroviral Inactivation by Ozone. *Journal of the Environmental Engineering Division, Proceedings of the American Society of Civil Engineering*, 107(EES):887-901.
- Roy, D., E.S.K. Chian and R.S. Engelbrecht. 1982a. Mathematic Model for Enterovirus Inactivation by Ozone. *Water Research*, 16(7):667-673.
- Roy, D., R.S. Englebrecht and E.S.K. Chian. 1982b. Comparative Inactivation of Six Enteroviruses by Ozone. *Journal of the American Water Works Association*, 74(12):660-664.

- Roy, D., P.K.Y. Wong, R.S. Engelbrecht and E.S.K. Chian. 1981b. Mechanism of Enteroviral Inactivation by Ozone. *Applied and Environmental Microbiology*, 41:718-723.
- Rubin, A.J., D.P. Evers, C.M. Eyman and E.L. Jarroll. 1989. Inactivation of Gerbil-Cultured *Giardia lamblia* Cysts by Free Chlorine. *Applied and Environmental Microbiology*, 55(10):2592-2594.
- Scaccia, C. and H.M. Rosen. 1978. Ozone Contacting: What is the Answer? *Ozonews*, 5(10, Pt. 2):1-8.
- Schaefer, F.W., III. 1990. Methods for Excystation of *Giardia*. In *Giardiasis, Volume 3*. Edited by E. A. Meyer.. Elsevier, Amsterdam, pp. 111-136.
- Schuler, P.F. and M.M. Ghosh. 1990. Diatomaceous Earth Filtration of Cysts and Other Particulates Using Chemical Additives. *Journal of the American Water Works Association*, 82(12):67-75.
- Schuler, P.F., M.M. Ghosh and P. Gopalan. 1991. Slow Sand and Diatomaceous Earth Filtration of Cysts and Other Particulates. *Water Research*, 25(8):995-1005.
- Schulgen, B., A. Amirtharajah and S.C. Jones. 1996. Effectiveness of Static Mixers for Coagulation in Water Treatment. In *Proceedings of the American Water Works Association Annual Conference*. American Water Works Association, Denver, CO, pp. 121-147.
- Schulz, C.R., G.C. Schafran, L.B.J. Garrett and R.A. Hawkins. 1995. Evaluating a High-Efficiency Ozone Injection Contactor. *Journal of the American Water Works Association*, 87(8):85-99.

- Schulz, R. and P.W. Prendeville. 1993. Designing High Concentration Ozone Contactors for Water Treatment Plants. *Ozone: Science and Engineering*, 15(3):245-266.
- Scott, D.B.M. and E.C. Leshner. 1963. Effect of Ozone on Survival and Permeability of *Escherichia coli*. *Journal of Bacteriology*, 85:567-576.
- Scott, K.N., R.L. Wolfe and M.H. Stewart. 1992. Pilot-Plant-Scale Ozone and Peroxone Disinfection of *Giardia muris* Seeded into Surface Water Supplies. *Ozone: Science and Engineering*, 14(1):71-90.
- Seber, G.A.F. and C.J. Wild. 1989. *Nonlinear Regression*. John Wiley & Sons, New York, NY, 78 p.
- Selleck, R.E., B.M. Saunier and H.F. Collins. 1978. Kinetics of Bacterial Deactivation with Chlorine. *American Society of Civil Engineers Journal of the Environmental Engineering Division*, 104:1197-1212.
- Severin, B.F., M.T. Suidan and R.S. Engelbrecht. 1983. Kinetic Modeling of U.V. Disinfection of Water. *Water Research*, 17(11):1669-1678.
- Shinriki, N., K. Ishizaki, T. Yoshizaki, K. Miura and T. Ueda. 1988. Mechanism of Inactivation of Tobacco Mosaic Virus with Ozone. *Water Research*, 22(7):933-938.
- Shulz, C.R., G.C. Shafran, L.B. Garrett and R. Hawkins. 1995. Evaluating a High-Efficiency Ozone Injection Contactor. *Journal of the American Water Works Association*, 87(8):85-99.
- Singer, P.C. 1990. Assessing Ozonation Research Needs in Water Treatment. *Journal of the American Water Works Association*, 82(10):78-88.

- Slifko, T.R., A. Coulliette, D.E. Huffman and J.B. Rose. 2000. Impact of Purification Procedures on the Viability and Infectivity of *Cryptosporidium parvum* Oocysts. *Water Science and Technology*, 41(7):23-29.
- Slifko, T.R., D. Friedman, J.B. Rose and W. Jakubowski. 1997. An Invitro Method for Detecting Infectious *Cryptosporidium* Oocysts with Cell Culture. *Applied and Environmental Microbiology*, 63(9):3669-3674.
- Slifko, T.R., D.E. Huffman and J.B. Rose. 1999. A Most-Probable-Number Assay for Enumeration of Infectious *Cryptosporidium parvum* Oocysts. *Applied and Environmental Microbiology*, 65(9):3936-3941.
- Smith, D.W. and H. Zhou. 1994. Theoretical Analysis of Ozone Disinfection Performance in a Bubble Column. *Ozone: Science and Engineering*, 16(5):429-441.
- Smith, H.V., L.J. Robertson, R.A. Gilmour, G.P. Morris, R.W.A. Girdwood and P.G. Smith. 1993. The Occurrence and Viability of *Giardia* Cysts in Scottish Raw and Final Waters. *Journal of the Institution of Water and Environmental Management*, 7(6):632-635.
- Smith, H.V., L.J. Robertson and J.E. Ongerth. 1995. Cryptosporidiosis and Giardiasis: The Impact of Waterborne Transmission. *Aqua*, 44(6):258-274.
- Smith, H.V. and J.B. Rose. 1998. Waterborne cryptosporidiosis: Current status. *Parasitology Today*. Jan, 14(1):14-22.
- Solo-Gabriele, H. and S. Neumeister. 1996. US Outbreaks of Cryptosporidiosis. *Journal of the American Water Works Association*, 88(9):76-86.

- Somiya, I., S. Fujii, N. Kishimoto and R.-H. Kim. 2000a. Development of a Mathematical Model of *Cryptosporidium* Inactivation by Ozonation. *Water Science and Technology*, 41(7):173-180.
- Somiya, I., S. Fujii, N. Kishimoto and R.-H. Kim. 2000b. Development of an ATP Assay as a Surrogate Indicator of Viability of *Cryptosporidium parvum* Oocysts. *Water Science and Technology*, 41(7):181-188.
- Sotelo, J.L., F.J. Beltrán, F.J. Benitez and J. Beltrán-Heredia. 1989. Henry's Law Constant for the Ozone-Water System. *Water Research*, 23(10):1239-1246.
- Sproul, O.J., R.M. Pfister and C.K. Kim. 1982. The Mechanism of Ozone Inactivation of Water Borne Viruses. *Water Science and Technology*, 14:303-314.
- Stahelin, J. and J. Hoigné. 1982. Decomposition of Ozone in Water: Rate of Initiation by Hydroxide Ions and Hydrogen Peroxide. *Environmental Science and Technology*, 16(10):676-681.
- Stahelin, J. and J. Hoigné. 1985. Decomposition of Ozone in Water in the Presence of Organic Solutes Acting as Promoters and Inhibitors of Radical Chain Reactions. *Environmental Science and Technology*, 19(12):1206-1213.
- States, S., M. Scheuring, R. Evans, E. Buzza, B. Movahead, T. Gigliotti and L. Casson. 2000. Membrane Filtration and Posttreatment. *Journal of the American Water Works Association*, 92(8):59-68.
- Taghi-Kilani, R., L.L. Gyürék, P.J. Millard, G.R. Finch and M. Belosevic. 1996. Nucleic Acid Stains as Indicators of *Giardia muris* Viability Following Cyst Inactivation. *International Journal for Parasitology*, 26(6):637-646.

- Tate, C.H. and K. Fox Arnold. 1990. Health and Aesthetic Aspects of Water Quality. In *Water Quality and Treatment: A Handbook of Community Water Supplies*. Edited by F. W. Pontius. McGraw-Hill, New York, NY, pp. 63-156.
- Thompson, R.C.A. and J.A. Reynoldson. 1993. Giardia and giardiasis. *Advances in Parasitology*, 32:71-160.
- Toenniessen, G.H. and D.J. Johnson. 1970. Heat Shocked *Bacillus subtilis* Spores as an Indicator of Virus Disinfection. *Journal of the American Water Works Association*, 62(9):589-593.
- Tomiak, R.B., J.L. Rennecker and B. Mariñas. 1998. Modeling of *Cryptosporidium parvum* Oocyst Inactivation in a Pilot-Scale Bubble-Diffuser Ozone Contactor. In *Proceedings of the American Water Works Association Water Quality Technology Conference*. American Water Works Association, Denver, CO.
- Tomiyasu, H., H. Fukutomi and G. Gordon. 1985. Kinetics and Mechanism of Ozone Decomposition in Basic Aqueous Solution. *Inorganic Chemistry*, 24(19):2962-2966.
- Trussell, R.R. and J.-L. Chao. 1977. Rational Design of Chlorine Contact Facilities. *Journal of the Water Pollution Control Federation*, 49(4):659-667.
- U.S. Environmental Protection Agency. 1989. Drinking Water; National Primary Drinking Water Regulations; Filtration, Disinfection; Turbidity, *Giardia lamblia*, Viruses, *Legionella*, and Heterotrophic Bacteria; Final Rule. *Federal Register*, 54(124):27486-27541.
- U.S. Environmental Protection Agency. 1998a. National Primary Drinking Water Regulations: Disinfectants and Disinfection Byproducts; Final Rule. *Federal Register*, 63(241):69389-69476.

- U.S. Environmental Protection Agency. 1998b. National Primary Drinking Water Regulations: Interim Enhanced Surface Water Treatment Rule. *Federal Register*, 63(241):69477-69521.
- U.S. Environmental Protection Agency. 1999. *Alternative Disinfectants and Oxidants Guidance Manual*. Office of Water, Washington, DC.
- Wallis, P.M., S.L. Erlandsen, J.L. Isaac-Renton, M.E. Olson, W.J. Robertson and H. van Keulen. 1996. Prevalence of *Giardia* Cysts and *Cryptosporidium* Oocysts and Characterization of *Giardia* spp. Isolated from Drinking Water in Canada. *Applied and Environmental Microbiology*, 62(8):2789-2797.
- Wallis, P.M., A. van Roodselaar, M. Neuwirth, P.D. Roach, J.M. Buchanan-Mappin, and H. Mack. 1990. Inactivation of *Giardia* Cysts in a Pilot Plant Using Chlorine Dioxide and Ozone. In *Proceedings of the American Water Works Association Water Quality Technology Conference*. American Water Works Association. Denver, CO, pp 695-708.
- Watson, H.E. 1908. A Note on the Variation of the Rate of Disinfection with Change in the Concentration of the Disinfectant. *Journal of Hygiene (Cambridge)*, 8:536-592.
- Wei, J.H. and S.L. Chang. 1975. A Multi-Poisson Distribution Model for Treating Disinfection Data. In *Disinfection of Water and Wastewater*. Edited by J. D. Johnson. Ann Arbor Science, Ann Arbor, MI, pp. 11-47.
- Wickramanayake, G.B., A.J. Rubin and O.J. Sproul. 1984a. Inactivation of *Giardia lamblia* Cysts with Ozone. *Applied and Environmental Microbiology*, 48(3):671-672.

- Wickramanayake, G.B., A.J. Rubin and O.J. Sproul. 1984b. Inactivation of *Naegleria* and *Giardia* Cysts in Water by Ozonation. *Journal of the Water Pollution Control Federation*, 56(8):983-988.
- Wickramanayake, G.B., A.J. Rubin and O.J. Sproul. 1985. Effects of Ozone and Storage Temperature on *Giardia* Cysts. *Journal of the American Water Works Association*, 77(8):74-77.
- Wolfe, R.L., M.H. Stewart, S. Liang and M.J. McGuire. 1989a. Disinfection of Model Indicator Organisms in a Drinking Water Pilot Plant by Using Peroxone. *Applied and Environmental Microbiology*, 55:2230-2241.
- Wolfe, R.L., M.H. Stewart, K.N. Scott and M.J. McGuire. 1989b. Inactivation of *Giardia muris* and Indicator Organisms Seeded in Surface Water Supplies by Peroxone and Ozone. *Environmental Science and Technology*, 23(6):744-745.
- Woodmansee, D.B. 1987. Studies of *In Vitro* Excystation of *Cryptosporidium parvum* from Calves. *Journal of Protozoology*, 34(4):398-402.
- Xiao, L., R.P. Herd and D.M. Rings. 1993. Concurrent infections of *Giardia* and *Cryptosporidium* on two Ohio farms with calf diarrhea. *Veterinary Parasitology*, 51(1-2):41-48.
- Xiao, L.H. and R.P. Herd. 1994. Infection Patterns of *Cryptosporidium* and *Giardia* in Calves. *Veterinary Parasitology*, 55(3):257-262.
- Yurteri, C. and M.D. Gurol. 1988. Ozone Consumption in Natural Waters: Effects of Background Organic Matter, pH and Carbonate Species. *Ozone: Science and Engineering*, 10:277-290.

- Zhou, H. and D.W. Smith. 1994. Kinetics of Ozone Disinfection in a Completely Mixed System. *Journal of Environmental Engineering*, 120(4):841-858.
- Zhou, H., D.W. Smith and S.J. Stanley. 1994. Modeling of Dissolved Ozone Concentration Profiles in Bubble Columns. *Journal of Environmental Engineering*, 120(4):821-839.
- Zhou, H.D. and D.W. Smith. 2000. Ozone Mass Transfer in Water and Wastewater Treatment: Experimental Observations Using a 2D Laser Particle Dynamics Analyzer. *Water Research*, 34(3):909-921.
- Zhu, Q. 1990. Ozone Disinfection Of Sewage In A Static Mixer Contacting Reactor System On A Plant Scale. *Ozone: Science and Engineering*, 13(3):313-328.
- Zhu, Q., C. Liu and Z. Xu. 1989a. Study of Contacting Systems in Water and Wastewater Disinfection by Ozone. 1. Mechanism of Ozone Transfer and Inactivation Related to the Contacting Method Selection. *Ozone: Science and Engineering*, 11(2):169-188.
- Zhu, Q., C. Liu and Z. Xu. 1989b. Study of Contacting Systems in Water and Wastewater Disinfection by Ozone. 2. Mathematical Models of the Ozone Disinfection Process With a Static Mixer. *Ozone: Science and Engineering*, 11(2):189-207.
- Zwietering, T.N. 1959. The Degree of Mixing in Continuous Flow Systems. *Chem. Eng. Sci.*, 11(1):1-15.

**APPENDIX A      INFORMATION FROM DOSE-RESPONSE EXPERIMENTS  
WITH *CRYPTOSPORIDIUM PARVUM* OOCYSTS AND  
*GIARDIA MURIS* CYSTS (CHAPTER 6)**

Table A-1 Results of five dose response experiments with experimental *C. parvum* oocysts

<b>Dose Response Experiment</b>	<b>Oocyst Age (days)</b>	<b>Inoculum Size <i>d</i></b>	<b>No. of Mice in Cohort</b>	<b>No. of Mice Positive for Infection</b>
1	16	25	10	3
		50	10	5
		100	10	9
		200	10	10
2	30	25	10	1
		50	10	5
		100	10	6
		200	10	10
3	44	25	10	6
		50	10	5
		100	10	6
		200	10	10
4	58	25	10	2
		50	10	4
		100	10	4
		200	10	8
5	72	25	10	4
		50	10	5
		100	10	5
		200	10	8

Table A-2 Information from *G. muris* dose-response experiments with adult-male C3H/HeN mice used to develop the latent period dose-response model.

Trial	Cysts in Inoculum $d_0$	Cyst production on successive days post infection (DPI)										Latent Period LP, d
		1	2	3	4	5	6	7	8	9	10	
1	100 000	1.8	1.8	5.0	6.6	6.1	6.3	6.2				2.6
	10 000	1.8	1.8	2.6	5.6	5.9	6.1	6.1				3.5
	1 000	1.8	1.8	1.8	4.3	6.0	6.1	6.2				3.9
	100	1.8	1.8	2.5	2.9	4.1	5.8	6.1				4.8
	10	1.8	1.8	2.4	1.8	1.8	2.7	4.5	5.3			6.8
2	100 000	2.7	2.7	4.8	5.9	5.9	6.0					2.7
	10 000	2.7	2.7	2.8	5.4	5.7	6.0	6.0				3.5
	1 000	2.7	2.7	2.0	3.5	5.3	5.9	6.0	5.9			4.3
	100	2.7	2.7	2.1	2.2	2.8	4.5	5.1	5.2	5.6		5.9
	10	2.7	2.7	2.2	2.0	3.5	5.0	5.0	4.8	5.1	5.8	6.1
3	100 000	2.5	2.5	4.8	6.3	6.1	6.5					2.7
	10 000	2.5	2.5	2.5	5.9	6.3	6.8	6.3				3.5
	1 000	2.5	2.5	2.5	2.5	6.1	6.1	6.3	6.5			4.5
	100	2.5	2.5	2.5	2.5	4.7	5.5	5.6	6.1	6.2		4.8
	10	2.5	2.5	2.5	2.5	2.5	2.5	5.6	6.2	5.8		6.6
4	10				1.9	3.1	4.5	4.4	4.3	5.3	6.1	6.4

Table Notes:

- Cyst production is shown as the  $\log_{10}$  of the average cyst production of the mouse cohort in cysts/g wet feces.
- A < value for cyst production indicates that no cysts were observed under microscopic analysis with a hemocytometer. The value is the detection limit and is based on the observation of 1 cysts and the average daily wet feces output per mouse and observation of 4 hemocytometer wells.
- Information for experiment 3 was extracted from Labatiuk (1992)

**APPENDIX B**

**INFORMATION FROM BATCH REACTOR OZONATION  
TRIALS WITH *BACILLUS SUBTILIS* (ATCC 6633)  
SPORES SUSPENDED IN PHOSPHATE BUFFERED  
WATER (CHAPTER 7)**

**Table B-1** Batch reactor ozonation trials with *Bacillus subtilis* (ATCC 6633) spores. All trials were conducted in 0.05 M ozone demand-free phosphate buffered ozone laboratory water at 3°C.<sup>1</sup>

Trial	pH	$C_a$	$t_b$	Direct UV Absorbance @ 260 nm						Indigo Trisulphonate Colorimetric Method						$\log N$	$\log N_0$	$-\log(N/N_0)$	$\pm 95\%$ conf.
				$C_0$	$C_f$	$C_a - C_0$	$k_d$	$C_{avg}$	$C_{avg}t$	$C_0$	$C_f$	$C_a - C_0$	$k_d$	$C_{avg}$	$C_{avg}t$				
		mg/L	min	mg/L	mg/L	mg/L	/min	mg/L	mg× min/L	mg/L	mg/L	mg/L	/min	mg/L	mg× min/L	log- units	log- units	log-units	log- units
1	6	1.59	10.0	1.76	1.29	-0.17	0.031	1.51	15.1	2.07	1.46	-0.48	0.035	1.75	17.5	2.1	5.5	3.4	0.4
2	6	0.94	6.0	0.99	0.77	-0.05	0.041	0.87	5.2	1.22	1.02	-0.28	0.030	1.11	6.7	5.7	5.5	-0.2	0.4
3	6	1.55	6.0	1.66	1.31	-0.11	0.039	1.48	8.9	2.15	1.61	-0.60	0.048	1.87	11.2	4.5	5.5	1.0	0.2
4	6	1.00	10.0	1.10	0.74	-0.10	0.040	0.90	9.0	1.44	0.93	-0.44	0.044	1.17	11.7	4.3	5.5	1.3	0.5
5	6	1.53	15.0	1.57	1.00	-0.04	0.030	1.26	18.9	2.04	1.12	-0.51	0.040	1.54	23.0	1.9	5.8	3.8	0.5
6	6	1.03	15.0	1.14	0.77	-0.11	0.026	0.95	14.2	1.41	0.89	-0.38	0.031	1.13	16.9	2.3	5.8	3.5	0.3
7	6	0.98	19.0	0.97	0.21	0.01	0.081	0.49	9.4	0.97	0.19	0.01	0.086	0.48	9.1	1.9	5.8	1.9	0.3
8	6	1.61	7.30	1.67	1.26	-0.05	0.038	1.45	10.6	1.98	1.48	-0.37	0.040	1.71	12.5	3.7	5.6	2.0	0.4
9	8	2.02	10.0	2.15	1.16	-0.13	0.062	1.60	16.0	2.40	1.32	-0.38	0.060	1.81	18.1	1.8	5.8	4.0	0.4
10	8	1.01	4.0	1.08	0.81	-0.07	0.071	0.94	3.7	1.49	1.07	-0.48	0.081	1.27	5.1	5.8	5.8	0.1	0.4
11	8	0.96	10.0	1.06	0.50	-0.10	0.075	0.74	7.4	1.29	0.64	-0.33	0.071	0.93	9.3	4.6	5.4	0.8	0.5
12	8	1.99	4.0	1.96	1.55	0.03	0.058	1.75	7.0	2.55	1.77	-0.56	0.091	2.14	8.5	4.9	5.4	0.5	0.1
13	8	1.92	15.0	1.89	0.83	0.03	0.055	1.29	19.3	2.14	0.94	-0.22	0.055	1.46	21.9	1.4	5.6	4.3	0.4
14	8	1.14	15.0	1.15	0.46	-0.01	0.061	0.75	11.3	1.46	0.57	-0.32	0.063	0.94	14.1	2.5	5.6	3.1	0.2
15	8	1.53	7.0	1.64	1.20	-0.11	0.045	1.41	9.8	2.01	1.31	-0.48	0.061	1.64	11.4	2.9	5.8	2.9	0.2
16	8	2.04	8.0	2.06	1.37	-0.02	0.051	1.69	13.6	1.98	1.43	0.06	0.040	1.69	13.5	2.7	5.6	2.9	0.3

<sup>1</sup>Spore stock preparation A was used for all trials.

Table B-2 Batch reactor ozonation trials with *Bacillus subtilis* (ATCC 6633) spores. All trials were conducted in 0.05 M ozone demand-free phosphate buffered ozone laboratory water at 12°C.<sup>1</sup>

Trial	pH	$C_a$	$t_b$	Direct UV Absorbance @ 260 nm						Indigo Trisulphonate Colorimetric Method						log $N$	log $N_0$	$-\log(N/N_0)$	$\pm 95\%$ conf.
				$C_0$	$C_f$	$C_a - C_0$	$k_d$	$C_{avg}$	$C_{avg}^f$	$C_0$	$C_f$	$C_a - C_0$	$k_d$	$C_{avg}$	$C_{avg}^f$				
		mg/L	min	mg/L	mg/L	mg/L	/min	mg/L	mg $\times$ min/L	mg/L	mg/L	mg/L	/min	mg/L	mg $\times$ min/L	log-units	log-units	log-units	log-units
1	6	1.57	12.3	1.60	0.94	-0.03	0.04	1.24	15.3	2.0	1.08	-0.5	0.05	1.51	18.5	1.5	5.5	4.0	0.7
2	6	1.54	4.0	1.71	1.37	-0.17	0.06	1.54	6.1	1.9	1.47	-0.4	0.07	1.69	6.8	2.8	5.5	2.7	0.6
3	6	0.98	12.0	1.13	0.73	-0.15	0.04	0.92	11.0	1.1	0.82	-0.1	0.03	0.96	11.6	2.3	5.8	3.5	0.3
4	6	0.98	4.1	1.01	0.80	-0.03	0.06	0.90	3.7	1.2	0.95	-0.2	0.06	1.08	4.4	4.9	5.8	0.9	0.2
5	6	1.28	12.0	1.31	0.78	-0.03	0.04	1.02	12.2	1.5	0.81	-0.3	0.05	1.13	13.6	2.1	5.8	3.8	0.4
6	6	1.32	4.0	1.42	1.09	-0.10	0.07	1.25	5.0	1.7	1.17	-0.4	0.09	1.42	5.7	4.0	5.8	1.8	0.3
7	6	1.00	10.0	1.11	0.81	-0.11	0.03	0.95	9.5	1.2	0.97	-0.2	0.02	1.07	10.7	2.0	5.3	3.3	0.4
8	6	0.59	4.0	0.55	0.47	0.04	0.04	0.51	2.0	0.8	0.59	-0.2	0.06	0.67	2.7	5.5	5.3	-0.2	0.2
9	8	2.32	12.0	2.36	0.59	-0.04	0.12	1.27	15.3	2.9	0.66	-0.5	0.12	1.50	18.0	1.5	5.5	4.0	0.7
10	8	2.57	4.0	2.54	1.49	0.03	0.13	1.97	7.9	3.1	1.72	-0.5	0.14	2.33	9.3	2.1	5.5	3.4	0.5
11	8	1.48	12.0	1.67	0.51	-0.19	0.10	0.98	11.7	1.8	0.45	-0.3	0.12	0.98	11.8	1.9	5.8	3.8	0.5
12	8	1.48	4.0	1.53	0.94	-0.05	0.12	1.21	4.9	1.8	1.00	-0.3	0.15	1.36	5.4	3.1	5.8	2.7	0.3
13	8	1.73	5.0	1.84	1.09	-0.11	0.10	1.43	7.2	2.1	1.30	-0.4	0.10	1.66	8.3	2.1	5.4	3.3	0.3
14	8	0.75	4.0	0.85	0.48	-0.10	0.14	0.65	2.6	1.0	0.51	-0.2	0.16	0.71	2.8	5.5	5.4	-0.1	0.5
15	8	1.79	12.0	2.01	0.63	-0.22	0.10	1.19	14.3	2.2	0.59	-0.4	0.11	1.21	14.5	1.2	5.7	4.5	0.5
16	8	1.49	6.1	0.73	0.42	0.76	0.09	0.56	3.4	0.9	0.47	0.6	0.11	0.67	4.1	4.8	5.7	0.9	0.2

<sup>1</sup>Spore stock preparation A was used for all trials.

**Table B-3** Batch reactor ozonation trials with *Bacillus subtilis* (ATCC 6633) spores. All trials were conducted in 0.05 M ozone demand-free phosphate buffered ozone laboratory water at 22°C.<sup>1</sup>

Trial	pH	$C_a$	$t_b$	Direct UV Absorbance @ 260 nm						Indigo Trisulphonate Colorimetric Method						log $N$	log $N_0$	-log( $N/N_0$ )	± 95% conf.
				$C_0$	$C_f$	$C_a - C_0$	$k_d$	$C_{avg}$	$C_{avg}t$	$C_0$	$C_f$	$C_a - C_0$	$k_d$	$C_{avg}$	$C_{avg}t$				
		mg/L	min	mg/L	mg/L	mg/L	/min	mg/L	mg× min/L	mg/L	mg/L	mg/L	/min	mg/L	mg× min/L	log- units	log- units	log-units	log- units
1	6	1	10.0	1.06	0.53	-0.06	0.07	0.76	7.6	1.28	0.65	-0.28	0.07	0.93	9.3	2.1	5.6	3.4	0.2
2	6	1.78	5.0	2.10	1.51	-0.32	0.07	1.79	8.9	2.44	1.71	-0.66	0.07	2.05	10.3	1.7	5.6	3.9	0.4
3	6	1.89	10.0	2.02	1.17	-0.13	0.05	1.56	15.6	2.38	1.52	-0.49	0.05	1.91	19.1	0.5	5.3	4.8	0.5
4	6	0.99	5.0	1.10	0.70	-0.11	0.09	0.88	4.4	1.39	0.86	-0.40	0.10	1.10	5.5	2.5	5.3	2.8	0.3
5	6	0.76	4.0	0.76	0.55	0.00	0.08	0.65	2.6	0.88	0.64	-0.12	0.08	0.75	3.0	3.3	5.5	2.2	0.3
6	6	0.48	2.0	0.50	0.34	-0.02	0.20	0.41	0.8	0.61	0.43	-0.13	0.17	0.51	1.0	5.8	5.5	-0.3	0.2
7	6	0.69	8.0	0.70	0.39	-0.01	0.07	0.53	4.3	0.84	0.47	-0.15	0.07	0.63	5.1	2.0	5.3	3.3	0.2
8	6	0.47	3.0	0.47	0.32	0.00	0.13	0.39	1.2	0.58	0.39	-0.11	0.13	0.48	1.4	5.7	5.3	-0.4	0.2
9	6	0.63	4.0	0.54	0.38	0.09	0.09	0.46	1.8	0.67	0.49	-0.04	0.08	0.58	2.3	5.1	5.5	0.4	0.1
10	8	1.36	10.0	1.41	0.15	-0.05	0.22	0.57	5.7	1.43	0.19	-0.07	0.20	0.61	6.1	1.5	5.6	4.1	0.5
11	8	2.93	5.0	3.21	1.11	-0.28	0.21	1.97	9.9	3.74	1.22	-0.81	0.22	2.25	11.2	1.4	5.6	4.2	0.4
12	8	2.74	10.0	2.96	0.30	-0.22	0.23	1.16	11.6	3.50	0.32	-0.76	0.24	1.33	13.3	1.1	5.5	4.4	0.4
13	8	1.43	5.0	1.52	0.34	-0.09	0.30	0.78	3.9	1.88	0.38	-0.45	0.32	0.94	4.7	2.1	5.5	3.4	0.3
14	8	0.99	4.0	1.06	0.32	-0.07	0.30	0.62	2.5	1.23	0.37	-0.24	0.30	0.72	2.9	2.9	5.5	2.6	0.3
15	8	0.66	2.0	0.66	0.33	0.00	0.35	0.48	1.0	0.81	0.43	-0.15	0.32	0.60	1.2	5.7	5.5	-0.2	0.2
16	8	0.68	3.0	0.80	0.35	-0.12	0.27	0.55	1.6	0.78	0.33	-0.10	0.29	0.52	1.6	5.5	5.3	-0.3	0.3
17	8	1.2	12.0	1.24	0.08	-0.04	0.23	0.42	5.1	1.40	0.08	-0.20	0.24	0.46	5.5	1.8	5.3	3.5	0.3
18	8	0.8	4.0	0.70	0.24	0.10	0.27	0.43	1.7	0.67	0.34	0.13	0.17	0.49	1.9	5.0	5.4	0.5	0.1

<sup>1</sup>Spore stock preparation A was used for all trials.

**APPENDIX C      EXPERIMENTAL DATA AND INFORMATION FROM  
TRANSFER EFFICIENCY MEASUREMENT  
EXPERIMENTS WITH THE STATIC MIXER OZONE  
CONTACTOR (CHAPTER 8).**

Table C-1 Information from ozone transfer efficiency experiments with the static mixer ozone contactor.

TRIAL	Units	1	2	3	4	5	6	7	8	9	10
<u>Operating Conditions</u>											
Feed Water Flow, $Q_f$	L/min	10.8	10.8	10.8	10.8	10.8	12.1	12.1	12.1	16.5	15.6
Feed Gas Flow, $G$	L/min	0.47	0.47	0.47	0.47	0.14	0.14	0.14	0.14	0.11	0.41
SMX Inlet Pressure	psig	7.3	7.4	7.3	7.4	5.5	7.3	7	6.9	6.9	7.6
SMX Outlet Pressure	psig	4.0	4	4	4	3.9	3.9	3.9	4	4.5	4.3
Bubble Column Height, $H$	m	2.3	2.3	2.3	2.3	2.3	2.3	2.3	2.3	0.45	0.45
<u>Feed Water</u>											
DPD Total Chlorine	mg/L	0.2	0.17	0.19		0.26		0.26			0.32
pH				8.2	8.4	8.2	8.2	8.4	8.2	8.3	8.4
Temperature	°C	16.8	16.9	17.3	16.2	16.9	15.2	16.5	16.1	16.3	15.9
<u>Off-Gas Analysis</u>											
Volume Collected	L	2.2	2.13	3.05	1.89	1.42	1.83	3.61	2.15	2.145	2.01
Vol. $\text{Na}_2\text{S}_2\text{O}_3$ Titrant	mL	7.5	12.75	2.6	10.75	3.25	5.15	1.65	5.6	5.6	6.4
<u>Feed Gas Analysis</u>											
Vol. Gas Collected	L	1.1	1.02	1.48	1.02	1.04	1.03	1.09	1.04	1.07	1.12
Vol. $\text{Na}_2\text{S}_2\text{O}_3$ Titrant	mL	17.9	32.05	5.7	26.7	30.55	39.5	8.05	39.75	39.15	19.1
Wet Test Meter Temp.	°C	23.3	23.3	23.5	23.5	23.5	23.3	23.3	23.3	23.5	23.5
Barometric Pressure	mmHg	710	710	710	710	710	710	710	710	709	709
Vol. Correction Factor		0.9	0.88	0.87	0.87	0.87	0.87	0.87	0.87	0.86	0.87
<u>Dissolved Ozone</u>											
<u>Conc. by UV 260</u>											
SMX Outlet	mg/L	0.22	1.46	0.11	1.17	0.50	0.47	0.15	0.66	0.99	0.71
Column Inlet	mg/L	1.96	4.21	0.65	4.19	1.20	1.57	0.33	1.25	1.47	1.83
Column Mid-Height	mg/L	1.25	3.19	0.43	2.80	0.88	1.18	0.24	1.14		
Column Outlet	mg/L	1.17	2.99	0.42	2.75	0.96	1.47	0.23	0.85	0.95	1.03
<u>Calculated Variables</u>											
$G/Q_f$	%	4.3	4.35	4.32	4.33	1.26	1.17	1.17	1.16	0.67	2.61
SMX Sup. Velocity, $v_s$	m/s	0.93	0.93	0.93	0.93	0.93	1.04	1.04	1.04	1.42	1.34
Feed Gas Ozone Conc. $Y_f$	$\text{g/m}^3$	46.5	85.7	10.4	70.9	79.6	103.9	20.0	103.5	99.2	46.2
Off Gas Ozone Conc. $Y_o$	$\text{g/m}^3$	9.2	16.3	2.3	15.4	6.2	7.6	1.2	7.1	7.1	8.6
Transfer Efficiency, $TE$	%	80.2	80.9	77.9	78.3	92.2	92.7	93.8	93.2	92.9	81.3
<u>Mass Balance</u>											
Ozone Addition Rate	mg/L	2.0	3.7	0.5	3.1	1.0	1.2	0.2	1.2	0.7	1.2
Ozone Transfer Rate	mg/L	1.6	3.0	0.4	2.4	0.9	1.1	0.2	1.1	0.6	1.0
Ozone Loss	mg/L	0.4	0.0	-0.1	-0.3	0.0	-0.3	0.0	0.3	-0.3	-0.1
Mass Balance Closure	%	38	1	-17	-12	-3	-23	-6	32	-35	-5

Table C-1 (continued)

TRIAL	Units	11	12	13	14	15	16	17	18	19	20
<u>Operating Conditions</u>											
Feed Water Flow, $Q_f$	L/min	6.7	10.8	7.1	16.1	11.6	7.4	11.5	11.1	11.0	7.0
Feed Gas Flow, $G$	L/min	0.30	0.29	0.30	0.27	0.47	0.09	0.14	0.29	0.29	0.09
SMX Inlet Pressure	psig	4.6	6.5	5	9	6.6	4.5	6.1	6.4	6.5	4.5
SMX Outlet Pressure	psig	3.6	4	3.6	4.4	3.9	3.6	4.1	4	4	3.7
Bubble Column Height, $H$	m	0.45	1.4	2.3	2.3	0.45	0.45	0.45	1.4	1.4	2.3
<u>Feed Water</u>											
DPD Total Chlorine	mg/L		0.23			0.33			0.36	0.27	
pH		8.4	8.3	8.4	8.5	8.5	8.5	8.5	8.5	8.2	8.3
Temperature	°C	16.2	17	16	15.9	16.3	16.6	16.4	16.5	16.5	16.7
<u>Off-Gas Analysis</u>											
Volume Collected	L	2.07	2.02	2.11	2.17	2.04	1.21	1.21	2.12	2.02	1.14
Vol. $\text{Na}_2\text{S}_2\text{O}_3$ Titrant	mL	7.6	5.8	8.64	3.25	3.55	11.2	6.9	6.6	5.25	4.8
<u>Feed Gas Analysis</u>											
Vol. Gas Collected	L	1.4	1.12	1.66	1.1	1.21	1.01	1.03	2.1	1.19	0.9
Vol. $\text{Na}_2\text{S}_2\text{O}_3$ Titrant	mL	15.25	16.6	15.5	18.9	8	39.1	44.15	33.95	17.2	33.65
Wet Test Meter Temp.	°C	23.5	23.6	23.7	23.8	23.5	23.3	23.2	23.1	23.7	23.7
Barometric Pressure	mmHg	709	690	690	690	690	690	690	690	693	693
Vol. Correction Factor		0.89	0.86	0.86	0.86	0.86	0.86	0.86	0.86	0.87	0.87
<u>Dissolved Ozone</u>											
<u>Conc. by UV 260</u>											
SMX Outlet	mg/L	0.35	0.33	0.31	0.49	0.28	0.48	0.60	0.43	0.46	0.50
Column Inlet	mg/L	2.00	1.88	0.83	0.93	1.24	2.47	2.26	1.87	1.53	1.57
Column Mid-Height	mg/L			0.78	0.70						1.48
Column Outlet	mg/L	0.81	1.06	0.68	0.76	0.53	1.17	0.99	0.86	0.81	1.22
<u>Calculated Variables</u>											
$G/Q_f$	%	4.42	2.72	4.18	1.69	4.03	1.16	1.19	2.63	2.65	1.23
SMX Sup. Velocity, $v_s$	m/s	0.58	0.93	0.61	1.39	0.99	0.64	0.99	0.95	0.95	0.60
Feed Gas Ozone Conc., $Y_f$	$\text{g/m}^3$	29.5	41.3	26.0	47.8	18.4	107.8	119.3	45.0	40.1	103.6
Off Gas Ozone Conc., $Y_o$	$\text{g/m}^3$	10.0	8.0	11.4	4.2	4.8	25.8	15.9	8.7	7.2	11.7
Transfer Efficiency, $TE$	%	66.3	80.6	56.1	91.3	73.7	76.1	86.7	80.7	82.0	88.7
<u>Mass Balance</u>											
Ozone Addition Rate	mg/L	1.3	1.1	1.1	0.8	0.7	1.3	1.4	1.2	1.1	1.3
Ozone Transfer Rate	mg/L	0.9	0.9	0.6	0.7	0.5	1.0	1.2	1.0	0.9	1.1
Ozone Loss	mg/L	0.1	-0.2	-0.1	0.0	0.0	-0.2	0.2	0.1	0.1	-0.1
Mass Balance Closure	%	7	-15	-10	-3	3	-18	23	11	8	-7

Table C-1 (continued)

TRIAL	Units	21	22	23	24	25	26	27	28	29	30	31
<u>Operating Conditions</u>												
Feed Water Flow, $Q_f$	L/min	11.5	11.5	15.9	15.9	16.3	15.7	11.1	11.1	7.7	10.0	10.0
Feed Gas Flow, $G$	L/min	0.47	0.14	0.42	0.19	0.19	0.19	0.29	0.29	0.30	0.14	0.14
SMX Inlet Pressure	psig	7.1	6.2	9	8.6	9	8.8	6.5	6.5	5.5	6.1	6.1
SMX Outlet Pressure	psig	4.1	4	4.5	4.4	4.5	4.5	4	4	3.6	4	4
Bubble Column Height, $H$	m	2.3	2.3	2.3	2.3	0.45	1.4	1.4	1.4	2.3	1.4	1.4
<u>Feed Water</u>												
DPD Total Chlorine	mg/L		0.32			0.24			0.48	0.29		
pH			8.5	8.5	8.5	8.0	8.3	8.6	8.5	8.0		
Temperature	°C	16.6	16.2	15.9	16.5	16.9	16.6	7	7	16.6	16.2	16.2
<u>Off-Gas Analysis</u>												
Volume Collected	L	2.05	1.28	2.24	1.73	2.02	1.95	2.01	2.06	2.35	2.06	2.13
Vol. $\text{Na}_2\text{S}_2\text{O}_3$ Titrant	mL	3.2	3.6	4.1	4.4	7.4	6.6	5.4	5.25	5.95	11.1	12.34
<u>Feed Gas Analysis</u>												
Vol. Gas Collected	L	1.19	1.25	1.05	1.01	1.23	1.05	1.04	1.06	1.4	1.03	1.03
Vol. $\text{Na}_2\text{S}_2\text{O}_3$ Titrant	mL	10.3	50.3	16.1	41.75	46.6	43.1	16.2	16.05	15.7	42.9	42.9
Wet Test Meter Temp.	°C	23.7	23.5	23.4	23.4	23.2	23	22.7	22.7	23	23	23
Barometric Pressure	mmHg	693	693	693	693	700	700	700	700	694	694	694
Vol. Correction Factor		0.87	0.87	0.87	0.87	0.88	0.88	0.88	0.88	0.87	0.87	0.87
<u>Dissolved Ozone</u>												
<u>Conc. by UV 260</u>												
SMX Outlet	mg/L	0.46	0.67	0.66	0.93	0.84	0.97	0.57	0.49	0.24	0.73	0.73
Column Inlet	mg/L	0.95	1.36	1.20	1.57	1.10	1.57	1.13	1.06	1.12	2.08	2.08
Column Mid-Height	mg/L	0.94	1.09	1.00	1.30					1.03		
Column Outlet	mg/L	0.85	1.10	0.97	1.27	1.03	1.24	1.02	0.93	0.80	1.22	1.22
<u>Calculated Variables</u>												
$G/Q_f$	%	4.09	1.19	2.63	1.19	1.17	1.21	2.65	2.65	3.92	1.37	1.37
SMX Sup. Velocity, $v_s$	m/s	0.99	0.99	1.37	1.37	1.40	1.35	0.96	0.96	0.67	0.86	0.86
Feed Gas Ozone Conc., $Y_f$	g/m <sup>3</sup>	24.0	111.5	42.5	114.6	103.9	112.6	42.7	41.5	31.0	115.2	115.2
Off Gas Ozone Conc., $Y_o$	g/m <sup>3</sup>	4.3	7.8	5.1	7.0	10.0	9.3	7.4	7.0	7.0	14.9	16.0
Transfer Efficiency, $TE$	%	82.0	93.0	88.1	93.8	90.3	91.8	82.8	83.2	77.4	87.1	86.1
<u>Mass Balance</u>												
Ozone Addition Rate	mg/L	1.0	1.3	1.1	1.4	1.2	1.4	1.1	1.1	1.2	1.6	1.6
Ozone Transfer Rate	mg/L	0.8	1.2	1.0	1.3	1.1	1.3	0.9	0.9	0.9	1.4	1.4
Ozone Loss	mg/L	0.0	0.1	0.0	0.0	0.1	0.0	-0.1	0.0	0.1	0.2	0.1
Mass Balance Closure	%	-5	12	1	1	7	1	-8	-2	18	12	11

**APPENDIX D**

**EXPERIMENTAL DATA AND INFORMATION FROM  
CHALLENGE EXPERIMENTS WITH *BACILLUS SUBTILIS*  
SPORES IN THE EXPERIMENTAL STATIC MIXER  
CONTACTOR AND IN BATCH REACTORS (CHAPTER 9)**

Table D-1 Static mixer contactor challenge experiments with *B. subtilis* spores:  
Ozonation conditions based on UV 260 absorbance method.

Trial	Units	34	35	36	37	38	39	40	41
<b>SMX Conditions</b>									
Feed Flow, $Q_f$	L/min	7.36	15.58	15.92	6.43	6.87	16.06	16.28	8.04
Gas Flow, $G$	L/min	0.092	0.391	0.197	0.203	0.092	0.388	0.196	0.2
Sup. Vel. $v_s$	m/s	0.63	1.34	1.37	0.55	0.59	1.38	1.40	0.69
$G/Q_f$	%	1.25	2.51	1.24	3.16	1.34	2.42	1.20	2.49
RFS Flow, $Q_{RFS}$	L/min	1.95	2.03	2.03	2.04	1.99	2.1	2.09	2.1
Pressure Drop, $\Delta p$	kPa	6.2	32.4	29.64	9.65	6.2	31.02	28.26	5.51
<b>Water</b>									
Avg. Temp	°C	16.6	16.0	15.8	16.4	15.6	15.4	16.2	16.4
DPD Total $Cl_2$	mg/L	0.06	0.18	0.19	0.12	0.19	0.2	0.21	0.42
pH		7.6	7.6	7.5	7.7	7.8	7.9	7.8	7.8
<b>Ozone Conc.</b>									
SMX Out	mg/L	0.22	0.57	0.76	0.50	0.46	0.58	0.57	0.62
Column In	mg/L	0.85	1.03	1.27	1.32	1.41	1.09	0.85	1.41
RFS In	mg/L	0.78	0.78	1.21	1.13	1.07	1.06	0.79	1.16
RFS 1/4	mg/L	0.66	0.75	1.06	1.04	1.01	1.01	0.68	1.13
RFS 1/2	mg/L	0.59	0.68	0.94	0.92	0.95	0.96	0.60	1.01
RFS 3/4	mg/L	0.49	0.69	0.93	0.88	0.84	0.90	0.56	0.96
RFS Out	mg/L	0.40	0.64	0.87	0.78	0.75	0.84	0.43	0.77
<b>Column</b>									
$t_m$	min	0.72	0.46	0.45	0.83	0.77	0.44	0.44	0.66
$C_{avg}$	mg/L	0.81	0.90	1.24	1.22	1.23	1.07	0.82	1.28
<b>RFS</b>									
$t_m$ 1/4	min	3.8	3.7	3.7	3.6	3.7	3.5	3.5	3.5
$t_m$ 1/2	min	7.9	7.6	7.6	7.5	7.7	7.3	7.3	7.3
$t_m$ 3/4	min	11.7	11.3	11.2	11.1	11.5	10.8	10.9	10.9
$t_m$ Out	min	15.6	15.1	15.1	15.0	15.4	14.5	14.6	14.6
$C_0$	mg/L	0.78	0.78	1.18	1.13	1.09	1.07	0.79	1.20
$k_d$	min <sup>-1</sup>	0.040	0.013	0.022	0.024	0.023	0.016	0.037	0.026
<b>Cumulative</b>									
$C_{avg} t_m$									
RFS In	mg×min/L	0.59	0.41	0.56	1.01	0.95	0.47	0.36	0.84
RFS 1/4	mg×min/L	3.33	3.19	4.69	4.93	4.86	4.14	2.98	4.90
RFS 1/2	mg×min/L	5.84	6.03	8.75	8.76	8.70	7.84	5.42	8.85
RFS 3/4	mg×min/L	7.84	8.56	12.25	12.03	11.99	11.12	7.41	12.22
RFS Out	mg×min/L	9.63	11.07	15.62	15.16	15.16	14.35	9.23	15.43

Table D-2 Static mixer contactor challenge experiments with *B. subtilis* spores:  
Ozonation conditions based on the indigo trisulphonate method.

Trial	Units	34	35	36	37	38	39	40	41
<b>SMX Conditions</b>									
Feed Flow, $Q_f$	L/min	7.36	15.58	15.92	6.43	6.87	16.06	16.28	8.04
Gas Flow, $G$	L/min	0.092	0.391	0.197	0.203	0.092	0.388	0.196	0.2
Sup. Vel. $v_s$	m/s	0.63	1.34	1.37	0.55	0.59	1.38	1.40	0.69
$G/Q_f$	%	1.25	2.51	1.24	3.16	1.34	2.42	1.20	2.49
RFS Flow, $Q_{RFS}$	L/min	1.95	2.03	2.03	2.04	1.99	2.1	2.09	2.1
Pressure Drop, $\Delta p$	kPa	6.2	32.4	29.64	9.65	6.2	31.02	28.26	5.51
<b>Water</b>									
Avg. Temp	°C	16.6	16.0	15.8	16.4	15.6	15.4	16.2	16.4
DPD Total $Cl_2$	mg/L	0.06	0.18	0.19	0.12	0.19	0.2	0.21	0.42
pH		7.6	7.6	7.5	7.7	7.8	7.9	7.8	7.8
<b>Ozone Conc.</b>									
SMX Out	mg/L	0.64	0.72	0.69	0.66	0.56	0.69	0.74	0.70
Column In	mg/L	1.41	1.17	1.42	1.45	1.33	1.28	1.03	1.66
RFS In	mg/L	1.34	0.97	1.47	1.27	1.35	1.08	0.92	1.62
RFS 1/4	mg/L	1.16	0.91	1.30	1.23	1.30	0.97	0.81	1.26
RFS 1/2	mg/L	0.95	0.83	1.12	1.04	1.28	0.84	0.68	1.07
RFS 3/4	mg/L	0.85	0.80	1.00	0.99	1.08	0.70	0.65	1.08
RFS Out	mg/L	0.75	0.77	0.98	0.94	1.02	0.66	0.58	0.91
<b>Column</b>									
$t_m$	min	0.72	0.46	0.45	0.83	0.77	0.44	0.44	0.66
$C_{avg}$	mg/L	1.37	1.07	1.44	1.36	1.34	1.17	0.97	1.64
<b>RFS</b>									
$t_m$ 1/4	min	3.8	3.7	3.7	3.6	3.7	3.5	3.5	3.5
$t_m$ 1/2	min	7.9	7.6	7.6	7.5	7.7	7.3	7.3	7.3
$t_m$ 3/4	min	11.7	11.3	11.2	11.1	11.5	10.8	10.9	10.9
$t_m$ Out	min	15.6	15.1	15.1	15.0	15.4	14.5	14.6	14.6
$C_0$	mg/L	1.33	0.96	1.45	1.29	1.38	1.09	0.91	1.54
$k_d$	min <sup>-1</sup>	0.039	0.016	0.030	0.023	0.018	0.037	0.032	0.039
<b>Cumulative</b>									
$C_{avg} t_m$									
RFS In	mg×min/L	1.0	0.5	0.7	1.1	1.0	0.5	0.4	1.1
RFS 1/4	mg×min/L	5.7	3.9	5.7	5.6	6.0	4.1	3.5	6.2
RFS 1/2	mg×min/L	10.0	7.4	10.5	10.0	11.0	7.5	6.4	10.9
RFS 3/4	mg×min/L	13.5	10.4	14.5	13.8	15.3	10.3	8.8	14.7
RFS Out	mg×min/L	16.6	13.4	18.2	17.5	19.5	12.8	11.0	18.2

Table D-3 Microorganism enumeration information from laboratory study with static mixer ozone contactor experiments with *B. subtilis* spores.

<b>Trial</b>	<b>34</b>	<b>35</b>	<b>36</b>	<b>37</b>	<b>38</b>	<b>39</b>	<b>40</b>	<b>41</b>
Spore Stock	B	C	B	C	C	C	B	B
<u>Log Spore Conc.</u>								
Feed	4.6	4.8	4.2	5.0	5.0	4.5	4.1	4.7
SMX Out	4.3	4.7	4.2	4.9	5.0	4.6	4.0	4.6
RFS In	4.3	4.6	4.2	5.0	4.9	4.4	4.0	4.7
RFS 1/4	4.2	4.5	3.7	4.2	4.3	4.4	4.1	4.0
RFS 1/2	2.2	3.0	1.5	1.9	1.7	2.9	3.1	0.9
RFS 3/4	0.1	0.8	-0.3	0.2	0.1	0.5	1.4	0.0
RFS Out	-0.1	-0.2	-0.3	-0.1	-1.1	-0.2	0.1	-0.8
<u>Log Inactivation</u>								
SMX Out	0.30	0.01	0.01	0.04	0.07	-0.03	0.11	0.11
RFS In	0.3	0.1	-0.1	0.0	0.1	0.1	0.1	0.0
RFS 1/4	0.3	0.2	0.5	0.7	0.7	0.2	0.0	0.7
RFS 1/2	2.5	1.7	2.7	3.0	3.3	1.6	1.0	3.7
RFS 3/4	4.5	3.9	4.5	4.7	5.0	4.0	2.7	4.7
RFS Out	4.6	4.9	4.5	5.0	6.1	4.7	4.0	5.5
<u>95 % Confidence Interval</u>								
SMX Out	0.5	0.1	0.5	0.2	0.2	0.2	0.4	0.4
RFS In	0.4	0.3	0.3	0.2	0.2	0.4	0.4	0.3
RFS 1/4	0.4	0.1	0.7	0.2	0.5	0.2	0.4	0.3
RFS 1/2	0.3	0.2	0.4	0.4	0.3	0.3	0.4	0.2
RFS 3/4	0.4	0.1	0.9	0.2	0.3	0.2	0.4	0.4
RFS Out	0.3	0.1	0.4	0.2	0.6	0.2	0.5	0.9

**Table D-4** Batch reactor ozonation trials with *B. subtilis* (ATCC 6633) spores. All trials were conducted in samples of feed water from the static mixer ozone contactor at 16°C.

Trial	pH	$C_a$	$t_b$	Direct UV Absorbance @ 260 nm						Indigo Trisulphonate Colorimetric Method						log $N$	log $N_0$	-log ( $N/N_0$ )	± 95% conf.
				$C_0$	$C_f$	$C_a - C_0$	$k_d$	$C_{avg}$	$C_{avg}t$	$C_0$	$C_f$	$C_a - C_0$	$k_d$	$C_{avg}$	$C_{avg}t$				
		mg/L	min	mg/L	mg/L	mg/L	/min	mg/L	mg× min/L	mg/L	mg/L	mg/L	/min	mg/L	mg× min/L	log- units	log-units	log-units	log-units
1	7.8	1.8	7.0	0.70	0.41	1.10	0.08	0.55	3.8	1.13	0.59	0.7	0.09	0.83	5.9	4.7	5.9	1.2	0.2
2	7.8	2.08	20.0	0.85	0.18	1.23	0.08	0.43	8.6	1.28	0.21	0.8	0.09	0.59	11.8	2.8	5.9	3.2	0.3
3	7.8	2.37	30.0	1.27	0.08	1.10	0.09	0.43	13.0	1.79	0.11	0.6	0.09	0.60	18.1	1.9	5.9	4.0	0.2
5	7.8	2.49	12.0	1.20	0.31	1.29	0.11	0.66	7.9	1.84	0.30	0.7	0.15	0.85	10.2	2.1	6.0	3.8	0.2
6	7.8	1.51	3.0	0.47	0.31	1.04	0.14	0.39	1.2	0.75	0.41	0.8	0.20	0.56	1.7	6.0	6.0	0.0	0.2
7	7.8	1.77	20.0	0.83	0.15	0.94	0.09	0.40	8.0	1.20	0.20	0.6	0.09	0.56	11.1	2.3	6.0	3.7	0.2
9	7.8	1.46	12.0	0.71	0.34	0.75	0.06	0.50	6.0	1.19	0.52	0.3	0.07	0.81	9.7	3.0	6.1	3.0	0.3
10	7.8	2.48	3.0	1.71	1.03	0.77	0.17	1.34	4.0	2.55	1.42	-0.1	0.20	1.93	5.8	5.0	6.1	1.1	0.1
11	7.8	2.07	7.0	1.34	0.52	0.73	0.14	0.87	6.1	1.87	0.71	0.2	0.14	1.20	8.4	3.0	6.1	3.1	0.3
14	7.8	1.81	10.0	1.04	0.53	0.77	0.07	0.76	7.6	1.38	0.68	0.4	0.07	0.99	9.9	2.5	6.0	3.5	0.2
15	7.8	1.45	7.0	0.73	0.39	0.72	0.09	0.54	3.8	0.98	0.59	0.5	0.07	0.77	5.4	5.1	6.0	0.9	0.2
17	7.8	2.93	19.0	1.84	0.26	1.09	0.10	0.81	15.4	2.78	0.27	0.1	0.12	1.08	20.6	1.2	6.0	4.8	0.2
18	7.8	2.08	6.0	1.08	0.45	1.00	0.15	0.72	4.3	1.80	0.56	0.3	0.19	1.06	6.4	4.3	6.0	1.7	0.2
19	7.8	1.85	3.0	0.90	0.56	0.95	0.16	0.71	2.1	1.36	0.87	0.5	0.15	1.10	3.3	5.9	6.0	0.1	0.2
22	7.8	1.91	15.5	1.99	0.52	-0.08	0.09	1.10	17.0	2.19	0.60	-0.3	0.08	1.23	19.0	0.7	5.5	4.8	0.2
23	7.8	1.89	4.0	1.98	1.19	-0.09	0.13	1.55	6.2	2.47	1.45	-0.6	0.13	1.91	7.7	3.0	5.5	2.5	0.2
25	7.8	1.9	15.0	2.07	0.51	-0.17	0.09	1.11	16.7	2.43	0.58	-0.5	0.10	1.29	19.3	1.1	6.3	5.2	0.3
26	7.8	2.02	10.0	2.09	0.91	-0.07	0.08	1.42	14.2	2.55	1.04	-0.5	0.09	1.68	16.8	1.7	6.3	4.6	0.3
27	7.8	1.93	4.0	2.12	1.42	-0.19	0.10	1.74	7.0	2.42	1.77	-0.5	0.08	2.08	8.3	3.3	6.3	3.0	0.2

**Notes:** Trials 1 through 15 were conducted with spore batch preparation B. Trials 16 through 27 were conducted with spore batch preparation C.

**APPENDIX E      INFORMATION FROM CHALLENGE EXPERIMENTS IN  
THE EXPERIMENTAL STATIC MIXER OZONE  
CONTACTOR AND BATCH OZONE REACTORS WITH  
*CRYPTOSPORIDIUM PARVUM* OOCYSTS (CHAPTER 10)**

Table E-1 Static mixer contactor experiments with *Cryptosporidium parvum* oocysts:  
Ozonation conditions based on UV 260 absorbance method.

Trial	Units	43	44	45	46	47	48	49	50	51
<b>SMX Conditions</b>										
Feed Flow, $Q_f$	L/min	7.29	7.48	7.9	7.49	7.6	12.96	7.49	7.49	16.01
Gas Flow, $G$	L/min	0.092	0.92	0.093	0.093	0.093	0.203	0.093	0.093	0.20
Sup. Vel. $v_s$	m/s	0.63	0.64	0.68	0.64	0.65	1.12	0.64	0.64	1.38
$G/Q_f$	%	1.26	1.23	1.18	1.24	1.22	1.57	1.24	1.24	1.26
RFS Flow, $Q_{RFS}$	L/min	2.05	2.05	2.06	2.06	2.06	2.05	2.05	2.09	2.09
Pressure Drop, $\Delta p$	kPa	6.2	5.51	7.58	6.89	7.58	34.46	7.58	7.58	31.7
<b>Water</b>										
Avg. Temp	°C	22.2	21.6	22.3	21.7	21.9	21.9	21.8	22.3	21.7
DPD Total $Cl_2$	mg/L	0.02	0.10	0.18	0.02	0.13	0.13	0.00	0.14	0.23
pH		7.2	7.9	8.1	7.9	7.8	7.8	7.7	8.0	7.8
<b>Ozone Conc.</b>										
SMX Out	mg/L	0.33	0.27	0.35	0.22	0.25	0.33	0.27	0.23	0.37
Column In	mg/L	0.72	0.59	0.82	0.70	0.71	0.62	0.68	0.62	0.63
RFS In	mg/L	0.51	0.54	0.74	0.55	0.61	0.56	0.53	0.55	0.51
RFS 1/4	mg/L	0.38	0.45	0.66	0.52	0.51				
RFS 1/2	mg/L	0.30	0.44	0.59	0.51	0.43	0.56	0.49	0.47	0.45
RFS 3/4	mg/L	0.28	0.34			0.32				
RFS Out	mg/L	0.22	0.30	0.53	0.34	0.27	0.50	0.41	0.39	0.39
<b>Column</b>										
$t_m$	min	0.73	0.71	0.67	0.71	0.70	0.55	0.71	0.71	0.45
$C_{avg}$	mg/L	0.60	0.56	0.78	0.62	0.66	0.59	0.60	0.58	0.56
<b>RFS</b>										
$t_m$ 1/4	min	3.6	3.6	1.8	1.8	3.7				
$t_m$ 1/2	min	7.5	7.5	3.6	3.6	7.6	1.81	1.8	1.8	1.8
$t_m$ 3/4	min	11.1	11.1			11.3				
$t_m$ Out	min	14.9	14.9	7.5	7.4	15.1	3.63	3.6	3.6	3.6
$C_0$	mg/L	0.50	0.53	0.73	0.57	0.62	0.57	0.54	0.55	0.51
$k_d$	min <sup>-1</sup>	0.055	0.037	0.047	0.059	0.055	0.028	0.070	0.091	0.075
<b>Cumulative <math>C_{avg}t_m</math></b>										
RFS In	mg×min/L	0.44	0.40	0.52	0.44	0.46	0.32	0.43	0.41	0.25
RFS 1/4	mg×min/L	2.08	2.21	1.78	1.41	2.52	0.32	0.43	0.41	0.25
RFS 1/2	mg×min/L	3.50	3.89	2.93	2.29	4.30	1.33	1.34	1.31	1.10
RFS 3/4	mg×min/L	4.59	5.27	0.52	0.44	5.66	0.32	0.43	0.41	0.25
RFS Out	mg×min/L	5.52	6.52	5.09	3.88	6.81	2.28	2.15	2.07	1.85

Table E-2 Static mixer contactor experiments with *Cryptosporidium parvum* oocysts: ozonation conditions based on indigo trisulphonate method.

Trial		43	44	45	46	47	48	49	50	51
<b>SMX Conditions</b>										
Feed Flow, $Q_f$	L/min	7.29	7.48	7.9	7.49	7.6	12.96	7.49	7.49	16.01
Gas Flow, $G$	L/min	0.092	0.92	0.093	0.093	0.093	0.203	0.093	0.093	0.20
Sup. Vel. $v_s$	m/s	0.63	0.64	0.68	0.64	0.65	1.12	0.64	0.64	1.38
$G/Q_f$	%	1.26	12.30	1.18	1.24	1.22	1.57	1.24	1.24	1.26
RFS Flow, $Q_{RFS}$	L/min	2.05	2.05	2.06	2.06	2.06	2.05	2.05	2.09	2.09
Pressure Drop, $\Delta p$	kPa	6.2	5.51	7.58	6.89	7.58	34.46	7.58	7.58	31.7
<b>Water</b>										
Avg. Temp	°C	22.2	21.6	22.3	21.7	21.9	21.9	21.8	22.3	21.7
DPD Total $Cl_2$	mg/L	0.02	0.10	0.18	0.02	0.13	0.13	0.00	0.14	0.23
pH		7.2	7.9	8.1	7.9	7.8	7.8	7.7	8.0	7.8
<b>Ozone Conc.</b>										
SMX Out	mg/L	0.41	0.27	0.54	0.34	0.26	0.33	0.30	0.23	0.40
Column In	mg/L	0.85	0.59	1.09	0.82	0.94	0.62	0.80	0.73	0.63
RFS In	mg/L	0.72	0.54	0.92	0.64	0.76	0.56	0.78	0.59	0.57
RFS 1/4	mg/L	0.58	0.45	0.81	0.62	0.62				
RFS 1/2	mg/L	0.51	0.44	0.77	0.56	0.52	0.56	0.80	0.51	0.46
RFS 3/4	mg/L	0.43	0.34			0.43				
RFS Out	mg/L	0.39	0.30	0.59	0.47	0.34	0.50	0.69	0.45	0.42
<b>Column</b>										
$t_m$	min	0.73	0.71	0.67	0.71	0.70	0.55	0.71	0.71	0.45
$C_{avg}$	mg/L	0.78	0.56	1.00	0.72	0.85	0.59	0.79	0.66	0.60
<b>RFS</b>										
$t_m$ 1/4	min	3.6	3.6	1.8	1.8	3.7				
$t_m$ 1/2	min	7.5	7.5	3.6	3.6	7.6	1.81	1.8	1.8	1.8
$t_m$ 3/4	min	11.1	11.1			11.3				
$t_m$ Out	min	14.9	14.9	7.5	7.4	15.1	3.63	3.6	3.6	3.6
$C_0$	mg/L	0.71	0.65	0.92	0.65	0.76	0.71	0.80	0.59	0.56
$k_d$	min <sup>-1</sup>	0.040	0.026	0.056	0.041	0.053	0.025	0.031	0.077	0.091
<b>Cumulative <math>C_{avg}t_m</math></b>										
RFS In	mg×min/L	0.57	0.40	0.67	0.51	0.59	0.32	0.56	0.47	0.27
RFS 1/4	mg×min/L	2.96	2.64	2.24	1.63	3.13	0.32	0.56	0.47	0.27
RFS 1/2	mg×min/L	5.17	4.82	3.65	2.68	5.36	1.58	1.97	1.45	1.19
RFS 3/4	mg×min/L	6.95	6.66	0.67	0.51	7.07	0.32	0.56	0.47	0.27
RFS Out	mg×min/L	8.55	8.41	6.25	4.67	8.53	2.79	3.30	2.31	1.97

Table E-3 Infectivity analysis with the CD-1 mouse infectivity assay in the static mixer contactor experiments with *Cryptosporidium parvum* oocysts.

Trial	Sample	Oocyst Recovery	$d_0$	Mice in Cohort	Mice Infected	$P$	$d$	log Inactivation - log ( $d/d_0$ )	Average log Inactivation -log ( $d/d_0$ )
43	Feed	73	50	5	3	0.60	71	-0.15	-0.15
			500	5	5	1.00	> 18	< 0.52	
	SMX Out	67	50	3	2	0.67	89	-0.25	-0.25
			500	4	4	1.00	> 121	< 0.62	
			5 000	5	5	1.00	> 152	< 1.52	
	RFS Out	67	500	5	0	0.00	< 18	> 1.45	3.12
5 000			5	0	0.00	< 18	> 2.45		
50 000			5	2	0.40	38	3.12		
44	Feed	64	50	5	3	0.60	71	-0.15	-0.15
			500	5	5	1.00	> 152	< 0.52	
	SMX Out	55	50	5	3	0.60	71	-0.15	-0.15
			500	5	5	1.00	> 152	< 0.52	
			5 000	5	5	1.00	> 152	< 1.52	
	RFS Out	64	1 000	5	0	0.00	< 18	> 1.75	> 3.25
10 000			5	1	0.20	18	2.75		
100 000			5	1	0.20	< 18	> 3.75		
45	Feed	63	50	5	4	0.80	152	-0.48	-0.48
			500	5	5	1.00	> 152		
	SMX Out	44	50	5	2	0.40	38	0.12	0.32
			500	5	4	0.80	152	0.52	
			5 000	5	5	1.00	> 152	< 1.5	
	RFS Out	43	500	5	0	0.00	< 18	> 1.44	3.12
5 000			5	0	0.00	< 18	> 2.44		
50 000			5	2	0.40	38	3.12		
46	Feed	43	50	5	1	0.20	18	0.45	0.65
			500	5	3	0.60	71	0.85	
	SMX Out	30	50	7	1	0.14	13	0.59	0.97
			500	8	2	0.25	22	1.36	
	RFS Out	10	2 000	7	1	0.14	13	2.19	2.30
			20 000	8	5	0.63	77	2.42	

Table E-3 (continued)

Trial	Sample	Oocyst Recovery	$d_0$	Mice in Cohort	Mice Infected	$P$	$d$	log Inactivation - log ( $d/d_0$ )	Average log Inactivation -log ( $d/d_0$ )
47	Feed	32	50	5	1	0.20	18	0.45	0.45
			500	5	5	1.00	> 152	< 0.52	
	SMX Out	25	50	7	3	0.43	41	0.08	0.08
		500	8	8	1.00	> 234	< 0.33		
RFS Out	17	9 000 90 000	50	7	1	0.14	13	2.84	3.37
			500	8	1	0.13	11	3.90	
48	Feed	17	50	6	1	0.17	15	0.53	0.64
			500	6	4	0.67	89	0.75	
	RFS Out	22	1 000 10 000	10 10	6 8	0.60 0.80	71 152	1.15 1.82	1.48
49	Feed	51	50	6	3	0.50	52	-0.01	0.21
			500	6	5	0.83	180	0.44	
	RFS Out	6	1 000 10 000	10 10	2 9	0.20 0.90	18 284	1.75 1.55	1.65
50	Feed	52	50	5	3	0.60	71	-0.15	0.18
			500	5	4	0.80	152	0.52	
	RFS Out	63	500 5 000	8 7	1 2	0.13 0.29	11 25	1.64 2.29	1.97
51	Feed	56	50	5	2	0.40	38	0.12	0.12
			500	5	5	1.00	> 152	< 0.52	
	RFS Out	60	500 5 000	8 7	1 6	0.13 0.86	11 208	1.64 1.38	1.51
<sup>1</sup> 52	Feed	48	50	5	1	0.20	18	0.45	0.45
			500	5	5	1.00	> 152	< 0.52	
RFS Out	61	50 500	50	7	3	0.43	41	0.08	0.45
			500	8	5	0.63	77	0.81	

<sup>1</sup>No ozone addition control trial.

**Table E-4** Ozonation conditions in batch ozone reactor experiments with *Cryptosporidium parvum* oocysts. All trials were conducted in samples of feed water from the static mixer ozone contactor at 22°C.

Trial	pH	$C_a$	$t_b$	Direct UV Absorbance @ 260 nm						Indigo Trisulphonate Colorimetric Method						$-\log(N/N_0)$
				$C_0$	$C_f$	$C_a - C_0$	$k_d$	$C_{avg}$	$C_{avg}t$	$C_0$	$C_f$	$C_a - C_0$	$k_d$	$C_{avg}$	$C_{avg}t$	
		mg/L	min	mg/L	mg/L	mg/L	/min	mg/L	mg× min/L	mg/L	mg/L	mg/L	/min	mg/L	mg× min/L	
1	7.8	1.43	12	1.55	0.23	-0.12	0.16	0.69	8.34	1.72	0.31	-0.29	0.14	0.82	9.85	2.7
2	7.9	0.8	12.3	0.88	0.2	-0.08	0.12	0.46	5.63	0.95	0.18	-0.15	0.13	0.46	5.7	2.8
3	7.9	0.79	4	1.04	0.5	-0.25	0.18	0.74	2.94	0.99	0.23	-0.2	0.13	0.78	3.13	1.9
4	7.8	1.35	12	1.43	0.24	-0.08	0.15	0.67	8.02	1.79	0.3	-0.44	0.15	0.83	9.98	2.8
5	7.8	0.79	4.9	0.77	0.31	0.02	0.19	0.51	2.46	0.85	0.4	-0.06	0.16	0.6	2.9	1.4
6	7.9	0.79	4	0.81	0.28	-0.02	0.26	0.5	1.99	1	0.33	-0.21	0.28	0.61	2.42	2.2
7	7.9	0.79	12	0.77	0.04	0.02	0.25	0.24	2.91	0.92	0.04	-0.13	0.27	0.27	3.28	2.3

Table E-5 Infectivity analysis with the neonatal CD-1 mouse infectivity assay in the batch ozone reactor experiments with *Cryptosporidium parvum* oocysts.

Trial	Sample	Oocyst Recovery	$d_0$	Mice in Cohort	Mice Infected	$P$	$d$	log Inactivation - log ( $d/d_0$ )	Average log Inactivation -log ( $d/d_0$ )
1	Exposure	23	10 000 100 000	5 10	2 6	0.40 0.60	38 71	2.42 3.15	2.79
	Control	55	50 500	5 4	2 4	0.40 1.00	38 > 121	0.12 < 0.62	
2	Exposure	11	500 5 000 50 000	5 5 5	0 1 2	0.00 0.20 0.40	< 18 18 38	> 1.45 2.45 3.12	2.79
	Control	24	50 500	5 5	2 5	0.40 1.00	38 > 152	0.12 < 0.52	
3	Exposure	39	500 5 000 50 000	5 5 5	0 3 5	0.00 0.60 1.00	< 18 71 > 152	> 1.45 1.85 < 2.52	1.85
	Control	54	50 500	5 5	4 5	0.80 1.00	152 > 152	-0.48 < 0.52	
4	Exposure	27	100 1 000 10 000	5 5 5	0 0 1	0.00 0.00 0.20	< 18 < 18 18	> 1.45 > 1.75 2.75	2.75
	Control	73	50 500	5 5	1 2	0.20 0.40	18 38	0.45 1.12	
5	Exposure	21	1 000 10 000	7 8	4 7	0.57 0.88	65 234	1.19 1.63	1.41
	Control	64	50 500	5 5	3 5	0.60 1.00	71 > 152	-0.15 < 0.52	
6	Exposure	51	500 5 000	7 8	0 3	0.00 0.38	< 13 35	> 1.59 2.16	2.16
7	Exposure	57	1 000 10 000	7 8	0 4	0.00 0.50	< 13 52	> 1.89 2.29	2.29
	Control	58	50 500	5 5	3 5	0.60 1.00	71 > 152	-0.15 < 0.52	

**APPENDIX F                    INFORMATION FROM CHALLENGE EXPERIMENTS IN  
THE STATIC MIXER OZONE CONTACTOR AND BATCH  
OZONE REACTORS WITH *GIARDIA MURIS* CYSTS  
(CHAPTER 11)**

Table F-1 Static mixer ozone contactor experiments with *Giardia muris* cysts:  
Ozonation conditions based on the UV 260 absorbance method.

Trial	Units	54	55	56	57	58	59
<b>SMX Conditions</b>							
Feed Flow, $Q_f$	L/min	5.29	13.35	4.55	15.37	5.01	15.43
Gas Flow, $G$	L/min	0.09	0.2	0.09	0.2	0.09	0.21
Sup. Vel. $v_s$	m/s	0.46	1.15	0.39	1.32	0.43	1.33
$G/Q_f$	%	1.70	1.50	1.98	1.30	1.80	1.36
RFS Flow, $Q_{RFS}$	L/min	2.04	2.07	2.03	2.07	2.05	2.03
Pressure Drop, $\Delta p$	kPa	11.0	40.7	7.6	33.8	9.7	36.5
<b>Water</b>							
Avg. Temp	°C	21.9	22.0	21.7	21.5	22.0	22.1
DPD Total $Cl_2$	mg/L	0.22	0.21	0.12	0.21	0.18	0.03
pH		7.7	7.9	8.0	7.9	7.8	7.8
<b>Ozone Conc.</b>							
SMX Out	mg/L	0.05	0.04	0.05	0.06	0.02	0.05
Column In	mg/L	0.15	0.08	0.16	0.11	0.10	0.10
RFS In	mg/L	0.08	0.08	0.11	0.09	0.07	0.06
RFS 1/2	mg/L	0.06	0.04	0.09	0.07	0.05	0.04
RFS Out	mg/L	0.05	0.05	0.08	0.06	0.03	0.03
<b>Column</b>							
$t_m$	min	1.21	0.60	1.31	0.51	1.25	0.51
$C_{avg}$	mg/L	0.11	0.08	0.13	0.10	0.09	0.08
<b>RFS</b>							
$t_m$ 1/2	min	1.8	1.8	1.8	1.8	1.8	1.84
$t_m$ Out	min	3.7	3.6	3.7	3.6	3.6	3.67
$C_0$	mg/L	0.08	0.07	0.11	0.09	0.07	0.06
$k_d$	min <sup>-1</sup>	0.153	0.179	0.096	0.128	0.230	0.201
<b>Cumulative <math>C_{avg t_m}</math></b>							
RFS In	mg×min/L	0.13	0.05	0.17	0.05	0.11	0.04
RFS 1/2	mg×min/L	0.27	0.16	0.35	0.19	0.21	0.13
RFS Out	mg×min/L	0.37	0.25	0.51	0.31	0.28	0.20

Table F-2 Static mixer ozone contactor experiments with *Giardia muris* cysts:  
Ozonation conditions based on the indigo trisulphonate method.

Trial	Units	54	55	56	57	58	59
<b>SMX Conditions</b>							
Feed Flow, $Q_f$	L/min	5.29	13.35	4.55	15.37	5.01	15.43
Gas Flow, $G$	L/min	0.09	0.2	0.09	0.2	0.09	0.21
Sup. Vel. $v_s$	m/s	0.46	1.15	0.39	1.32	0.43	1.33
$G/Q_f$	%	1.70	1.50	1.98	1.30	1.80	1.36
RFS Flow, $Q_{RFS}$	L/min	2.04	2.07	2.03	2.07	2.05	2.03
Pressure Drop, $\Delta p$	kPa	11.0	40.7	7.6	33.8	9.7	36.5
<b>Water</b>							
Avg. Temp	°C	21.9	22.0	21.7	21.5	22.0	22.1
DPD Total $Cl_2$	mg/L	0.22	0.21	0.12	0.21	0.18	0.03
pH		7.7	7.9	8.0	7.9	7.8	7.8
<b>Ozone Conc.</b>							
SMX Out	mg/L	0.05	0.07	0.05	0.07	0.02	0.05
Column In	mg/L	0.15	0.07	0.16	0.12	0.08	0.09
RFS In	mg/L	0.08	0.06	0.12	0.11	0.06	0.08
RFS 1/2	mg/L	0.06	0.06	0.11	0.09	0.05	0.05
RFS Out	mg/L	0.05	0.03	0.09	0.07	0.04	0.03
<b>Column</b>							
$t_m$	min	1.21	0.60	1.31	0.51	1.25	0.51
$C_{avg}$	mg/L	0.11	0.07	0.14	0.11	0.07	0.09
<b>RFS</b>							
$t_m$ 1/2	min	1.8	1.8	1.8	1.8	1.8	1.84
$t_m$ Out	min	3.7	3.6	3.7	3.6	3.6	3.67
$C_0$	mg/L	0.08	0.07	0.12	0.11	0.06	0.08
$k_d$	min <sup>-1</sup>	0.116	0.152	0.065	0.127	0.058	0.255
<b>Cumulative <math>C_{avtm}</math></b>							
RFS In	mg×min/L	0.13	0.04	0.18	0.06	0.09	0.04
RFS 1/2	mg×min/L	0.26	0.15	0.38	0.23	0.18	0.16
RFS Out	mg×min/L	0.37	0.23	0.56	0.37	0.27	0.23

**Table F-3 Latent period infectivity analysis in adult-male C3H HeN mice for static mixer ozone contactor experiments with *Giardia muris*.**

Trial	Sample	Cyst Recovery %	Cysts in Inoculum $d_0$	Cyst production on successive days post infection (DPI)						Latent Period LP, d	Live Cysts in Inoculum $d$	$-\log (d/d_0)$	
				2	3	4	5	6	7				8
153	Feed	7	4 940	< 1.9	2.9	5.2	5.9				3.5	7,596	-0.19
	SMX Out	3	2 500	< 1.9	1.9	4.8	5.9				3.7	3,933	-0.20
	RFS Out	5	3 380	< 1.9	< 1.9	3.1	5.8	5.9			4.3	797	0.63
54	Feed	10	8 310	< 2.0	2.0	5.4	5.8				3.1	5,491	0.18
	SMX Out	17	13 700	< 2.0	3.8	5.8					4.6	22,951	-0.22
	RFS Out	0.3	220	< 2.0	2.9	3.6	4.1	5.1	5.4		3.6	376	-0.23
55	Feed	11	7 560	< 2.0	3.2	5.5					3.3	12,541	-0.22
	SMX Out	14	9 810	< 2.0	3.7	5.7					3.2	20,325	-0.32
	RFS Out	2	1 440	< 2.0	< 2.0	< 2.0	< 2.0	< 2.0	< 2.0	< 2.0	> 6.5	< 10	> 2.2
56	Feed	39	23 500	< 2.0	4.4	5.9					2.9	53,401	-0.36
	SMX Out	31	15 800	< 2.0	3.7	5.7					3.2	20,103	-0.11
	RFS Out	3	3 000	< 2.0	< 2.0	2.9	3.2	4.9	5.3	5.8	5.3	86	1.54
57	Feed	64	33 900	< 2.0	5.1	6.1					2.8	83,177	-0.39
	SMX Out	41	24 100	< 2.0	4.7	5.9					2.6	130,412	-0.73
	RFS Out	19	10 800	< 2.0	< 2.0	3.3	4.8	5.7	5.7	5.8	4.5	537	1.30

<sup>1</sup>No ozone addition control trial.

Table F-3 (Continued)

Trial	Sample	Cyst Recovery %	Cysts in Inoculum $d_0$	Cyst production on successive days post infection (DPI)								Latent Period LP, d	Live Cysts in Inoculum $d$	-log ( $d/d_0$ )
				2	3	4	5	6	7	8				
58	Feed	30	6 690	< 2.1	< 2.1	5.5						3.6	5,993	0.05
	SMX Out	28	13 600	< 2.1	3.2	5.9						3.3	15,011	-0.04
	RFS Out	12	10 900	< 2.1	< 2.1	2.1	2.1	2.1	2.1	2.1	2.1	> 6.5	< 10	> 3.04
59	Feed	30	19 100	< 2.1	4.4	6.1						2.9	58,832	-0.49
	SMX Out	22	25 400	< 2.1	4.0	5.9						2.6	133,887	-0.72
	RFS Out	11	27 300	< 2.1	< 2.1	2.1	2.1	2.1	4.2	4.7		> 6.5	< 10	> 3.44

298

Notes:

- Cyst production is shown as the log<sub>10</sub> of the average cyst production of the mouse cohort in cysts/g wet feces.
- A < value for cyst production indicates that no cysts were observed under microscopic analysis with a hemocytometer. The value is the detection limit and is based on the observation of 1 cysts and the average daily wet feces output per mouse and observation of 4 hemocytometer wells.
- maximum latent period determined in the dose response experiments is 6.5 days.
- In trials 57, 58 and 59, the 8 L samples were split and were filtered through two 47mm PCTE membrane filters(4 L per filter) to improve cyst recovery. In all other trials, only 1 membrane filter was used for all 8 L.

**Table F-4** Batch ozonation trials with *Giardia muris* cysts and simplified Hom model predictions. Experimental information extracted from Charles Labatiuk Ph. D. thesis (1992).

<b>Trial</b>	<b>pH</b>	<b>Batch Time <math>t_b</math></b>	<b>Applied Ozone <math>C_a</math></b>	<b>Initial Ozone <math>C_0</math></b>	<b>Final Ozone <math>C_f</math></b>	<b><math>C_{avg}</math></b>	<b><math>C_{avg}t_b</math></b>	<b>Measured <math>-\log N/N_0</math></b>	<b>Hom Model Prediction <math>-\log N/N_0</math></b>	<b>Model Error</b>
		min	mg/L	mg/L	mg/L	mg/L	mg×min/L			
A1	6.7	5	0.62	0.47	0.3	0.38	1.88	4.2	3.71	0.49
A2	6.7	5	0.64	0.52	0.4	0.46	2.28	4.2	3.84	0.36
B1	6.7	5	0.26	0.18	0.1	0.13	0.67	3.1	3.10	0.00
B2	6.7	5	0.3	0.22	0.1	0.15	0.74	3.1	3.15	-0.05
C1	6.7	5	2.55	2.14	1.3	1.67	8.34	4.4	4.83	-0.43
C2	6.7	0.58	0.13	0.07	0.04	0.05	0.03	1.2	1.79	-0.59
D1	6.7	0.58	0.28	0.15	0.2	0.17	0.10	2.2	2.21	-0.01
30-4	7.6	2	2.73	2.1	1.36	1.69	3.38	3.4	4.12	-0.72
30-7	7.6	7	1.54	1.48	0.29	0.66	4.59	4	4.35	-0.35
36-4	7.6	5	0.82	0.7	0.36	0.50	2.51	5.1	3.91	1.19

Notes:

- All trials were conducted in ozone demand-free 0.05 M phosphate buffered ultrapure water at 22°C.

**APPENDIX G      CALCULATION OF THE NUMBER OF OZONE  
MOLECULES TO OOCYSTS IN A DISSOLVED OZONE  
SOLUTION**

**Assumptions:**

- Oocysts are 5  $\mu\text{m}$  in diameter and are spherical
- Concentration of dissolved ozone is 1 mg/L
- Molecular weight of ozone is 48 g/gmole

Volume of a single oocyst,  $V_o$ :

$$V_o = 1/6 \pi d^3 = 1/6 \pi (5 \times 10^{-6})^3 = 6.5 \times 10^{-17} \text{ m}^3 = 6.5 \times 10^{-14} \text{ L}$$

No. ozone molecules of per L @ 1 mg/L:

$$\begin{aligned} &= 1 \text{ mg/L} / [(48 \text{ mg/mole})(1000 \text{ mmole/gmole})] \times 6.02 \times 10^{23} \text{ molecules/gmole} \\ &= 1.3 \times 10^{19} \text{ molecules/L} \end{aligned}$$

No. ozone molecule per oocysts:

$$= (1.3 \times 10^{19} \text{ molecules/L}) / (6.5 \times 10^{-14} \text{ L/oocyst}) = 8 \times 10^5 \text{ O}_3 \text{ molecules/oocyst}$$

**APPENDIX H      CALCULATIONS OF HYDRODYNAMIC CONDITIONS  
WITHIN THE STATIC MIXER**

## **CALCULATION OF VELOCITY GRADIENT, G, IN THE EXPERIMENTAL STATIC MIXER:**

The velocity gradient was estimated using the conventional definition of G as given by Camp and Stein (1943):

$$G = \sqrt{\frac{P}{\mu V}}$$

For the static mixer, the power dissipation was estimated from the measured pressure drop that was provided in Tables D-1, D-2, E-1, E-1 and F-1 and F-2. Based on the information in these tables, approximate pressure drop,  $\Delta p$ , was:

Case 1:  $Q_f = 7 \text{ L/min}$ ,  $v_s = 0.6 \text{ m/s} \rightarrow \Delta p = 6 \text{ kPa}$

Case 2:  $Q_f = 16 \text{ L/min}$ ,  $v_s = 1.4 \text{ m/s} \rightarrow \Delta p = 32 \text{ kPa}$

Calculations were done base on a water temperature of 22°C and the following values for the water properties:

Specific Weight,  $\gamma = 9.78 \text{ kN/m}^3$

Viscosity,  $\mu = 0.957 \times 10^{-3} \text{ Ns/m}^2$

Density,  $\rho = 998 \text{ kg/m}^3$

The volume of the static mixer was taken to be the volume of the 3 mixing elements themselves:

$$V = 3 \times (0.015 \text{ m}) (3.14/4)(0.0157\text{m})^2 = 8.7 \times 10^{-6} \text{ m}^3 \quad (8.7 \text{ mL})$$

The power dissipation was estimated from the pressure drop as follows:

$$P = \gamma Q_f h_L = \gamma Q_f \frac{\Delta p}{\rho g}$$

where,  $h_L$ , was the head loss across the static mixer.

Case 1:  $v_s = 0.6 \text{ m/s}$

$$\begin{aligned} P &= (9780 \text{ N/m}^3)(0.007 \text{ m}^3/\text{min})(6000 \text{ Pa})/[(998 \text{ kg/m}^3)(9.81 \text{ m/s}^2)(60 \text{ s/min})] \\ &= 0.7 \text{ Nm/s} = 0.7 \text{ W} \end{aligned}$$

$$G = [(0.7 \text{ Nm/s})/(0.957 \times 10^{-3} \text{ Ns/m}^2)(8.7 \times 10^{-6} \text{ m}^3)]^{1/2} = 9\,200$$

Case 2:  $v_s = 1.4 \text{ m/s}$

$$\begin{aligned} P &= (9780 \text{ N/m}^3)(0.016 \text{ m}^3/\text{min})(32000 \text{ Pa})/[(998 \text{ kg/m}^3)(9.81 \text{ m/s}^2)(60 \text{ s/min})] \\ &= 8.5 \text{ Nm/s} \end{aligned}$$

$$G = [(8.5 \text{ Nm/s})/(0.957 \times 10^{-3} \text{ Ns/m}^2)(8.7 \times 10^{-6} \text{ m}^3)]^{1/2} = 32\,000$$

## **CALCULATION OF THE ENERGY DISSIPATION RATE IN THE EXPERIMENTAL STATIC MIXER**

Energy dissipation,  $\varepsilon$ , rate was calculated using the expression provided by Taweel and Walker (1983)

$$\varepsilon = \frac{v_s \Delta p}{L_{sm} \rho}$$

where,  $L_{sm}$ , represented the length of the mixer. For the experimental system,  $L_{sm} = 3 \times 15 \text{ mm} = 45 \text{ mm} = 0.045 \text{ m}$ .

**Case 1:**  $v_s = 0.6 \text{ m/s}$

$$\varepsilon = [(0.6 \text{ m/s})/(0.045 \text{ m})] \times [(6000 \text{ Pa})/(998 \text{ kg/m}^3)] = 80 \text{ J/(kg s)}$$

**Case 2:**  $v_s = 1.4 \text{ m/s}$

$$\varepsilon = [(1.4 \text{ m/s})/(0.045 \text{ m})] \times [(32000 \text{ Pa})/(998 \text{ kg/m}^3)] = 1 \text{ 000 J/(kg s)}$$

## **CALCULATION OF THE KOLMOGOROFF SCALE OF TURBULENCE**

Based on Kolmogoroff, the minimum turbulent eddy size,  $\eta$ , can be estimated from the energy dissipation rate and the properties of the fluid according to (Nauman and Buffham 1983)

$$\eta = \left( \frac{\mu^3}{\rho^3 \varepsilon} \right)^{1/4}$$

**Case 1:**  $v_s = 0.6 \text{ m/s}$

$$\eta = \{(0.957 \times 10^{-3} \text{ Ns/m}^2)^3 / (998 \text{ kg/m}^3)^3 (80 \text{ J/kgs})\}^{1/4} = 0.00001 \text{ m} = 10 \text{ }\mu\text{m}$$

**Case 2:**  $v_s = 1.4 \text{ m/s}$

$$\eta = \{(0.957 \times 10^{-3} \text{ Ns/m}^2)^3 / (998 \text{ kg/m}^3)^3 (1000 \text{ J/kgs})\}^{1/4} = 0.0000054 \text{ m} = 5 \text{ }\mu\text{m}$$

**APPENDIX I            CALCULATIONS OF THE HYDRODYNAMIC REGIME IN  
THE GREATER VANCOUVER DISTRICT GVRD  
COAQUITLAM FACILITY OZONE CONTACTOR**

## **CALCULATION OF REYNOLDS NUMBER**

For the purposes of this calculation, the physical dimensions and operating parameters of the GVRD ozone were assumed to be:

Length,  $L = 1000$  m

Diameter,  $d = 3$  m

Hydraulic Residence Time,  $\tau = 10$  min

Liquid Velocity,  $v = (L/\tau) = (1000 \text{ m})/(10 \text{ min}) = 100 \text{ m/min} = 1.7 \text{ m/s}$

Calculations were done based on a water temperature of 22°C and the following values for the water properties:

Viscosity,  $\mu = 0.957 \times 10^{-3} \text{ Ns/m}^2$

Density,  $\rho = 998 \text{ kg/m}^3$

The Reynold's number for flow in a pipe was calculated from the following:

$$N_{Re} = \frac{\rho dv}{\mu}$$

Therefore,

$$N_{Re} = (998 \text{ kg/m}^3)(3 \text{ m})(1.7 \text{ m/s})/(0.957 \times 10^{-3} \text{ Ns/m}^2) = 5.3 \times 10^6$$

From page 284, Figure 20 in Levenspeil (1972), the intensity of dispersion,  $D/ud$ , in a turbulent pipe at this  $N_{Re}$  is approximately 0.2. The dispersion number,  $D/uL$  was calculated by multiplying the intensity of dispersion by the geometric factor,  $d/L$ :

$$D/uL = (0.2)(3 \text{ m}/1000 \text{ m}) = 6 \times 10^{-4}$$

According to the axial dispersion model and the CFSTR-in-series model, the normalized variance of the residence time distribution,  $\sigma_\theta^2$ , is related to the dispersion number and the number of CFSTRs in series,  $J$ , as follows (Levenspiel 1972):

$$\sigma_\theta^2 = 2 \frac{D}{uL} + 8 \left( \frac{D}{uL} \right)^2 = \frac{1}{J}$$

Substituting values:

$$\sigma_\theta^2 = 2(6 \times 10^{-4}) + 8(6 \times 10^{-4})^2 = 1.2 \times 10^{-3}$$

Therefore, the number of CFSTRs in series for the GVRD pipeline contactor was estimated to be:

$$J = 1/1.2 \times 10^{-3} = 83$$

**APPENDIX J      CURRICULUM VITAE**

## **CURRICULUM VITAE**

**STEPHEN A. CRAIK, MSc., PEng.**

1997 - to date: Teaching and Research Assistant, Dept. of Civil and Environmental Engineering, University of Alberta, Edmonton, AB, Canada.

1990 - 1997: Senior Research Engineer, Dow Chemical Canada, Fort Saskatchewan, AB, Canada.

1990: M. Sc. Chemical Engineering, University of Alberta, Edmonton, AB, Canada.

1987 - 1989: Teaching Assistant, Dept. of Chemical Engineering, University of Alberta, Edmonton, AB, Canada.

1987: B. Sc. Chemical Engineering, University of New Brunswick, NB, Canada

### **PUBLICATIONS IN REFEREED JOURNALS**

1. Belosevic, M., Craik, S. A., Stafford, J. L., Neumann, N. F., Kruithof, J. and D. W. Smith, 2001. Studies on the Resistance/Reactivation of *Giardia muris* and *Cryptosporidium parvum* to UV. *FEMS Microbiology Letters*, in press.
2. Craik, S. A., Weldon, D., Finch, G. R., Bolton, J. and M. Belosovic. 2001. Inactivation of *Cryptosporidium parvum* by Low and Medium Pressure Ultraviolet Radiation, *Water Research*, 35(6):1387-1398.
3. Craik, S. A., Finch, G. R., Bolton, J. and M. Belosovic. 2000. Inactivation of *Giardia muris* by Low Pressure Ultraviolet Radiation, *Water Research*, 34(18):4325-4332.
4. Craik, S. A, Fedorak, P. M., Hrudey, S. E. and M. R. Gray.1992. Kinetics of Methanogenic Degradation of Phenol by Activated-Carbon-Supported and Granular Biomass, *Biotechnology and Bioengineering*, Vol. 40, 777-786.
5. Craik, S. A, Gray, M. R., Hrudey, S. E. and P. M. Fedorak. 1991. Thermogravimetric Determination of Biomass on Activated Carbon, *Environmental Technology*. Vol. 12, 489-496.

### **SUBMITTED FOR PUBLICATION IN REFEREED JOURNALS**

1. Craik, S. A., Finch, G., Leparc, J. and M. Chandrakanth, 2001. The Effect of Ozone Gas-Liquid Contacting Conditions in a Static Mixer on Microorganism Reduction. *Ozone: Science and Engineering*, submitted for publication.

2. Craik, S. A., Smith, D. W., Belosevic, M. and M. Chandrakanth, 2001. Use of *Bacillus subtilis* spores as Model Microorganisms for Ozonation of *Cryptosporidium parvum* in Drinking Water Treatment. *Journal of Environmental Engineering and Science*, submitted for publication.
3. Lewin, N., Craik, S. A., Smith, D. W. and M. Belosevic, 2001. Sequential Inactivation of *Cryptosporidium* Using Ozone Followed by Free Chlorine in Natural Water. *Ozone: Science and Engineering*, in press.

### **CONFERENCE PROCEEDINGS**

1. Craik, S. A., Smith, D. W., Li. H. and M, Belosevic. 2001. Options for Microorganism Reduction for Cold water Utilities. *In: Proceedings of the American Water Works Association Annual Conference 2001*. American Water Works Association, Denver, CO.
2. Craik, S. A., Smith, D. W., Neumann, N. F., Kruithof, J., Stafford, J. and M. Belosevic. Effect of Ultraviolet Light on *Cryptosporidium parvum* Oocysts and *Giardia muris* Cysts in Various Drinking Waters. *In: Proceedings of the 1<sup>st</sup> International Congress of the International Ultraviolet Association*. The International Ultraviolet Association, Ayr, ON.
3. Smith, D. W., Craik, S. A., K. Farahbakhsh, Li. H. and M. Belosevic. 2001. Review of Microorganism Reduction Options for Cold Regions Utilities. *In: Sixth Annual Research and Development Conference on Rural Sanitation*. Alaska Water and Wastewater Management Association, Anchorage, AL.
4. Craik, S. A., Smith, D. W., Chandrakanth, M. and Belosevic. 2000. Reaction Engineering Analysis of *Cryptosporidium parvum* Inactivation in a Laboratory-Scale Static Mixer Ozonation System. *In: Water Quality and Technology Conference Proceedings*. American Water Works Association, Denver, CO.
5. Craik, S., Finch, G., Leparc J. and M. Chandrakanth. Considerations in the Process Design of Ozone Contacting Systems for Microbial Reduction. *In: Proceedings of the 2000 Annual Conference of the International Ozone Association Pan American Group*. International Ozone Association, Stamford, CT.
6. Chandrakanth, M., Prevost, M., Finch, G., Craik, S. and J. Leparc. An evaluation of static mixers at bench- and pilot-scale for enhanced ozone dissolution and disinfection in drinking water treatment. *In: Proceedings of the American Water*

Works Association National Conference. American Water Works Association, Denver, CO.

### **OTHER CONFERENCE PRESENTATIONS AND SEMINARS**

1. Craik, S. A., Smith, D. W. and M. Belosevic. Current State of UV Research at the University of Alberta. *Presented at: BC Hydro Innovative Electrotechnologies in Water and Wastewater Treatment Seminar, May 10-11, Vancouver, BC.*
2. Craik, S. A., Smith, D. W. and M. Belosevic. Ozone Static Mixer Contactor for *Cryptosporidium parvum* Reduction by Ozone. *Presented at: BC Hydro Innovative Electrotechnologies in Water and Wastewater Treatment Seminar, May 10-11, Vancouver, BC.*
3. Craik, S. A., Smith, D. W. and M. Belosevic. Ultraviolet Light for Microorganism Reduction in Drinking Water. Summary of Research at the University of Alberta. *Presented at: University of Calgary Drinking Water Workshop, April 9, 2001, Calgary, Alberta. BC.*
4. Craik, S. A. Nuemann, N. F. and M. Belosevic. Effect of Ultraviolet Light on *Giardia muris* Cysts in Drinking Water Determined by Loss of Infectivity in Mice. *Presented at: Giardia in the Rockies, Oct 18-20, 2000. Canmore, AB.*
5. Finch, G., Craik, S., Bircher, K., Bolton, J., Gyürék L., Neumann, N.F. and M. Belosevic, Inactivation of Encysted Parasites Using Medium-Pressure Ultraviolet Radiation Drinking Water. Canadian Water and Wastewater Association 9<sup>th</sup> Annual Water and Wastewater Conference, Regina, SK, May 16-18, 2000.
6. Craik, S., Finch G., Bircher K., Degan D. and D. Rector, Inactivation of Encysted Parasites Using Medium-Pressure Ultraviolet Radiation Drinking Water. 2000 British Columbia Water and Wastewater Association Conference, Victoria, BC, April 15 – 19, 2000.

## **TECHNICAL REPORTS**

1. Craik, S. A., Smith, D. W., M. Belosevic and J. Stafford. Inactivation of Protozoan Pathogens in City of Kelowna Drinking Water by Ultraviolet Radiation. Dept. of Civil and Environmental Engineering, University of Alberta, Edmonton AB, Prepared for City of Kelowna, May 7, 2001.
2. Smith, D. W., Craik, S. A., M. Belosevic and J. Stafford. Inactivation of Water-Borne Viruses, Spore-Forming Bacteria and Protozoan Pathogens in EPCOR Water by Ultraviolet Radiation. Dept. of Civil and Environmental Engineering, University of Alberta, Edmonton AB, Prepared for EPCOR Water Services, February 20, 2001.
3. Belosevic, M., Neumann, N. F., Smith, D. W. and S. A. Craik. Inactivation of Water-borne Viruses, Spore-Forming Bacteria and Protozoan Pathogens by Medium Pressure Ultraviolet Light Irradiation, Dept. of Biological Sciences and Medical Microbiology & Immunology, Prepared for N.V. PWN Water Supply Company North Holland, November 2000.
4. Finch, G. R., Craik, S. A. and M. Belosovic. Effect of Medium Pressure Ultraviolet Radiation on Encysted *Cryptosporidium parvum* and *Giardia muris*. Dept. of Civil and Environmental Engineering, University of Alberta, Prepared for Calgon Carbon Corporation. Sept. 8, 1999.

## **AWARDS**

1998 - 2000 Natural Sciences and Engineering Research Council (NSERC) PGSB Graduate Scholarship  
1987 - 1989 Natural Sciences and Engineering Research Council (NSERC) PGSA Graduate Scholarship  
1987 Society of Chemical Industry Merit Award  
1983 - 85 University of New Brunswick Undergraduate Scholarship